Adipose stem cell-derived extracellular matrix – comparative characterization and evaluation as a biomaterial

Dissertation

der Mathematisch-Naturwissenschaftlichen Fakultät

der Eberhard Karls Universität Tübingen

zur Erlangung des Grades eines

Doktors der Naturwissenschaften

(Dr. rer. nat.)

vorgelegt von

M. Sc. Svenja Nellinger

aus Stuttgart

Tübingen

2022

Gedruckt mit Genehmigung der Mathematisch-Naturwissenschaftlichen Fakultät der Eberhard Karls Universität Tübingen.

Tag der mündlichen Qualifikation:	20.05.2022
Dekan:	Prof. Dr. Thilo Stehle
1. Berichterstatter:	Prof. Dr. Katja Schenke-Layland
2. Berichterstatter:	Prof. Dr. Petra J. Kluger

A million dreams is all it's gonna take

A million dreams for the world we're gonna make

“A million dreams”, Pasek and Paul

TABLE OF CONTENTS

LIST OF FIGURES

LIST OF TABLES

ABBREVIATIONS

3D	three dimensional
acdECM	adipose stem cell-derived extracellular matrix
Ang	angiopoietin
ASC	adipose-derived stem cell
bFGF	basic fibroblast growth factor
BM	basement membrane/ basal membrane
cdECM	cell-derived extracellular matrix
CS	Chondroitin sulfate
CuAAC	copper-catalyzed azide-alkyne cycloaddition
dECM	decellularized extracellular matrix
DNA	deoxyribonucleic acid
DS	dermatan sulfate
ECM	extracellular matrix
FACIT	Fibril-associated collagen with interrupted triple helices
GAG	glycosaminoglycans
HA	hyaluronan
Hep	heparin
HS	heparan sulfate
IEDDA	inverse electron- demand Diels-Alder
KS	keratan sulfate
LOX	lysyl oxidase
MBV	Matrix-bound vesicle
MGE	Metabolic Glycoengineering
mvEC	Microvascular endothelial cells
PDGF	platelet-derived growth factor
PG	proteoglycans
RNA	ribonucleic acid
S1P	sphingosine-1-phosphate
scdECM	stem cell-derived extracellular matrix
sGAG	sulfated glycosaminoglycans
SIS	small intestinal submucosa
SLRP	small leucine-rich repeat proteoglycan
SPAAC	strain-promoted alkyne-azide cycloaddition
VEGF	vascular endothelial growth factor

ABSTRACT

The extracellular matrix (ECM) is the non-cellular part of tissues and represents the natural environment of the cells. Next to structural stability, it provides various physical, chemical, and mechanical cues that strongly regulate and influence cellular behavior and are required for tissue morphogenesis, differentiation, and homeostasis. Due to its promising characteristics, ECM is used in a wide range of tissue engineering and regenerative medicine approaches as a biomaterial for coatings and scaffolds. To date, there are two sources for ECM material. First, native ECM is generated by the removal of the residing cells of a tissue or organ (decellularized ECM; dECM). Secondly, cell-derived ECM (cdECM) can be generated by and isolated from *in vitro* cultured cells. Although both types of ECM were intensively used for tissue engineering and regenerative medicine approaches, studies directly characterizing and comparing them are rare. Hence, in the first part of this thesis, dECM from adipose tissue and cdECM from stem cells and adipogenic differentiated stem cells from adipose tissue (ASCs) were characterized towards their macromolecular composition, structural features, and biological purity. The dECM was found to exhibit higher levels of collagens and lower levels of sulfated glycosaminoglycans compared to cdECMs. Structural characteristics revealed an immature state of collagen fibers in cdECM samples. The obtained results revealed differences between the two ECMs that can relevantly impact cellular behavior and subsequently experimental outcome and should therefore be considered when choosing a biomaterial for a specific application. The establishment of a functional vascular system in tissue constructs to realize an adequate nutrient supply remains challenging. In the second part, the supporting effect of cdECM on the self-assembled formation of prevascular-like structures by microvascular endothelial cells (mvECs) was investigated. It could be observed that cdECM, especially adipogenic differentiated cdECM, enhanced the formation of prevascular-like structures. An increased concentration of proangiogenic factors was found in cdECM substrates. The demonstration of cdECMs capability to induce the spontaneous formation of prevascular-like structures by mvECs highlights cdECM as a promising biomaterial for adipose tissue engineering. Depending on the purpose of the ECM material chemical modification might be necessary. In the third and last part, the chemical functionalization of cdECM with dienophiles (terminal alkenes, cyclopropene) by metabolic glycoengineering (MGE) was demonstrated. MGE allows the chemical functionalization of cdECM via the natural metabolism of the cells and without affecting the chemical integrity of the cdECM. The incorporated dienophile chemical groups can be specifically addressed via catalysts-free, cell-friendly inverse electron-demand Diels-Alder

reaction. Using this system, the successful modification of cdECM from ASCs with an active enzyme could be shown. The possibility to modify cdECM via a cell-friendly chemical reaction opens up a wide range of possibilities to improve cdECM depending on the purpose of the material. Altogether, this thesis highlighted the differences between adipose dECM and cdECM from ASCs and demonstrated cdECM as a promising alternative to native dECM for application in tissue engineering and regenerative medicine approaches.

ZUSAMMENFASSUNG

Die extrazelluläre Matrix (englisch: extracellular matrix: ECM) ist der nichtzelluläre Teil von Gewebe und Organen und stellt die natürliche Umgebung der Zellen dar. Neben struktureller Stabilität interagiert sie über zahlreiche physikalische, chemische und mechanische Signale mit den Zellen und reguliert so das Verhalten der Zellen und darüber hinaus die Morphogenese, Differenzierung und Homöostase von Geweben. Aufgrund ihrer vielversprechenden Eigenschaften wird die ECM umfangreich im Tissue Engineering und in der regenerativen Medizin als (Bio)Material eingesetzt. Bislang stehen zwei Quellen für ECM zur Verfügung. Erstens kann native ECM durch die Entfernung der in einem Gewebe oder Organ vorhandenen Zellen (dezellularisierte ECM; dECM) gewonnen werden. Neben dieser nativer dECM kann ECM aus im Labor kultivierten Zellen gewonnen werden (englisch: cell-derived ECM; cdECM). Obwohl beide Arten von ECM umfangreich im Tissue Engineering und in der regenerativen Medizin eingesetzt werden, gibt es nur wenige Studien, die sie systematisch charakterisieren und direkt miteinander vergleichen. Im ersten Teil dieser Thesis werden dECM aus dem Fettgewebe und cdECM aus Stammzellen und adipogen differenzierten Stammzellen aus dem Fettgewebe (englisch: adipose-derived stem cells; ASCs) hinsichtlich ihrer makromolekularen Zusammensetzung, strukturellen Merkmale und biologischen Reinheit untersucht. Es konnte gezeigt werden, dass die dECM im Vergleich zur cdECM einen höheren Anteil an Kollagenen und einen geringeren Anteil an sulfatierten Glykosaminoglykanen aufweist. Die Untersuchung der strukturellen Merkmale zeigte, dass die Kollagenfasern in der cdECM einen noch unreifen Zustand aufweisen. Die erzielten Ergebnisse lassen Unterschiede zwischen den beiden ECMs erkennen, die das zelluläre Verhalten und damit Versuchsergebnisse maßgeblich beeinflussen können und daher bei der Auswahl eines Biomaterials für eine bestimmte Anwendung berücksichtigt werden sollten. Die Integration eines funktionellen Gefäßsystems in Gewebekonstrukte zur Realisierung einer ausreichenden Nährstoffversorgung bleibt weiterhin eine Herausforderung. Im zweiten Teil dieser Thesis wird die unterstützende Wirkung von cdECM auf die Ausbildung von gefäßähnlichen Strukturen durch mikrovaskuläre Endothelzellen (mvECs) untersucht. Es konnte beobachtet werden, dass die cdECM, insbesondere die adipogen differenzierte cdECM, die Bildung von gefäßähnlichen Strukturen deutlich fördert. Weiterhin wurde in den cdECM Substraten eine erhöhte Konzentration von pro-angiogenen Faktoren gemessen. Die Fähigkeit von cdECMs, die spontane Bildung von gefäßähnlichen Strukturen durch mvECs zu induzieren, hebt cdECM als vielversprechendes Biomaterial für das Tissue Engineering hervor.

Je nach Verwendungszweck des ECM-Materials kann eine chemische Modifizierung erforderlich oder hilfreich sein. Im dritten und letzten Teil dieser Thesis wurde die chemische Funktionalisierung von cdECM mit dienophilen Gruppen (endständigen Alkenen, Cyclopropenen) durch metabolisches Glykoengineering (MGE) gezeigt. MGE ermöglicht die chemische Funktionalisierung von cdECM mittels des natürlichen Stoffwechsels der Zellen und ohne Veränderung der chemischen Integrität der cdECM selbst. Die eingebauten dienophilen Gruppen können über eine katalysatorfreie, zellfreundliche Diels-Alder-Reaktion mit inversem Elektronenbedarf gezielt adressiert werden. Über dieses chemische System konnte die erfolgreiche Modifikation von cdECM aus ASCs mit einem aktiven Enzym gezeigt werden. Die Möglichkeit, cdECM über eine zellfreundliche chemische Reaktion zu modifizieren, eröffnet eine breite Palette von Möglichkeiten zur Anpassung der cdECM, je nach Verwendungszweck des Materials. Insgesamt hat diese Thesis die Unterschiede zwischen dECM aus dem Fettgewebe und cdECM von ASCs hervorgehoben und gezeigt, dass cdECM eine vielversprechende Alternative zur nativen dECM für die Anwendung im Tissue Engineering und in der regenerativen Medizin darstellt.

PUBLICATIONS AND CONTRIBUTIONS

The presented cumulative thesis is based on the following publications, which are published in international peer-reviewed journals:

1. **Cell-derived and enzyme-based decellularized extracellular matrix exhibit compositional and structural differences that are relevant for its use as a biomaterial**

   Svenja Nellinger, Ivana Mrsic, Silke Keller, Simon Heine, Alexander Southan, Monika Bach, Ann-Cathrin Volz, Thomas Chassé, Petra J. Kluger

   Biotechnology and Bioengineering. 2022; 1– 15. DOI: 10.1002/bit.28047

2. **Adipose stem cell-derived Extracellular Matrix represents a promising Biomaterial by inducing spontaneous formation of Prevascular-like Structures by MvECs**

   Svenja Nellinger, Isabelle Schmidt, Simon Heine, Ann-Cathrin Volz and Petra J. Kluger

   Biotechnology and Bioengineering. 2020;1–13. DOI: 10.1002/bit.27481

3. **An Advanced "clickECM" that Can be Modified by the Inverse-Electron Demand Diels-Alder Reaction**

   Svenja Nellinger, Mareike A. Rapp, Alexander Southan, Valentin Wittmann, Petra J. Kluger

   *ChemBioChem***.** 2022, 23. DOI: 10.1002/cbic.202100266

Contributions to the publications:

No.	Accepted for publication	Number of authors	Position of the candidate in the list of authors	Scientific ideas by candidate [%]	Data generation by candidate [%]	Interpretation and analysis by candidate [%]	Paper writing by candidate [%]
1	Yes	9	1	90	80	90	80
2	Yes	5	1	90	95	90	80
3	Yes	5	1	75	75	75	75

Further contributions of the PhD candidate:

Conference paper:

- **Generation of an azide-modified extracellular matrix by adipose-derived stem cells using metabolic glycoengineering**

  Svenja Nellinger*, Silke Keller, Alexander Southan, Valentin Wittmann, Ann-Cathrin Volz and Petra J. Kluger

  Current Directions in Biomedical Engineering, vol. 5, no. 1, 2019, pp. 393-395.

  DOI: 10.1515/cdbme-2019-0099 (full text provided under Appendix I)

- **Cell-derived Extracellular Matrix as maintaining Biomaterial for adipogenic differentiation**

  Svenja Nellinger, Simon Heine, Ann-Cathrin Volz and Petra J. Kluger*

  Current Directions in Biomedical Engineering, vol. 6, no. 3, 2020, pp. 410-413.

  DOI: 10.1515/cdbme-2020-3106 (full text provided under Appendix II)

Participation in national and international conferences:

Year & Venue	Conference	Type	Title of contribution
2017 Dresden	Annual Conference on Biomedical Engineering	Poster	Chemically modified micro grooved PDMS surfaces influence adipose-derived stem cell behavior
2017 Würzburg	Annual Meeting of the German Society for Biomaterials (DGBM)	Poster	Actin cytoskeleton organization and nucleus orientation of adipose-derived stem cells on micro structured PDMS surfaces
2018 Maastricht	Conference of the European Society for Biomaterials	Poster	Advancement of *click*ECM technique by metabolic glycoengineering using synthetic dienophile-modified monosaccharide derivates
2018 Braunschweig	Annual Meeting of the German Society for Biomaterials (DGBM)	Poster	Devitalized extracellular matrix as smart biomaterial for adipose-derived stem cell differentiation
2019 Frankfurt	Annual Conference on Biomedical Engineering	Poster + conference paper	Generation of an azide-modified extracellular matrix by adipose-derived stem cells using metabolic glycoengineering
2020 online	Annual Conference on Biomedical Engineering	Poster + conference paper	Cell-derived extracellular matrix as maintaining biomaterial for adipogenic differentiation
2021 online	Annual Meeting of the German Society for Biomaterials (DGBM)	Oral presentation	Decellularized native ECM vs cell-derived ECM – a systematically characterization and comparison

1 INTRODUCTION

1.1 The Extracellular Matrix

Tissues are composed of specific cells and a non-cellular component, the extracellular matrix (ECM). The ECM is a complex three-dimensional network structure consisting of interconnected fibrillary and non-fibrillary macromolecules, synthesized and secreted by the residing cells. As it is continuously remodeled by the cells using specific proteases (e.g. matrix metalloproteases), it is a highly dynamic structure [1,2]. The ECM not only provides physical and structural stability to tissues but also initiates crucial biochemical and biomechanical cues that regulate numerous cellular processes including adhesion, proliferation, migration, and differentiation. The physical, chemical, and topographical features of the ECM are highly tissue-specific and generate the characteristic properties of a tissue, such as its tensile and compressive strength and elasticity. By providing specific binding sites, ECM serves as a reservoir for growth factors and cytokines that can be presented to specific receptors on cell surfaces at relevant times [1–3]. Next to signaling proteins ECM also provides binding sites for cell membrane receptors (e.g. integrins) that sense the ECM and initiate a cellular response via the interaction with the actin cytoskeleton [4,5].

Depending on its structure and composition ECM can be divided into two major subtypes, i.e. pericellular and interstitial ECM [1,6]. Pericellular ECM is a narrow space surrounding individual cells that is in close contact with the cells and exhibits a distinct composition from the interstitial ECM. A well-known type of pericellular ECM is the basement membrane which is a sheet-like structure that separates the cells from the surrounding connective tissue. The interstitial ECM is present in the connective tissue and mainly comprises different types of collagen, elastin, fibronectin, and proteoglycans [1,2,7,8]. **Figure 1** gives an overview of the main components of the ECM and their interaction with cellular structures.

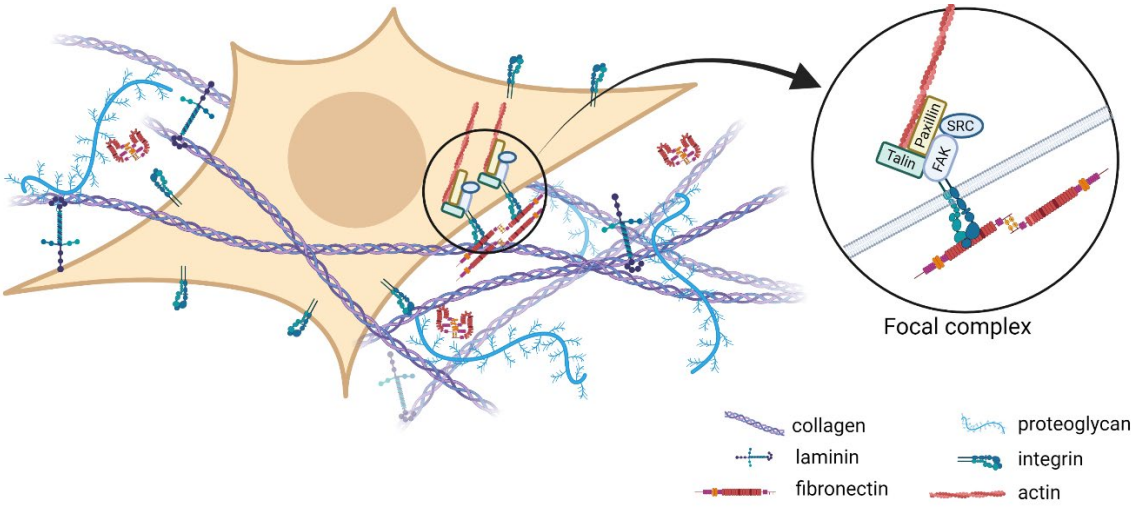

Figure 1: Schematic overview of ECM structures and focal complex. The ECM consists of various fibrous proteins like collagens, proteoglycans with GAGs and cell adhesion proteins like laminin and fibronectin. Via focal complexes the ECM interact and influence the actin cytoskeleton and thereby various cellular signaling pathways. (FAK: focal adhesion kinase, SRC: Src kinase). Created with BioRender.com

1.1.1 ECM components

The ECM is composed of two main components: Ground substance and fibrous proteins. Further, anchor proteins for cell-ECM interactions (e.g. fibronectin and laminins), and ECM-bound and soluble growth factors can be found. The fibrous components built a stable network that provides adhesion sites for the molecules of the ground substance [1–3,9]. In the following, the main ECM compounds are described in more detail.

Ground substance

The ground substance consists of glycosaminoglycans (GAGs), proteoglycans (PGs), and glycoproteins which include among others anchor proteins like fibronectin and laminins [10–12]. GAGs are unbranched, negatively charged heteropolysaccharides with repeating disaccharide structures. The disaccharide subunits are linked via 1,4-glycosidic bonds that are linked via a 1,3-glycosidic bond to an amino sugar, like *N*-acetylglucosamine or *N*-acetyl galactosamine. Depending on variations in the disaccharide sequence and sulfonylation degree, six subgroups of sulfated (s)GAGs are defined: Chondroitin sulfate (CS), dermatan sulfate (DS), heparin (Hep), heparan sulfate (HS), hyaluronan (hyaluronic acid; HA), and keratan sulfate (KS) [13–16]. In contrast to the other GAGs, which are synthesized in the Golgi apparatus, HA is synthesized by transmembrane proteins and is the only non-sulfated GAG [14]. GAGs are involved in the maintenance of turgor and enhance the elasticity of ECM. Next to their structural functions in ECM, GAGs are known to influence cellular behavior (e.g. migration, proliferation, and differentiation) and to have a

beneficial effect in regenerative processes, like wound healing and angiogenesis [14,15]. In **Figure 2** the structure of proteoglycans is shown.

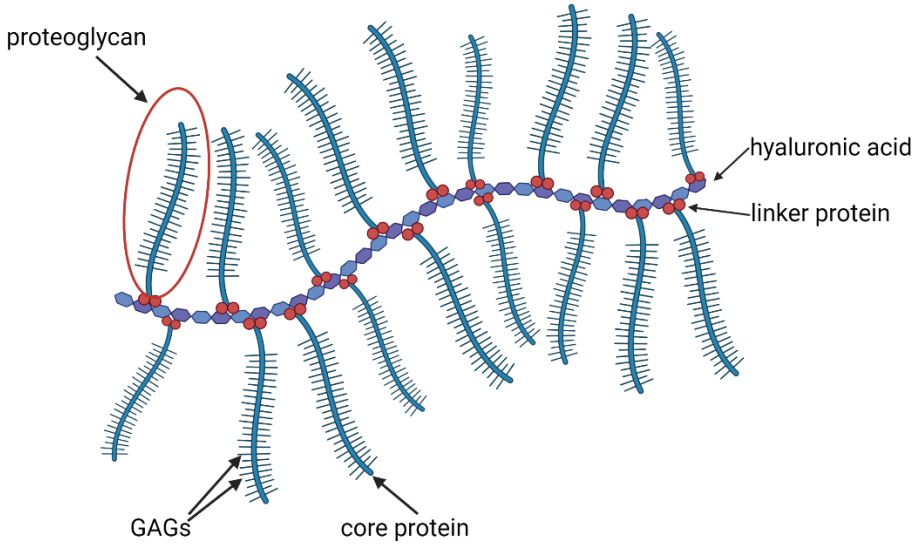

Figure 2: Schematic structure of a proteoglycan. PGs consist of one or more sGAGs bound to a core protein. The type and number of attached sGAGs are responsible for their physiological functions including regulation matrix mechanics and cellular behavior. Created with BioRender.com

PGs are composed of GAG chains covalently linked to a core protein [17]. According to their localization, PGs can be classified into fours subgroups: intracellular PGs, extracellular PGs, pericellular PGs, and cell-surface PGs [9]. Other classifications e.g. after their linked sGAGs or protein structure, can also be found. **Table 1** gives an overview of the members of the above-mentioned different PG subgroups, their localization, and the respective sGAG chains. PGs are ubiquitously expressed by all cell types and fill the majority of the extracellular space in the form of a hydrated gel. They have various functions including buffering, hydration, binding of growth factors, and force-resistance [18,19]. Next to regulating matrix mechanics, they act as integrators of different signaling pathways regulating cellular behavior by acting as coreceptors for growth factors and interacting with enzymes that are continuously remodeling the ECM [20,21]. The covalently attached sGAG chains are principally responsible for most of the physiological functions. Extracellular PGs aggrecan, versican, neuronan, and brevican are responsible for the compressive-resistant features of cartilage, the tensile strength of skin and tendon, and the mineralization of the bone matrix. Decorin is mainly found in connective tissue ECM and perlecan is an important component of basement membrane (BM) [21].

Table 1: Overview of the four subgroups of PG classified according to their localization (adapted from [9,14]**).** SLRP: small leucine-rich repeat proteoglycan; CSPG: Chondroitin sulfate proteoglycan; NG: neuron-glial antigen; GPI: glycosylphosphatidylinositol; GPC: glypican; Hep: heparin; CS: chondroitin sulfate; KS: keratan sulfate; DS: dermatan sulfate; HS: heparan sulfate

Location/ Class	Proteoglycan	GAG chains
Intracellular		
Secretory Granules	Serglycin	Hep
Extracellular PGs		
Hyalectanes	Aggrecan	CS/KS
	Versican, Neuronan, Brevican	CS
SLRPs	Biglycan	CS
	Decorin	DS
	Fibromodulin, Lumican	KS
SPOCK	Testican	HS
Pericellular		KS
BM	Perlecan, Agrin, Collagen XVIII	HS
	Collagen XV	CS/HS
Cell surface		
Transmembrane	Syndecans 1-4	HS
	CSPG4/NG2, Phosphacan	CS
	Betaglycan	CS/HS
GPI anchored	GPC-1-6	HS

Fibrous proteins

Collagens

Collagens are the most abundant proteins in the ECM. To date, 28 types of collagens are identified in mammals, with types I - III making up 80-90 % of the collagen in the human body [22–24]. Collagens comprised of different procollagen α chains (α1, α2, and α3) that are post-translational modified. This includes the hydroxylation of proline and lysine residues and the glycosylation of lysine [25,26]. Polypeptide α-chains contain a variable number of Gly-X-Y repeats, where X and Y often are proline and 4-hydroxyproline, respectively. After release from the endoplasmic reticulum into the cytoplasm, the α-chains assemble into homo- or heterotrimeric helical bundles to form the procollagen triple helix molecule. Procollagen is released to extracellular, converted

to tropocollagen by proteolytic removal of the N- and C-propeptides and assembled to fibrils and/ or networks, depending on the type of collagen [27].

Fibril-forming collagens (I, II, III, V, XI, XXIV, XXVII) self-assemble into fibrils of various diameters and different structures. Covalent cross-linking of the collagens is initiated by the enzymes of the lysyl oxidase (LOX) family, to stabilize the fibers and provide their mechanical properties [28]. Collagens I, II, III, V, and XI are the most extensively characterized and investigated fibrillar collagens. Subtypes I, III, and V are found in a variety of tissues. Subtype II is mainly found in cartilage, associated with subtype XI, which regulates fibril assembly, and functional properties in tendon [29,30].

Fibril-associated collagen with interrupted triple helices (FACITs) (IX, XII, XIV, XVI, XIX, XX, XXI, XXII) do not form fibrils by themselves. They are associated with the surface of fibrillar collagens. Collagen IX is covalently linked to the surface of collagen II, and collagens XII and XIV are associated with collagen I fibrils. Collagen XV is associated with BM and forms a bridge linking large, banded fibrils, likely fibrils containing collagens I and III [31,32].

Collagen forming beaded filaments (VI) and collagen forming anchoring fibrils (VII) are special within the collagen family. Collagen VI contains von Willebrand factor and Kunitz family of serine protease inhibitor domains and forms end-to-end beaded filaments. It is found in a wide range of tissues where it forms structural links with cellular structures [27,33]. Collagen VII is the major component of the anchoring fibrils at the dermal-epidermal junction [27]. It plays a role in wound closure by enhancing fibroblast migration and cytokine secretion [34].

Network-forming collagens include collagens IV, VIII, and X. Collagen IV represents the prototypical network-forming collagen, which is associated with the BM [27]. Collagen VIII is a major component of the Descemet's membrane – the specialized BM of the corneal endothelium [35] - and subendothelial matrices. The related collagen X is found in the hypertrophic zone of growth plate cartilage [36].

Membrane-associated collagens (XIII, XVII, XXIII, XXV) are transmembrane proteins that have a short cytosolic N-terminal domain and long interrupted triple-helical extracellular domains, which can be proteolytically shed by furin-like proprotein convertases. Collagens XIII and XXV have cell adhesive properties and occur in numerous cell types [22]. Collagen XVII is mainly expressed in basal keratinocytes and can be found in hemidesmosomes [37].

Multiplexins (XV, XVIII) are a subtype of collagens decorated with GAGs and associated with the BM [31]. Collagen XV plays a role in the regulation of cell adhesion and migration whereas collagen XVIII is required for the maintenance of the BM and regulates cell survival, maintenance, differentiation, and inflammation [38].

Elastic fibers

Together with fibrillin, elastin builds a highly elastic network of elastic fibers in the ECM. They endow connective tissues with the critical properties of elasticity and resilience. Cells secrete the soluble tropoelastin molecules into the extracellular space [39]. Tropoelastin mainly consists of hydrophobic amino acids (glycine, alanine, valine, and proline) and exhibits small amounts of hydroxyproline. Extracellularly, tropoelastin is cross-linked via lysin side chains and surrounded by fibrillin. Similar to collagens this cross-linking is initiated by members of the LOX family [40]. This is a highly complex and multistage process named elastogenesis. As shown in **Figure 3** mature elastic fibers exhibit a "random coil" structure which allows the stretching of 100-200 % of their original length and the retraction to the original shape [41]. The production of functional elastic fibers *in vivo* occurs during the neonatal stages and decreases after birth [42,43]. The turnover of elastic fibers is extremely slow and under normal conditions, there is no elastogenesis in adult life leading to an accumulation of damages in elastic fibers over a lifetime [44–46].

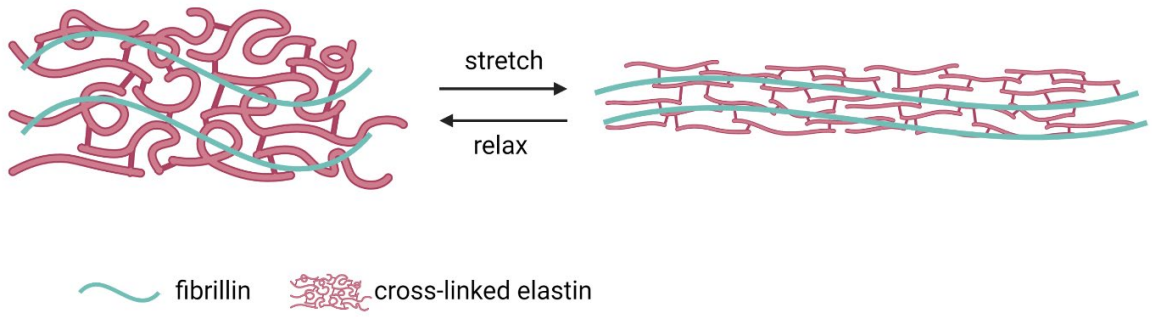

Figure 3: Elastic fibers. Single elastin molecules are secreted by the cells and assemble extracellularly with fibrillin. Cross-linking via enzymes of the lysyl oxidase family (LOX) leads to fibers with a "random-coil" structure. This specific structure enables stretching of the fiber to 100-200 % of their initial length and the retraction to the initial shape. Created with Biorender.com

Reticular fibers

Reticular fibers consist of one or more strands of collagen III building very thin fibers (< 2µm). They built a highly branched network of thin reticular fibers mostly covered with glycoproteins. Reticular fibers are associated with the BM, lymphatic organs, and blood vessels where they act as a supporting mesh [47,48].

<u>Other components present in ECM</u>

In addition to their function as structural proteins, ECM proteins interact with cell surface receptors and regulate numerous biological processes either as full-length proteins or via their bioactive fragments (matricryptins and matrikines) released by proteolysis e.g. during tissue

remodeling [49,50]. In 2016 Huleihel *et al.* first described a subpopulation of extracellular vesicles that are bound within the ECM (matrix-bound vesicles; MBVs) and have the potential to highly influence its bioactivity (e.g. macrophage activation and differentiation) [51]. These MBVs contain microRNA and are released after enzymatic degradation as it occurs during natural ECM turnover in tissues by cell-derived enzymes [51,52]. Further, cell-secreted bioactive molecules (e.g. growth factors, cytokines, and enzymes) accumulate within the ECM and can partly be bound by the ECM protein [53,54]. Similar to MBVs, ECM-bound bioactive molecules can be released after ECM degradation.

1.1.2 Basement membrane

The BM is a thin special type of ECM that can be found on the basal side of epithelial or endothelial cells and is important for the from and structure of the overlying tissues [55]. BM structures can also be found around adipocytes in adipose tissue [56]. The composition of the BM is highly diverse, dynamic, and tissue-specific. Typically the BM consists of a network of laminin and collagen IV linked with several additional ECM proteins, such as nidogen, perlecan, fibulin, and argin [57,58]. Recent studies showed that laminins together with collagen IV built a stable scaffold of BM and proteins like nidogen, fibulin and agrin are more dynamic components of the BM. These mobile BM components might allow the response of BM to changes in tissue [59]. **Figure 4** shows the structure of BM and the stable and mobile components.

Laminins are deposited by the cells and are assembled along with collagen IV, nidogens, argin, and perlecan and representing an essential part of the BM. They are heterotrimers comprising of an α-, a β- and a γ- subunit that are assembled to a cross-, Y, or rod-shaped molecule. To date, five α chains, three β chains, and three γ chains are known which can assemble to different isoforms [60,61]. Laminin molecules interact with each other as well as with other ECM molecules participating in the organization of the ECM. Further, Laminin interacts with the cell membrane receptors integrin and dystroglycan, which cause actin cytoskeleton rearrangement that in turn have functional consequences on cell behavior (e.g. adhesion, migration, and differentiation). Laminins are shown to be crucial in embryonic development, organogenesis and are an important player in wound repair and angiogenesis [62,63].

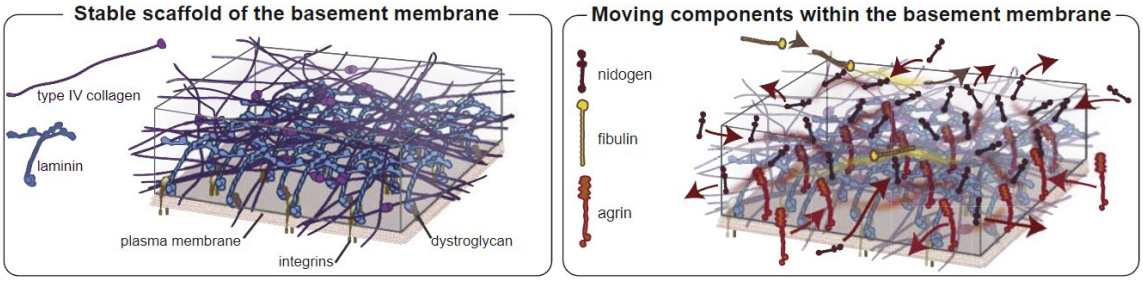

Figure 4: Structure of the basement membrane. Laminins and collagen IV form a stable scaffold. The most dynamic proteins in the BM are moving proteins like nidogen, fibulin, and argin. The dynamic of the BM allows response to changes in the tissue [59][1].

1.2 The extracellular matrix as a biomaterial

There are a variety of different definitions for the term "biomaterial". One widespread definition is employed by the American National Institute of Health that describes biomaterial as "*any substance or combination of substances, other than drugs, synthetic or natural in origin, which can be used for any period of time, which augments or replaces partially or totally any tissue, organ or function of the body, in order to maintain or improve the quality of life of the individual*" [64,65]. Biomaterials are used in different (bio)medical applications, such as surgical instruments, catheters or screws, and implants, differing in their type of material and remaining time in the body. Since the 1950s biomaterials go through an enormous development (**Figure 5**). The first generation of biomaterials includes metals and alloys that do not elicit an adverse reaction in the biological system (bioinert). Due to poor adhesion and implant loosening the second generation of biomaterials was developed, which were capable to form complex bonds with the biological tissue (bioactive). Simultaneously, researchers studied bioresorbable materials. In the next step, research was focused on materials that are being degraded in a controlled manner and promoting a natural integration of the implant with the tissue (third generation). Since around 2010 the fourth generation of biomaterials moved to the fore: biomimetic materials for application in tissue engineering. Although the natural ECM would best represent the natural environment of the cells, these materials are mainly natural biopolymers like collagen and other single ECM molecules [66–68].

[1] Reprinted from *Comprehensive Endogenous Tagging of Basement Membrane Components Reveals Dynamic Movement within the Matrix Scaffolding*, Daniel P. Keeley,Eric Hastie,Ranjay Jayadev,Laura C. Kelley,Qiuyi Chi,Sara G. Payne,Jonathan L. Jeger,Brenton D. Hoffman,David R. Sherwood, Dev Cell. 2020 Jul 6;54(1):60-74, Copyright (2022) with permission from Elsevier

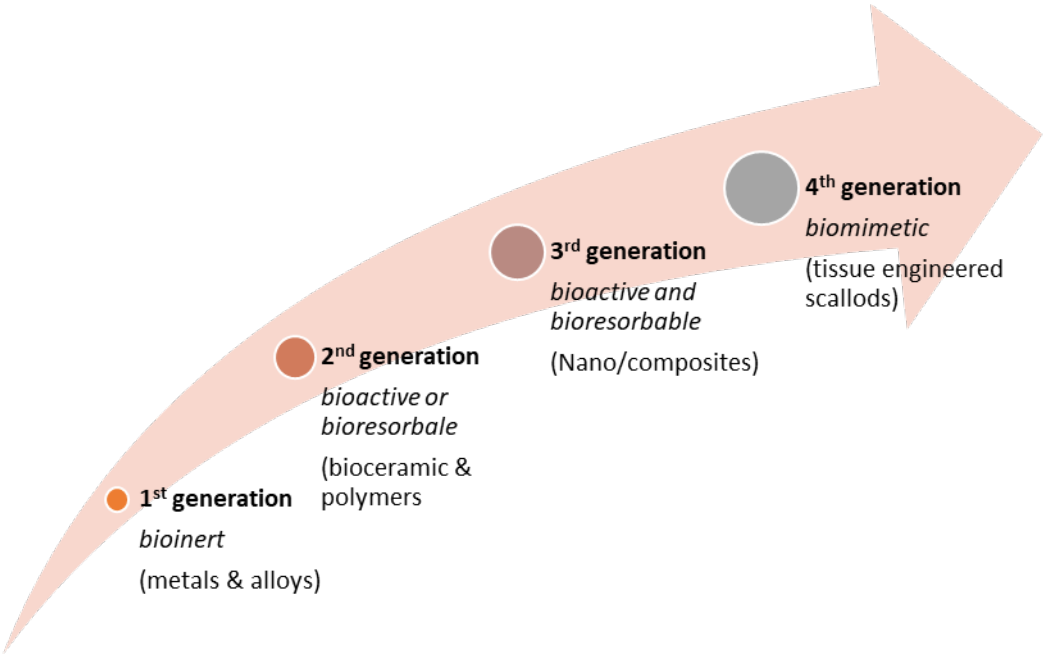

Figure 5: "Evolution" of biomaterials. Since the 1950s biomaterials developed through different stages from bioinert materials that did not interact with the host tissue to biomimetic materials that aim to reflect the natural environment of the cells.

These molecules are used as coatings, as scaffold material, or as a component of hybrid materials in combination with synthetic materials [69–72]. In hybrid materials, the desirable characteristics of biological molecules are combined with the good mechanical/ physical characteristic of synthetic materials. The advantages of the use of single ECM molecules are their simplicity in the generation, application, and processing. Due to the extreme complexity, to date it is not possible to rebuild the natural ECM as the most natural environment of cells. Thus, researchers focus on the use of natural ECM as a biomaterial. To date, this natural ECM can be generated in two ways:

1. **Decellularization of native tissues/organs (dECM)**
2. **Generation of cell-derived ECM (cdECM)**

1.2.1 Decellularized tissues/organs

Since the conception of decellularized tissue was introduced methods and application of dECM evolved (**Figure 6**) [73]. The first reported decellularization (muscle tissue) was performed by Poel *et al*. in 1948 [74]. In the 1970s Hjelle *et al.* demonstrated the isolation of BM from rat kidney [75]. Badylak and his team reported the isolation of ECM from small intestine submucosa (SIS) for Achilles tendon repair [76]. Since then a variety of whole organ decellularization were reported (heart [77], lung [78,79], liver [80], kidney [81]). With the upcoming of 3D printing, dECM was

regarded as a promising biomaterial for the development of bioinks [82,83]. Pati *et al*. demonstrated the printability of dECM from adipose tissue, cartilage tissue, and cardiac tissue [84].

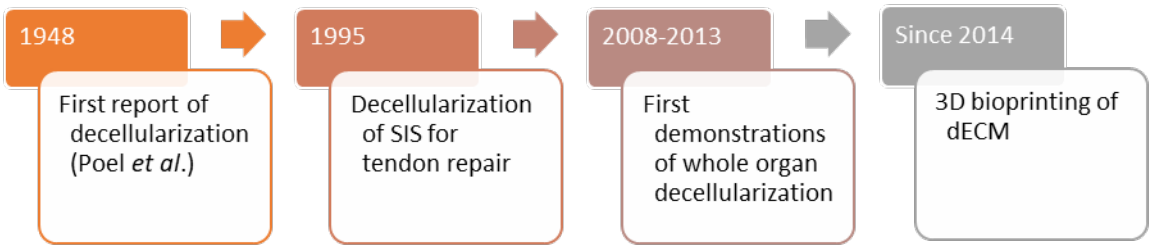

Figure 6: Timeline of decellularization methods. Since the first reported decellularization in 1948 this method was continuously further developed for compete tissues and organs. With the upcoming of 3D bioprinting dECM is also seen as an interesting material for bioinks. (SIS: small intestinal submucosa)

The aim of the decellularization of tissues and organs is the removal of cellular structures to obtain scaffolds with the original shape of the tissue/ organ with simultaneous conservation of the natural composition and structure of the biomolecules [85]. The removal of the cellular structures reduces the immunological host reaction and the risk of disease transmission when the scaffold is used as a transplant [86]. Especially for the use of xenogeneic ECM, this is a critical factor. A variety of different decellularized tissues are used in research and clinical application for example heart valves [87–89], adipose tissue [90,91], skin [92,93], SIS [94–96], urinary bladder [97,98], tendon [99,100], and vascular structures [101,102].

The methods for decellularization can be divided into three groups whereby the different methods can also be combined:

- **Chemical decellularization**
- **Physical decellularization**
- **Enzymatic decellularization**

Chemical decellularization protocols are based on alcohols, solvents, acids, bases, ionic and non-ionic detergents. This method is seen as quite efficient for tissue exhibiting a dense structure. The greatest disadvantage of this method is the impact of the used – mostly harsh - chemicals on the ECM molecules. For example, GAGs are known to be very sensitive against detergents [86,103]. *Physical decellularization* methods include temperature (e.g. freeze-thaw cycles), pressure, sonication, and mechanical treatment. These methods are mainly cost-effective and relatively simple in the implementation. However, the structure of ECM can be damaged and cellular debris remains in the ECM which makes further steps necessary to remove them [104]. For *enzymatic*

decellularization enzymes like nucleases, proteases, collagenases, galactosidases, phospholipases, and dispase are used to specifically degrade cellular components. These components have to be removed in subsequent processing steps [103].

In **Figure 7** the parameters influencing the yielded dECM are shown. The parameter that cannot be influenced is the donor of the tissue/organ. It is known that also in dECM composition and characteristics there can be high donor variations depending on species, age, sex, diseases, and health status of the donor [105–109]. These factors can highly influence the "quality" of the yielded dECM when used as a scaffold material in tissue engineering by altering the behavior of re-seeded cells *in vitro* or incorporating efficiency and host response *in vivo*. Another parameter is the tissue source which has a great impact on the composition of the dECM. As described in 4.1 the ECM is highly tissue-specific which has to be considered for the generation of dECM as a biomaterial for a specific application. For example, ECM from adipose tissue is less dense and softer than ECM from tendon. The last parameter influencing the yielded dECM is the decellularization and processing method. As described above different decellularization methods have a different impact on dECM composition and structure. Thus, the decellularization and processing methods have to be combined in the best way to conserve dECM structures relevant for the intended use. In general, the availability of specific tissues – especially from human origin - (e.g. heart, liver, tendon) is limited which in turn limits the availability of the respective dECM.

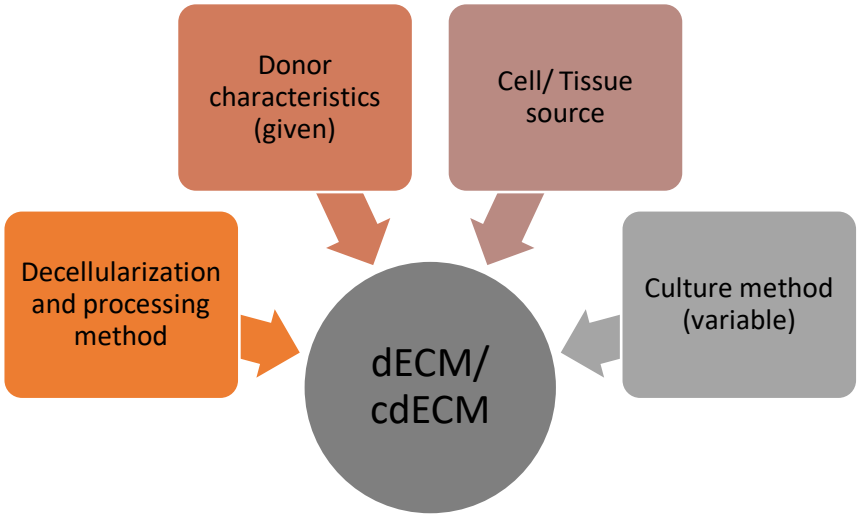

Figure 7: Parameters influencing the composition and characteristics of dECM and cdECM. Donor characteristics (e.g. age, health, sex) and cell/ tissue source are given parameters. Variable parameters include decellularization method (physical, chemical and/or mechanical) and processing methods. For cdECM the culture method (culture under hypoxia, media supplementation etc.) represents an additional variable parameter that can be used to adjust cdECM characteristics.

1.2.2 Cell-derived ECM

A promising alternative to dECM is the generation of cell-derived ECM (cdECM) by the *in vitro* culture of cells and subsequent removal of cellular structures from the secreted cdECM. This secreted cdECM exhibits a complex and specific biomolecule composition and can imitate the natural dECM of the cells in wide parts [85]. In contrast to dECM, cdECM did not exhibit the same physical characteristics and structural organization/ shape as the original tissue. To date different methods of cdECM production were used: The deposition of cdECM in 2D cell culture on planar surfaces [110], the deposition of cdECM in/ on 3D scaffold materials [111], and the generation of spheroids for 3D cdECM aggregates [112]. All of those methods hold their advantages that need to be balanced depending on the purpose of the generated cdECM. Several cell types (e.g. fibroblasts, bone marrow-derived mesenchymal stem cells (MSCs), adipose-derived stem cells (ASCs), endothelial cells (ECs)) were shown to deposit cdECM during cell culture that can be successfully isolated [110,113–115]. In **Figure 7** the parameters influencing the yielded cdECM are shown. For decellularization of cdECM mostly chemical decellularization using hypotonic solutions is chosen. These hypotonic solutions lead to the lysis of the cells and cellular debris can be washed out of the remaining cdECM. By the use of enzymes, critical components like DNA and RNA can be degraded and removed in subsequent steps. Compared to the other chemicals listed in 4.2.1, hypotonic solutions are gentler to the ECM molecules which might lead to a good preservation of sensitive ECM structures like sGAGs.

A major benefit of cdECM towards dECM is its tunability. Culture methods like mechanical or biochemical conditioning of the cells open up the possibilities for the production of a wide range of different cdECMs (**Figure 7**). For example, stem cells can be differentiated into specific lineages to generate cdECM from differentiated cells. Further, cdECM from cells cultured under different conditions e.g. hypoxia, different substrate stiffness, and different topographies, can be produced that exhibit different characteristics. Hypoxia was shown to improve the deposition of collagen [116,117] and substrate topography influences fiber alignment of secreted cdECM [118]. This allows cdECM to be tuned extensively for its intended purpose. The possibility to choose and/ or combine cell type(s) and cell source(s) leads to much higher variability of the generated cdECM compared to dECM. For example, combining two or more cell types to produce cdECM [119] it might be possible to yield a more physiological cdECM as in native tissue the ECM is also produced by several cells of the tissue. Using primary cells, the donor characteristics like age, sex, and health status also play an important role comparable to dECM generation. For example, it was shown that cells from younger donors mostly produce a “younger” ECM compared to cells from older donors. This “young” cdECM can rejuvenate “older” cells when cultured on the “young” ECM

[120]. Primary cells are more likely to produce a cdECM that exhibits the most native ECM composition whereas, cell lines might produce a cdECM with an altered composition. In specific applications also, the generation of cdECM from tumor cells might be interesting. Further applications of cdECM are its use as a cell culture substrate for the culture of sensitive cells like embryonic stem cells [85]. The possibility of cryoconservation of cells theoretically leads to high availability of cdECM as cells can be stored, thawed, and expanded when needed.

One of the drawbacks of cdECM as a biomaterial is the low amount that can be generated from standard cell culture and related costs of production. Several scale-up approaches are trying to solve this issue [121]. For example, the addition of ascorbic acid increases collagen secretion and matrix proteinase inhibitors have been shown to increase collagen content in isolated cdECM [122,123]. Macromolecules in culture medium were shown to enhance ECM deposition by a process called macromolecular crowding [124]. Further, targeted genetic alteration and the use of pharmaceutical small molecules were shown to be able to enhance ECM generation *in vitro* [121]. For all those approaches the possibility of alteration in cdECM composition and structure must be assumed and taken into consideration for the intended use of the cdECM. **Table 2** gives an overview of the advantages and disadvantages of dECM and cdECM.

Table 2: Advantages and disadvantages of Decellularized native ECM (dECM) and cell-derived ECM (cdECM)

	Advantages	**disadvantages**
dECM	Composition/ shape of the origin tissue High mechanical stability	Shortage of donor tissue Donor variations Higher immunogenicity
cdECM	Tunability Consistency Lower immunogenicity	Not native tissue composition/ structure Low mechanical stability Low yielded amount

1.3 Cell-derived extracellular matrix as a biomaterial for soft tissue engineering

Depending on body composition adipose tissue makes up to 25% [125]. Next to energy storage, temperature isolation, and mechanical protection, adipose tissue serves as an endocrine organ. Cells of the adipose tissue are known to secrete hormones like leptin, which is involved in energy homeostasis and cytokines, that modulate immune cells [126,127]. Under healthy conditions, it is a highly vascularized tissue [128]. The main cell type in adipose tissue are adipocytes [129]. They exhibit a vacuole filled with triglycerides that claim up to 95% of the volume of the cell. Adipocytes can reach a diameter of 200µm and are covered by a specialized BM [130]. While adipocytes are the most abundant cell type, a variety of additional cells types can be found in adipose tissue.
ASCs are the progenitor cells of adipocytes and are classified as MSCs. They can develop to mature adipocytes but were also shown to be able to differentiate into other cell types including chondrocytes, osteoblasts, and smooth muscle cells *in vitro* [131]. Microvascular endothelial cells (mvECs) form the capillaries that are found in high numbers in adipose tissue. They supply the cells with oxygen and nutrients and manage the removal of waste products of metabolism. MvECs exhibit a high level of cell-cell contacts that mainly consists of a protein known as PECAM-1 or CD31 [132]. Among others, additional cells that can be found in adipose tissue are macrophages as the immune component of the tissues, fibroblasts as the main producers of ECM, and perivascular cells that support the vascular structures [133,134].

1.3.1 Human adipose tissue-derived ECM

Compared to other tissues, like liver, heart, or bone, human adipose tissue is relatively good available and can be harvested with minimal invasiveness. In most cases, adipose tissue accrues as a waste product in cosmetic surgery or liposuction. Thus, human adipose tissue-derived ECM represents a biomaterial that is relatively good availably. Human sourcing reduces the concerns associated with immune reaction and xenogeneic disease transmission typically associated with the use of animal products. As adipose tissue exhibits a soft structure and a comparatively loose ECM it can be decellularized using relatively gentle protocols. To date, there is a wide range of approaches that use human adipose dECM as a scaffold material for soft tissue engineering [135–138]. In 2010 Flynn *et al*. described a method to decellularize adipose tissue and isolate large volumes of intact ECM with a well-preserved 3D structure [135]. They demonstrated that the yielded adipose tissue-derived dECM provided an inductive microenvironment for adipogenic differentiation of ASCs. These findings were confirmed by other studies [47,136,137,139,140]. To date, a variety of different decellularization protocols were described for human adipose tissue

[90,91,136]. The yielded adipose tissue dECM was used in a wide range of different types/ shapes of scaffold (e.g. sheets, microspheres, films, tubes, beads, and injectable gels). Human adipose dECM can be used in the hydrated stage or can be freeze-dried to achieve a porous scaffold material. By neutralization after pepsin treatment adipose dECM-hydrogels can be generated [141,142]. With the advent of 3D bioprinting, adipose dECM was further processed for the associated development of bioinks [84,138].

1.3.2 Human adipose stem cell derived ECM

Human ASCs can be isolated from adipose tissue with minimal invasiveness and can be expanded and differentiated into different lineages *in vitro* [143]. Comparable to the widely used fibroblasts, ASCs can secrete their cdECM during cell culture, which can be isolated using hypotonic solutions (see 4.2.2) [144]. One advantage of the use of ASCs for the generation of cdECM is the possibility to generate cdECM from different developmental stages. In their stem cell stage, ASCs secrete stem cell ECM (scdECM), and when differentiated cdECM from different mesenchymal tissues can be generated [145]. For example, also cdECM from tissues that are not available in high amounts (e.g. bone or cartilage) can be generated *in vitro*. Adipose cdECM (acdECM) was widely used in different tissue engineering and biomedical approaches and was demonstrated to be an inductive biomaterial. Several studies demonstrated the ability of ASC-derived cdECM to induce cellular differentiation of cells when cultured on the acdECM [85,114,146]. For example, acdECM induce adipogenic differentiation, cdECM from chondrogenic differentiated ASCs induce chondrogenic differentiation and cdECM from osteogenic differentiated ASCs induce osteogenic differentiation [145]. Adipose cdECM was also used in the designing of scaffolds for soft tissue engineering approaches. The deposition of cdECM from ASCs was used to decorate 3D scaffold materials to functionalize bioinert materials and make them bioactive by inducing adipogenic differentiation [147].

1.4 Metabolic Glycoengineering

Depending on the application it is useful to equip the ECM with specific chemical groups. These functional groups can be addressed via chemical reactions to, for example, link specific bioactive molecules to the ECM or to adjust the physical characteristics of the ECM by cross-linking. The possibilities that this functionalization brings with it are very diverse. As a chemical reaction for such functionalization of ECMs bioorthogonal reactions has proven themselves. These reactions have the advantage that they do not influence natural biological processes [148–150]. One prominent bioorthogonal reaction is the copper-catalyzed azide-alkyne cycloaddition (CuAAC). This reaction belongs to the so-called "*click*" reactions, which describe a type of highly selective reaction with high reaction efficiency, stereo- and regio-specificity, and high reactions yields [148,149,151,152]. Next to the unspecific functionalization of ECM using carbodiimide chemistry and the incorporation of unnatural amino acids (alkynyl methionine) into the cdECM, metabolic glycoengineering (MGE) represents a promising method to incorporate functional groups, like azido-groups, into the cdECM. Using MGE alterations of cdECM proteins and loss of functions, like it can be occurred by using carbodiimide chemistry can be prevented and no non-natural amino acids like the alkynyl methionine are used [153]. In contrast to the carbodiimide chemistry which can be used for all ECMs, incorporation of non-natural amino acids and MGE can only be used for the modification of cdECM. The modification of cdECM using MGE was first described by Ruff *et al*. in 2017 who incorporated azido-groups into the cdECM of human dermal fibroblasts [154]. During MGE chemically modified paracetylated monosaccharides are supplemented into the cell culture medium (paracetylated monosaccharides are membrane-permeable). The modified monosaccharides were metabolized by the cell and incorporated into the intracellular and extracellular sugar structures (e.g. glycans, proteoglycans, proteolipids) [155]. One big disadvantage of the use of CuAAC in biological systems is the cytotoxicity of copper ions that are needed as catalyst [148,149,151,152,156]. Bertozzi *et al.* developed a copper-free alternative, the strain-promoted alkyne-azide cycloaddition (SPAAC), which is based on strained cyclic alkynes as an alternative to terminal alkynes [157]. Their intrinsic energy leads to a chemical reaction and supersedes the use of a catalyst. Another alternative reaction that does not need any toxic catalyst is the inverse-electron-demand Diels-Alder reaction (IEDDA). This approach is based on the incorporation of dienophile modified monosaccharides into the ECM which undergo an IEDDA reaction with tetrazines. Different dienophiles were shown to be incorporated into the ECM using MGE including terminal alkenes [158–160], strained cyclic alkenes, such as cyclopropenes [161,162], bicyclononynes [163], and norbornenes [164]. As these groups have different reaction kinetics they can be used for sequential modification of the ECM with different tetrazines [165].

Further, it can be combined with the SPAAC reaction and photo click reaction enabling multiple labeling after the incorporation of differently modified monosaccharides [166].

1.5 Vascularization in tissue engineering

In vivo, the formation of new blood vessels is a strictly regulated and complex process named angiogenesis. As a response to hypoxic circumstances, several cells can secrete vascular endothelial growth factor (VEGF), which induces proliferation in endothelial cells and the adoption of a tip cell phenotype that can sprout and invade the surrounding BM. Stalk cells follow the tip cell and proliferate and lumenize the new sprout. During this process, platelet-derived growth factor (PDGF) is secreted to attract pericytes that support the new vessel structure. Among others, well-known pro-angiogenic factors initiating and supporting the formation of new blood vessels are basic fibroblast growth factor (bFGF), angiopoietins (Ang), and sphingosine-1-phosphate (S1P) [167,168].

In vitro vascularization remains one of the major bottlenecks in tissue engineering approaches. A vascular system is important to enabling an appropriate supply of oxygen and nutrients of the core cells and the removal of waste products. In most tissues, cells are found at a maximum distance of 200 µm from blood vessels – the diffusion limit of oxygen [169,170]. After implantation of tissue engineered constructs, the development of vascular(-like) structures by ECs can be observed in most cases. This is partly a response to a pro-inflammatory status that is induced by the surgical procedure. However, this spontaneous vascularization occurs mostly too slow to provide an adequate supply of the core cells of the construct within an adequate time frame [171,172]. Further, the incorporation of a vascular system would enormously enhance the physiology of tissue engineered *in vitro* testing systems. Therefore, different approaches aim to incorporate a vascular/supply system into tissue-engineered constructs. These include scaffold design [173,174] (including 3D (bio)printing of vascular structures [175]), inclusion of pro-angiogenic factors and co-culture of mvECs with “feeder cells” (that also secrete pro-angiogenic factors) to achieve *in vitro* (pre-)vascularization [172,176]. Next to a variety of synthetic materials several of the natural ECM proteins (e.g. collagen I [177,178] and fibrin [179,180]) are known to play a pivotal role in embryonic and pathological angiogenesis and were shown to induce vessel formation of mvECs *in vitro*. Also, natural ECM from native blood vessels was shown to induce angiogenesis [181,182]. Despite enormous progress has been made, to date, no adequate solution has been found for the inclusion of a functional vascular system into tissue-engineered constructs.

2 OBJECTIVE AND MOTIVATION

As the natural ECM represents the natural environment of cells and its well-known bioactivity and promising characteristics ECM – dECM and cdECM - is a popular biomaterial in tissue engineering and regenerative medicine approaches. The overall aim of this thesis is the detailed investigation of cdECM from ASCs regarding its use as a biomaterial for tissue engineering and regenerative medicine. In the first part, the cdECM from ASCs is systematically characterized and compared to the native adipose tissue-derived dECM to reveal compositional and structural differences of the two ECMs that have the potential to influence cellular behavior when used as a biomaterial. In the next step cdECM in its stem cell state and the adipogenic differentiated stage is investigated towards its capability to induce the formation of prevascular-like structures by mvECs. As the vascularization of tissue-engineered constructs remains an obstacle in tissue engineering this would highlight cdECM from ASCs as a promising biomaterial for vascularized tissue engineering. In the last part of this thesis, the modification of cdECM from ASCs with dienophile groups that are specifically addressable via cell-friendly inverse-electron demand Diels-Alder reaction is demonstrated, which opens up a wide range of applications of this cdECM by individual modification.

Against this background the following hypotheses were evaluated:

(H1) Native adipose tissue dECM and cdECM from adipose-derived stem cells differ in their macromolecular composition and structural features (addressed in **Paper I**)

(H2) The demonstrated differences between adipose tissue dECM and cdECM from adipose-derived stem cells can be assessed as relevant for its use as a biomaterial (discussed in **Paper I**)

(H3) Stem cell and adipogenic differentiated cdECM supports the formation of prevascular-like structures by microvascular endothelial cells (addressed in **Paper II**)

(H4) cdECM from adipose-derived stem cells can be functionalized via metabolic glycoengineering using different dienophile modified monosaccharides enabling the catalyst-free and cell-friendly modification via inverse-electron demand Diels-Alder reaction (addressed in **Paper III**)

3 PAPER I – CHARACTERIZATION AND COMPARISON

This chapter is originally published in the journal *Biotechnology and Bioengineering (DOI: 10.1002/bit.28047)* [2]. In this study native decellularized extracellular matrix (ECM) from adipose tissue and cell-derived ECM from adipose-derived stem cells (stem cell state and adipogenic differentiated) are systematically characterized and compared regarding protein content, macromolecular composition, and biological purity (**Figure 8**).

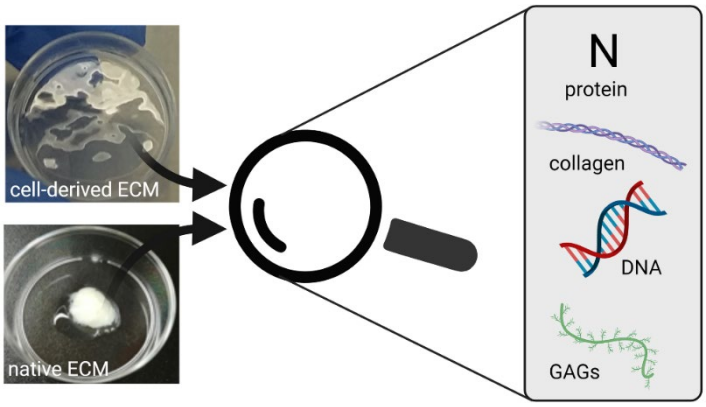

Figure 8: Graphical abstract Paper I (Cell-derived and enzyme-based decellularized extracellular matrix exhibit compositional and structural differences that are relevant for its use as a biomaterial)

Differences are shown in macromolecular composition, structural features, and biological purity. The dECM was found to exhibit higher levels of collagens and lower levels of sulfated glycosaminoglycans (sGAGs) compared to cdECMs. Further, structural characteristics revealed an immature state of the fibrous part of cdECM samples. These differences might be relevant for the cellular behavior of reseeded cells and affect the experimental outcome and should therefore be considered when choosing a biomaterial for a specific application or interpreting obtained results. Thus, within the framework of this study, the first hypothesis (H1) could be confirmed. In addition, the impact of the obtained results on cellular behavior is assessed (H2).

[2] Reprinted from *Cell-derived and enzyme-based decellularized extracellular matrix exhibit compositional and structural differences that are relevant for its use as a biomaterial*. Nellinger, S., Mrsic, I., Keller, S., Heine, S., Southan, A., Bach, M., Volz, A.-C., Chassé, T., & Kluger, P. J.; Biotechnology and Bioengineering, 2022, 1– 15. with permission from Wiley-VCH GmbH under CC-BY-NC 4.0

Cell-derived and enzyme-based decellularized extracellular matrix exhibit compositional and structural differences that are relevant for its use as a biomaterial

Svenja Nellinger[1], Ivana Mrsic[2], Silke Keller[3, 4], Simon Heine[1], Alexander Southan[5], Monika Bach[6], Ann-Cathrin Volz[1], Thomas Chassé[2], Petra J. Kluger[7]*

[1] *Reutlingen Research Institute, Reutlingen University, Reutlingen, Germany*

[2] *Institute of Physical and Theoretical Chemistry, Eberhard Karls University Tübingen, Tübingen, Germany*

[3] *3R-Center for In Vitro Models and Alternatives to Animal Testing, Eberhard Karls University Tübingen, Tübingen, Germany*

[4] *Department for Microphysiological Systems, Institute of Biomedical Engineering, Faculty of Medicine of the Eberhard Karls University Tübingen, Tübingen, Germany*

[5] *Institute of Interfacial Process Engineering and Plasma Technology, University of Stuttgart, Stuttgart, Germany*

[6] *Biomedicine and Materials Sciences, Natural and Medical Sciences Institute at the University of Tübingen, Reutlingen, Germany*

[7] *School of Applied Chemistry, Reutlingen University, Reutlingen, Germany*

Keywords:
adipose-derived stem cells, biomaterial, cell-derived matrix, decellularization, extracellular matrix

Abstract

Due to its availability and minimal invasive harvesting human adipose tissue-derived extracellular matrix (dECM) is often used as a biomaterial in various tissue engineering and healthcare applications. Next to dECM, cell-derived ECM (cdECM) can be generated by and isolated from in vitro cultured cells. So far both types of ECM were investigated extensively towards their application as (bio)material in tissue engineering and healthcare. However, a systematic characterization and comparison of soft tissue dECM and cdECM is still missing. In this study, we characterized dECM from human adipose tissue, as well as cdECM from human adipose-derived stem cells (ASCs), towards their molecular composition, structural characteristics, and biological purity. The dECM was found to exhibit higher levels of collagens and lower levels of sulfated glycosaminoglycans (sGAGs) compared to cdECMs. Structural characteristics revealed an immature state of the fibrous part of cdECM samples. By the identified differences, we aim to support researchers in the selection of a suitable ECM-based biomaterial for their specific application and the interpretation of obtained results.

Introduction

For healthcare applications (e.g. tissue-engineered implants, innovative wound dressing, coating of devices, or bioinks for bioprinting approaches) good biocompatibility of a biomaterial is a necessity. The next level in the performance of a biomaterial is its bioactivity, which enables the materials to support and enhance regeneration or cell ingrowth. One very promising material with bioactive characteristics is the harvested extracellular matrix (ECM). The ECM represents the natural environment of cells. It is a fibrous network of proteins, proteoglycans, and glycosaminoglycans (GAGs), arranged in a highly tissue-specific manner and is produced and secreted by the resident cells (Frantz et al., 2010; Mecham, 2012; Theocharis et al., 2016). This results in the establishment of specialized local microenvironments, which contribute to the differentiation and maintenance of tissue-specific cellular phenotypes and functions. Cells recognize the chemical and mechanical cues provided by ECM via membrane receptors (e.g. integrins) that trigger intracellular signaling cascades resulting in the expression of genes that regulate cellular survival, proliferation, migration, differentiation, and apoptosis (Daley & Yamada, 2013). Reciprocally, resident cells are rebuilding and remodeling the surrounding ECM by biochemical modification (e.g. cross-linking), degradation, and reassembly (P. Lu et al., 2011). Furthermore, bioactive molecules derived from cells can be stored in and released from the ECM when necessary (Brizzi et al., 2012). These processes are tightly regulated during tissue

development, homeostasis, and aging as well as in response to injury (Frantz et al., 2010; Miller et al., 2020; Rousselle et al., 2019).

Great efforts were made to develop synthetic biomaterials mimicking native ECM. However, given the complexity of ECM and the incomplete understanding of its composition and structure, fabricating materials that fully mimic the structure and composition of native ECM is very challenging. One successful method to obtain tissue-specific ECM, besides the de novo generation, is the decellularization of organs or tissues. A variety of different decellularization strategies have been usually described involving a combination of physical, chemical, and enzymatic treatments. Every decellularization method invariably disrupts the ECM to some degree (Thomas-Porch et al., 2018). However, dECM has been extensively used as a substrate for in vitro cell culture systems to maintain tissue-specific cellular phenotypes and modulate cell proliferation and differentiation (Pati et al., 2014). In addition, dECM was used as a scaffold material for tissue models, which can serve as an alternative to animal testing of drugs and chemicals and as an in vitro model for the investigation of disease development and respective therapy approaches. In the context of the emerging field of three-dimensional (3D) bioprinting, dECM was also investigated as a component for bioinks (Kim et al., 2018; Pati et al., 2015; Tan et al., 2017; Turner et al., 2012).

For several years, an alternative method for the generation of tissue-specific ECM has moved into the focus of researchers: cell-derived ECM (cdECM). Cells produce ECM in vitro, which can be isolated by decellularization. Thus, cells from different tissue sources can be used to generate (autologous) tissue-specific ECM. Moreover, ECM characteristics can be modulated and ECM can be generated and maintained in a pathogen-free environment (Hussey et al., 2018; H. Lu et al., 2011). In addition, cdECM can be customized by controlling cell culture conditions like oxygen concentration, mechanical preconditioning, or specific chemical modification using metabolic glycoengineering (MGE - modification of GAGs with functional chemical groups using the natural cellular metabolism and subsequent modification with specific molecules like growth factors or enzymes) (Fitzpatrick & McDevitt, 2015; Keller, Wörgötter, et al., 2020; Ruff et al., 2017). CdECM from different tissues and developmental stages thereof can be generated by selecting specific cell types. For example, such a cdECM can be obtained by the use of e.g. mesenchymal stem cells (MSCs). These show several advantages, including high availability, functional plasticity, and low immunogenicity (C. Brown et al., 2019). Among the various sources of MSCs, adipose-derived stem cells (ASCs) represent a promising cell source for the generation of cdECM. Compared to bone marrow-derived MSCs, they can be easily obtained from adipose tissue in large quantities with little patient discomfort. Further, they exhibit a comparable differentiation potential into cells of mesodermal origin (adipogenic, osteogenic, and chondrogenic lineage) (Si et al., 2019). CdECM

was investigated in a range of studies towards its influencing potential on cells and its prospective use as a biomaterial (V. Guneta et al., 2018). Spontaneous differentiation and subsequent loss of stem cell pheno- and genotype represent a major issue in stem cell culture. Stem cell ECM exhibits the promising potential to maintain stem cells in vitro by providing a stem cell-typical environment (stem cell niche) that may prevent these spontaneous differentiation events (Agmon & Christman, 2016; Novoseletskaya et al., 2019).

Both ECM sources – dECM from native adipose tissue and cdECM from cultured ASCs – are applied in healthcare biomaterial research extensively (Abaci & Guvendiren, 2020; Chiang et al., 2021; Fitzpatrick & McDevitt, 2015; Flynn, 2010; Pati et al., 2015; Rossi et al., 2018; Wolf et al., 2012). The dECM is mainly used to generate 3D tissue constructs for in vitro as well as in vivo applications (Flynn, 2010; Pati et al., 2014, 2015), whereas cdECM is particularly used for the coating of different biomaterials to enhance bioactivity or as 2D sheets (Vipra Guneta et al., 2016; Magnan et al., 2018; Rossi et al., 2018). Reviews are comparing the dECM and cdECM from different tissues (Sun et al., 2018; Sutherland et al., 2015; Xing et al., 2020). However, studies characterizing and directly comparing the composition of the ECM of different sources (native and cell-derived) and the impact on cellular behavior are missing so far. As it is well known that macromolecular, structural, and chemical features are responsible for the performance of a biomaterial, these characteristics will have to be taken into consideration when choosing the ideal biomaterial for a specific application.

In this study, dECM from native adipose tissue, as well as in vitro-generated cdECM (both stem cell ECM (scdECM) and adipogenic ECM (acdECM)) were characterized and compared systematically. The different ECMs were investigated in terms of their elementary and macromolecular composition, their structural characteristic and their biological purity after processing (Figure 1). With this innovative approach, we compared the ECM of both sources directly and evaluated their potential as biomaterials for tissue engineering approaches.

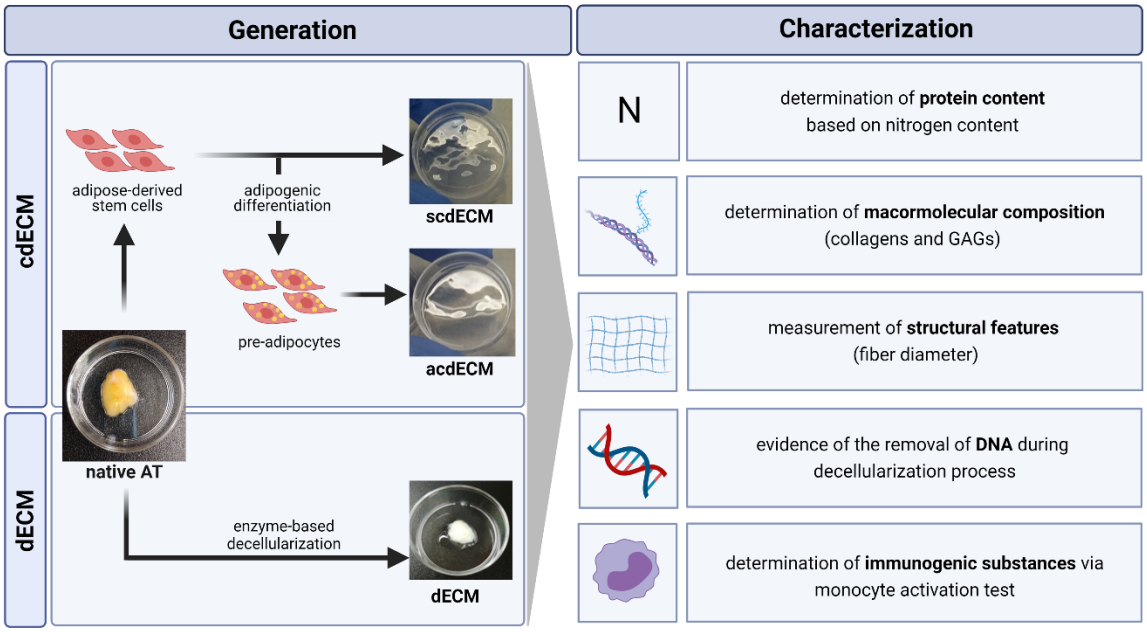

Figure 1: Schematic overview of the study and the performed analyses. Decellularized native extracellular matrix (dECM) was generated by enzyme-based decellularization of human native adipose tissue (AT) from human biopsies. For the generation of cell-derived ECM (cdECM), adipose-derived stem cells (ASCs) were isolated from native AT biopsies and expanded to yield an adequate cell number. Subsequently, ASCs were seeded into cell culture polystyrene dishes for the generation of cdECM and either cultured with growth medium (for generation of stem cell-derived ECM (scdECM)) or adipogenic differentiation medium (for generation of adipogenic cell-derived ECM (acdECM)). CdECM was harvested on day 7 and day 14 of cell culture. DECM and cdECM samples were analyzed for their elementary and macromolecular composition, their structural characteristics and the remaining DNA content (Diameter (d) petri dish: 35 mm). Created with BioRender.com.

Materials and Methods

All research was carried out in accordance with the rules for the investigation of human subjects as defined in the Declaration of Helsinki. Patients provided written agreement in compliance with the Landesärztekammer Baden-Württemberg (F-2012- 078, for normal skin from elective surgeries).

Decellularization of adipose tissue

Adipose tissue samples were obtained from patients undergoing plastic surgery (Dr. Ziegler; Klinik Charlottenhaus, Stuttgart, Germany). For their transport, tissue samples were transferred in phosphate-buffered saline with calcium and magnesium ions (PBS+) and were stored for a maximum of 24 h at 4°C. Decellularization was performed according to the detergent-free enzyme-based protocol published by Flynn et.al. (Flynn, 2010). Briefly, tissue samples were cut into pieces ranging from masses between 20 g and 25 g. After three freeze-thaw cycles in hypotonic tris buffer (10 mM tris base and 5 M methylenediaminetetraacetic acid (EDTA); pH 8.0) samples were incubated in enzymatic digestion solution 1 (0.25 % trypsin/ 0.1 % EDTA) overnight,

followed by an isopropanol (99.9 %) treatment for 48 h to remove lipids. Next, samples were washed three times in washing buffer (8 g/L NaCl, 200 mg/L KCl, 1 g/L Na2HPO4, and 200 mg/L KH2PO4; pH 8.0) and again treated with enzymatic digestion solution 1 for another 6 h. Subsequently, samples were washed three times and treated with enzymatic digestion solution 2 (55 mM Na2HPO4, 17 mM KH2PO4, 4.9 mM MgSO4·7H2O, 15,000 U DNase type II (from bovine pancreas), and 2000 U lipase type VI-S (from porcine pancreas)). Afterward, extraction of lipids was done by incubating the samples in isopropanol (99.9 %) for 16 h at RT. Last, samples were washed three times and stored in sterile PBS- at 4°C. All solutions were supplemented with 1 % penicillin/ streptomycin (P/S).

Generation of cell-derived extracellular matrix

ASCs were isolated from human adipose tissue samples as described before.(Volz et al., 2017) ASCs were initially seeded at a density of 5 x 103 cells/cm2 in a serum-free MSC growth medium (MSCGM; PELOBiotech, containing 5 % human platelet lysate and 1 % P/S).

For the generation of cell-derived ECM, ASCs were seeded into petri dishes (d=14.5 cm) at a density of 2.5 x 104 cells/cm2 in MSCGM. At confluence, medium was changed to adipogenic differentiation medium (Dulbecco's Modified Eagle Medium (DMEM) with 10 % FCS, 1 µg/mL insulin, 1 µg/mL dexamethasone, 100 µM indomethacin, 500 µM 3-isobutyl-1- methylxanthine, and 50 µg/mL sodium ascorbate) or growth medium (DMEM with 10 % FCS and 50 µg/mL sodium ascorbate). Conditioned medium exchange (half of the medium was removed and replaced with fresh medium) was performed every second day for the approaches in adipogenic differentiation medium and complete medium exchange was performed every second day for the approaches in growth medium. On days 7 and 14 cells were lysed using hypotonic 4 mM ammonium hydroxide solution and isolated cdECM was washed three times with ultrapure water (modified after [21]). All media were supplemented with 1 % P/S. ASCs were used up to passage three.

As the water content in freshly isolated cdECM is high, cdECM was concentrated using ultracentrifugation tubes (Amicon® Ultra Filter, Merck, Germany) with a molecular weight cut-off of 10 kDa.(Keller, Wörgötter, et al., 2020) To achieve a homogeneous ECM solution for quantitative assays, concentrated cdECM was recovered and homogenized using lysis tubes (Lysing Matrix Z; MP Biomedicals™, Germany) and the homogenizer FastPrep-24™ 5G (MP Biomedicals™, Germany) (Keller, Wörgötter, et al., 2020). Homogenization was performed in three cycles with 60 s of lysing and a 1 min break. Keller et al. previously demonstrated that biological activity of the ECM is maintained during concentration and homogenization of cdECM (Keller, Wörgötter, et al., 2020). The dry weight of cdECM samples was determined by freeze-drying.

Elementary analysis and X-ray photoelectron spectroscopy measurement

ECM samples were lyophilized and a minimum of 10mg of ECM sample (dry weight) was used for the analysis following DIN EN ISO 16948 after dry combustion. Samples were burned in the oxygen stream at 900 °C. During oxidative combustion, molecular nitrogen and the oxidation products CO2, H2O, NO, NO2, SO2, and SO3 were formed from the elements C, N, and S. The resulting gas mixture was cleaned and separated into its components. The nitrogen oxides were quantitatively reduced to molecular N2 at the copper contact in the reduction tube and then determined relatively with an accuracy of up to ± 0.1 % using a thermal conductivity detector (Vario El Cube, Elementar Analysensysteme GmbH, Germany). Total protein content was estimated based on the percentage nitrogen content determined by elementary analysis multiplied with the conversion range for connective tissue recommended by Keller et al (Keller, Liedek, et al., 2020).

$$\text{Total protein [\%]} = \text{nitrogen content} \times 5.25 < \text{total protein} < \text{nitrogen content} \times 5.88 \quad (1)$$

For X-ray photoelectron spectroscopy (XPS) analysis, concentrated cdECM and dECM samples were homogenized and 100 µL of the ECM suspension was dried at room temperature onto a silicon wafer (1 cm x 1 cm). The samples were measured with XPS using a multi-chamber ultrahigh vacuum system, with a base pressure of 8 × 10-10 mbar. The system was equipped with a Phoibos 100 analyzer and a 1d- delay line detector (SPECS, Germany). Al-Kα radiation of an Al/Mg anode (XR-50 m X-ray source, hν = 1486.6 eV) was used for the measurements. The survey spectra were collected with the following parameters: 50 eV pass energy, 0.2 s dwell time and 0.5 eV step width. The spectral analysis was done in the software Unifit version 2018 (Unifit scientific software GmbH, Germany) (Hesse et al., 2004). The atomic composition was obtained from the atomic percentages, calculated with Wagner sensitivity factors (Wagner, 1983) after Shirley background subtraction. The spectra were [0.1] normalized to maximum peak height. Charge correction was done by shifting the C 1s peak to 285.0 eV.

Histological staining

For histological staining, dECM samples were directly fixed with 4 % paraformaldehyde (10 min per 1 mm diameter of the sample; Roti Histofix; Carl Roth, Germany), cdECM samples were concentrated and afterward the yielded dense three-dimensional cdECM construct was fixed with 4 % paraformaldehyde. Fixed samples were dehydrated with ascending alcohol solutions and embedded in paraffin. Histological sections (5 µm) were produced using a microtome (Autocut

1140, Reichert-Jung, Germany). After deparaffinization and rehydration by descending alcohol solutions of histological sections, histological staining (Alcian blue PAS for the staining of proteoglycans and basal membrane and MOVAT pentachrome for the staining of elastic fibers and collagens) were performed according to the manufacturer's protocols (Morphisto GmbH, Germany). Images were taken with an Axio Observer microscope and an Axiocam 305 color using the software ZENblue (Carl Zeiss, Germany).

Hydroxyproline and sGAG assay

To determine the total collagen content of ECM samples, HP assay was performed based on Keller et al. (Keller, Liedek, et al., 2020) and Capella-Monsonis et al..(Capella-Monsonís et al., 2018) Briefly, lyophilized ECM samples were hydrolyzed overnight in concentrated hydrochloric acid at 110 °C. To remove the insoluble carbohydrate fraction, samples were centrifuged at 15.000 g for 10 min. The following solutions were prepared: HP standard solutions (0 µg/mL, 1 µg/mL, 2.5 µg/mL, 5 µg/mL, 10 µg/mL, 20 µg/mL); diluent (isopropanol/ water, 1:1); chloramine T reagent (0.2625 g chloramine T diluted in 18.75 mL), citrate buffer (17.19 g sodium acetate, 18.75 g tri-sodium citrate-dihydrate, 2.75 g citric acid diluted in 200 mL ultrapure water which afterwards was mixed with 200 mL isopropanol and brought to a final volume of 500 mL with ultrapure water); Ehrlich's reagent (2 g 4-(dimethylamino)benzaldehyde (p-DMAB) diluted with 3 mL 70 % perchloric acid (HClO4) and mixed with 16.7 mL isopropanol).

110 µL of samples and standard were mixed with 254 µL diluent and 176 µL chloramine T reagent, citrate buffer, and incubated at RT for 10 min. 460 µL of Ehrlich's reagent was added and incubated at 70 °C for 10 min. 200 µL of samples and standards were transferred in a transparent 96-well plate and absorbance was measured at 555 nm (Tecan Safire 2, Tecan Trading AG, Switzerland). Reagent blank was subtracted from the measured values. HP content was calculated from the standard curve and the conversation range for connective tissue recommended by Keller et al. (Keller, Liedek, et al., 2020). Collagen content was given in % of dry weight and calculated using the equation:

$$\text{collagen content [\%]} = \text{HP content} / 0.0135 < \text{collagen content} < \text{HP content} / 0.0180 \quad (2)$$

To determine the content of sulfated glycosaminoglycans (sGAGs), lyophilized ECM samples were used for the sGAG assay according to the manufacturer's protocol (Blyscan™ Assay, Biolcolor Ltd., UK). Briefly, 5 mg of lyophilized samples were digested with 1 mL papain solution (0.2 M Na2HPO4

· 2H2O, pH6.4, 0.4 % EDTA, 0.08 % cysteine HCl, 0.8 % NaCH3COO-, 0.5 % papain solution, Sigma-Aldrich) at 65 °C overnight. Subsequently, samples were centrifuged at 10,000 g for 10 min and the supernatant was used for the assay, which was performed according to the manufacturer's instructions. Absorbance was measured at 656 nm (Tecan Safire 2, Tecan Trading AG, Switzerland).

Immunofluorescence staining

For immunofluorescence staining of ECM-specific proteins (collagen type IV and laminins), histological sections were produced according to 2.4. Deparaffinized and rehydrated sections were heat-unmasked in target retrieval buffer (pH 9.0) for 20 min in a steam cooker to unveil epitopes. Unspecific binding sites were blocked with blocking solution (3 % bovine serum albumin in PBS-) for 1 h at RT. Primary antibodies (rabbit-anti-Col IV (1:200); mouse-anti-fibronectin (1:200); rabbit-anti-Col I (1:200); rabbit-anti-laminin (1:200)) were diluted in blocking solution and incubated for 1 h at RT. Samples were washed with washing buffer (0.1 % Tween-20 in PBS-) followed by incubation with the secondary antibodies (goat-anti-rabbit-AlexaFluor® 488 (1:250); goat-anti-mouse-Cy 3 (1:250), diluted in blocking solution) for 30 min at RT. A secondary antibody control was carried along to ensure the specificity of the antibodies. Images were taken with an Axio Observer microscope and Axiocam305 color using the software ZENblue (Carl Zeiss, Germany).

Scanning-Electron-Microscopic (SEM) analysis

Samples were fixed with 2 % glutaraldehyde for 45 min at RT and dehydrated with increasing alcohol concentration followed by treatment with hexadimethylsiloxane. After incubation, samples were air-dried at RT. Samples were sputtered with platinum (Argon, 0.05 mbar, 50 s, 65 mm distance, 40 mA/470 V, 17 °C; SCD 050, Balzers, Germany). SEM images were taken using a Hitachi SU8030 (Hitachi, Japan). The images were acquired using secondary electrons (SE) with an upper detector (U), 1.0 kV acceleration voltage of the electron beam, and a magnification of ×50.0 k.

Degree of swelling: To determine the degree of swelling, lyophilized ECM samples were weighed (=dry weight). After incubation, in deionized water for 24 h, samples were weighed again (=wet weight) and the degree of swelling was calculated with the equation:

$$\text{Degree of swelling [\%]} = (\text{wet weight} - \text{dry weight})/(\text{dry weight}) \times 100 \quad (3)$$

DNA quantification

Homogenized ECM samples were treated with 1500 U/mL DNase (DNase I from bovine pancreas, Roche, Germany) at 37°C overnight. The remaining DNA in untreated and treated ECM samples was isolated by the DNA extraction kit for tissue samples (GeneOn GmbH, Germany). For qualitative assessment of the DNA content, hematoxylin and eosin staining, as well as 4,6-diamidino-2-phenylindole (DAPI) staining of sections prepared according to 2.4, was performed. Photometric quantification of the DNA content per mg dry weight in ECM samples was performed using a picogreen staining (Pico488, Lumiprobe GmbH, Germany) according to the manufacturer's instructions. As a standard for double-stranded DNA (dsDNA), lambda-DNA (fisher scientific GmbH, Germany) was used.

Statistics

Elementary analysis and qualitative experiments (staining and SEM) were performed once with samples from three different biological donors (n=3). All other quantitative experiments were performed three times, using samples from three different biological donors (n=9). Data were analyzed by one-way analysis of variance (ANOVA) with a Bonferroni posthoc test using Origin 2018b. Statistical significances were stated as $p < 0.05$ (*), very significant as $p < 0.01$ (**), and highly significant as $p < 0.001$ (***).

Results and Discussion

Quantification of total protein content

In a study comparing widely used bioanalytical methods for the characterization of ECM materials, Keller et al. demonstrated that colorimetric assays are not suitable for the determination of the total protein content of ECM materials. Instead, the estimation of total protein based on total nitrogen content provided the most reliable results (Keller, Liedek, et al., 2020). In this study, elementary and XPS analyses were performed for the estimation of the total protein content of dECM, acdECM, and scdECM as a bulk material and as a coating. By elementary analysis, the mass fraction of nitrogen (N) of the bulk material was determined (Table 1). From the relative amount of nitrogen, the amount of protein in the individual samples could be estimated using equation (1) according to Keller et al.(Keller, Liedek, et al., 2020) In their study, Keller et al. demonstrated that one specific conversion factor derived from the composition of only one ECM protein component is not sufficient to describe the complex composition of ECM. Thus, they recommended stating the protein content in a tissue-specific range. The used range includes the conversion factors for collagen type I (5.25), collagen type III (5.31), collagen type IV (5.69 (α1)),

fibronectin (5.88), and laminins (5.66). It was shown that the conversion factors for native connective tissue also lie within this range.(Keller, Liedek, et al., 2020) In this study, the calculated range of protein content for dECM was found to be 42.6 (±19.2) % – 47.7 (±21.5) % and lied between the ranges of acdECM with 36.9 (±7.5) % - 41.3 (±8.4) % and scdECM with 52.3 (±0.9) % - 58.6 (±1.0) %. As expected, the calculated protein content of scdECM is comparable to the results of Keller et al. who obtained a protein content of 53 (±4) % - 59 (±4) % in ECM derived from human dermal fibroblasts. For dECM and acdECM d14 slightly lower amounts of nitrogen and consequently protein content were measured. At the same time, measured nitrogen content in dECM showed a higher variance. The higher standard deviations may indicate impurities in the dECM and acdECM samples or may highlight high donor-dependent variations in the composition of the ECMs caused by differences in the expression profile during adipogenic differentiation (Gregoire et al., 1998). However, to date, we have no conclusive explanation for this phenomenon. XPS analysis was performed to analyze the elementary composition of ECM coatings. XPS is a surface-sensitive method with an information depth of 7 – 9 nm. The atomic percentages calculated from the XPS spectra are essentially the elementary composition of the ECM surface layers. In Table 1 the results of the XPS analysis are shown. Results indicate that there is no difference in the total protein content within the ECM samples. Complete results of XPS analysis including carbon percentages and results of cdECM from day 7 are shown in supplementary figure 1. The XPS analysis generally showed lower amounts of protein content. As shown in supplementary figure 1 the carbon percentage is comparable in all samples. Thus the lower nitrogen/ protein content measured in the XPS analysis compared to the results of the elementary analysis can be explained by atmospheric contaminations of e.g. carbon containing compounds (Graubner et al., 2004; Mrsic et al., 2021). These contaminations are caused by the adsorption of molecules from the surrounding atmosphere onto the samples during preparation. As XPS is a surface-sensitive method, these contaminations lead to a reduced detection of other elements, like nitrogen. This may result in an underestimation of their elemental contents as observed in our case. The joint consideration of the nitrogen/protein quantification results from both methods leads to the expectation that there are no appreciable differences in protein content between the ECM samples. However, further studies should investigate this more comprehensively. Further methods like quantification of amino acids or mass spectrometry might help to get more consistent results.

Table 1: Protein content of dECM and cdECM samples. Elementary analysis: ECM samples were lyophilized and elementary analysis was performed using the bulk material. XPS analysis: Concentrated and homogenized ECM samples were dried onto silicon wafers and the coating was analyzed by XPS. From the determined percentage of nitrogen, the percentage of protein content was calculated using the equation (1) (n=3).

	Elementary analysis		**XPS analysis**	
	N [%]	**calc. protein content [%]**	**N [%]**	**calc. protein content [%]**
dECM	8.1 (±3.7)	42.6 (±19.2) – 47.7 (±21.5)	5.0 (±0.2)	26.1 (±0.8) – 29.2 (±0.9)
acdECM	7.0 (±1.4)	36.9 (±7.5) – 41.3 (±8.4)	5.1 (±1.0)	27.0 (±5.4) – 30.2 (±6.0)
scdECM	9.9 (±0.2)	52.3 (±0.9) – 58.6 (±1.0)	4.3 (±0.7)	22.8 (±3.8) – 25.5 (±4.3)

Macromolecular composition

In addition to the elementary analysis of ECM samples, their macromolecular composition was determined. To detect possible changes in composition during growth and adipogenic differentiation of cdECM, additional samples from day 7 were examined. To get an impression of the macromolecular composition of ECM samples, histological staining was performed. For histological characterization of important extracellular structures, Alcian blue PAS and MOVAT pentachrome staining were done (Figure 2,A). By Alcian blue PAS, proteoglycans are stained in blue and the basal membrane is stained in purple. The basal membrane is an extracellular matrix structure that separates epithelial or endothelial tissues from the underlying stroma (Randles et al., 2017). It can further be found around adipocytes in mature AT (Pierleoni et al., 1998). DECM exhibited large parts of the preserved basal membrane (purple). No basal membrane, but high amounts of proteoglycans (blue) was found in cdECM samples. Based on the histological staining it can be presumed that there is no difference in proteoglycan composition and distribution between the different cdECM samples. By MOVAT pentachrome staining, ground substance (non-fibrous components like proteoglycans and glycosaminoglycans (green)), collagens (yellow), and elastic fibers (black) were stained. A high amount of ground substance and collagens was found in dECM. Furthermore, elastic fibers were observed in dECM samples. In all cdECM samples, high amounts of ground substance but no elastic fibers were found. The absence of elastic fibers in cdECMs leads to the assumption that these cdECMs exhibit an immature state of development. This can be explained by several studies which have shown before that in the absence of mechanical stimuli elastin synthesis and formation of elastic fibers are lower in vitro (Eoh et al., 2017; Hinderer et al., 2015). Overview staining with hematoxylin and eosin (HE) and a picrosirius

staining (for the visualization of the homogenous distribution of collagens in all samples) is shown in supplementary figure 2.

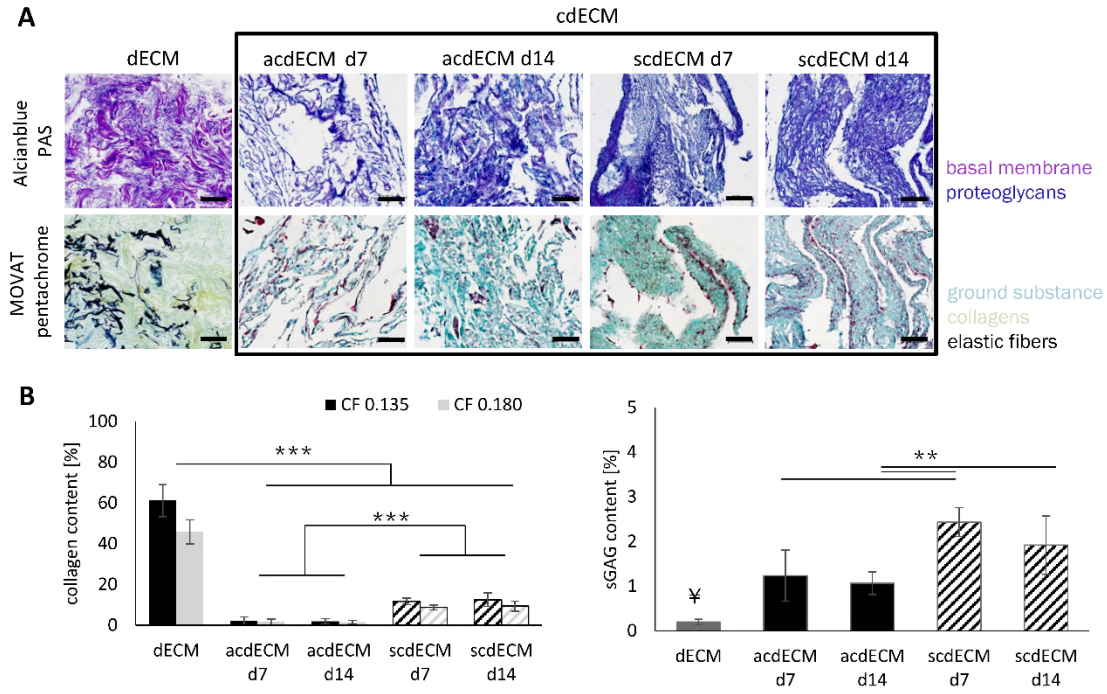

Figure 2: Macromolecular composition of ECM samples. A: Histological staining: Alcian blue PAS and MOVAT Pentachrome staining were performed on histological sections of dECM, acdECM, and scdECM samples. Alcian blue PAS staining: proteoglycans (blue) and basal membrane (purple). MOVAT Pentachrome staining: ground substance (green), collagen (yellow) and elastic fibers (black) (Scale bars: 100µm; n=3) B: Quantification of collagens and sGAGs: Collagen content in ECM samples was determined via HP assay and was normalized to the dry weight (DW) of the sample (CF = conversion factor). The amount of sGAGs was determined by a colorimetric sGAG assay and normalized to the DW. (** $p \leq 0.01$; *** $p \leq 0.001$; ¥ $p \leq 0.001$ to all other samples; n=9)

In the next step, the two main components of ECM – collagens and sGAGs– were quantified (Figure 2,B). Results were normalized to the dry weight (DW) of the samples and given in percent. For quantification of collagen content, a hydroxyproline (HP) assay was performed and collagen content was calculated based on this assay. The amino acid HP is mainly contained in collagens and only to a limited amount in elastin (Capella-Monsonís et al., 2018). Thus, the HP content can be used for the quantification of collagens. For the calculation, the conversion range from 0.135 to 0.180 was used, based on the findings of Keller et al. The used conversion range includes the conversion factors for collagen type I (0.135) and collagen type III (0.180). The conversion factors for native connective tissue lie also within this range (Keller, Liedek, et al., 2020). Results indicated a significantly higher amount of collagens in dECM (45.9 (±5.9) % – 61.2 (±7.9) %) compared to all cdECM samples. Within the cdECM approaches, significantly higher collagen content was found in

scdECM samples (scdECM d7: 8.8 (±1.2) % – 11.8 (±1.6) %), scdECM d14: 9.4 (±2.5) % – 12.6 (±3.3) %) compared to the acdECM samples (acdECM d7: 1.6 (±1.5) % – 2.1 (±2.0) %, acdECM d14: 1.5 (±0.9) % – 2.0 (±1.2) %). These results are in line with the MOVAT pentachrome staining (collagens stained in yellow) with the most intense staining in dECM. The amount of collagens in scdECM samples found in this study are in the same order of magnitude as the values shown by Keller et al. with 12 – 16 % in cdECM from juvenile human skin fibroblasts (Keller, Liedek, et al., 2020). Interestingly, the HP assay revealed the highest collagen content to be present in dECM and the lowest collagen content in acdECMs. One reason why we observed higher collagen content in dECM might be the presence of elastic fibers, which were only found in dECM (see histological staining) and which contain little amounts of HP. However, that does not explain the enormous differences between dECM and cdECM samples. A further explanation might be the maturing/culture period. The dECM has grown over several years, whereas the cdECM was generated in only 7 to 14 days in vitro. During collagen synthesis, tropocollagen is secreted by the cells and assembled extracellularly to form mature collagen fibers (Myllyharju & Kivirikko, 2004). In native tissue, collagen fibers are completely polymerized and may be preserved during decellularization. In cell culture, the tropocollagen is partly released into the cell culture medium or loosely attached to the cell surrounding and may get lost during medium exchange and decellularization (Shendi et al., 2019). The differences in collagen content between acdECM and scdECM samples could be explained by alterations in protein expression during adipogenic differentiation. The relative concentrations of collagen type I and collagen type III decline by 80 – 90 % during adipogenic differentiation and the secretion of collagen type IV and the glycoprotein nidogen increases (Aratani & Kitagawa, 1988; Gregoire et al., 1998). As the interactions of cells and ECM proteins play a pivotal role in cellular development and behavior, these differences should be considered when choosing a material for a specific application.

Quantification of sGAGs revealed a significantly lower amount in dECM (0.20 (±0.06) %) compared to all cdECM approaches. Within the cdECM approaches, scdECM d7 (2.43 (±0.32) %) exhibited a significantly higher amount of sGAGs compared to both acdECM approaches (acdECM d7: 1.24 (±0.57) %, acdECM d14: 1.07 (±0.25) %). Further, the sGAG content of scdECM d14 (1.92 (±0.65) %) was significantly higher compared to acdECM d14. As it is well known that sGAGs have a positive impact on cellular behavior regarding regenerative capacity and angiogenesis/ neo-vascularization, which remains a major obstacle in tissue engineering (Köwitsch et al., 2018; Salbach et al., 2012), ECMs containing higher amounts of sGAGs, which are on top preserved during decellularization would be favorable. The noticeable low amount of sGAG in dECM could be explained by the harsh decellularization method used for native tissue. GAGs are known to be

very sensitive to a variety of agents used in decellularization protocols (B. N. Brown et al., 2011; Crapo et al., 2011). The reported amount of preserved sGAGs in dECM from human adipose tissue ranges from 0.05 % up to 0.4 % (Song et al., 2018; L. Wang et al., 2013; Young et al., 2011). Reported sGAG content in different native human tissues range from 0.3 % to 0.7 % (Eckert et al., 2013; Johnson et al., 2014; Wei et al., 2005). This indicates a loss of sGAGs during decellularization of up to 70% in our study. However, the high amount of lipids within AT seems to interfere with the reliable determination of sGAGs in native AT. The available data about the sGAG content in native AT and on the reduction of sGAGs during decellularization of native AT is rare and varies extremely. Song et al. found no significant reduction of sGAGs after decellularization (Song et al., 2018), whereas Pati et al. described a reduction of about 60 % (Pati et al., 2014). In general, the usually performed normalization of the values to the dry weight leads to questionable comparability of native and decellularized tissue, since the removal of cellular components leads to distorted values. In this study, we found that cdECM represents a promising alternative to dECM, as the amount of sGAGs is up to 12-fold higher in scdECM from day 7 compared to dECM. Previously, Schenke-Layland et al. found 3.1 % of sGAGs in non-decellularized fibroblast-derived ECM sheets (Schenke-Layland et al., 2009), which indicates adequate preservation of sGAGs in cdECM during the decellularization process in our study. Keller et al. investigated the sGAG content in fibroblast-derived ECM (Keller, Liedek, et al., 2020). Compared to their results (2.4 %) the amount of sGAG determined in this study was found to be in the same order of magnitude. As GAGs are known to exhibit a positive influence on cellular behavior in regenerative processes (e.g. proliferation, vascularization), cdECM containing and preserving higher amounts of GAGs represent a promising material in regenerative applications.

Expression of proteins associated with basal membrane

The basal membrane plays a fundamental role in cellular anchorage, as a physical barrier, and in signaling (Leclech et al., 2021). Thus, the preservation of basal membrane structures during decellularization would be beneficial for healthcare approaches. Histological staining suggested the presence of superordinate structures, like the basal membrane, in dECM, but not in cdECM samples (Figure 2). Two of the main components of the basal membrane are collagen type IV and laminins (Kalluri, 2003; Yurchenco & Schittny, 1990). In the next step, the presence of these basal membrane-associated ECM proteins collagen type IV and laminins, was proven by an immunofluorescence staining (Figure 3). After decellularization, a heterogeneous distribution of dense and loosely packed structures was observed in dECM. For all cdECM approaches – regardless of the time point of isolation - densely packed structures with ubiquitous staining of

ECM-specific proteins were found. Qualitative analysis of the immunofluorescence images did not indicate differences between the investigated ECM samples. This indicates that basal membrane proteins are also present in cdECM but do not exhibit the specific structure of the basal membrane, which might prevent the binding of the dye in histological staining. Immunofluorescence staining of ECM-specific proteins collagen type I and fibronectin are shown in supplementary figure 3.

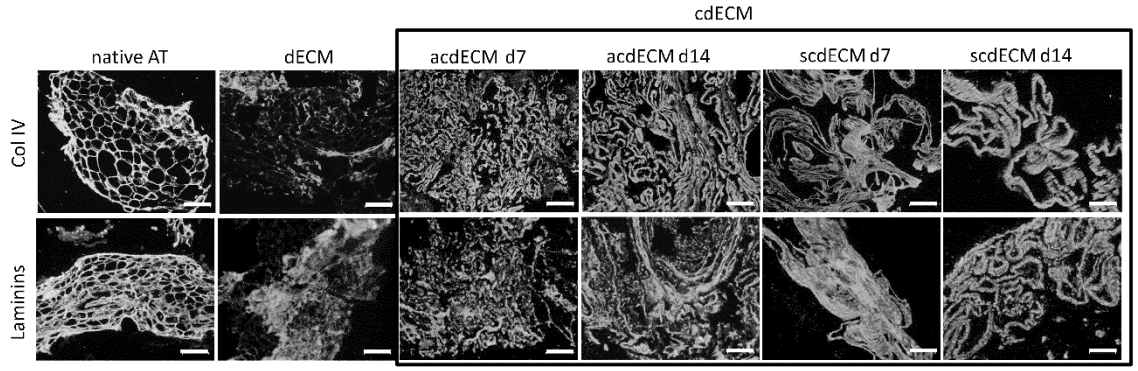

Figure 3: Immunofluorescence staining of basal membrane proteins collagen type IV and laminins. The presence of proteins collagen type IV and laminins were proven by immunofluorescence staining. (Scale bar: 200µm; n=3)

Previous studies demonstrated that laminin, which is mainly found in the basal membrane, contributes to the formation and maintenance of vascular structures (MALINDA et al., 1999; Ponce et al., 1999). After homogenization, which is necessary for further processing as biomaterial, the structure of the basal membrane is very likely disrupted in all ECM samples. Thus, the presence of basal membrane proteins (e.g. collagen type IV and laminins) may play a stronger role than the specific structure of the basal membrane. If a well-developed basal membrane as a biomaterial is desired epithelial or endothelial cells, that mainly produce basal membrane in vivo and in vitro, in monoculture or co-culture with other cell types can be used. This is especially useful for the coating of synthetic materials when the original structure can be restored and is not disrupted by further processing of a harvested cdECM (Carvalho et al., 2019; Junka et al., 2020). Dao Thi et al. recently described a method to polarize stem cells using a growth factor gradient in trans wells yielding hepatocyte-like cells with an apical and a basolateral side (Dao Thi et al., 2020). Despite in vivo adipocytes does not exhibit this polarization this method might be promising to enhance basal membrane secretion of cdECM.

Structural characterization

Topographical characteristics are known to strongly influence cellular behavior such as proliferation and differentiation (Ko et al., 2016; Shi et al., 2014; Z. Wang et al., 2016). For example, Abagnale et al. showed that ASCs, without specific differentiation media, underwent osteogenesis on 2 µm thick microfibers but adipogenesis on microfibers with a diameter of 15 µm. However, no upregulation of specific differentiation markers was observed on fiber diameters thinner than 400 nm (Abagnale et al., 2015). Fiber diameter as the primary topographical feature of fibrous materials such as ECM was evaluated by SEM. In Figure 4, SEM images of the dECM and cdECM are shown. A significantly higher fiber diameter in dECM (63.9 (± 12.8) nm) compared to cdECM samples (acdECM d7: 35.9 (±9.2) nm; acdECM d14: 37.7 (±11.2) nm; scdECM d7: 36.7 (±7.7) nm; scdECM d14: 37.3 (±11.2) nm) was observed. The immature state of collagen fibers in cdECM previously indicated by the histological staining (Figure 2) could also be observed in the SEM analysis. The mature collagen fibers of dECM exhibited the characteristic cross stripes with an average distance of 65 nm (black arrows), derived from the assembly of the tropocollagen molecules, whereas no stripes were found in cdECM samples.

The influence of these features on cell fate has to be considered when using the materials for specific applications and if necessary soluble factors are needed to prevent unwanted differentiation events. As longer culture periods are not practicable for the generation of a biomaterial, different culture methods, such as macromolecular crowding, hypoxia, reduced frequency of medium replacement, and reduction of serum concentration can be tested to increase the maturity and diameter of the collagen fibers of cdECM, if needed (Assunção et al., 2020). The period for the generation of a biomaterial that can be assumed to be suitable strongly depends on the intended use. For the generation of cdECM, which is used for in vitro applications (e.g. the built-up of tissue models) and in vivo application where it can be generated in advance (allogenic products) culture periods of a few weeks can be seen as feasible. In contrast for the treatment of patients with autologous material, only generation periods of a few days can be seen as feasible.

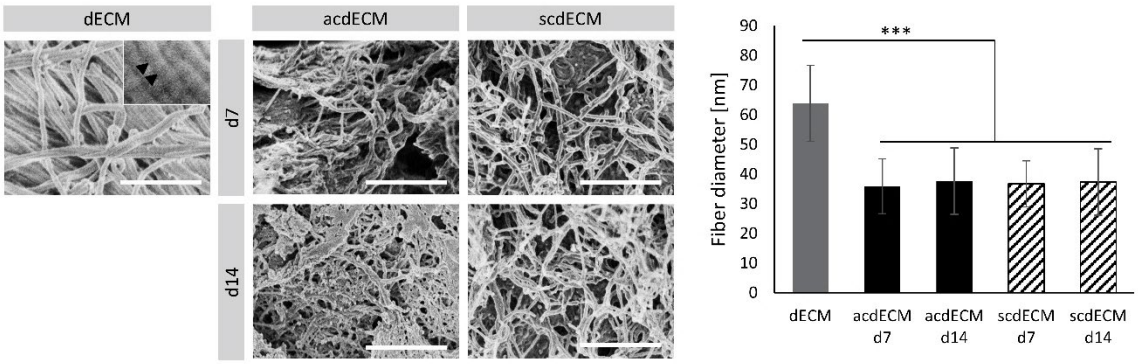

Figure 4: Analysis of fiber diameter of the different ECM samples: Fiber diameter was determined with ImageJ using SEM images of ECM samples (n=9). Black arrows: horizontal stripes with a distance of 65 nm. (Scale bar: 1µm; *** $p \leq 0.001$)

Degree of swelling

The degree of swelling describes the ability of a material to bind water, which has a high impact on the materials' physical properties. The ability of a material to bind water depends on structural characteristics (e.g. pore size) and chemical properties (e.g. charge). Thus, differences in the degree of swelling indicate differences in structural and chemical material characteristics. Figure 5 shows the degree of swelling of dECM and cdECM samples. It was found that acdECM from both time points (acdECM d7: 2357.6 (±201.1) % (this value was already published by us in (Nellinger et al., 2020)) and acdECM d14: 2329.4 (±118.7) %) exhibited a higher degree of swelling compared to dECM (1288.1 (±383.3) %). Further, acdECM exhibited a higher degree of swelling compared to scdECM d7 (scdECM d7: 1624.3 (±96.4) % (this value is already published by us in (Nellinger et al., 2020))) independent of the day. The degree of swelling of scdECMd14 (1764.5 (±421.0) %) was significantly lower compared to acdECM d7, within the different evaluation days of cdECM.

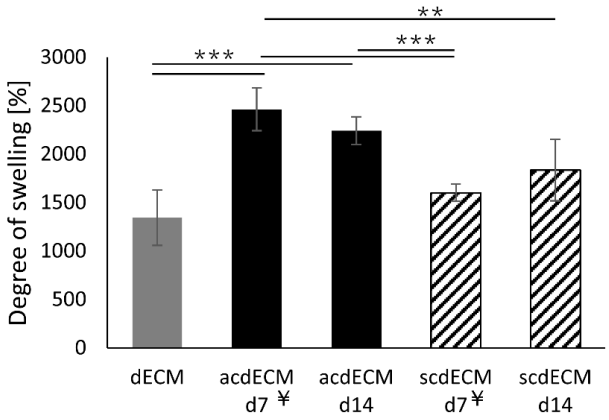

Figure 5: Degree of swelling. The degree of swelling was calculated from the dry and wet weight of ECM samples according to equation (3) and displayed in percentual amount. (¥ = data from [68]; ** $p \leq 0.01$; *** $p \leq 0.001$; n=9)

One possible explanation for the differences in the degree of swelling between the ECM samples is different degrees of cross-linking. A higher degree of cross-linking leads to a lower swelling degree. With the results of this study, it can be assumed that with the higher collagen content the degree of cross-linking is higher in scdECM samples compared to acdECM, leading to a lower degree of swelling in scdECM samples. Interestingly, the swelling degree of dECM was found to be comparable to scdECM. This might be explained by the mature state of dECM (as demonstrated by SEM) and therefore a higher degree of cross-linking compared to acdECM.

It is well known that physical characteristics influence cellular behavior strongly. (Engler et al., 2006; Kshitiz et al., 2012) For example, Guneta et al. demonstrated increased proliferation and adipogenic differentiation of ASCs on alginate scaffolds with decreasing stiffness (Vipra Guneta et al., 2016). Furthermore, Subbiah et al. showed that an increase of cross-linking of cdECM is accompanied by a rise of stiffness and a shift from adipogenic differentiation to osteogenic differentiation (Subbiah et al., 2016). Considering these results, it can be assumed that acdECM, produced in this study, may also favor adipogenic differentiation, whereas scdECM and dECM may favor chondrogenic and osteogenic differentiation. Thus, next to the structural characteristics, the degree of swelling of the ECMs must be considered when using ECM as a biomaterial to prevent unwanted differentiation events.

DNA content

Removal of DNA is a critical indicator for successful decellularization. It is known that remaining DNA can contribute to cytocompatibility problems and immunogenic reactions upon reintroduction of cells (B. N. Brown et al., 2009). A limit of residual DNA for its use as biomaterial is not officially defined, however, the postulated limit of 50 ng/mg by Capro et al. is generally accepted (Crapo et al., 2011). The absence of remaining DNA in decellularized cdECM and dECM samples was proven by a HE and DAPI staining for qualitative evidence and by a Pico488 assay for quantitative evidence. In Figure 6, histological stainings of dECM and scdECMd7 are exemplarily shown. The HE staining revealed a strong decrease of DNA (blue/purple) for both approaches after treatment with DNase (w/ DNase) compared to the samples without DNase treatment (w/o DNase). In addition, DAPI staining indicated a strong reduction of the nucleic acid content in samples treated with DNase compared to untreated samples. Untreated and DNase treated dECM and cdECM samples exhibited a DNA content below the postulated limit of 50 ng/mg DW in the treated samples. For dECM samples a significantly lower amount of DNA was observed (7.9 (±4.5) ng/mg) compared to all cdECM approaches (acdECM d7: 37.0 (±17.8) ng/mg; acdECM d14: 46.0

(±2.9) ng/mg; scdECM d7: 28.4 (±22.8) ng/mg; scdECM d14: 43.2 (±4.5) ng/mg) after the treatment with DNase.

The variation of DNA content in untreated ECM of the different origins was most likely caused by the difference in the present cell number in the samples. Due to the large portion of big mature adipocytes in native AT, it exhibited the lowest total cell number per volume, whereas the cdECM approaches proportionally exhibited a higher number of cells resulting in a higher amount of remaining DNA in the decellularized samples.

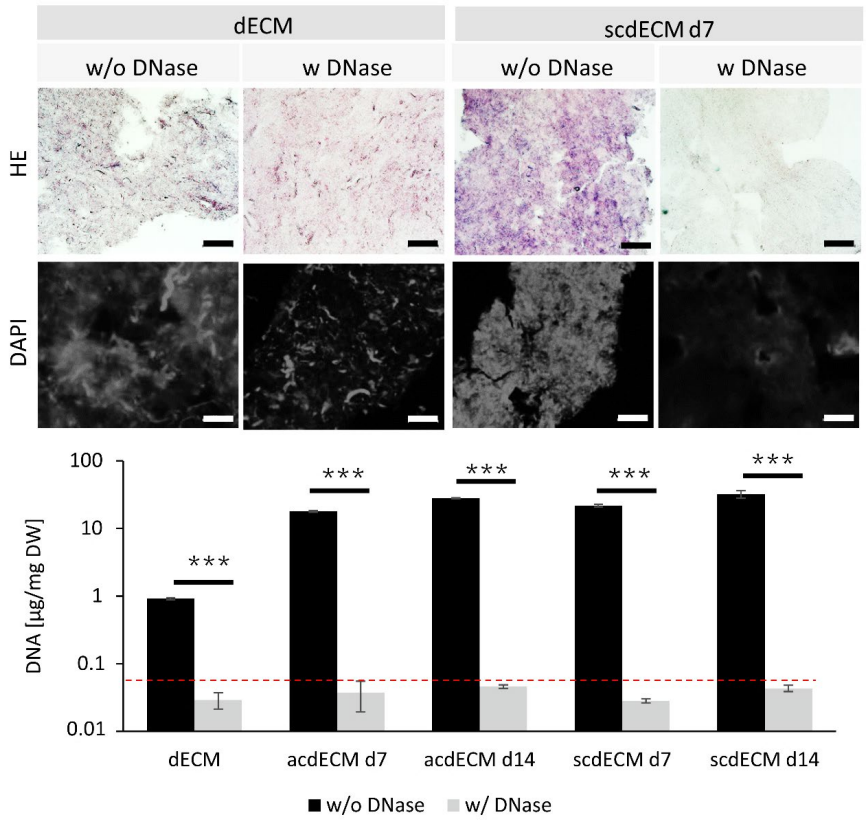

Figure 6: DNA content after treatment with DNase. To remove the remaining DNA, ECM samples were treated with 1500 U/mL of DNase. To determine DNA content in ECM samples, HE and DAPI staining were performed on histological sections of ECM samples with and without DNase treatment (n=3). Quantification of total DNA content in DNase-treated ECM samples was performed using Pico488. (*** $p \leq 0.001$; red dotted line: 50 ng/mg DW; n=9)

General aspects

Due to their different appearance, the decellularization protocols of the two ECMs differ in the used solutions and time by default in current studies (Flynn, 2010; V. Guneta et al., 2018; Magnan et al., 2018, 2021; Song et al., 2018). In this study, dECM was decellularized using relatively harsh chemicals and enzymes (no detergents which are classified as critical were used) whereas cdECM was treated with a relatively gentle hypotonic solution and nucleases. It is to be assumed that this

will have a great impact on some of the obtained results in this study (preservation of GAGs and the degree of swelling). However, in our opinion, this would rather be another reason for the use of cdECM whenever possible. This would, further, have the advantage that no chemicals remain in the material that could have a potentially negative effect on cells in vivo or in vitro.

Next to the demonstrated characteristics and differences also general aspects, such as costs of production, mechanical properties, and tunability have to be considered when choosing between dECM and cdECM as a biomaterial. Native adipose tissue can be harvested with low invasiveness in relatively high amounts and frequently is a waste product from plastic surgery. Depending on the used protocol the decellularization process includes the treatment with costly enzymes. However, relatively high amounts of dECM can be achieved with little effort. In contrast, the culture of ECM producing cells over several weeks with the needed consumables and media supplements is much more expensive. Especially since the yielded amount of cdECM which can be produced in one cell culture flask or plate is extremely low. Thus, the upscaling of cdECM production is a key step towards its widespread use in tissue engineering and healthcare. Next to the usual supplemented sodium L-ascorbate that increases collagen secretion, further methods are known to enhance cdECM yield. These include pharmaceutical substances that affect cellular pathways (e.g. TGF-beta pathway that was shown to cause increased ECM secretion (Biancheri et al., 2014)) and genetic alterations that lead to overexpression of ECM proteins (Chan et al., 2021). However, as these techniques are extremely invasive the resulting cdECMs need to be carefully studied before being used for biomedical applications. A less invasive method that is currently used is macromolecular crowding which enhances the polymerization of collagen fibers extracellularly.

For further processing it is necessary for both ECMs to homogenize the material except the original shape is sought to be reseeded with cells. For tissue engineering and healthcare applications in most cases, the original shape does not need to be restored. When the ECM is blended with another (hydrogel)material or used as a coating it has to be homogenized to achieve a homogeneous distribution of the ECM with the hydrogel or on the surface. Thus, the mechanical properties of the ECM material itself can be more or less neglected. Regarding the tunability of the ECM, cdECM brings a great advantage as it can be equipped with specific addressable functional groups using metabolic glycoengineering (MGE) (Gutmann et al., 2018; Ruff et al., 2017). During MGE the cells metabolize a modified sugar derivate and incorporate it into the glycocalyx and the ECM. The functional group can then be used to covalently and site-directed link bioactive molecules, like growth factors, or can be used to crosslink the ECM with another material or with itself in a controllable manner. In contrast, the modification of native unmodified dECM

occurs randomly and is not site-directed which may impact the effect of the bioactive molecules by covering the bioactive epitope(s). Further, the modification and crosslinking of dECM is performed with chemicals that may alter the structure of the ECM and therefore its impact on the cells when used for tissue engineering and healthcare applications (AC et al., 2018; Subbiah et al., 2016).

One aspect which needs to be investigated in cdECM is the binding of serum proteins to cdECM structures. CdECM is produced using fetal calf serum (FCS) containing media. As it is well known that there are high batch-to-batch variations in FCS and proteins can be bound to ECM and thus remain in the material. This might be a concern regarding the reproducibility of cell experiments (Boyd & Thomas, 2017). However, also in dECM donor variations might have an impact on the outcome of in vitro and in vivo experiments. Thus, the standardization of cdECM production using defined media would turn this disadvantage of cdECM into an advantage against the dECM where the donor variation cannot be eliminated.

In future studies, dECM and cdECM from further tissues should be characterized and investigated and a more detailed investigation of ECM proteins should be performed. Due to the complexity of the ECM colorimetric assays might be error-prone (comparable to total protein quantification). A more reliable method might be mass spectrometry. This method complements the results of the present study as it enables the identification and quantification of individual proteins and allows their classification (Johnson et al., 2016). This in turn would give more insight into the functionalities of the different ECMs. Based on further studies characterizing and comparing dECM and cdECM from different tissues, the range of methods needed to be performed to work with a well-defined ECM material can be reduced. From our point of view histological staining (Movat Pentachrome and Alcianblue PAS), quantification of sGAG, and remaining DNA represent a feasible amount of experiments that monitor the efficiency and reproducibility decellularization process and can be performed in most laboratories.

Conclusion

In the present study, we compared dECM and cdECM from stem cells and adipogenic differentiated ASCs towards their macromolecular composition and their structural features. We found that cdECM exhibited more sGAGs which are beneficial for regenerative processes. The thinner collagen fibers and of cdECM indicate its immature state and the accompanying differences in topography might have an impact on cell fate. With the differences identified, we aim to support researchers in the decision, which ECM is suitable as a biomaterial for their specific application. The differences between the ECMs investigated have the potential to highly influence

experimental outcomes and therefore should be considered when choosing a biomaterial for tissue engineering or healthcare application. Next to the found characteristics and differences, to date, general aspects, such as costs of production and possibilities in the tunability have to be considered. To find the ideal material for a specific application the aim of the planned study has to be opposed to the advantages and disadvantages of both ECM materials.

Conflict of interests

The authors have no conflict of interest to declare.

Data availability statement

The data that support the findings of this study are available from the corresponding author upon reasonable request.

Acknowledgments

We acknowledge the financial support of the Ministry of Science, Research and the Arts (Baden-Württemberg, Germany), for the University of Tuebingen and the Reutlingen University under the program “Intelligent Process and Material Development in Biomateriomics”

The authors kindly thank Prof. Dr. Katja Schenke-Layland (University of Tuebingen) and Prof. Dr. Ralf Kemkemer (Reutlingen University) for the helpful discussion of the results and Isabelle Schmidt (Reutlingen University) for the support in the experimental procedure and the Analytical Chemistry Unit (University of Hohenheim) for the performance of the elementary analysis. The authors thank Elke Nadler for SEM measurements. The SEM/S(T)EM was cofounded by the German Science Foundation (DFG) under contract no. INST37/829-1FUGG. Silke Keller kindly acknowledges the Peter and Traudl Engelhorn Foundation for its financial support through her PhD scholarship

References

Abaci, A., & Guvendiren, M. (2020). Designing Decellularized Extracellular Matrix-Based Bioinks for 3D Bioprinting. *Advanced Healthcare Materials*, *9*(24), 2000734. https://doi.org/10.1002/ADHM.202000734

Abagnale, G., Steger, M., Nguyen, V. H., Hersch, N., Sechi, A., Joussen, S., Denecke, B., Merkel, R., Hoffmann, B., Dreser, A., Schnakenberg, U., Gillner, A., & Wagner, W. (2015). Surface topography enhances differentiation of mesenchymal stem cells towards osteogenic and adipogenic lineages. *Biomaterials*, *61*, 316–326. https://doi.org/10.1016/j.biomaterials.2015.05.030

AC, B., M, G., T, L., & L, M. (2018). Bioorthogonal strategies for site-directed decoration of biomaterials with therapeutic proteins. *Journal of Controlled Release : Official Journal of the Controlled Release Society*, *273*, 68–85. https://doi.org/10.1016/J.JCONREL.2018.01.018

Agmon, G., & Christman, K. L. (2016). Controlling stem cell behavior with decellularized extracellular matrix scaffolds. In *Current Opinion in Solid State and Materials Science* (Vol. 20, Issue 4, pp. 193–201). Elsevier Ltd. https://doi.org/10.1016/j.cossms.2016.02.001

Aratani, Y., & Kitagawa, Y. (1988). Enhanced synthesis and secretion of type IV collagen and entactin during adipose conversion of 3T3-L1 cells and production of unorthodox laminin complex. *Journal of Biological Chemistry*, *263*(31), 16163–16169. https://doi.org/10.1016/s0021-9258(18)37573-2

Assunção, M., Dehghan-Baniani, D., Yiu, C. H. K., Später, T., Beyer, S., & Blocki, A. (2020). Cell-Derived Extracellular Matrix for Tissue Engineering and Regenerative Medicine. In *Frontiers in Bioengineering and Biotechnology* (Vol. 8, p. 602009). Frontiers Media S.A. https://doi.org/10.3389/fbioe.2020.602009

Biancheri, P., Giuffrida, P., Docena, G. H., MacDonald, T. T., Corazza, G. R., & Di Sabatino, A. (2014). The role of transforming growth factor (TGF)-β in modulating the immune response and fibrogenesis in the gut. *Cytokine & Growth Factor Reviews*, *25*(1), 45–55. https://doi.org/10.1016/J.CYTOGFR.2013.11.001

Boyd, D. F., & Thomas, P. G. (2017). Towards integrating extracellular matrix and immunological pathways. *Cytokine*, *98*, 79–86. https://doi.org/10.1016/J.CYTO.2017.03.004

Brizzi, M. F., Tarone, G., & Defilippi, P. (2012). Extracellular matrix, integrins, and growth factors as tailors of the stem cell niche. *Current Opinion in Cell Biology*, *24*(5), 645–651. https://doi.org/10.1016/j.ceb.2012.07.001

Brown, B. N., Freund, J. M., Han, L., Rubin, J. P., Reing, J. E., Jeffries, E. M., Wolf, M. T., Tottey, S., Barnes, C. A., Ratner, B. D., & Badylak, S. F. (2011). Comparison of three methods for the derivation of a biologic scaffold composed of adipose tissue extracellular matrix. *Tissue Engineering - Part C: Methods*, *17*(4), 411–421. https://doi.org/10.1089/ten.tec.2010.0342

Brown, B. N., Valentin, J. E., Stewart-Akers, A. M., McCabe, G. P., & Badylak, S. F. (2009). Macrophage phenotype and remodeling outcomes in response to biologic scaffolds with and without a cellular component. *Biomaterials*, *30*(8), 1482–1491. https://doi.org/10.1016/j.biomaterials.2008.11.040

Brown, C., McKee, C., Bakshi, S., Walker, K., Hakman, E., Halassy, S., Svinarich, D., Dodds, R., Govind, C. K., & Chaudhry, G. R. (2019). Mesenchymal stem cells: Cell therapy and regeneration potential. In *Journal of Tissue Engineering and Regenerative Medicine* (Vol. 13, Issue 9, pp. 1738–1755). John Wiley and Sons Ltd. https://doi.org/10.1002/term.2914

Capella-Monsonís, H., Coentro, J. Q., Graceffa, V., Wu, Z., & Zeugolis, D. I. (2018). An experimental toolbox for characterization of mammalian collagen type I in biological specimens. *Nature Publishing Group*, *13*. https://doi.org/10.1038/nprot.2017.117

Carvalho, M. S., Silva, J. C., Udangawa, R. N., Cabral, J. M. S., Ferreira, F. C., da Silva, C. L., Linhardt, R. J., & Vashishth, D. (2019). Co-culture cell-derived extracellular matrix loaded electrospun microfibrous scaffolds for bone tissue engineering. *Materials Science and Engineering: C*, *99*, 479–490. https://doi.org/10.1016/J.MSEC.2019.01.127

Chan, W. W., Yu, F., Le, Q. B., Chen, S., Yee, M., & Choudhury, D. (2021). Towards Biomanufacturing of Cell-Derived Matrices. *International Journal of Molecular Sciences 2021, Vol. 22, Page 11929*, *22*(21), 11929. https://doi.org/10.3390/IJMS222111929

Chiang, C.-E., Fang, Y.-Q., Ho, C.-T., Assunção, M., Lin, S.-J., Wang, Y.-C., Blocki, A., & Huang, C.-C. (2021). Bioactive Decellularized Extracellular Matrix Derived from 3D Stem Cell Spheroids under Macromolecular Crowding Serves as a Scaffold for Tissue Engineering. *Advanced Healthcare Materials*, *10*(11), 2100024. https://doi.org/10.1002/ADHM.202100024

Crapo, P. M., Gilbert, T. W., & Badylak, S. F. (2011). An overview of tissue and whole organ decellularization processes. In *Biomaterials* (Vol. 32, Issue 12, pp. 3233–3243). Elsevier. https://doi.org/10.1016/j.biomaterials.2011.01.057

Daley, W. P., & Yamada, K. M. (2013). ECM-modulated cellular dynamics as a driving force for tissue morphogenesis. *Current Opinion in Genetics and Development*, *23*(4), 408–414. https://doi.org/10.1016/j.gde.2013.05.005

Dao Thi, V. L., Wu, X., Belote, R. L., Andreo, U., Takacs, C. N., Fernandez, J. P., Vale-Silva, L. A., Prallet, S., Decker, C. C., Fu, R. M., Qu, B., Uryu, K., Molina, H., Saeed, M., Steinmann, E., Urban, S., Singaraja, R. R., Schneider, W. M., Simon, S. M., & Rice, C. M. (2020). Stem cell-derived polarized hepatocytes. *Nature Communications 2020 11:1*, *11*(1), 1–13. https://doi.org/10.1038/s41467-020-15337-2

Eckert, C. E., Fan, R., Mikulis, B., Barron, M., Carruthers, C. A., Friebe, V. M., Vyavahare, N. R., & Sacks, M. S. (2013). On the biomechanical role of glycosaminoglycans in the aortic heart valve leaflet. *Acta Biomaterialia*, *9*(1), 4653–4660. https://doi.org/10.1016/j.actbio.2012.09.031

Engler, A. J., Sen, S., Sweeney, H. L., & Discher, D. E. (2006). Matrix Elasticity Directs Stem Cell Lineage Specification. *Cell*, *126*(4), 677–689. https://doi.org/10.1016/j.cell.2006.06.044

Eoh, J. H., Shen, N., Burke, J. A., Hinderer, S., Xia, Z., Schenke-Layland, K., & Gerecht, S. (2017). Enhanced elastin synthesis and maturation in human vascular smooth muscle tissue derived from induced-pluripotent stem cells. *Acta Biomaterialia*, *52*, 49–59. https://doi.org/10.1016/j.actbio.2017.01.083

Fitzpatrick, L. E., & McDevitt, T. C. (2015). Cell-derived matrices for tissue engineering and regenerative medicine applications. In *Biomaterials Science* (Vol. 3, Issue 1, pp. 12–24). Royal Society of Chemistry. https://doi.org/10.1039/c4bm00246f

Flynn, L. E. (2010). The use of decellularized adipose tissue to provide an inductive microenvironment for the adipogenic differentiation of human adipose-derived stem cells. *Biomaterials*, *31*(17), 4715–4724. https://doi.org/10.1016/j.biomaterials.2010.02.046

Frantz, C., Stewart, K. M., & Weaver, V. M. (2010). The extracellular matrix at a glance. *Journal of Cell Science*, *123*(24), 4195 LP – 4200. https://doi.org/10.1242/jcs.023820

Graubner, V. M., Jordan, R., Nuyken, O., Schnyder, B., Lippert, T., Kötz, R., & Wokaun, A. (2004). Photochemical modification of cross-linked poly(dimethylsiloxane) by irradiation at 172 nm. *Macromolecules*, *37*(16), 5936–5943. https://doi.org/10.1021/ma049747q

Gregoire, F. M., Smas, C. M., & Sul, H. S. (1998). Understanding adipocyte differentiation. In *Physiological Reviews* (Vol. 78, Issue 3, pp. 783–809). American Physiological Society. https://doi.org/10.1152/physrev.1998.78.3.783

Guneta, V., Zhou, Z., Tan, N. S., Sugii, S., Wong, M. T. C., & Choong, C. (2018). Recellularization of decellularized adipose tissue-derived stem cells: Role of the cell-secreted extracellular matrix in cellular differentiation. *Biomaterials Science*, *6*(1), 168–178. https://doi.org/10.1039/c7bm00695k

Guneta, Vipra, Loh, Q. L., & Choong, C. (2016). Cell-secreted extracellular matrix formation and differentiation of adipose-derived stem cells in 3D alginate scaffolds with tunable properties. *Journal of Biomedical Materials Research Part A*, *104*(5), 1090–1101. https://doi.org/10.1002/jbm.a.35644

Gutmann, M., Braun, A., Seibel, J., & Lühmann, T. (2018). Bioorthogonal Modification of Cell Derived Matrices by Metabolic Glycoengineering. *ACS Biomaterials Science and Engineering*,

4(4), 1300–1306. https://doi.org/10.1021/acsbiomaterials.8b00264

Hesse, R., Chassé, T., Streubel, P., & Szargan, R. (2004). Error estimation in peak-shape analysis of XPS core-level spectra using UNIFIT 2003: how significant are the results of peak fits? *Surface and Interface Analysis*, *36*(10), 1373–1383. https://doi.org/10.1002/sia.1925

Hinderer, S., Shen, N., Ringuette, L. J., Hansmann, J., Reinhardt, D. P., Brucker, S. Y., Davis, E. C., & Schenke-Layland, K. (2015). In vitro elastogenesis: Instructing human vascular smooth muscle cells to generate an elastic fiber-containing extracellular matrix scaffold. *Biomedical Materials (Bristol)*, *10*(3), 034102. https://doi.org/10.1088/1748-6041/10/3/034102

Hussey, G. S., Dziki, J. L., & Badylak, S. F. (2018). Extracellular matrix-based materials for regenerative medicine. In *Nature Reviews Materials* (Vol. 3, Issue 7, pp. 159–173). Nature Publishing Group. https://doi.org/10.1038/s41578-018-0023-x

Johnson, T. D., Dequach, J. A., Gaetani, R., Ungerleider, J., Elhag, D., Nigam, V., Behfar, A., & Christman, K. L. (2014). Human versus porcine tissue sourcing for an injectable myocardial matrix hydrogel. *Biomaterials Science*, *2*(5), 735–744. https://doi.org/10.1039/c3bm60283d

Johnson, T. D., Hill, R. C., Dzieciatkowska, M., Nigam, V., Behfar, A., Christman, K. L., & Hansen, K. C. (2016). Quantification of Decellularized Human Myocardial Matrix: A Comparison of Six Patients. *Proteomics. Clinical Applications*, *10*(1), 75. https://doi.org/10.1002/PRCA.201500048

Junka, R., Quevada, K., & Yu, X. (2020). Acellular polycaprolactone scaffolds laden with fibroblast/endothelial cell-derived extracellular matrix for bone regeneration. *Journal of Biomedical Materials Research - Part A*, *108*(2), 351–364. https://doi.org/10.1002/JBM.A.36821/FORMAT/PDF

Kalluri, R. (2003). Basement membranes: Structure, assembly and role in tumour angiogenesis. In *Nature Reviews Cancer* (Vol. 3, Issue 6, pp. 422–433). Nature Publishing Group. https://doi.org/10.1038/nrc1094

Keller, S., Liedek, A., Shendi, D., Bach, M., Tovar, G. E. M., Kluger, P. J., & Southan, A. (2020). Eclectic characterisation of chemically modified cell-derived matrices obtained by metabolic glycoengineering and re-assessment of commonly used methods. *RSC Advances*, *10*(58), 35273–35286. https://doi.org/10.1039/d0ra06819e

Keller, S., Wörgötter, K., Liedek, A., Kluger, P. J., Bach, M., Tovar, G. E. M., Tovar, G. E. M., & Southan, A. (2020). Azide-Functional Extracellular Matrix Coatings as a Bioactive Platform for Bioconjugation. *ACS Applied Materials and Interfaces*, *12*(24), 26868–26879. https://doi.org/10.1021/acsami.0c04579

Kim, B. S., Kwon, Y. W., Kong, J. S., Park, G. T., Gao, G., Han, W., Kim, M. B., Lee, H., Kim, J. H., & Cho, D. W. (2018). 3D cell printing of in vitro stabilized skin model and in vivo pre-vascularized skin patch using tissue-specific extracellular matrix bioink: A step towards advanced skin tissue engineering. *Biomaterials*, *168*, 38–53. https://doi.org/10.1016/j.biomaterials.2018.03.040

Ko, E., Alberti, K., Lee, J. S., Yang, K., Jin, Y., Shin, J., Yang, H. S., Xu, Q., & Cho, S. W. (2016). Nanostructured tendon-derived scaffolds for enhanced bone regeneration by human adipose-derived stem cells. *ACS Applied Materials and Interfaces*, *8*(35), 22819–22829. https://doi.org/10.1021/acsami.6b05358

Köwitsch, A., Zhou, G., & Groth, T. (2018). Medical application of glycosaminoglycans: a review. *Journal of Tissue Engineering and Regenerative Medicine*, *12*(1), e23–e41. https://doi.org/10.1002/term.2398

Kshitiz, Park, J., Kim, P., Helen, W., Engler, A. J., Levchenko, A., & Kim, D.-H. (2012). Control of stem cell fate and function by engineering physical microenvironments. *Integrative Biology*, *4*(9), 1008–1018. https://doi.org/10.1039/c2ib20080e

Leclech, C., Natale, C. F., & Barakat, A. I. (2021). The basement membrane as a structured surface – role in vascular health and disease. In *Journal of Cell Science* (Vol. 133, Issue 18). Company of Biologists Ltd. https://doi.org/10.1242/jcs.239889

Lu, H., Hoshiba, T., Kawazoe, N., Koda, I., Song, M., & Chen, G. (2011). Cultured cell-derived extracellular matrix scaffolds for tissue engineering. *Biomaterials*, *32*(36), 9658–9666. https://doi.org/10.1016/j.biomaterials.2011.08.091

Lu, P., Takai, K., Weaver, V. M., & Werb, Z. (2011). ExtracellularMatrix Degradation andRemodeling in Development and Disease. *Cold Spring Harb Perspect Biol*. https://doi.org/10.1101/cshperspect.a005058

Magnan, L., Kawecki, F., Labrunie, G., Gluais, M., Izotte, J., Marais, S., Foulc, M.-P., Lafourcade, M., & L'Heureux, N. (2021). In vivo remodeling of human cell-assembled extracellular matrix yarns. *Biomaterials*, *273*, 120815. https://doi.org/10.1016/j.biomaterials.2021.120815

Magnan, L., Labrunie, G., Marais, S., Rey, S., Dusserre, N., Bonneu, M., Lacomme, S., Gontier, E., & L'Heureux, N. (2018). Characterization of a Cell-Assembled extracellular Matrix and the effect of the devitalization process. *Acta Biomaterialia*, *82*, 56–67. https://doi.org/10.1016/j.actbio.2018.10.006

MALINDA, K. M., NOMIZU, M., CHUNG, M., DELGADO, M., KURATOMI, Y., YAMADA, Y., KLEINMAN, H. K., & PONCE, M. L. (1999). Identification of laminin α1 and β1 chain peptides active for endothelial cell adhesion, tube formation, and aortic sprouting. *The FASEB Journal*, *13*(1), 53–62. https://doi.org/10.1096/fasebj.13.1.53

Mecham, R. P. (2012). Overview of extracellular matrix. *Current Protocols in Cell Biology*, *SUPPL.57*, 1–16. https://doi.org/10.1002/0471143030.cb1001s57

Miller, A. E., Hu, P., & Barker, T. H. (2020). Feeling Things Out: Bidirectional Signaling of the Cell–ECM Interface, Implications in the Mechanobiology of Cell Spreading, Migration, Proliferation, and Differentiation. *Advanced Healthcare Materials*, *9*(8), 1–24. https://doi.org/10.1002/adhm.201901445

Mrsic, I., Bäuerle, T., Ulitzsch, S., Lorenz, G., Rebner, K., Kandelbauer, A., & Chassé, T. (2021). Oxygen plasma surface treatment of polymer films—Pellethane 55DE and EPR-g-VTMS. *Applied Surface Science*, *536*, 147782. https://doi.org/10.1016/j.apsusc.2020.147782

Myllyharju, J., & Kivirikko, K. I. (2004). Collagens, modifying enzymes and their mutations in humans, flies and worms. In *Trends in Genetics* (Vol. 20, Issue 1, pp. 33–43). Elsevier Ltd. https://doi.org/10.1016/j.tig.2003.11.004

Nellinger, S., Schmidt, I., Heine, S., Volz, A. C., & Kluger, P. J. (2020). Adipose stem cell-derived extracellular matrix represents a promising biomaterial by inducing spontaneous formation of prevascular-like structures by mvECs. *Biotechnology and Bioengineering*, *117*(10), 3160–3172. https://doi.org/10.1002/bit.27481

Novoseletskaya, E. S., Grigorieva, O. A., Efimenko, A. Y., & Kalinina, N. I. (2019). Extracellular Matrix in the Regulation of Stem Cell Differentiation. In *Biochemistry (Moscow)* (Vol. 84, Issue 3, pp. 232–240). Pleiades Publishing. https://doi.org/10.1134/S0006297919030052

Pati, F., Ha, D. H., Jang, J., Han, H. H., Rhie, J. W., & Cho, D. W. (2015). Biomimetic 3D tissue printing for soft tissue regeneration. *Biomaterials*, *62*, 164–175. https://doi.org/10.1016/j.biomaterials.2015.05.043

Pati, F., Jang, J., Ha, D. H., Won Kim, S., Rhie, J. W., Shim, J. H., Kim, D. H., & Cho, D. W. (2014). Printing three-dimensional tissue analogues with decellularized extracellular matrix bioink. *Nature Communications*, *5*(1), 1–11. https://doi.org/10.1038/ncomms4935

Pierleoni, C., Verdenelli, F., Castellucci, M., & Cinti, S. (1998). Fibronectins and basal lamina molecules expression in human subcutaneous white adipose tissue. *European Journal of Histochemistry*, *42*(3), 183–188. https://europepmc.org/article/med/9857243

Ponce, M. L., Nomizu, M., Delgado, M. C., Kuratomi, Y., Hoffman, M. P., Powell, S., Yamada, Y., Kleinman, H. K., & Malinda, K. M. (1999). Identification of endothelial cell binding sites on the laminin γ1 chain. *Circulation Research*, *84*(6), 688–694. https://doi.org/10.1161/01.RES.84.6.688

Randles, M. J., Humphries, M. J., & Lennon, R. (2017). Proteomic definitions of basement membrane composition in health and disease. In *Matrix Biology* (Vols. 57–58, pp. 12–28).

Elsevier B.V. https://doi.org/10.1016/j.matbio.2016.08.006

Rossi, E., Guerrero, J., Aprile, P., Tocchio, A., Kappos, E. A., Gerges, I., Lenardi, C., Martin, I., & Scherberich, A. (2018). Decoration of RGD-mimetic porous scaffolds with engineered and devitalized extracellular matrix for adipose tissue regeneration. *Acta Biomaterialia*, *73*, 154–166. https://doi.org/10.1016/j.actbio.2018.04.039

Rousselle, P., Montmasson, M., & Garnier, C. (2019). Extracellular matrix contribution to skin wound re-epithelialization. *Matrix Biology*, *75–76*, 12–26.

Ruff, S. M., Keller, S., Wieland, D. E., Wittmann, V., Tovar, G. E. M., Bach, M., & Kluger, P. J. (2017). clickECM: Development of a cell-derived extracellular matrix with azide functionalities. *Acta Biomaterialia*, *52*, 159–170. https://doi.org/10.1016/j.actbio.2016.12.022

Salbach, J., Rachner, T. D., Rauner, M., Hempel, U., Anderegg, U., Franz, S., Simon, J.-C., Lorenz, &, & Hofbauer, C. (2012). Regenerative potential of glycosaminoglycans for skin and bone. *J Mol Med*. https://doi.org/10.1007/s00109-011-0843-2

Schenke-Layland, K., Rofail, F., Heydarkhan, S., Gluck, J. M., Ingle, N. P., Angelis, E., Choi, C. H., MacLellan, W. R., Beygui, R. E., Shemin, R. J., & Heydarkhan-Hagvall, S. (2009). The use of three-dimensional nanostructures to instruct cells to produce extracellular matrix for regenerative medicine strategies. *Biomaterials*, *30*(27), 4665–4675. https://doi.org/10.1016/j.biomaterials.2009.05.033

Shendi, D., Marzi, J., Linthicum, W., Rickards, A. J., Dolivo, D. M., Keller, S., Kauss, M. A., Wen, Q., McDevitt, T. C., Dominko, T., Schenke-Layland, K., & Rolle, M. W. (2019). Hyaluronic acid as a macromolecular crowding agent for production of cell-derived matrices. *Acta Biomaterialia*, *100*, 292–305. https://doi.org/10.1016/j.actbio.2019.09.042

Shi, Z., Neoh, K. G., Kang, E. T., Poh, C. K., & Wang, W. (2014). Enhanced endothelial differentiation of adipose-derived stem cells by substrate nanotopography. *Journal of Tissue Engineering and Regenerative Medicine*, *8*(1), 50–58. https://doi.org/10.1002/term.1496

Si, Z., Wang, X., Sun, C., Kang, Y., Xu, J., Wang, X., & Hui, Y. (2019). Adipose-derived stem cells: Sources, potency, and implications for regenerative therapies. In *Biomedicine and Pharmacotherapy* (Vol. 114, p. 108765). Elsevier Masson SAS. https://doi.org/10.1016/j.biopha.2019.108765

Song, M., Liu, Y., & Hui, L. (2018). Preparation and characterization of acellular adipose tissue matrix using a combination of physical and chemical treatments. *Molecular Medicine Reports*, *17*(1), 138–146. https://doi.org/10.3892/mmr.2017.7857

Subbiah, R., Hwang, M. P., Du, P., Suhaeri, M., Hwang, J.-H., Hong, J.-H., & Park, K. (2016). Tunable Crosslinked Cell-Derived Extracellular Matrix Guides Cell Fate. *Macromolecular Bioscience*, *16*(11), 1723–1734. https://doi.org/10.1002/mabi.201600280

Sun, Y., Yan, L., Chen, S., & Pei, M. (2018). Functionality of decellularized matrix in cartilage regeneration: A comparison of tissue versus cell sources. In *Acta Biomaterialia* (Vol. 74, pp. 56–73). Acta Materialia Inc. https://doi.org/10.1016/j.actbio.2018.04.048

Sutherland, A. J., Converse, G. L., Hopkins, R. A., & Detamore, M. S. (2015). The Bioactivity of Cartilage Extracellular Matrix in Articular Cartilage Regeneration. *Advanced Healthcare Materials*, *4*(1), 29–39. https://doi.org/10.1002/ADHM.201400165

Tan, Q. W., Zhang, Y., Luo, J. C., Zhang, D., Xiong, B. J., Yang, J. Q., Xie, H. Q., & Lv, Q. (2017). Hydrogel derived from decellularized porcine adipose tissue as a promising biomaterial for soft tissue augmentation. *Journal of Biomedical Materials Research - Part A*, *105*(6), 1756–1764. https://doi.org/10.1002/jbm.a.36025

Theocharis, A. D., Skandalis, S. S., Gialeli, C., & Karamanos, N. K. (2016). Extracellular matrix structure. *Advanced Drug Delivery Reviews*, *97*, 4–27. https://doi.org/10.1016/j.addr.2015.11.001

Thomas-Porch, C., Li, J., Zanata, F., Martin, E. C., Pashos, N., Genemaras, K., Poche, J. N., Totaro, N. P., Bratton, M. R., Gaupp, D., Frazier, T., Wu, X., Ferreira, L. M., Tian, W., Wang, G., Bunnell, B. A., Flynn, L., Hayes, D., & Gimble, J. M. (2018). Comparative proteomic analyses of human

adipose extracellular matrices decellularized using alternative procedures. *Journal of Biomedical Materials Research - Part A*, *106*(9), 2481–2493. https://doi.org/10.1002/jbm.a.36444

Turner, A. E. B., Yu, C., Bianco, J., Watkins, J. F., & Flynn, L. E. (2012). The performance of decellularized adipose tissue microcarriers as an inductive substrate for human adipose-derived stem cells. *Biomaterials*, *33*(18), 4490–4499. https://doi.org/10.1016/j.biomaterials.2012.03.026

Volz, A. C., Huber, B., Schwandt, A. M., & Kluger, P. J. (2017). EGF and hydrocortisone as critical factors for the co-culture of adipogenic differentiated ASCs and endothelial cells. *Differentiation*, *95*, 21–30. https://doi.org/10.1016/j.diff.2017.01.002

Wagner, C. D. (1983). Sensitivity factors for XPS analysis of surface atoms. *Journal of Electron Spectroscopy and Related Phenomena*, *32*(2), 99–102. https://doi.org/10.1016/0368-2048(83)85087-7

Wang, L., Johnson, J. A., Zhang, Q., & Beahm, E. K. (2013). Combining decellularized human adipose tissue extracellular matrix and adipose-derived stem cells for adipose tissue engineering. *Acta Biomaterialia*, *9*(11), 8921–8931. https://doi.org/10.1016/j.actbio.2013.06.035

Wang, Z., Lin, M., Xie, Q., Sun, H., Huang, Y., Zhang, D. D., Yu, Z., Bi, X., Chen, J., Wang, J., Shi, W., Gu, P., & Fan, X. (2016). Electrospun silk fibroin/poly(lactide-co-ε-caprolactone) nanofibrous scaffolds for bone regeneration. *International Journal of Nanomedicine*, *11*, 1483–1500. https://doi.org/10.2147/IJN.S97445

Wei, H. J., Liang, H. C., Lee, M. H., Huang, Y. C., Chang, Y., & Sung, H. W. (2005). Construction of varying porous structures in acellular bovine pericardia as a tissue-engineering extracellular matrix. *Biomaterials*, *26*(14), 1905–1913. https://doi.org/10.1016/j.biomaterials.2004.06.014

Wolf, M. T., Daly, K. A., Brennan-Pierce, E. P., Johnson, S. A., Carruthers, C. A., D'Amore, A., Nagarkar, S. P., Velankar, S. S., & Badylak, S. F. (2012). A hydrogel derived from decellularized dermal extracellular matrix. *Biomaterials*, *33*(29), 7028–7038. https://doi.org/10.1016/j.biomaterials.2012.06.051

Xing, H., Lee, H., Luo, L., & Kyriakides, T. R. (2020). Extracellular matrix-derived biomaterials in engineering cell function. In *Biotechnology Advances* (Vol. 42, p. 107421). Elsevier Inc. https://doi.org/10.1016/j.biotechadv.2019.107421

Young, D. A., Ibrahim, D. O., Hu, D., & Christman, K. L. (2011). Injectable hydrogel scaffold from decellularized human lipoaspirate. *Acta Biomaterialia*, *7*(3), 1040–1049. https://doi.org/10.1016/j.actbio.2010.09.035

Yurchenco, P. D., & Schittny, J. C. (1990). Molecular architecture of basement membranes. *The FASEB Journal*, *4*(6), 1577–1590. https://doi.org/10.1096/fasebj.4.6.2180767

Supplementary information

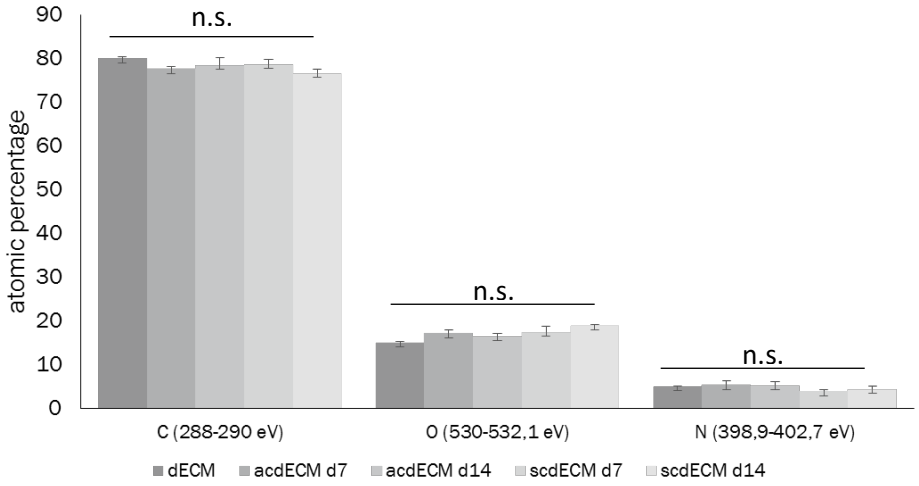

Supplementary Figure 1: XPS analysis of ECM coatings. (n.s.= not significant)

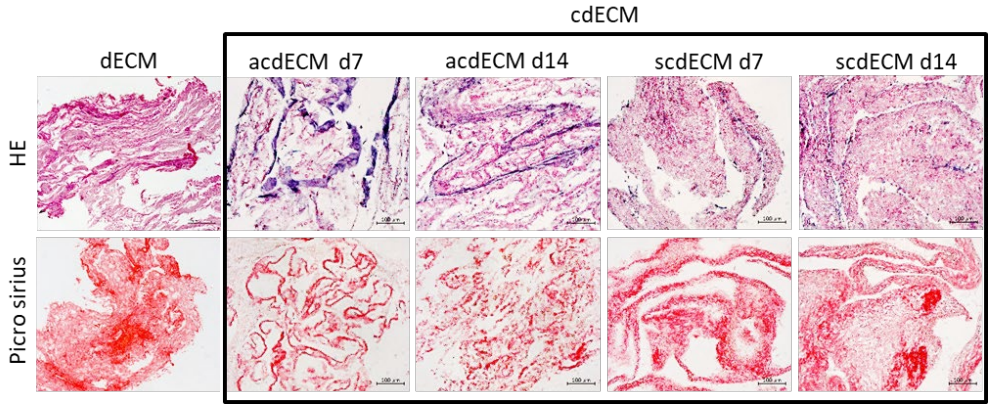

Supplementary Figure 2: HE and picrosirius staining

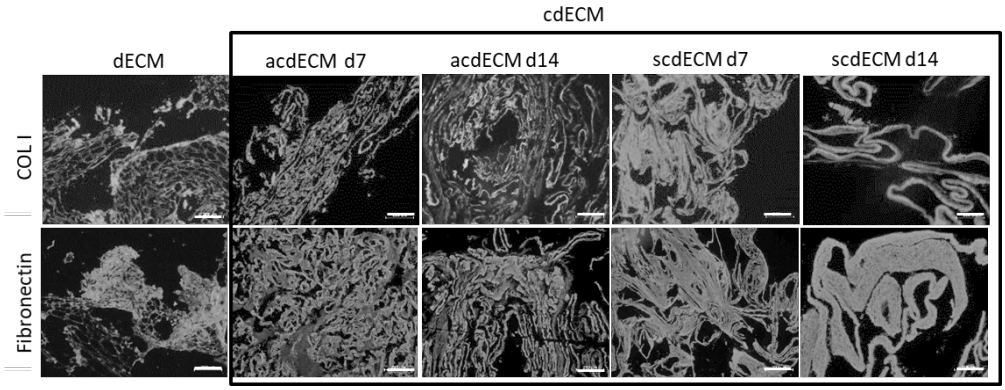

Supplementary Figure 3. Immunofluorescence staining of collagen type I and fibronectin

4 PAPER II – SUPPORT OF PREVASCULAR-LIKE STRUCTURE FORMATION

This chapter is originally published in the journal *Biotechnology and Bioengineering (*DOI: 10.1002/bit.27481) [3]. In this study the supporting effect of cdECM from ASCs in the stem cell state and adipogenic differentiation state on the formation of prevascular-like structures is investigated (Figure 9).

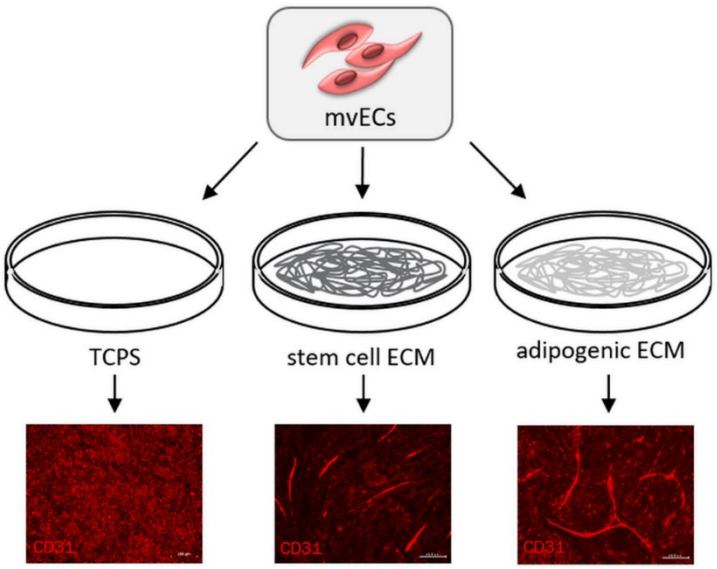

Figure 9: Graphical abstract Paper II (Adipose stem cell-derived Extracellular Matrix represents a promising Biomaterial by inducing spontaneous formation of Prevascular-like Structures by MvECs)

All cell-derived ECM (cdECM) substrates enabled mvEC growth with high viability. It was shown that mvECs cultured on cdECM self-assemble to prevascular-like structures. This effect is enhanced on adipogenic differentiated cdECM where longer and higher branched structures could be found compared to stem cell cdECM. The obtained results confirm the third hypothesis (H3). An increased concentration of pro-angiogenic factors was found in cdECM substrates. These results highlight cdECM as promising biomaterial for adipose tissue engineering.

[3] Reprinted from *Adipose stem cell-derived extracellular matrix represents a promising biomaterial by inducing spontaneous formation of prevascular-like structures by mvECs;* Nellinger S, Schmidt I, Heine S, Volz AC, Kluger PJ. Biotechnol Bioeng. 2020 Oct;117(10):3160-3172. with permission from Wiley-VCH GmbH under CC-BY 4.0

Adipose stem cell-derived Extracellular Matrix represents a promising Biomaterial by inducing spontaneous formation of Prevascular-like Structures by MvECs

Svenja Nellinger, [a] Isabelle Schmidt, [b] Simon Heine, [a] Ann-Cathrin Volz [a] and Petra J. Kluger [b*]

[a] *Reutlingen University, Reutlingen Research Institute, Reutlingen, Germany*

[b] *Reutlingen University, School of Applied Chemistry, Reutlingen, Germany*

Keywords adipose-derived stem cells; biomaterials; extracellular matrix; prevascular-like structures; tissue engineering.

Abstract

Tissue constructs of physiologically relevant scale require a vascular system to maintain cell viability. However, in vitro vascularization of engineered tissues is still a major challenge. Successful approaches are based on a feeder layer (FL) to support vascularization. Here, we investigated whether the supporting effect on the self-assembled formation of prevascular-like structures by microvascular endothelial cells (mvECs) originates from the FL itself or from its extracellular matrix (ECM). Therefore, we compared the influence of ECM, either derived from adipose-derived stem cells (ASCs) or adipogenically differentiated ASCs, with the classical cell-based FL. All cell-derived ECM (cdECM) substrates enabled mvEC growth with high viability. Prevascular-like structures were visualized by immunofluorescence staining of endothelial surface protein CD31 and could be observed on all cdECM and FL substrates but not on control substrate collagen I. On adipogenically differentiated ECM, longer and higher branched structures could be found compared with stem cell cdECM. An increased concentration of proangiogenic factors was found in cdECM substrates and FL approaches compared with controls. Finally, the expression of proteins associated with tube formation (E-selectin and thrombomodulin) was confirmed. These results highlight cdECM as promising biomaterial for adipose tissue engineering by inducing the spontaneous formation of prevascular-like structures by mvECs.

Introduction

Adipose tissue is a highly metabolic and vascularized tissue. In native tissue, a dense capillary network provides the supply of nutrients and inspiratory gases to the residing cells and removes their waste products. Since the diffusion limit of oxygen is less than 200 µm (Olive, Vikse, & Trotter, 1992; Thomlinson & Gray, 1955), the centers of large tissue constructs experience necrosis and volume loss without a functional vascular network. Consequently, there is an urgent need for fast vascularization following implantation of adipose tissue implants to maintain tissue mass and viability. In addition, for the in vitro use of tissue constructs, for example as a testing system, a stable functional vascular system would be desirable to allow constructs of a larger size and to maintain comprehensive cell behavior. Furthermore, such vascularized tissue constructs would allow in vitro investigations regarding the development and therapy of vascular diseases.

The inclusion of a functional vascular system remains one of the biggest challenges in three-dimensional (3D) tissue engineering. To date, there are several strategies to vascularize engineered 3D tissue constructs, e.g. functionalized scaffolds, perfusion bioreactors, co-culture and in vivo approaches (Laschke & Menger, 2016). Pro-angiogenic factors immobilized in the scaffold material were found to enhance vascularization (Laschke et al., 2008; Yoon, Chung, Lee,

& Park, 2006). For example, vascular endothelial growth factor (VEGF) and basic fibroblast growth factor (bFGF), are known to induce vessel formation and platelet-derived growth factor (PDGF) β supports stabilization of the newly formed vessels (Gaengel, Genove, Armulik, & Betsholtz, 2009). Different co-culture systems, including monolayer or spheroid cultures, demonstrated spontaneous formation of vascular-like structures (Walser et al., 2013; Wenz, Tjoeng, Schneider, Kluger, & Borchers, 2018). In particular, the co-culture of endothelial cells (ECs) with adipose-derived stem cells (ASCs) showed a beneficial effect on prevascular-like structure formation (Verseijden et al., 2012; Volz, Hack, Atzinger, & Kluger, 2018). Abovementioned techniques help to prevascularize a construct, but the complete vascularization is only achieved post implantation in vivo (Laschke, Strohe, et al., 2009; Laschke, Vollmar, & Menger, 2009). So far, there is no successful in vitro approach to create a physiological and functional vascular system, which ensures adequate stability and reproducibility. In most approaches, some type of feeder cells are used to support the formation of vascular-like structures by ECs. This living cellular part impedes a commercial application due to the difficult handling and storage. In contrast, lyophilized acellular biomaterials can be stored for long periods. Moreover, they evoke far fewer concerns regarding their application in regenerative medicine compared to the approaches including living cells. However, changes in structure and composition may occur during dehydration of natural materials. Thus, it has to be clarified if the processing of a biomaterial affects its ability to influence cellular behavior. To address this issue, next to the effect of the wet hydrogel-like form, the effect of the dehydrated materials on cellular behavior should be investigated.

A critical requirement for engineering tissue constructs is the use of a suitable scaffold that provides appropriate biological and physicochemical properties. The cell surrounding material also plays an important role in vascularization. There are several synthetic and natural scaffold materials used for vascularized tissue engineering approaches, e.g. polylactic acid, polyethylene glycol, collagen or hyaluronic acid. However, the extracellular matrix (ECM) as the natural environment of the cells in vivo represents the most physiological biomaterial. A variety of ECM-hybrid materials and pure decellularized ECM were investigated towards their ability to support stem cell differentiation and (neo)vascularization in vivo and in vitro (Adam Young, Bajaj, & Christman, 2014; Badylak, Freytes, & Gilbert, 2009; L. Flynn, Prestwich, Semple, & Woodhouse, 2009; L. E. Flynn, 2010). All these studies were performed with decellularized ECM derived from native tissue. For the past years, another source of natural ECM moves to the fore. In vitro generated cell-derived ECM (cdECM) was isolated from different cell-types (e.g. fibroblasts and ASCs) and used as a biomaterial in a variety of applications (Lu, Hoshiba, Kawazoe, & Chen, 2011; Lu, Hoshiba, Kawazoe, Koda, et al., 2011; Sart et al., 2016; Schenke-Layland et al., 2009; Wolchok

& Tresco, 2010). Several studies show that cdECMs, obtained from different cell-types, can induce adipogenic, chondrogenic and osteogenic differentiation of ASCs indicating its influence on cell fate (Dzobo et al., 2016; Guneta, Loh, & Choong, 2016; Guneta et al., 2017; Guo et al., 2013).

Our previous study revealed a spontaneous formation of prevascular-like structures by mvECs in a co-culture with adipogenically differentiated ASCs (Volz et al., 2018). In the following the term "prevascular-like structures" defines the aggregation/alignment of CD31 positive mvECs to fiber- or network-like structures, which stand out from the rest of the cellular monolayer. This term was previously used by Verseijden et al. to describe the alignment of ECs in spheroids without lumen formation (Verseijden, Posthumus-van Sluijs, Farrell, et al., 2010; Verseijden, Posthumus-van Sluijs, Pavljasevic, et al., 2010). The formation of vacuoles within ECs and subsequent lumenogenesis (tube formation) of prevascular-like structures requires the activation of cellular pathways and the transcription of different genes (Bayless & Davis, 2002). Further, the expression of E-selectin and thrombomodulin are shown to contribute to tube formation (Oh et al., 2007; Pan et al., 2017). In this study, we aimed to analyze whether the effect formation of prevascular-like structures by mvECs has to be attributed to cell-cell or cell-matrix interactions. The maintenance of the biological impact after processing and storage represents an important feature regarding the commercial application of biomaterials. The most common processing method for the preservation of biomaterials is drying. Consequently, we directly compared the effect of the hydrogel-like, wet cdECM and the dried cdECM as a coating regarding its ability to support the formation of prevascular-like structures by mvECs. The formation of vascular structures is a rather developmental process than a maintenance phenomenon as it can e.g. be found during (adipogenic) differentiation rather than in the stem cell niche. Thus, we tested whether there is a difference between cdECM derived from stem cells and adipogenically differentiated cells regarding their capability to induce prevascular-like structure formation.

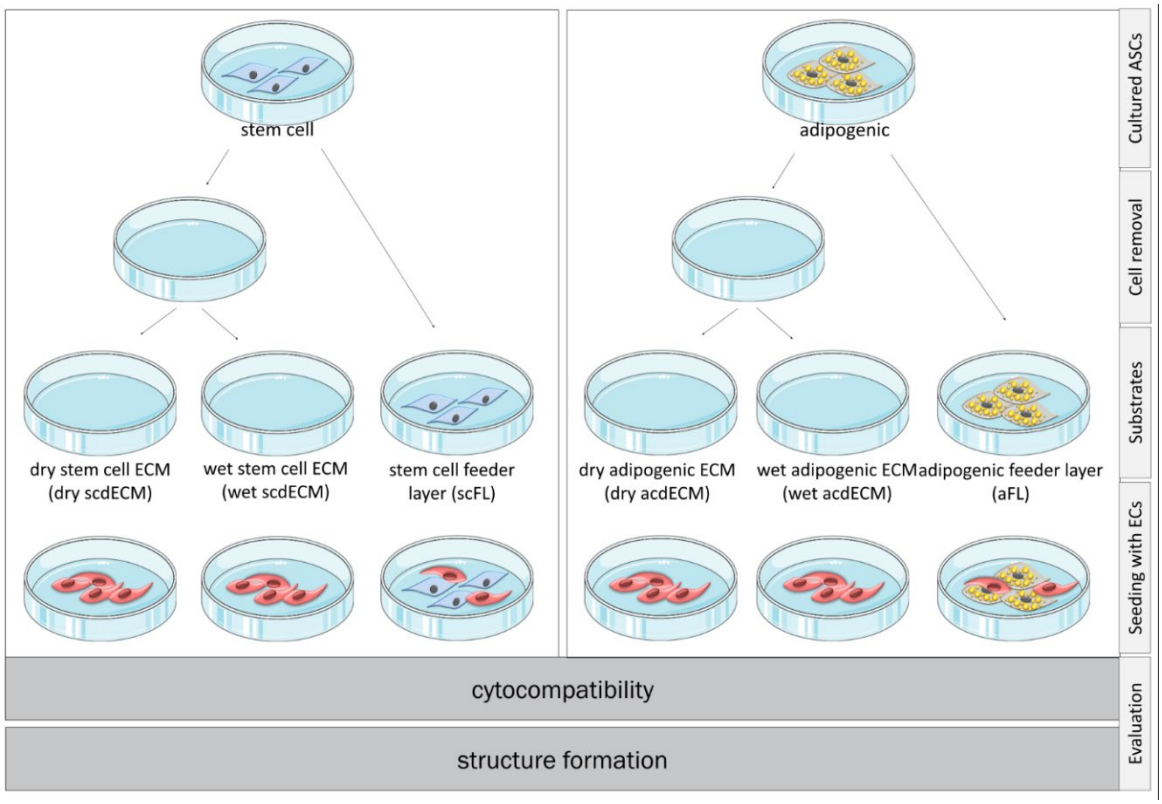

Figure 1: Schematic overview of the study procedure. The pro-angiogenic potential of different acellular and cellular substrates was analyzed. ASCs were cultured in growth and adipogenic differentiation medium respectively for 7 days. For acellular ECM substrates (cdECM), ASCs were removed and the remaining cdECM was dried or stored under wet conditions. For cellular substrates (FL), ASCs were not removed. MvECs were seeded onto the different substrates. Cytocompatibility was determined at day 3 and prevascular-like structure formation was determined at day 14 of cell culture.

Materials and Methods

All research was carried out in accordance with the rules for the investigation of human subjects as defined in the Declaration of Helsinki. Patients provided written agreement in compliance with the Landesärztekammer Baden-Württemberg (F-2012- 078, for normal skin from elective surgeries).

Cell isolation and expansion

ASCs were isolated from human tissue samples obtained from patients undergoing plastic surgery (Dr. Ziegler; Klinik Charlottenhaus, Stuttgart, Germany) as described before (Huber, Borchers, Tovar, & Kluger, 2016). ASCs were initially seeded at a density of 5x103 cells/cm2 in serum-free Mesenchymal Stem Cell (MSC) Growth Medium (MSCGM, PELOBiotech) containing 5 % human platelet lysate. ASCs were used up to passage three.

MvECs were isolated from juvenile foreskins (Dr. Yurttas, Stuttgart, Germany) as described before (Volz, Huber, Schwandt, & Kluger, 2017). Briefly, dermis was cut into small pieces and digested in

a dispase solution (2 U/ml; Serva Electrophoresis, Germany) overnight at 4 °C. After the removal of the epidermis, mvECs were isolated from the dermal layer by incubation with 0.05 % trypsin in ethylenediaminetetraacetic acid (EDTA; Life Technologies, Germany) for 40 min at 37 °C and mechanically isolated in mvEC Growth Medium-2 (EGM-2mv; Lonza, Switzerland). For cell expansion, mvECs were seeded with 5 x 10^3 cells/cm^2. MvECs were used up to passage three.

Generation of cell-derived extracellular matrix substrates and ASC feeder layer

ASCs were seeded into 8-well chamber slides (ibidi, Germany) and 24-well plates respectively at a density of 25 x103 cells/cm2 in serum-free MSCGM containing 5 % human platelet lysate. At confluency, medium was changed to either serum-containing GM (Dulbecco's Modified Eagle Medium (DMEM) with 10 % fetal calf serum (FCS) = scdECM) or adipogenic differentiation medium (DMEM with 10 % FCS, 1 µg/mL insulin, 1 µM dexamethasone, 100 µM indomethacin, 500 µM 3-isobutyl-1- methylxanthine = acdECM) both supplemented with 50 µg/mL Na-L-Ascorbate. The medium was changed every other day. At day 7, cells were lysed using hypotonic ammonium hydroxide solution and ECM was washed with ultrapure water. For dry ECM approaches (= dry), ECM was dried at room temperature (RT) and for wet ECM approaches (= wet), ECM was stored in ultrapure water until seeded with mvECs. Cellular substrates (= FL) were seeded with mvECs without lysis of ASCs (Figure 1).

Macroscopic pictures and degree of swelling

Macroscopic pictures of wet cdECM substrates were taken directly after cell removal. To investigate the water uptake and to calculate the degree of swelling, lyophilized cdECMs were weighed to determine the dry weight [weight (dry cdECM)]. Subsequently, cdECMs were swollen in demineralized water for 24 h at RT and weighed again [weight (swollen cdECM)].
The degree of swelling was calculated as:

$$\text{Degree of swelling [\%]} = (\text{weight (swollen cdECM)} - \text{weight (dry cdECM)}) / (\text{weight (dry cdECM)}) \times 100 \quad (1)$$

Immunofluorescence staining of fibronectin and quantification of pore size

For immunofluorescence (IF) staining of fibronectin, cdECM substrates were fixed in 4 % paraformaldehyde (Carl Roth, Germany) for 10 min followed by incubation with blocking solution, consisting of 3 % bovine serum albumin (Biomol, Germany) in 0.1 % Triton X (Sigma Aldrich, Germany) for 30 min to block unspecific binding sites. Subsequently, the primary antibody (mouse

anti-fibronectin, Santa Cruz, Germany; 1:200) was incubated for 1 h at RT. After washing three times with 0.1 % Tween-20 (SigmaAldrich, Germany) in PBS and, secondary antibody (anti-mouse Cy3, Dianova, Germany; 1:250) was incubated for 30 min at RT. Both were diluted in blocking solution. Images were taken with an Axio Observer microscope and Axiocam 506 mono using ZENblue software (Carl Zeiss, Germany). The pore size of the different cdECM substrates was quantified using ImageJ based on the IF images. The 100 largest pores for each image were determined and results are given as the mean.

Seeding of mvECs on cell-derived ECM and feeder layer

Isolated dry and wet cdECM substrates were re-seeded with mvECs at a density of 1 x 104 cells/cm2 in a defined mvEC adipocyte co-culture medium (Volz et al., 2018). For FL approaches mvECs were directly seeded on top of adipogenically differentiated and undifferentiated ASCs at a density of 1 x 104 cells/cm2 in defined co-culture medium, developed by us earlier (Volz et al., 2018). Cells were cultured for 14 days and the medium was changed every other day (Figure 1). As a control, all experiments were performed on collagen I (rat tail; 250 µg/mL in 0.1 % acetic acid) coated tissue culture polystyrene (COL I) and uncoated tissue culture polystyrene (TC). All media were supplemented with 1 % penicillin/streptomycin.

Cytocompatibility

Cytocompatibility of the cdECM substrates was demonstrated by the analysis of lactate dehydrogenase (LDH) in the cell culture supernatant. At day 3 after seeding, an LDH assay (TaKaRa Bio Europe, France) was performed according to the manufacturer's instructions. To exclude the remaining LDH from cell lysis, LDH concentration from supernatant from cdECM substrates without mvECs was determined. Values were subtracted from the LDH concentrations measured from mvECs on the different cdECM substrates. On day 14, live-dead staining was performed to assess the viability of cultured cells. Before staining the cells were washed in phosphate-buffered saline (PBS, Biochrom, Germany) and subsequently treated with staining solution, consisting of 200 ng/ml fluorescein diacetate (FDA, Sigma Aldrich, Germany) and 20 µg/mL propidium iodide (PI, Sigma Aldrich, Germany) in DMEM, for 15 min at 37 °C. Finally, cells were imaged in PBS with calcium and magnesium at RT with Axio Observer microscope and Axiocam 506 mono camera using ZENblue software (Carl Zeiss, Germany). The number of dead and viable cells was quantified using the software ImageJ and results are depicted as a percentage.

Immunofluorescence staining of cell-specific proteins

For IF staining of cell-specific proteins, cells were fixed in 4 % paraformaldehyde for 10 min and permeabilized for 10 min with 0.1 % Triton X in PBS. Following, cells were incubated in blocking solution, consisting of 3 % bovine serum albumin in 0.1 % Triton X for 30 min to block unspecific binding sites. Primary antibodies (mouse anti-CD31, 1:50, Dako, Germany; rabbit anti-CD31, 1:200, abcam, GB; goat anti-E-selectin, 1:200, R&D Systems, USA; sheep anti-thrombomodulin, 1:200, R&D Systems, USA) were diluted in blocking solution and incubated with samples for 2 h at RT. Secondary antibodies (anti-rabbit Alexa FluorTM 488, abcam, GB; anti-mouse Cy3, Dianova, Germany; donkey anti-sheep Alexa FluorTM 647, abcam, GB; donkey anti-goat Alexa FluorTM 594, abcam, GB) were diluted 1:250 in blocking solution and incubated with samples for 30 min at RT.

Enzyme-linked immunosorbent assay

For characterization of cdECM substrates regarding growth factors composition, substrates were washed 3 days in culture medium. For the characterization of FL, medium from day 3 was collected. Quantification of growth factors VEGF, bFGF and PDGFβ was performed using enzyme-linked immunosorbent assays (ELISA) (all PEPROTech, Germany) according to the manufacturer's instructions. The converted TMB was read out at 450 nm with a wavelength correction set at 620 nm (TECAN Saphire II, Tecan, Switzerland)

Statistical analysis

All experiments were performed at least three times, using cells from at least three different biological donors of ECs. The obtained data were compared by a one-way analysis of variance (ANOVA) with repetitive measurement and a Bonferroni post-hoc test using OriginPro 2018b. Statistical significances were stated as $*p \leq 0.05$, very significant as $**p \leq 0.01$ and highly significant as $***p \leq 0.001$.

Results

Macroscopic pictures and degree of swelling

Macroscopic pictures showed that wet scdECM and acdECM substrates exhibited a transparent gel-like appearance on the bottom of a petri dish (Figure 2). Determination of the degree of swelling of the different cdECM substrates revealed a higher water uptake capacity of acdECM (2357.6 (± 201.1) %) compared to the scdECM (1624.3 (± 96.4) %). Quantification of the pore size in the IF staining of fibronectin revealed smaller pores in the scdECM substrates compared to the acdECM substrates.

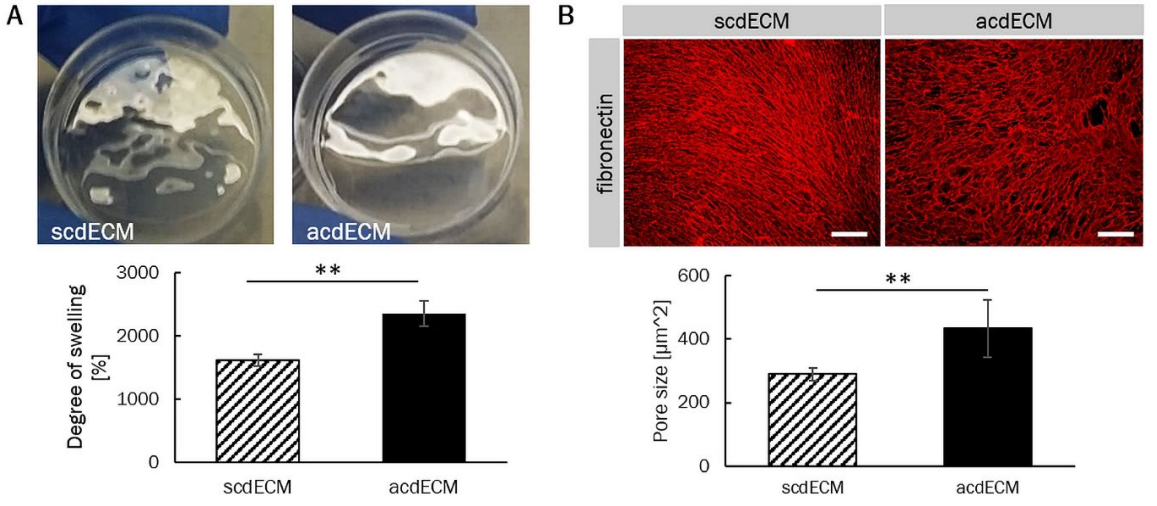

Figure 2: Degree of swelling of ECM substrates and staining of fibronectin and quantification of pore size. A: Macroscopic pictures of cdECM substrates show a transparent gel-like cdECM on the bottom of the petri dish. The degree of swelling was calculated in percent. Results revealed a higher swelling rate of acdECM compared to the scdECM (Diameter of the petri dish is 35 mm). B: Fixed cdECM samples were stained for fibronectin. Quantification of the pore sizes in fibronectin staining revealed smaller pores in the scdECM substrate compared to the acdECM substrate (Fibronectin indicated in red; scale bar: 200 µm). (** $p \leq 0.01$)

Acellular and cellular substrates are cytocompatible for mvECs

Cytocompatibility of the materials was determined by the measurement of the release of LDH after seeding with mvECs. LDH is an enzyme that is released during cell death and therefore can be used to quantify cytotoxicity. LDH release by mvECs seeded on the different substrates was measured 3 days after seeding (Figure 3, A). The values of TC were set as 100 (± 3.5) %. For cdECM substrates, values were normalized to TC. Results showed no significant increase of released LDH of mvECs when seeded on COL I coating (89.4 (± 13.8) %), dry scdECM (113.7 (± 31.0) %); dry acdECM (108.0 (± 29.0) %), wet scdECM (96.3 (± 33.4) %), or wet acdECM (93.4 (± 29.0) %). For the stem cell and adipogenic FL substrates, values were normalized to stem cell FL approach without mvECs (FL stem cell), which was set as 100 (± 3.3) %. For adipogenic FL (FL adipogenic: 157.9 (±

13.4) %) approach, a higher LDH release was found compared to stem cell FL. As in the cdECM approaches, no significant increase in LDH release was observed when mvECs were seeded onto the FL for stem cell and adipogenically differentiated cells (FL stem +mvECs: 126.1 (± 15.8) %; FL ad +mvECs: 176.8 (± 25.0) %).

The viability of mvECs cultured on the different substrates was assessed on day 14 after seeding with mvECs by live-dead staining with FDA and PI (Figure 3, B). Results showed that mvECs were viable on all acellular and FL substrates on day 14 and only a few dead cells could be found. Quantification of the percentage of dead cells revealed less than 1 % of dead cells on all acellular substrates (TC: 0.14 (± 0.08) %; COL I: 0.29 (± 0.21) %; dry scdECM: 0.46 (± 0.11) %; dry acdECM: 0.61 (± 0.13) %; wet scdECM: 0.25 (± 0.23) %; wet acdECM: 0.45 (± 0.26) %). On FL substrates higher amounts of dead cells were found in adipogenic approaches compared to the stem cell approach (FL stem cell: 0.25 (± 0.08) %; FL adipogenic: 4.58 (± 0.19) %; FL stem cell +mvECs: 0.37 (±0.18) %; FL adipogenic +mvECs: 3.25 (± 1.66) %).

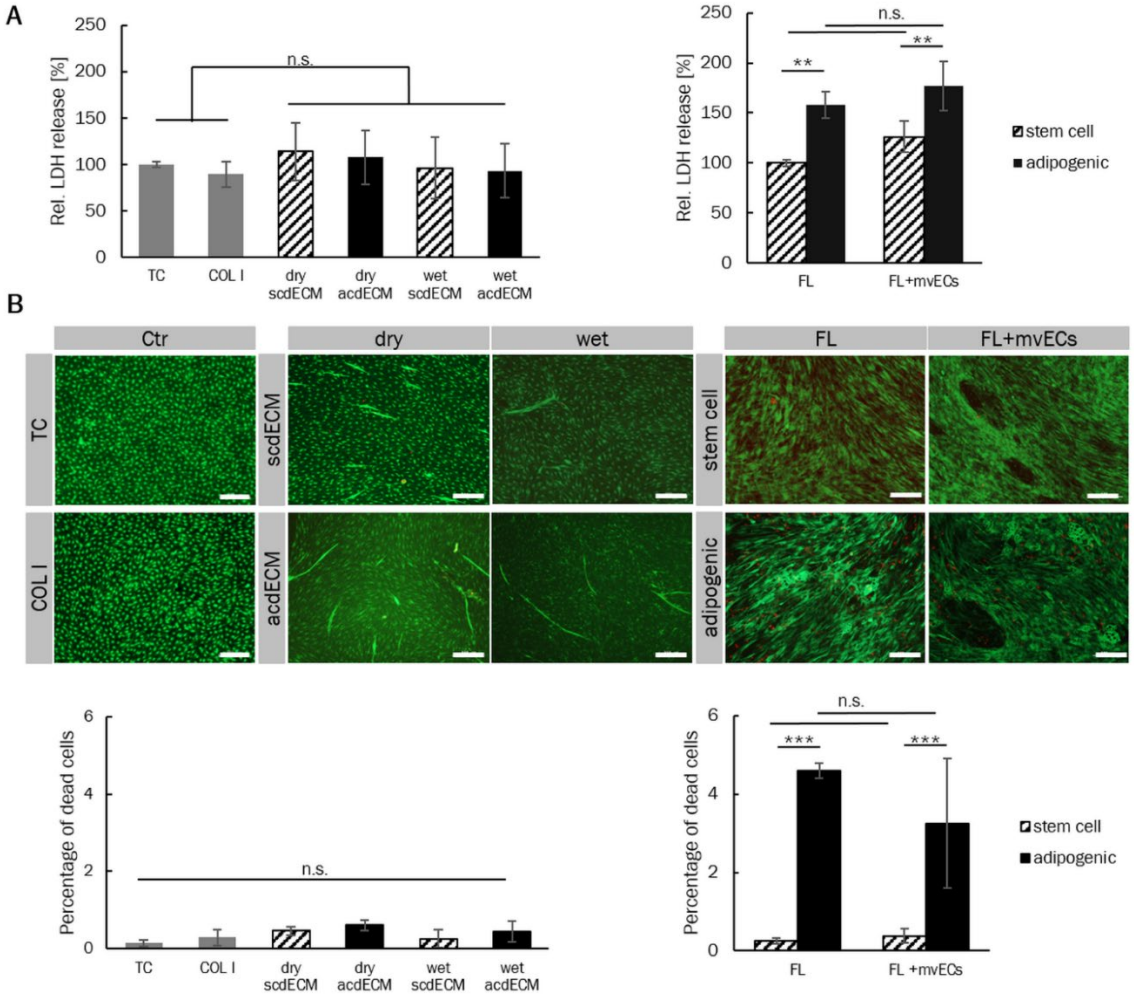

Figure 3: Cytocompatibility of the acellular and feeder layer substrates. 1 x 10^4 cells/cm^2 mvECs were seeded in a defined medium onto the different substrates. A: Relative LDH release was measured at day 3

after seeding with mvECs. For acellular substrates values were normalized to TC. No significant increase in LDH release could be observed on COL I coating or dry and wet cdECM for both, scdECM and acdECM. For FL approaches, values were normalized to stem cell FL without mvECs (FL stem cell). None of the FL approaches (stem cell and adipogenic differentiated) exhibited a significant increase of released LDH after seeding of mvECs (FL +mvECs), B: Live-dead staining (FDA, indicating alive cells displayed in green/PI, indicating dead cells, displayed in red) was performed on day 14 after seeding with mvECs. A confluent layer of viable cells was observed in all approaches. For each approach, the percentage of dead cells was quantified using ImageJ. The analysis revealed an amount of less than 1% of dead cells for all acellular substrates with no significant differences between the different substrates. In FL approaches a higher number of dead cells could be found in adipogenic approaches compared to stem cell approaches. Scale bar represents 200 µm. (n.s. = not significant; ** $p \leq 0.01$, *** $p \leq 0.001$)

Cell-derived ECM substrates support the formation of prevascular-like structures by mvECs

To investigate the effect of cdECM substrates on the formation of prevascular-like structures by mvECs, CD31 was visualized by IF staining (Figure 4). CD31 is a specific endothelial surface protein mainly localized on cell-cell connections and mainly responsible for the control of leukocyte transmigration in vivo (Piali et al., 1995). The staining pattern revealed that mvECs grew to a confluent cell layer on all acellular substrates. The degree of structure formation on the different substrates was analyzed and quantified using ImageJ on basis of the CD31 IF images. The formation of prevascular-like structures by mvECs was detected on all tested substrates in contrast to the controls (TC and COL I) on which no structure formation was observed. Higher magnification of the cellular monolayer or the prevascular-like structures shows the typical localization of CD31 at cell-cell contacts. Quantification of the structures' lengths revealed longer structures in wet acdECM (433.5 (± 293.1) µm) substrate compared to both scdECM substrates (dry: 235.9 (± 100.0) µm; wet: 232.9 (± 183.8) µm). Dry acdECM (297.2 (± 149.1) µm) substrates exhibited a slightly but not significantly higher structure length compared to dry and wet scdECM substrates. The lengths of prevascular-like structures found on the adipogenic FL (FL adipogenic: 483.5 (± 287.4) µm) were significantly longer than those of all other approaches except for wet acdECM substrate. Prevascular-like structures on stem cell FL exhibited an average length per structure of 302.1 (± 168.7) µm. Another essential criterion for the maturation of a vascular network is the formation of nodes. Therefore, the number of nodes formed by the mvECs on the different substrates was quantified. No nodes could be detected on the controls TC and COL I. In adipogenic approaches (dry acdECM: 1.2 (± 1.1); wet acdECM: 1.7 (±1.2); FL adipogenic: 6.7 (± 3.9)) the number of nodes was higher compared to the stem cell approaches (dry scdECM: 0.7 (± 0.4); wet scdECM: 0.2 (± 0.6); FL stem cell: 1.7 (± 1.5)) for all substrates. Furthermore, the number of nodes on wet acdECM was slightly but not significantly higher compared to the dry acdECM and comparable to stem cell FL. The significantly highest number of nodes could be observed in the adipogenic FL approach. To summarize, many short structures were identified on scdECM substrates, whereas on acdECM substrates the structures were longer and more branched. By co-

culture with the stem cell FL, mvECs formed islets of a confluent layer within the ASCs and prevascular-like structures sprouting from these islets were apparent. Long and highly branched prevascular-like structures were formed by mvECs on adipogenic FL.

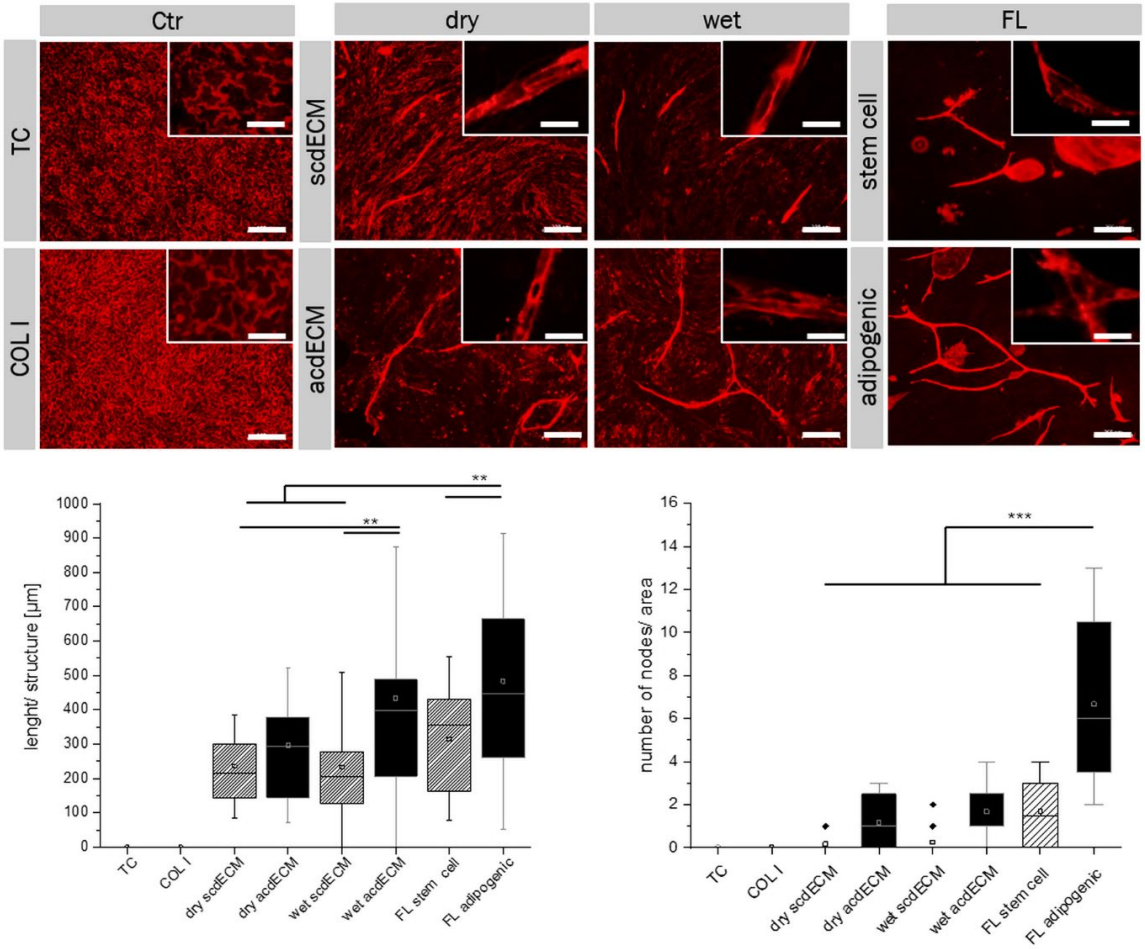

Figure 4: Formation of prevascular-like structures by mvECs on cellular and acellular ECM substrates. 1 x 104 mvECs /cm2 were seeded in defined co-culture medium onto the different substrates and were cultured for 14 days. Medium was changed three times a week. For determination of newly formed prevascular- like structures, IF staining of CD31 (indicated in red) was performed at day 14 after seeding with mvECs. On controls (TC and COL I) a confluent layer of mvECs could be observed without any structure formation. On cdECM substrates, the formation of prevascular-like structures could be observed with the strongest manifestation on wet acdECM. The highest degree of structure formation could be observed on adipogenic FL. On stem cell FL cluster formation of mvECs could be found and a considerably lower degree of structure formation compared to the adipogenic approach was detected. For each representative overview image, a magnified section of the cellular monolayer or the prevascular-like structures are pictured in the upper right corner to show the localization of CD31 at cell-cell contacts. Length per structure and number of formed nodes was quantified using ImageJ. Analysis revealed a significantly higher structure length of mvECs on wet acdECM substrate compared to dry acdECM and stem cell approaches (dry and wet scdECM) and comparable to FL approaches. Structure length on adipogenic FL was significantly higher compared to all approaches except wet acdECM. On adipogenic FL, a significantly higher number of nodes could be observed compared to all other approaches. (Scale bar overview image: 200 µm; scale bar magnified section: 25µm; * $p \leq 0.05$; ** $p \leq 0.01$; *** $p \leq 0.001$)

Quantification of pro-angiogenic factors on substrates

To confine which cdECM components are responsible for its pro-angiogenic effect, the relative concentration of growth factors VEGF, bFGF and PDGFβ were determined in the supernatant after washing the acellular substrates for 3 days (Figure 5). Values were normalized to TC. VEGF concentration was significantly higher for dry and wet acdECM substrates compared to all other acellular substrates. For quantification of growth factor concentrations on FL approaches cell culture supernatant from day 3 (corresponding to 3 days of washing of acellular substrates) was collected. A 10-fold higher concentration of VEGF could be found on in FL approaches with no difference between stem cell FL and adipogenic FL Significantly higher concentrations of bFGF could be found on in cdECM substrates compared to controls and on FL approaches higher concentration could be found compared to all other substrates. For PDGFβ a significantly higher concentration could be found on cdECM substrates compared to the controls. Between the different cdECM substrates no difference in PDGFβ concentration could be measured. On FL substrates, a higher concentration of PDGFβ could be found compared to acellular substrates but no difference between stem cell and adipogenically differentiated approach was observed.

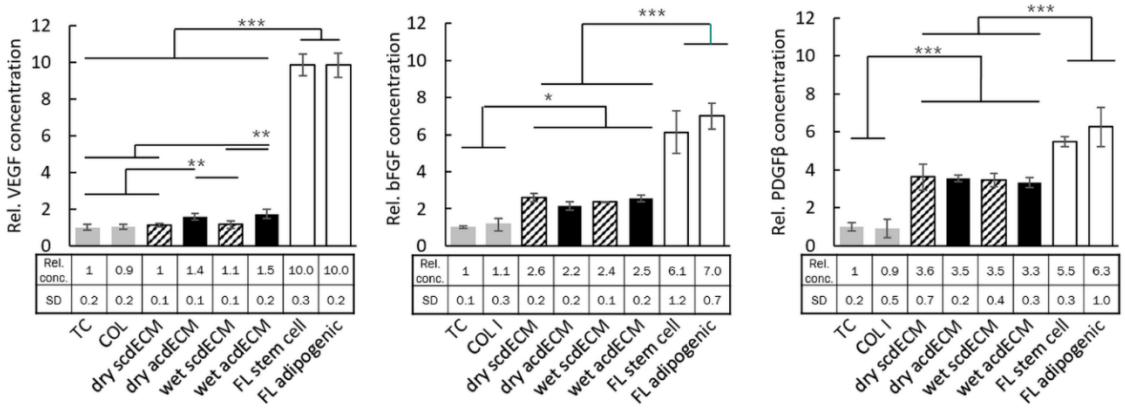

Figure 5: Pro-angiogenic factors concentration on cellular and acellular ECM substrates. For the determination of VEGF, bFGF and PDGFβ from the different substrates, supernatant from day 3 was investigated regarding the concentration of the growth factors using ELISA. For statistical analysis, values on TC were set as 1 and data were normalized to TC. For VEGF a significantly higher amount could be found in acdECM substrates (dry and wet) compared to all other acellular substrates including controls. FL substrates exhibited a 10-fold higher concentration of VEGF compared to acellular substrates. For bFGF a higher concentration could be found in cdECM substrates compared to controls. On FL approaches, a higher concentration could be found compared to all other approaches. For PDGFβ a significantly higher (3-fold) amount could be found in all cdECM substrates compared to the controls TC and COL I. Between the individual cdECM substrates no difference in remaining PDGFβ could be found. FL substrates exhibited significantly higher PDGFβ concentrations compared to acellular substrates. (* $p \leq 0.05$; ** $p \leq 0.01$; *** $p \leq 0.001$).

Expression of proteins associated with tube formation in newly formed prevascular-like structures

Recent studies showed that the expression of adhesion molecules E-selectin and thrombomodulin in ECs is associated with the tube formation of new blood vessels (Oh et al., 2007; Pan et al., 2017). To get an indication if lumenogenesis occurs to any extent, we investigated the expression of these proteins in the newly formed prevascular-like structures (Figure 6). Results of the IF staining revealed the expression of neither E-selectin nor thrombomodulin in mvECs cultured on TC or COL I. However, all newly formed prevascular-like structures showed expression of E-selectin and thrombomodulin on all cdECM substrates. Further, E-selectin and thrombomodulin expression of the prevascular-like structures were found in the newly formed prevascular-like structures on both FL approaches. E-selectin and thrombomodulin staining corresponded to the CD31 staining pattern of the prevascular-like structures (Supplementary figure 1).

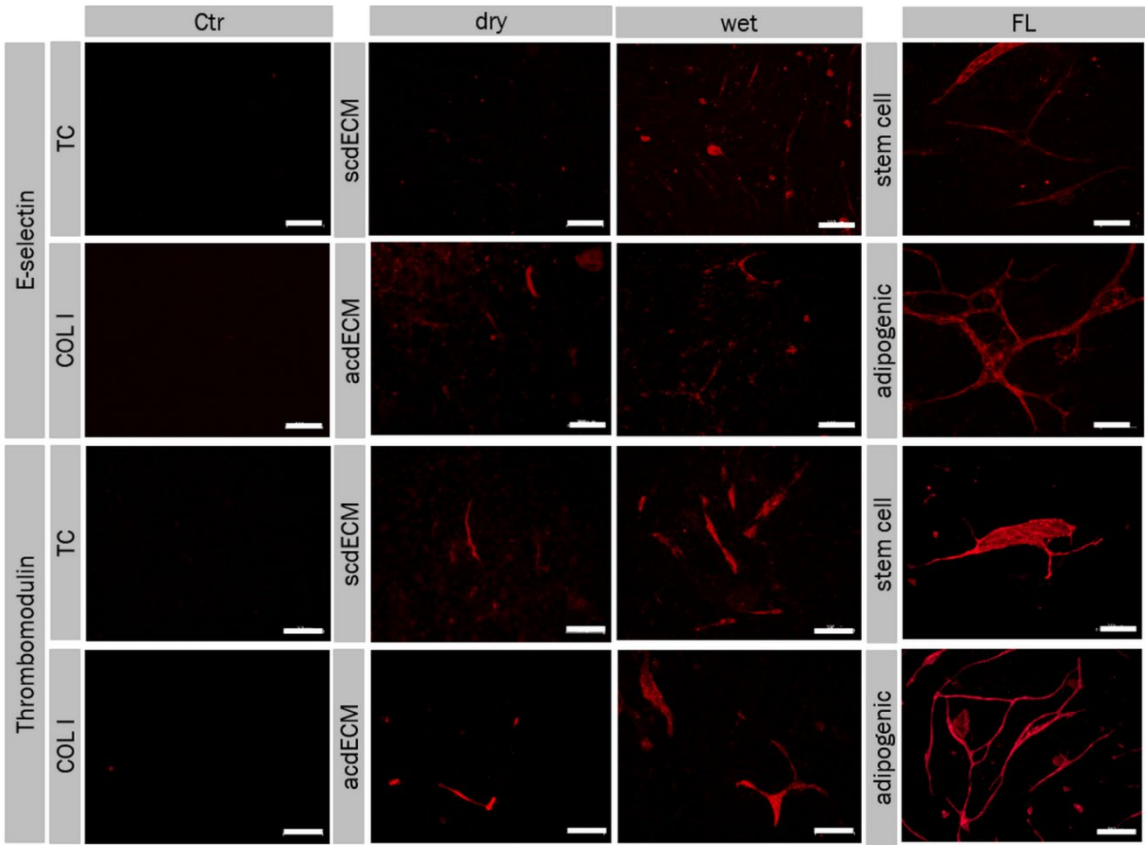

Figure 6: Expression of E-selectin and thrombomodulin by mvECs forming prevascular-like structures. 1 x 10^4 mvECs /cm^2 were seeded in defined co-culture medium onto the different substrates and were cultured for 14 days. Medium was changed three times a week. For both proteins, no specific staining was observed on controls (TC and COL I coating). For all acellular and cellular substrates, specific staining of E-selectin and thrombomodulin (both indicated in red) could be found mainly on the newly formed prevascular-like structures. (Scale bar: 200 µm)

Discussion

The implementation of a functional vascular system into an engineered tissue construct would address one of the major bottlenecks in tissue engineering and regenerative medicine. In the present study, we aimed to investigate the supportive effect of cdECM on the self-assembled formation of prevascular-like structures by mvECs for its use as a biomaterial for adipose tissue engineering compared to the well-established application of a supportive FL.

Determination of the degree of swelling revealed a higher capacity of water uptake of the adipogenic ECM compared to stem cell ECM. This effect can be explained by the larger pore size in acdECM shown by fibronectin staining. The development of larger pores in acdECM may be explained by morphological changes of ASCs during adipogenesis. By incorporating lipids, adipogenically differentiated ASCs develop a more spherical shape compared to the stem cells and substantially increase their volume (Moldovan et al., 2019). During adipogenesis ASCs further stop to proliferate which results in a lower total cell number in adipogenic approaches (Fajas, 2003). Thus the amount of cdECM in stem cell approaches may be higher which leads to more densely packed collagen fibers and smaller pores. The larger pores found in adipogenic ECM may also be able to enhance the degree of prevascular-like structure formation by mvECs. Chui et al. showed that larger pore size is associated with a higher degree of neovascularization in an in vitro PEG hydrogel model (Chiu et al., 2011). Furthermore, Artel et al. proposed an agent-based model indicating that pores of larger size support vascularization in a polymer scaffold (Artel, Mehdizadeh, Chiu, Brey, & Cinar, 2011).

Analysis of LDH release of mvECs on the substrates revealed no cytotoxic effects of the cdECM substrates, the FL cells or the controls (COL I coating and TC). Even on day 14 after seeding, a confluent viable monolayer of mvECs was observed which indicates a good cytocompatibility of the cdECM substrates and their possible use in tissue engineering. Nearly no dead mvECs were observed during the quantification of the live/dead staining on acellular substrates. For the stem cell FL approach, less than 1 % of dead cells could be found. However, on the adipogenic FL approach around 4 % of dead cells could be found for FL with and without mvECs. Adipogenically differentiated ASCs may be more sensitive to the change to the defined co-culture medium compared to the non-differentiated ASCs which leads to an increase of cell death. For comprehensive toxicological and immunogenic characterization further analysis is required, e.g. the analysis of the cdECM impact on the metabolic activity of the mvECs and for the intended in vivo use, biocompatibility of the cdECM has to be evaluated.

Visualization of mvECs on day 14 after seeding by staining of the specific surface protein CD31 showed the self-assembled formation of prevascular-like structures on all substrates except for

the controls COL I and TC. Structure formation on the adipogenic FL approach was in line with our previous study (Volz et al., 2018) as a lower degree of structure formation was found on the stem cell FL approach. In addition, on dry and wet cdECM approaches, the degree of prevascular-like structure formation on adipogenic ECM substrates was higher compared to the corresponding stem cell approach, which is reflected by longer structures and a higher number of nodes. The effect of enhanced structure formation on adipogenic substrates could be explained by the different secretomes of ASCs and (pre-)adipocytes (Kapur & Katz, 2013). It is well known that ASCs secrete a broad spectrum of pro-angiogenic proteins and they were often used as a delivery system of growth factors and cytokines in vascularization approaches (Kondo et al., 2009; Liu et al., 2011; Moon et al., 2006; Nakagami, Maeda, Kaneda, Ogihara, & Morishita, 2005; Rehman et al., 2004). For example, Matusda et al. showed that conditioned cell culture medium of ASCs positively influenced EC proliferation and the formation of new vessels in vivo (Matsuda et al., 2013). During adipogenic differentiation, ASCs secret further pro-angiogenic factors like leptin. Leptin is known to be upregulated during adipogenic differentiation and was shown to exhibit a pro-angiogenic effect itself but also upregulates the secretion of VEGF (Cao, Brakenhielm, Wahlestedt, Thyberg, & Cao, 2001). By secreting their specific set of proteins, ASCs and (pre-)adipocytes not only condition their cell culture medium but also their ECM which we use in this study as a biomaterial for induction of prevascular-like structure formation by mvECs. Thus, cdECM does not only contain a set of specific factors, but a broad spectrum pro-angiogenic factors with its synergistic effects needed for the successful formation of prevascular-like structures by ECs. Especially acdECM induces the formation of prevascular-like structures and seems to be able to stabilize the newly formed structures.

The two most important pro-angiogenic factors are VEGF and bFGF. Results revealed higher VEGF concentrations released from acdECM substrates compared to scdECM approaches. On FL approaches high amounts of VEGF were found, most likely produced by FL cells. These results are in line with the degree of prevascular-like structure formation. On acdECM approaches, longer and more branched structures were formed whereas on FL approaches the highest degree of structure formation occurred. Determination of the bFGF concentration in the different substrates revealed a higher concentration from cdECM substrates compared to controls and the highest bFGF concentration from FL approaches. Both factors – VEGF and bFGF – are able to induce the formation of new vascular structures (Marra et al., 2008; Murakami & Simons, 2008; Nissen et al., 2007; Tomanek, Hansen, & Christensen, 2008). Therefore, in our study, the induction of the formation of prevascular-like structures may among other events, be attributed to the synergistic effect of available VEGF and bFGF. We further investigated the amount of pro-angiogenic factor

PDGFβ from cdECM substrates. It is secreted by ECs during angiogenesis to attract perivascular cells, which stabilize the newly formed vessels (Gaengel et al., 2009). Further, PDGFβ was shown to induce vascular structure formation by modulating proliferation and tube formation of ECs (Battegay, Rupp, Iruela-Arispe, Sage, & Pech, 1994). PDGFβ can be found in all cdECM substrates as well as FL approaches. The PDGFβ concentration from FL approaches is higher compared to the other substrates which is in line with the higher degree of structure formation. In vivo, these growth factors are known to be partially bound to ECM after their secretion (Ostman, Andersson, Betsholtz, Westermark, & Heldin, 1991). To date, there are no studies investigating their binding capacity and protein half-life in in vitro generated cdECM.

A critical step in the formation of a new vascular system is the formation of a lumen in the vascular structure to enable perfusion with blood in vivo and culture medium in vitro. Recent studies show that the adhesion proteins E-selectin and thrombomodulin are associated with tube formation. In vivo, E-selectin is mainly contributing to the binding of immune cells by mediating adhesive interactions of circulating leukocytes with the endothelium (Ley & Tedder, 1995). Nevertheless, it also plays a role in the homing of endothelial progenitor cells (EPCs) and therefore promotes neovascularization. Studies showed that E-selectin potentiates angiogenesis in ischaemic tissue, by mediating EPC-endothelial interactions (Oh et al., 2007). During this process of neovascularization, EPCs are mobilized from the bone marrow into the circulation and recruited to new sites of vascularization, using cues that resemble an inflammatory response. Therefore, E-selectin plays a crucial role in EPC homing and following neovascularization and tube formation. Thrombomodulin is a transmembrane protein expressed on ECs acting as an anticoagulant (Dahlback & Villoutreix, 2005; Dittman & Majerus, 1990). The fourth and fifth region of an epidermal growth factor (EGF)-like region of thrombomodulin (TME45) was shown to stimulate the proliferation of human umbilical vein ECs and to promote tube formation and angiogenesis (Ikezoe et al., 2017). In this study, we use these proteins as indicators for the development of the prevascular-like structure towards a tubular vascular structure with a lumen. IF staining of E-selectin and thrombomodulin revealed specific expression of E- selectin almost exclusively on the newly formed prevascular-like structures. Thus, we suggest that newly formed prevascular-like structures exhibit promising characteristics to develop a lumen. The expression of E-selectin and thrombomodulin and their function in tube formation and neovascularization in vivo represent promising characteristics when considering implantation of prevascularized constructs.

Compared to ECM derived from native tissue, cdECM exhibited a variety of advantages which makes it a promising biomaterial for tissue engineering. For example, the possibility of autologous production without harvesting high amounts of autologous tissue and the generation of ECM from

different developmental stages. This study confirms a supportive effect of cdECM on the spontaneous formation of prevascular-like structures by mvECs. Further, it could be shown that dry cdECM partly maintains its biological properties regarding the induction of the self-assembled prevascular-like structure formation of mvECs with some restrictions. Drying of the cdECM would be a convenient method for improving storage possibilities when necessary. Due to the relatively low amounts of cdECM, which can be produced with current methods this study is limited to 2D approaches, which insufficiently reflect physiological conditions. Further studies should focus on the up-scaling of the generation of cdECM to enable the setup of continuative experiments in 3D constructs consisting of cdECM, which would better reflect in vivo situation.

Conclusion

In the present study, we demonstrated that cdECM (as a dry coating and as a wet hydrogel-like form) is able to induce the self-assembled formation of prevascular-like structures by mvECs and helps to support their maintenance. Mainly acdECM was confirmed as a promising material for adipose tissue engineering by supporting the formation of prevascular-like structures. In addition, scdECM also provides the ability to induce prevascular-like structure formation and can be used for approaches addressing other tissues. In further investigations regarding other lineage-specific cdECMs, the upscaling of cdECM generation and the transfer from 2D cell culture to 3D cell culture should be pursued.

Acknowledgments

This study was financially supported by the Landesgraduiertenförderung by the Ministry of Science, Research and the Arts (Baden-Württemberg, Germany) under the program “Intelligent Process and Material Development in Biomateriomics” (University of Tuebingen and Reutlingen University).

Conflicts of interest

The authors declare no conflict of interest.

References

Adam Young, D., Bajaj, V., & Christman, K. L. (2014). Award winner for outstanding research in the PhD category, 2014 Society for Biomaterials annual meeting and exposition, Denver, Colorado, April 16-19, 2014: Decellularized adipose matrix hydrogels stimulate in vivo neovascularization and adipose formation. J Biomed Mater Res A, 102(6), 1641-1651. doi: 10.1002/jbm.a.35109

Artel, A., Mehdizadeh, H., Chiu, Y. C., Brey, E. M., & Cinar, A. (2011). An agent-based model for the investigation of neovascularization within porous scaffolds. Tissue Eng Part A, 17(17-18), 2133-2141. doi: 10.1089/ten.TEA.2010.0571

Badylak, S. F., Freytes, D. O., & Gilbert, T. W. (2009). Extracellular matrix as a biological scaffold material: Structure and function. Acta Biomater, 5(1), 1-13. doi: 10.1016/j.actbio.2008.09.013

Battegay, E. J., Rupp, J., Iruela-Arispe, L., Sage, E. H., & Pech, M. (1994). PDGF-BB modulates endothelial proliferation and angiogenesis in vitro via PDGF beta-receptors. J Cell Biol, 125(4), 917-928. doi: 10.1083/jcb.125.4.917

Bayless, K. J., & Davis, G. E. (2002). The Cdc42 and Rac1 GTPases are required for capillary lumen formation in three-dimensional extracellular matrices. J Cell Sci, 115(Pt 6), 1123-1136.

Cao, R., Brakenhielm, E., Wahlestedt, C., Thyberg, J., & Cao, Y. (2001). Leptin induces vascular permeability and synergistically stimulates angiogenesis with FGF-2 and VEGF. Proc Natl Acad Sci U S A, 98(11), 6390-6395. doi: 10.1073/pnas.101564798

Chiu, Y. C., Cheng, M. H., Engel, H., Kao, S. W., Larson, J. C., Gupta, S., & Brey, E. M. (2011). The role of pore size on vascularization and tissue remodeling in PEG hydrogels. Biomaterials, 32(26), 6045-6051. doi: 10.1016/j.biomaterials.2011.04.066

Dahlback, B., & Villoutreix, B. O. (2005). The anticoagulant protein C pathway. FEBS Lett, 579(15), 3310-3316. doi: 10.1016/j.febslet.2005.03.001

Dittman, W. A., & Majerus, P. W. (1990). Structure and function of thrombomodulin: a natural anticoagulant. Blood, 75(2), 329-336.

Dzobo, K., Turnley, T., Wishart, A., Rowe, A., Kallmeyer, K., van Vollenstee, F. A., . . . Parker, M. I. (2016). Fibroblast-Derived Extracellular Matrix Induces Chondrogenic Differentiation in Human Adipose-Derived Mesenchymal Stromal/Stem Cells in Vitro. Int J Mol Sci, 17(8). doi: Artn 1259

10.3390/Ijms17081259

Fajas, L. (2003). Adipogenesis: a cross-talk between cell proliferation and cell differentiation. Ann Med, 35(2), 79-85. doi: 10.1080/07853890310009999

Flynn, L., Prestwich, G. D., Semple, J. L., & Woodhouse, K. A. (2009). Adipose tissue engineering in vivo with adipose-derived stem cells on naturally derived scaffolds. Journal of Biomedical Materials Research Part A, 89A(4), 929-941. doi: 10.1002/jbm.a.32044

Flynn, L. E. (2010). The use of decellularized adipose tissue to provide an inductive microenvironment for the adipogenic differentiation of human adipose-derived stem cells. Biomaterials, 31(17), 4715-4724. doi: 10.1016/j.biomaterials.2010.02.046

Gaengel, K., Genove, G., Armulik, A., & Betsholtz, C. (2009). Endothelial-mural cell signaling in vascular development and angiogenesis. Arterioscler Thromb Vasc Biol, 29(5), 630-638. doi: 10.1161/ATVBAHA.107.161521

Guneta, V., Loh, Q. L., & Choong, C. (2016). Cell-secreted extracellular matrix formation and differentiation of adipose-derived stem cells in 3D alginate scaffolds with tunable properties. J Biomed Mater Res A, 104(5), 1090-1101. doi: 10.1002/jbm.a.35644

Guneta, V., Zhou, Z., Tan, N. S., Sugii, S., Wong, M. T. C., & Choong, C. (2017). Recellularization of decellularized adipose tissue-derived stem cells: role of the cell-secreted extracellular matrix in cellular differentiation. Biomaterials Science, 6(1), 168-178. doi: 10.1039/c7bm00695k

Guo, Y., Zeng, Q. C., Yan, Y. X., Shen, L., Liu, L., Li, R. X., . . . Huang, S. J. (2013). Proliferative effect and osteoinductive potential of extracellular matrix coated on cell culture plates.

Springerplus, 2. doi: Artn 303
10.1186/2193-1801-2-303
Huber, B., Borchers, K., Tovar, G. E., & Kluger, P. J. (2016). Methacrylated gelatin and mature adipocytes are promising components for adipose tissue engineering. J Biomater Appl, 30(6), 699-710. doi: 10.1177/0885328215587450
Ikezoe, T., Yang, J., Nishioka, C., Pan, B., Xu, K., Furihata, M., . . . Yokoyama, A. (2017). The fifth epidermal growth factor-like region of thrombomodulin exerts cytoprotective function and prevents SOS in a murine model. Bone Marrow Transplant, 52(1), 73-79. doi: 10.1038/bmt.2016.195
Kapur, S. K., & Katz, A. J. (2013). Review of the adipose derived stem cell secretome. Biochimie, 95(12), 2222-2228. doi: 10.1016/j.biochi.2013.06.001
Kondo, K., Shintani, S., Shibata, R., Murakami, H., Murakami, R., Imaizumi, M., . . . Murohara, T. (2009). Implantation of Adipose-Derived Regenerative Cells Enhances Ischemia-Induced Angiogenesis. Arteriosclerosis Thrombosis and Vascular Biology, 29(1), 61-U167. doi: 10.1161/Atvbaha.108.166496
Laschke, M. W., & Menger, M. D. (2016). Prevascularization in tissue engineering: Current concepts and future directions. Biotechnology Advances, 34(2), 112-121. doi: 10.1016/j.biotechadv.2015.12.004
Laschke, M. W., Rucker, M., Jensen, G., Carvalho, C., Mulhaupt, R., Gellrich, N. C., & Menger, M. D. (2008). Incorporation of growth factor containing Matrigel promotes vascularization of porous PLGA scaffolds. J Biomed Mater Res A, 85(2), 397-407. doi: 10.1002/jbm.a.31503
Laschke, M. W., Strohe, A., Scheuer, C., Eglin, D., Verrier, S., Alini, M., . . . Menger, M. D. (2009). In vivo biocompatibility and vascularization of biodegradable porous polyurethane scaffolds for tissue engineering. Acta Biomater, 5(6), 1991-2001. doi: 10.1016/j.actbio.2009.02.006
Laschke, M. W., Vollmar, B., & Menger, M. D. (2009). Inosculation: connecting the life-sustaining pipelines. Tissue Eng Part B Rev, 15(4), 455-465. doi: 10.1089/ten.TEB.2009.0252
Ley, K., & Tedder, T. F. (1995). Leukocyte interactions with vascular endothelium. New insights into selectin-mediated attachment and rolling. J Immunol, 155(2), 525-528.
Liu, S., Zhang, H., Zhang, X., Lu, W., Huang, X., Xie, H., . . . Jin, Y. (2011). Synergistic angiogenesis promoting effects of extracellular matrix scaffolds and adipose-derived stem cells during wound repair. Tissue Eng Part A, 17(5-6), 725-739. doi: 10.1089/ten.TEA.2010.0331
Lu, H. X., Hoshiba, T., Kawazoe, N., & Chen, G. P. (2011). Autologous extracellular matrix scaffolds for tissue engineering. Biomaterials, 32(10), 2489-2499. doi: 10.1016/j.biomaterials.2010.12.016
Lu, H. X., Hoshiba, T., Kawazoe, N., Koda, I., Song, M. H., & Chen, G. P. (2011). Cultured cell-derived extracellular matrix scaffolds for tissue engineering. Biomaterials, 32(36), 9658-9666. doi: 10.1016/j.biomaterials.2011.08.091
Marra, K. G., DeFail, A., Clavijo-Alvarez, J. A., Badylak, S. F., Taieb, A., Schipper, B., . . . Rubin, J. P. (2008). FGF-2 enhances vascularization for adipose tissue engineering. Plast Reconstr Surg, 121(4), 1153-1164. doi: 10.1097/01.prs.0000305517.93747.72
Matsuda, K., Falkenberg, K. J., Woods, A. A., Choi, Y. S., Morrison, W. A., & Dilley, R. J. (2013). Adipose-derived stem cells promote angiogenesis and tissue formation for in vivo tissue engineering. Tissue Eng Part A, 19(11-12), 1327-1335. doi: 10.1089/ten.TEA.2012.0391
Moldovan, L. M. Y., Lustig, M., Naftaly, A., Mardamshina, M., Geiger, T., Gefen, A., & Benayahu, D. (2019). Cell shape alteration during adipogenesis is associated with coordinated matrix cues. J Cell Physiol, 234(4), 3850-3863. doi: 10.1002/jcp.27157
Moon, M. H., Kim, S. Y., Kim, Y. J., Kim, S. J., Lee, J. B., Bae, Y. C., . . . Jung, J. S. (2006). Human adipose tissue-derived mesenchymal stem cells improve postnatal neovascularization in a mouse model of hindlimb ischemia. Cellular Physiology and Biochemistry, 17(5-6), 279-290. doi: Doi 10.1159/000094140
Murakami, M., & Simons, M. (2008). Fibroblast growth factor regulation of neovascularization.

Curr Opin Hematol, 15(3), 215-220. doi: 10.1097/MOH.0b013e3282f97d98

Nakagami, H., Maeda, K., Kaneda, Y., Ogihara, T., & Morishita, R. (2005). Novel autologous cell therapy in ischemic limb disease through growth factor secretion by cultured adipose tissue-derived stromal cells. Hypertension, 46(4), 867-867.

Nissen, L. J., Cao, R., Hedlund, E. M., Wang, Z., Zhao, X., Wetterskog, D., . . . Cao, Y. (2007). Angiogenic factors FGF2 and PDGF-BB synergistically promote murine tumor neovascularization and metastasis. J Clin Invest, 117(10), 2766-2777. doi: 10.1172/JCI32479

Oh, I. Y., Yoon, C. H., Hur, J., Kim, J. H., Kim, T. Y., Lee, C. S., . . . Kim, H. S. (2007). Involvement of E-selectin in recruitment of endothelial progenitor cells and angiogenesis in ischemic muscle. Blood, 110(12), 3891-3899. doi: 10.1182/blood-2006-10-048991

Olive, P. L., Vikse, C., & Trotter, M. J. (1992). Measurement of Oxygen Diffusion Distance in Tumor Cubes Using a Fluorescent Hypoxia Probe. International Journal of Radiation Oncology Biology Physics, 22(3), 397-402. doi: Doi 10.1016/0360-3016(92)90840-E

Ostman, A., Andersson, M., Betsholtz, C., Westermark, B., & Heldin, C. H. (1991). Identification of a cell retention signal in the B-chain of platelet-derived growth factor and in the long splice version of the A-chain. Cell Regul, 2(7), 503-512. doi: 10.1091/mbc.2.7.503

Pan, B., Wang, X., Nishioka, C., Honda, G., Yokoyama, A., Zeng, L., . . . Ikezoe, T. (2017). G-protein coupled receptor 15 mediates angiogenesis and cytoprotective function of thrombomodulin. Sci Rep, 7(1), 692. doi: 10.1038/s41598-017-00781-w

Piali, L., Hammel, P., Uherek, C., Bachmann, F., Gisler, R. H., Dunon, D., & Imhof, B. A. (1995). CD31/PECAM-1 is a ligand for alpha v beta 3 integrin involved in adhesion of leukocytes to endothelium. J Cell Biol, 130(2), 451-460. doi: 10.1083/jcb.130.2.451

Rehman, J., Traktuev, D., Li, J., Merfeld-Clauss, S., Temm-Grove, C. J., Bovenkerk, J. E., . . . March, K. L. (2004). Secretion of angiogenic and antiapoptotic factors by human adipose stromal cells. Circulation, 109(10), 1292-1298. doi: 10.1161/01.CIR.0000121425.42966.F1

Sart, S., Yan, Y. W., Li, Y., Lochner, E., Zeng, C. C., Ma, T., & Li, Y. (2016). Crosslinking of extracellular matrix scaffolds derived from pluripotent stem cell aggregates modulates neural differentiation. Acta Biomater, 30, 222-232. doi: 10.1016/j.actbio.2015.11.016

Schenke-Layland, K., Rofail, F., Heydarkhan, S., Gluck, J. M., Ingle, N. P., Angelis, E., . . . Heydarkhan-Hagvall, S. (2009). The use of three-dimensional nanostructures to instruct cells to produce extracellular matrix for regenerative medicine strategies. Biomaterials, 30(27), 4665-4675. doi: 10.1016/j.biomaterials.2009.05.033

Thomlinson, R. H., & Gray, L. H. (1955). The histological structure of some human lung cancers and the possible implications for radiotherapy. Br J Cancer, 9(4), 539-549. doi: 10.1038/bjc.1955.55

Tomanek, R. J., Hansen, H. K., & Christensen, L. P. (2008). Temporally expressed PDGF and FGF-2 regulate embryonic coronary artery formation and growth. Arterioscler Thromb Vasc Biol, 28(7), 1237-1243. doi: 10.1161/ATVBAHA.108.166454

Verseijden, F., Posthumus-van Sluijs, S. J., Farrell, E., van Neck, J. W., Hovius, S. E. R., Hofer, S. O. P., & van Osch, G. J. V. M. (2010). Prevascular Structures Promote Vascularization in Engineered Human Adipose Tissue Constructs Upon Implantation. Cell Transplant, 19(8), 1007-1020. doi: 10.3727/096368910X492571

Verseijden, F., Posthumus-van Sluijs, S. J., Pavljasevic, P., Hofer, S. O. P., van Osch, G. J. V. M., & Farrell, E. (2010). Adult Human Bone Marrow- and Adipose Tissue-Derived Stromal Cells Support the Formation of Prevascular-like Structures from Endothelial Cells In Vitro. Tissue Engineering Part A, 16(1), 101-114. doi: 10.1089/ten.tea.2009.0106

Verseijden, F., Posthumus-van Sluijs, S. J., van Neck, J. W., Hofer, S. O., Hovius, S. E., & van Osch, G. J. (2012). Comparing scaffold-free and fibrin-based adipose-derived stromal cell constructs for adipose tissue engineering: an in vitro and in vivo study. Cell Transplant, 21(10), 2283-2297. doi: 10.3727/096368912X653129

Volz, A. C., Hack, L., Atzinger, F. B., & Kluger, P. J. (2018). Completely Defined Co-Culture of

Adipogenic Differentiated ASCs and Microvascular Endothelial Cells. Altex-Alternatives to Animal Experimentation, 35(4), 464-476. doi: 10.14573/altex.1802191

Volz, A. C., Huber, B., Schwandt, A. M., & Kluger, P. J. (2017). EGF and hydrocortisone as critical factors for the co-culture of adipogenic differentiated ASCs and endothelial cells. Differentiation, 95, 21-30. doi: 10.1016/j.diff.2017.01.002

Walser, R., Metzger, W., Gorg, A., Pohlemann, T., Menger, M. D., & Laschke, M. W. (2013). Generation of co-culture spheroids as vascularisation units for bone tissue engineering. Eur Cell Mater, 26, 222-233. doi: 10.22203/ecm.v026a16

Wenz, A., Tjoeng, I., Schneider, I., Kluger, P. J., & Borchers, K. (2018). Improved vasculogenesis and bone matrix formation through coculture of endothelial cells and stem cells in tissue-specific methacryloyl gelatin-based hydrogels. Biotechnology and Bioengineering, 115(10), 2643-2653. doi: 10.1002/bit.26792

Wolchok, J. C., & Tresco, P. A. (2010). The isolation of cell derived extracellular matrix constructs using sacrificial open-cell foams. Biomaterials, 31(36), 9595-9603. doi: 10.1016/j.biomaterials.2010.08.072

Yoon, J. J., Chung, H. J., Lee, H. J., & Park, T. G. (2006). Heparin-immobilized biodegradable scaffolds for local and sustained release of angiogenic growth factor. Journal of Biomedical Materials Research Part A, 79A(4), 934-942. doi: 10.1002/jbm.a.30843

Supplements

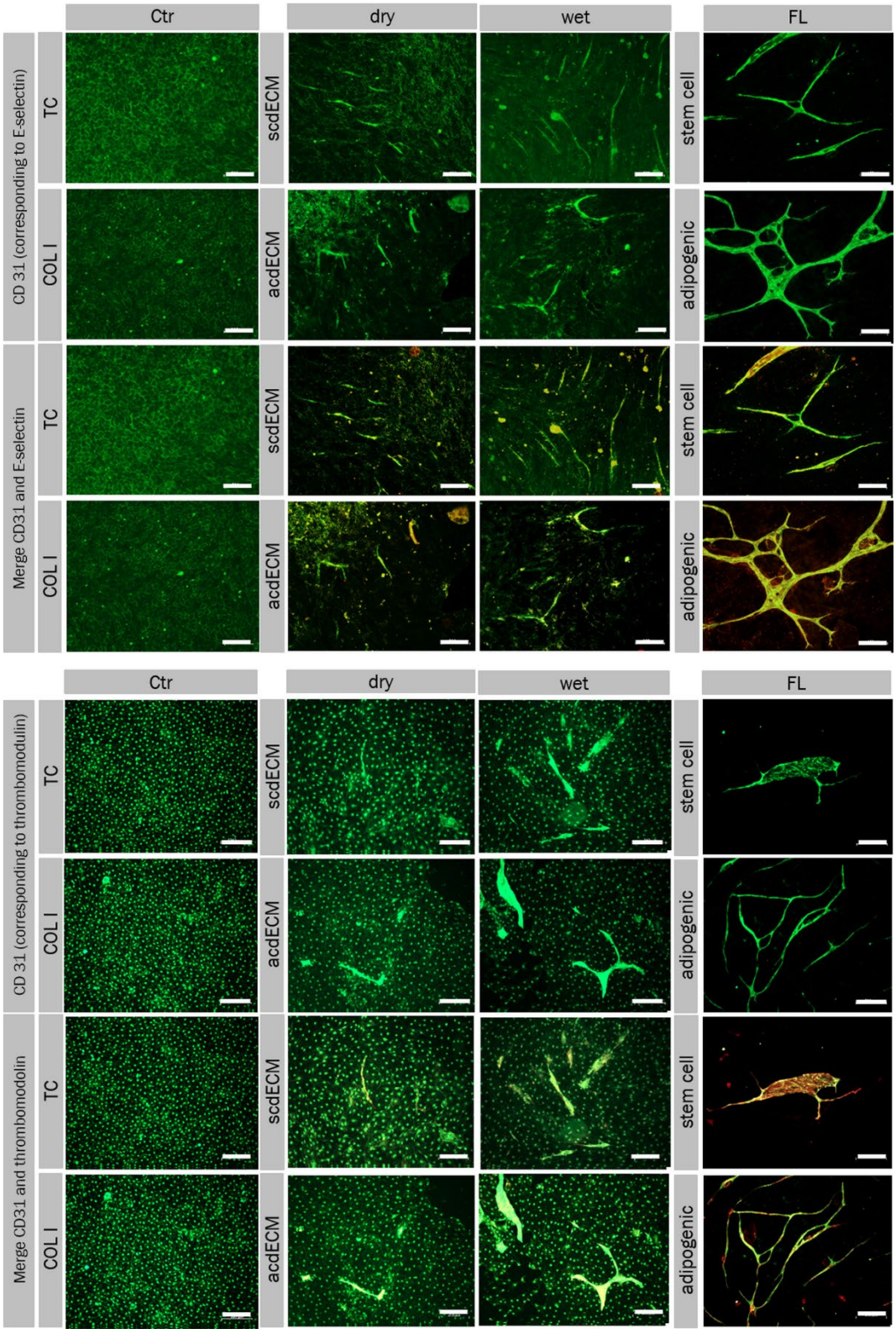

Supplementary Figure 1: CD31 staining and merged images of samples stained for E-selectin and thrombomodulin. Both corresponding to Figure 6. (Scale bar: 200µm; green: CD31, red: E-selectin and thrombomodulin in the different sections, white: Nuclei)

5 PAPER III – FUNCTIONALIZATION OF CDECM

This chapter was originally published in the journal *ChemBioChem* (DOI*:* 10.1002/cbic.202100266)[4]*.* In this study metabolic glycoengineering was employed to incorporate dienophiles (terminal alkenes and a cyclopropene) into the extracellular matrix (ECM) of adipose-derived stem cells (ASCs) (**Figure 10**).

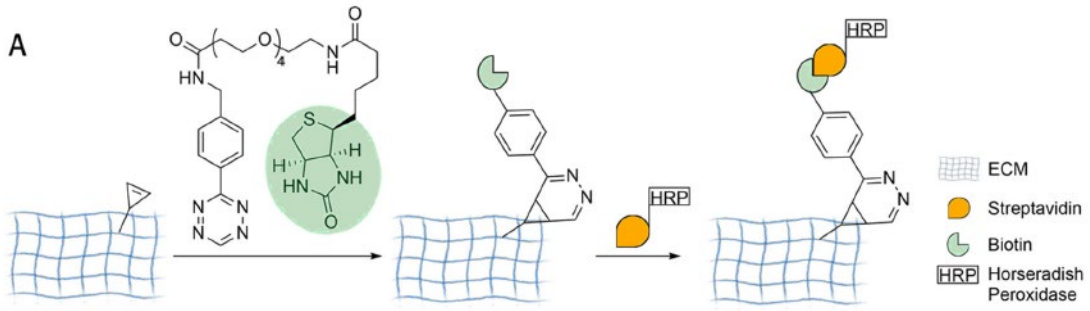

Figure 10: Graphical abstract Paper III (An Advanced "clickECM" that Can be Modified by the Inverse-Electron Demand Diels-Alder Reaction)

It was demonstrated that dienophiles were successfully incorporated into the ECM of ASCs by MGE. These results confirm the fourth hypothesis (H4). Further it was shown that functionalized cdECM can be successfully equipped with bioactive molecules via IEDDA reaction, which confirms fourth hypothesis (H4). Furthermore, it was proven that the functionalization itself has no impact on survival and proliferation of ASCs incorporated in a gellan gum-cdECM-hybrid hydrogel.

[4] Reprinted from *An Advanced 'clickECM' That Can be Modified by the Inverse-Electron-Demand Diels-Alder Reaction*; Nellinger S, Rapp MA, Southan A, Wittmann V, Kluger PJ. Chembiochem. 2022 Jan 5;23(1). with permission from Wiley-VCH GmbH under CC-BY-NC 4.0

An Advanced "clickECM" that Can be Modified by the Inverse-Electron Demand Diels-Alder Reaction

Svenja Nellinger,[a] Mareike A. Rapp,[b] Alexander Southan,[c] Valentin Wittmann,*[b] and Petra J. Kluger*[a]

[a] S. Nellinger, Prof. Dr. P. J. Kluger
Reutlingen Research Institute
Reutlingen University, School of Applied Chemistry
Alteburgstr. 150, 72762 Reutlingen, Germany
E-mail: Petra.Kluger@Reutlingen-University.de
[b] M. A. Rapp, Prof. Dr. V. Wittmann
Department of Chemistry and Konstanz Research School Chemical Biology (KoRS-CB)
University of Konstanz
Universitätsstr. 10, 78457 Konstanz, Germany
E-mail: mail@valentin-wittmann.de
[c] Dr. A. Southan
Institute of Interfacial Process Engineering and Plasma Technology
University of Stuttgart
Allmandring 5b, 70569 Stuttgart, Germany

Keywords: bioorthogonal chemistry • carbohydrates • extracellular matrix • inverse-electron-demand Diels-Alder reaction • metabolic engineering

Abstract

The extracellular matrix (ECM) represents the natural environment of the cells in tissue and therefore is a promising biomaterial in a variety of applications. Depending on the purpose it is necessary to equip the ECM with specific addressable functional groups for further modification with bioactive molecules, for controllable cross linking and/or covalent binding to surfaces. Metabolic glycoengineering (MGE) enables the specific modification of the ECM with such functional groups without affecting the native structure of the ECM. In a previous approach (S. M. Ruff, S. Keller, D. E. Wieland, V. Wittmann, G. E. M. Tovar, M. Bach, P. J. Kluger, Acta Biomater. 2017, 52, 159-170), we demonstrated the modification of an ECM with azido groups which can be addressed by biorthogonal copper-catalyzed azide-alkyne cycloaddition (CuAAC). Here we demonstrate the modification of an ECM with dienophiles (terminal alkenes, cyclopropene) which can be addressed by an inverseelectron- demand Diels-Alder (IEDDA) reaction. This reaction is cell friendly as there are no cytotoxic catalysts needed. We show the equipment of the ECM with a bioactive molecule (enzyme) and prove the functional groups itself not to influence cellular behavior. Thus, this new material has great potential for its use as biomaterial which can be individually modified in a wide range of applications.

Introduction

The extracellular matrix (ECM) is a complex network of various macromolecules, which is synthesized and assembled by the residing cells of a tissue. The main components of ECM are fibrous and nonfibrous collagens and various glycosaminoglycans and proteoglycans as well as adhesion proteins and enzymes.[1] As the ECM is the natural environment of the cells, it represents a promising biomaterial for regenerative medicine and tissue engineering approaches. Through cell-ECM-interaction, mainly mediated by the interaction of anchor proteins (e.g. integrins) and specific adhesion peptides (e.g. those containing the RGD sequence), a variety of cellular mechanisms are regulated related to the characteristics (e.g. stiffness, pore size) of the surrounding of the cell.[2] Also, different proteins (collagens, glycosaminoglycans (GAGs), proteoglycans) within the ECM and consequently the composition of the ECM have extensive impact on cellular behavior. Although individual ECM proteins are used as coating, scaffolds, and hydrogels in tissue engineering and regenerative medicine approaches, to date the complexity of the natural ECM cannot be rebuilt. Next to the decellularization of native tissues, in vitro generated cell-derived ECM represents a promising source for natural ECM. Among others, fibroblasts and mesenchymal stem cells were shown to produce relevant amounts of this cell-derived ECM.[3] Adipose-derived stem cells (ASCs), a subgroup of the mesenchymal stem cells,

represent a promising cell type as they can be obtained with minimal invasiveness and adipose tissue is permanently available. Previous studies demonstrated the high impact of natural ECM as coating or scaffold material on stem cell fate concerning adhesion, proliferation, and differentiation.[4] These cell-derived ECMs resemble the tissue specific ECM more closely than individual proteins and are used in a variety of applications.[3,5]

Depending on the application, it is desirable to covalently modify the ECM to achieve, for example, covalent linking on surfaces or cross-linking without affecting the structure or functionalization with molecules providing specific characteristics. One method to functionalize ECM is the application of amine-targeting strategies including N-hydroxysuccinimide (NHS) chemistry which ends up in unspecific conjugation to different amines. However, this unspecific conjugation can lead to a partial or full loss of the (bio)activity of the protein by the blockade of the active site.[6] Metabolic glycoengineering (MGE)[7] is a successful approach to introduce unnatural functional groups (so-called chemical reporter groups) into the glycan structures of glycoconjugates on the cell surface and within the ECM enabling site-directed conjugation of molecules. For MGE, cultured cells are treated with chemically modified monosaccharides which are metabolized by the cell and incorporated into the intra- and extracellular glycan structures. The incorporated chemical reporter group can now be reacted in a biorthogonal ligation reaction[8] which allows a chemoselective modification of the ECM without touching protein side chains. Previously, we[9] and others[10] reported the preparation of a functionalized ECM by MGE. For example, we demonstrated the incorporation of azide functionalities into the ECM of human fibroblasts[9a] and ASCs,[9b] which can be addressed via biorthogonal coppercatalyzed azide-alkyne cycloaddition (CuAAC).[11] We demonstrated different possible applications of the azide-modified 'clickECM' and showed, for example, the positive effect of a clickECM coating on the fibroblast culture and demonstrated the clickECM as a bioconjugation platform using biotinstreptavidin interaction.[12]

One disadvantage of this azide-modified clickECM is the need for copper as a catalyst for CuAAC. It is known that copper is cytotoxic, and it can be assumed that even after extensive washing significant amounts of copper remain in the ECM.[13] Alternative bioorthogonal ligation reactions that do not need any toxic catalyst include the strain-promoted azide-alkyne cycloaddition (SPAAC)[14] and the inverseelectron- demand Diels-Alder (IEDDA) reaction.[15] The latter has found widespread application as a bioorthogonal ligation reaction in various applications including MGE.[16] Dienophiles that undergo an IEDDA reaction with tetrazines and that have been used for MGE include terminal alkenes[17] and strained cyclic alkenes, such as cyclopropenes,[18] bicyclononynes,[19] and norbornenes.[20] These dienophiles can have markedly different

reaction kinetics enabling various applications including sequential modifications with different tetrazines.[21] Furthermore, the IEDDA reaction can be orthogonal to other bioorthogonal ligation reactions, such as the strain-promoted azide-alkyne cycloaddition (SPAAC) and the light-induced nitrile imine-alkene cycloaddition (photoclick reaction) enabling dual-[17a,18a] and even triple-orthogonal labeling[22] after incorporation of two or three differently modified monosaccharides. This opens future opportunities to modify the ECM simultaneously in two (or three) ways. These opportunities include but are not limited to the incorporation of bioactive molecules (e.g., growth factors or cell growth inhibiting molecules), enzymes, antibacterial substances, and cross-linking using specific linkers.

Here we present the investigation of a series of alkene-modified sugar derivatives and their suitability for the preparation of a new material, an advanced clickECM that can be modified by the IEDDA reaction. We demonstrate the incorporation of the dienophile functional group via the activity of a linked enzyme. Further, we show that the modification has no impact on the physical characteristics of gellan gum-ECM-hybrid hydrogels and the cellular behavior of encapsulated ASCs. These results highlight the possibilities of this new modified ECM material for different applications as the modification itself does not interfere with possible functionalization by, e.g., bioactive molecules.

Results and Discussion

Synthesis of modified monosaccharides

In previous experiments, Ac4GalNAz was demonstrated to be a suitable monosaccharide derivative for efficient incorporation into the ECM.[9a] For the preparation of a clickECM that can be modified by the IEDDA reaction, we thus synthesized a series of new dienophile-modified GalNAc derivatives (Scheme 1A). Galactosamine hydrochloride was neutralized with sodium methoxide and subsequently reacted with the respective alkene derivative activated either as succinimidyl carbonate (1a–c) or succinimidyl ester (1d). Acetylation with acetic anhydride in pyridine gave Ac4GalNBeoc, Ac4GalNPeoc, Ac4GalNHeoc, or Ac4GalNPtl. In addition, we synthesized the GalNAc derivatives depicted in Scheme 1B according to previously reported procedures (Ac4GalNAcryl,[23] Ac4GalNBtl,[17e] Ac4GalNHxl,[24] Ac4GalNCp[18g]). The GalNAc derivatives with terminal alkenes feature a lower reactivity in the IEDDA reaction than the cyclopropenyl derivative. However, they have a higher chemical stability which might be advantageous during the ECM preparation.

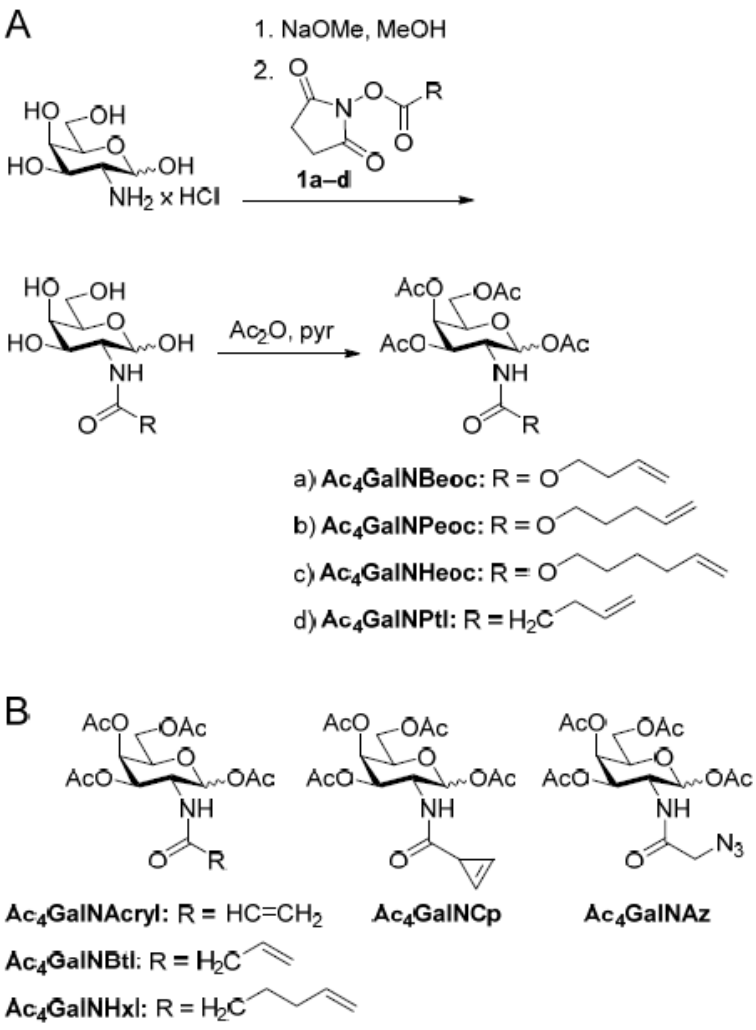

Scheme 1. A) Synthesis of dienophile-modified GalNAc derivatives. B) Investigated GalNAc derivatives that have been synthesized following published procedures.

Cytotoxicity of investigated modified monosaccharides

Good biocompatibility of the used monosaccharide derivates is needed to ensure the ECM-production capacity of the cells and to prevent the accumulation of unwanted cytokines in relevant concentrations within the produced ECM, which might exhibit a negative impact on the cells in further application of the ECM material. For example, the secretion and accumulation of tumor necrosis factor in the ECM might induce pro-inflammatory or even apoptotic pathways in cells that are in contact with the ECM material in further applications.[25]

To exclude any cytotoxic effects of the used monosaccharides, cell death (lactate dehydrogenase (LDH) assay) and metabolic activity (resazurin assay) after supplementation of the monosaccharides were determined (Figure 1). The LDH assay is based on the release of this enzyme during cell death, which can be colorimetrically quantified in the cell culture supernatant. The relative amount of LDH in the supernatant can be used to quantify cell death. The colorimetric

resazurin assay is based on the metabolic turnover of resazurin in the mitochondria of cells which reflects the metabolic activity of the cells.

The LDH release revealed no cytotoxic effects of any of the modified monosaccharides at the concentration used during MGE (100 µM) (Ac4GalNBeoc: (94.5 ± 11.8) %; Ac4GalNPeoc: (111.1 ± 19.1) %; Ac4GalNHeoc: (100.7 ± 14.0) %, Ac4GalNAcryl: (110.2 ± 9.1) %, Ac4GalNBtl: (103.6 ± 7.9) %, Ac4GalNPtl: (117.7 ± 35.2) %, Ac4GalNHxl: (109.5 ± 10.1) %, Ac4GalNCp: (60.2 ± 4.3) %) compared to the negative control ((100.0 ± 12.0) %) (Figure 1). Interestingly, the LDH release of ASCs treated with Ac4GalNCp was significantly lower compared to the other monosaccharides and the control, indicating an enhancing effect on cellular survival. However, the underlying mechanism of this effect is not known. The resazurin assay revealed that the metabolic activity of the ASCs treated with the modified monosaccharides (Ac4GalNBeoc: (87.1 ± 16.9) %; Ac4GalNPeoc: (89.8 ± 13.4) %; Ac4GalNHeoc: (90.4 ± 10.2) %; Ac4GalNAcryl: (79.7 ± 15.4) %; Ac4GalNBtl: (95.7 ± 8.4) %, Ac4GalNPtl: (89.9 ± 9.9) %; Ac4GalNHxl: (84.0 ± 12.3) %; Ac4GalNCp: (79.6 ± 14.8) %) was comparable to the negative control ((100.0 ± 2.2) %) (Figure 1). According to DIN EN ISO 10993-5, cytotoxic effects of a tested substance are indicated by a reduction of metabolic activity by 30 % or more following substance incubation (indicated by a red line). Thus, the results of the resazurin assay are in line with the LDH release and showed no cytotoxicity of the tested monosaccharides.

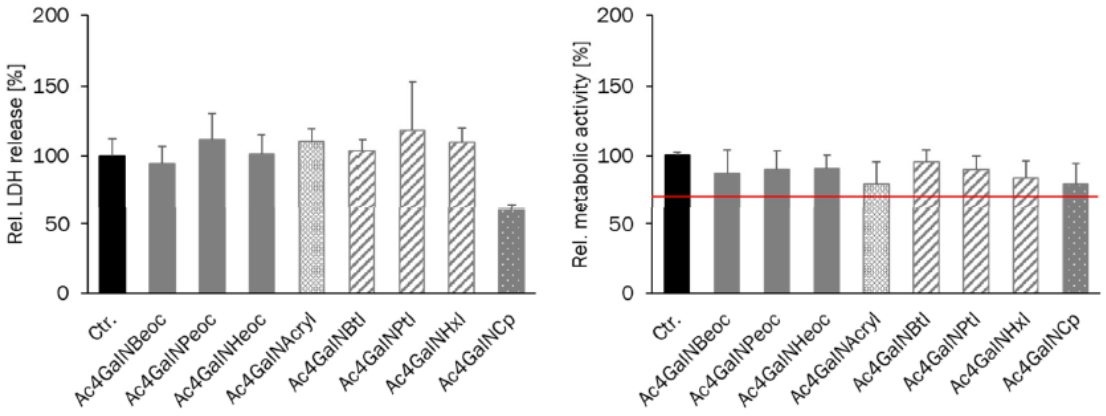

Figure 1. Cytotoxicity of monosaccharide derivatives. ASCs were seeded in growth medium at a density of 50.000 cells cm–2. Cytotoxicity of the monosaccharides was determined by measurement of LDH release (cell death) and resazurin turnover (metabolic activity) of ASCs treated with 100 µM of the compounds for 24 h. Negative control (Ctr.) was treated with sterile water. Values are the means of 3 independent experiments using cells from different donors (each 2 technical replicates) and normalized to the negative control, which was set as 100 %.

Incorporation of alkene-modified monosaccharides into the ECM

To prove the incorporation of the modified monosaccharides into the ECM by MGE, the presence of the functional groups was detected by tagging them with an enzyme and subsequent measurement of the enzymatic activity. This method was previously applied[12] and therefore considered as suitable for this purpose. By this method, we simultaneously demonstrated the incorporation of the functional groups and the possibility to covalently bind bioactive molecules such as enzymes to the ECM via the dienophile functional groups. Since all tested alkene-modified monosaccharides had a comparable low cytotoxicity, we focused on the carbamate-linked terminal alkenes because carbamate derivatives had higher incorporation efficiencies in previous studies on sialic acid labeling.[17c] In addition, we investigated Ac4GalNCp because of its much higher reactivity in the IEDDA reaction. The functional groups (terminal alkenes and cyclopropene) were ligated with a tetrazine-biotin conjugate by an IEDDA reaction (Figure 2 A). Subsequently, the biotin was labeled with horseradish peroxidase (HRP)-linked streptavidin. The unmodified negative control ECM (coECM) was treated in the same way as the samples. Addition of the substrate 3,3',5,5'-tetramethylbenzidine (TMB) allowed the quantification of HRP-tagged reporter groups by colorimetric detection.

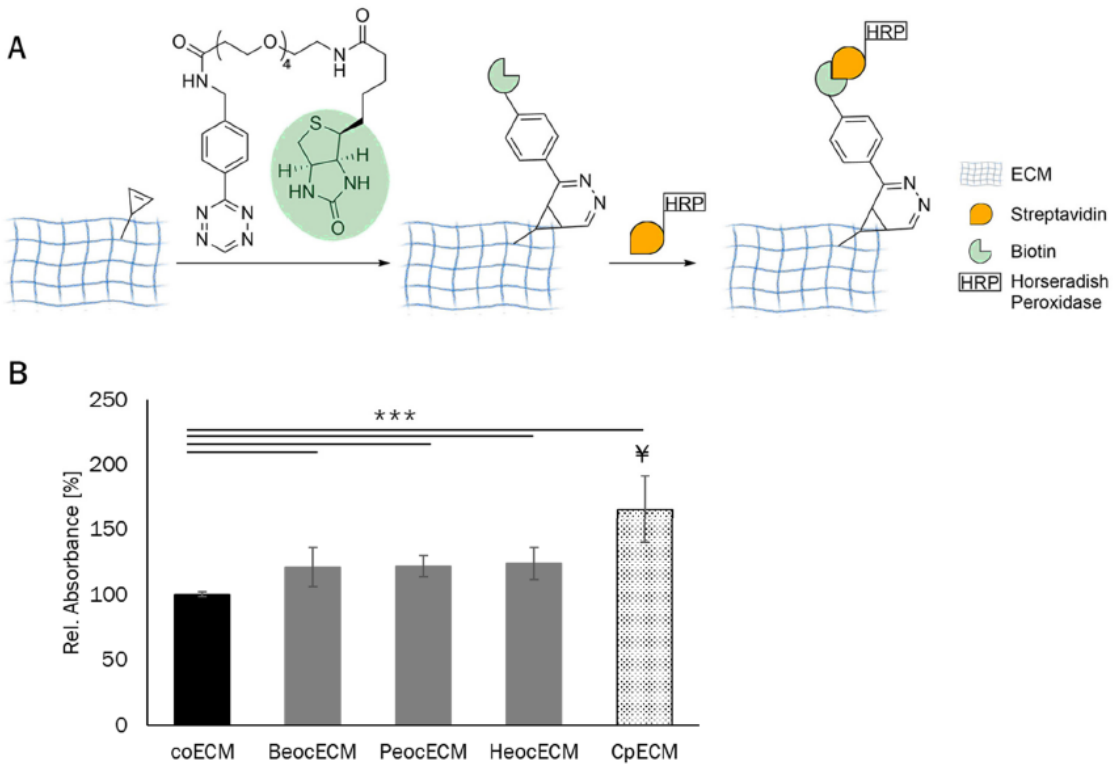

Figure 2. Detection of functional groups incorporated into the ECM. A) Schematic overview of the detection mechanism. Control ECM (coECM) and dienophile-modified ECM were concentrated, homogenized, and dried into a well plate, and incubated with a tetrazine-biotin conjugate (50 µM). After IEDDA reaction, biotin

residues were labeled with a streptavidin-HRP conjugate (6.6 µg/mL). Subsequent addition of HRP substrate TMB allowed the quantification of HRP by colorimetric detection of TMB turnover. B) Relative TMB turnover from 3 independent experiments using cells from different donors (each 2 technical replicates) normalized to the unmodified coECM (set to 100 %). *** $p \leq 0.001$, ¥ ≤ 0.001 to all other samples; partly created in BioRender.com

Figure 2 B shows the relative TMB turnover as an indicator for the incorporated functional groups. The value of the unmodified coECM was set to 100 % and values of the modified ECMs were normalized to the coECM. As expected, modified ECM produced by the use of dienophile-modified monosaccharides resulted in a significantly higher TMB turnover demonstrating successful functional group incorporation by this approach (BeocECM: (120.6 ± 14.8) %; PeocECM: (121.6 ± 8.1) %; HeocECM: (123.5 ± 12.2) %; CpECM: (165.6 ± 25.7) %). These results are in the same range as the results with an azide-modified clickECM that revealed a twofold turnover rate of the substrate compared to unmodified ECM.[12] The highest TMB turnover was found for the Cp modification. The labeling efficiency in MGE experiments depends on both the amount of reporter group incorporated and the chemical reactivity in the bioorthogonal ligation reaction.[16,17c] In case of the terminal alkenes, an increasing length of the side chain leads to higher reactivity in the IEDDA reaction. At the same time, it can be expected that the metabolic acceptance of the GalNAc derivative is lower with increasing length of the side chain. This might explain similar TMB turnover of the BeocECM, PeocECM, and HeocECM. Ac4GalNCp has a small reporter group and a high IEDDA reactivity which is in line with a higher TMB turnover of the CpECM. Since the Cp-modified ECM gave the highest TMB turnover, this material was used in all following experiments.

Impact of the advanced clickECM in 3D gellan gum-ECM-hybrid hydrogels

We showed that the incorporated dienophiles can be addressed by the IEDDA reaction. However, it cannot be ensured that all functional groups within the clickECM reacted with the tetrazine derivative. This also applies to a future modification of the clickECM, e.g., with growth factors using this system. Thus, we wanted to ensure that the functional group itself has no negative impact on cellular behavior. To investigate the influence of the functional group within the clickECM as biomaterial on cellular behavior, ASCs (300.000 cells/100 µL hydrogel) were encapsulated into ECM-gellan gum-hybrid hydrogels consisting of 1 wt% gellan gum and 0.25 wt% homogenized ECM (non-functionalized: coECM; azide-functionalized: AzECM; cyclopropene-functionalized: CpECM). Gellan gum is a mostly bioinert bacterial polysaccharide that is used in different tissue engineering approaches.[26] Gellan gum itself does not influence ASCs behavior and thus possible changes can be traced back to the ECM. Next to (bio)chemical characteristics, it is well known that the stiffness of a matrix has a high impact on cellular behavior.[2a,27] To

exclude differences in stiffness as a source for different behavior, rheological measurements were performed on hydrogels without ASCs (Figure 3). As a control, gellan gum hydrogels without ECM were measured (w/o ECM). The storage and loss modulus of the different hydrogels exhibit no significant differences. Thus, in this study, possible changes in cellular behavior of encapsulated ASCs can be traced back to the ECM and/or the modification with functional groups and not to differences in the stiffness of the hydrogel.

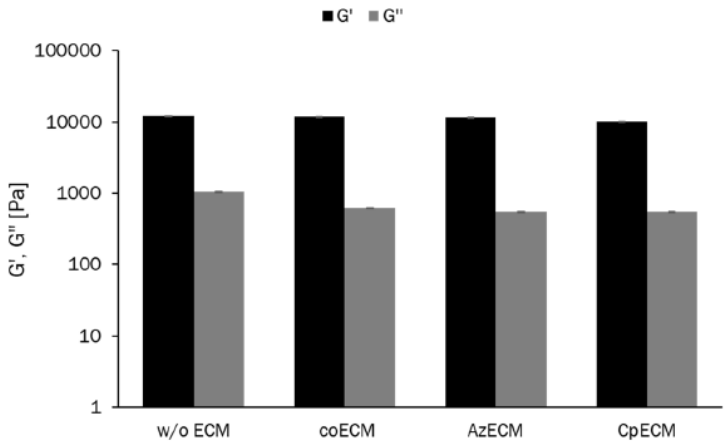

Figure 3. Stiffness of the hydrogels. For the determination of the stiffness of the hydrogels, ECM-gellan gum-hybrid hydrogels without ASCs were used (mean values of 3 independent experiments using cells from different donors). Determination of stiffness showed no significant difference between the different hybrid hydrogels.

The distribution of the ECM particles is a critical parameter for cell experiments that impacts the extent of possible interaction of cells with ECM and, therefore, the possible positive impact on cellular survival, proliferation, and differentiation.[4] To evaluate the distribution of the ECM particles within the hydrogels, we used ECM-gellan gum-hybrid hydrogels with encapsulated ASCs and performed hematoxylin eosin (HE) staining on histological slices (Figure 4). HE staining is a standard overview staining for the visualization of ECM structures in red and nuclei in blue. As expected, in the hydrogel without ECM no staining of ECM was found. In the hydrogels with ECM, a homogeneous distribution of ECM particles was observed. This ensures the proximity of ASCs and ECM throughout the hydrogel. For the determination of the cellular response to the different functional groups within the ECM materials in a 3D environment, ASCs were encapsulated into gellan gum-ECM-hybrid hydrogels (Figure 5). As controls, hydrogels without ECM and with azide-modified AzECM were used. After three days of culture in the growth medium, the impact of ECM and their functionalization was determined by the analysis of supernatant and live/dead staining of the cells. Using the supernatant, LDH release and resazurin assays were performed to

determine cell death and metabolic activity of the ASCs in contact with the different modified ECM materials (Figure 5 A). We were not able to detect a significant difference in LDH release between the different hydrogels, which indicates that the functional groups do not have a negative impact on the ASCs regarding cellular survival. Analogously, no difference in metabolic activity was found between the ASCs cultured with the different functionalized ECMs and the negative control. These results are in line with previous experiments in which no cytotoxic effects of the coating with azide modified ECM on human dermal fibroblasts were found.[12]

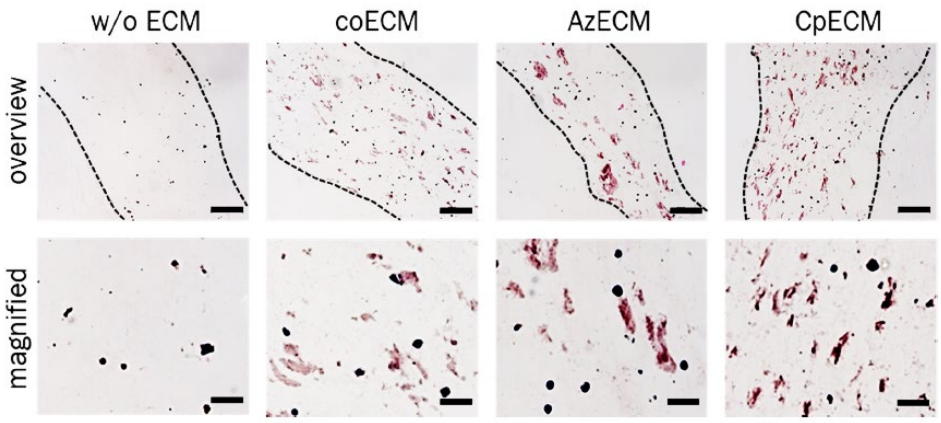

Figure 4. HE staining of gellan gum-ECM-hybrid hydrogels. For the histological staining, ECM-gellan gum-hybrid hydrogels with encapsulated ASCs (300.000 cells/100 µL hydrogel) were used. HE staining showed the presence and homogeneous distribution of the ECM particles within the gellan gum hydrogels for all samples. ECM particles are stained in rose/red and nuclei are stained in dark blue/black. Scale bar: overview: 200 µm; magnified: 50 µm

On day three of cell culture, live/dead staining was performed and analyzed concerning cellular survival and proliferation of the encapsulated ASCs by image analysis software (Figure 5 B). As expected, we observed that ASCs in hydrogels with ECM exhibited a higher survival rate and proliferation compared to the control without ECM. This effect was independent of the functionalization of the ECM. Previously, several studies demonstrated that ECM and ECM components enhance cellular adhesion, survival, and proliferation.[28] Within the samples with ECM, no differences could be observed between the differently modified ECMs or unmodified ECM. The results of the counting of viable and dead cells (Figure 5 C) do not coincide with the results of the LDH release, as a higher percentage of dead cells was found in the live/dead staining whereas no differences in LDH release were found. One possible explanation might be an irregular diffusion of the LDH protein within the hydrogel. LDH released from the encapsulated cells might be caught in the hydrogel and consequently cannot be measured in the supernatant. This further might explain the relatively high standard deviations found in the values of LDH determination.

Against this background, results from the image analysis seem to be more reliable. The results of the proliferation were given as the percentage of total cell number on day three relative to day zero. Next to the interaction with ECM, bioactive molecules such as growth factors are known to be bound to ECM and might enhance proliferation. We previously demonstrated the presence of different growth factors in ASC-derived ECM.[29] As there are no differences between the approaches with coECM and the functionalized ECMs (AzECM and CpECM), the functionalization exhibits no effect on the parameters shown in Figure 5 (cellular survival, proliferation, and metabolic activity) and therefore represents a promising method for ECM modification without unintentionally affecting cellular behavior.

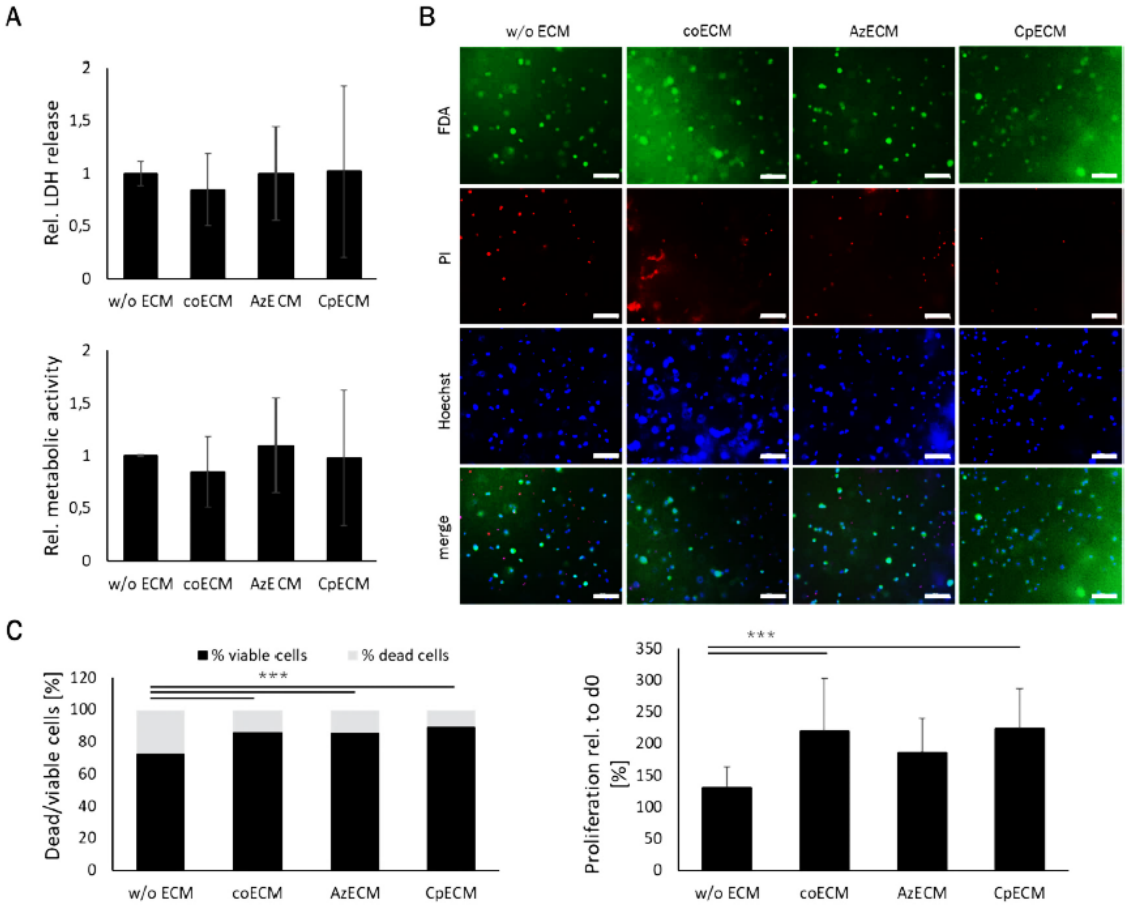

Figure 5. Impact of azide- and cyclopropene-modified ECM on cellular behavior of ASCs encapsulated in gellan gum hybrid hydrogels. 300.000 cells were encapsulated into gellan gum hybrid hydrogel containing different modified or unmodified types of ECM and cultured in growth medium for three days. A) To determine the apoptosis rate, an LDH assay was performed from the cell culture supernatant. Mean values of 3 independent experiments using cells from different donors (each 2 technical replicates) were normalized to the gellan gum without ECM. The metabolic activity of the encapsulated ASCs was determined using a resazurin assay, which is based on the metabolic turnover of the resazurin salt and a resulting color change. B) Representative figure of live/dead staining of the encapsulated ASCs. After three days of culture, viable cells were stained with fluorescein diacetate (FDA, green), and dead cells were stained with propidium iodide (PI, red). To get an overview of the total cell number nuclei were stained with Hoechst

(blue). C) Quantitative evaluation of the live/dead staining. Based on the images of the live/dead staining, cellular survival and relative proliferation were determined. For cellular survival, the number of viable and dead cells was determined and shown as a percentage. Proliferation was determined by counting of total cell numbers on day zero and day three and relative proliferation is shown as the increase of total cell number on day three relative to day zero (mean values of 3 independent experiments using cells from different donors (each 2 technical replicates)). Scale bar: 200 µm; *** $p \leq 0.001$

In general, these results demonstrate that the incorporated functional groups in the ECM themselves have no negative impact on encapsulated ASCs. Therefore, this new cell-derived ECM-based material provides a variety of possible applications including the equipment with bioactive molecules exhibiting desired effects and the possibility of cross-linking of the ECM itself by using corresponding linker molecules.[10,12] The great advantage over the previously reported functionalization of a clickECM by CuAAC is the independence of any catalyst which might exhibit cytotoxic effects or have any other impact on the ECM producing cells.

Conclusions

In this study, we demonstrated for the first time that it is possible to modify a cell-derived ECM with dienophiles as chemical reporter groups (functionalization) using MGE. The used monosaccharide derivatives exhibited no cytotoxic effects. A good cytocompatibility is important for monosaccharide derivates used in MGE to prevent cell death and the accumulation of unwanted cytokines with possible negative effects within the ECM. We were further able to show that the incorporated functional groups were addressable by an IEDDA reaction without the need for cytotoxic catalysts. In this way, it was possible to incorporate a bioactive enzyme. This feature opens numerous future applications, such as equipment of the ECM with desired growth factors, cross-linkers, and other molecules. Importantly, we demonstrated that the functional groups themselves have no impact on basic cellular behavior such as survival, metabolic activity, and proliferation. Thus, this new material provides great potential as a biomaterial in a variety of tissue engineering and regenerative medicine approaches as it allows the linking of molecules with desired effects without the need for cytotoxic catalysts.

Experimental Section

General methods. Reactions were monitored by TLC on silica gel 60 F254 (Merck) with detection under UV light (λ = 254 nm). Additionally, acidic ethanolic p-anisaldehyde solution or basic KMnO4 solution followed by gentle heating were used for visualization. Preparative flash column chromatography (FC) was performed with an MPLC-Reveleris X2 system from *Grace*. NMR spectra were recorded at room temperature with Avance III 400 and Avance III 600 instruments from Bruker. Chemical shifts are reported relative to solvent signals ($CDCl_3$: δ_H = 7.26 ppm, δ_C = 77.16 ppm; CD_3OD: δ_H = 4.87 ppm, δ_C = 49.00 ppm; D2O: δ_H = 4.73 ppm). The numbering of compounds is given in the supporting information. High-resolution mass spectra (HRMS) were obtained with a micrOTOF II instrument from *Bruker Daltonics*.

*General procedure for the synthesis of dienophile-modified GalNAc derivatives***.** Galactosamine hydrochloride (3.3 g, 15.3 mmol, 1 equiv.) was dissolved in dry MeOH (90 mL), and NaOMe (0.5 M in MeOH, 31 mL, 1 equiv.) was added. The reaction mixture was stirred for 1.5 h at rt and a solution of the alkene derivative 1a–d) (1.04 equiv.) in dry MeOH (90 mL) was added. After having been stirred at rt for 18 h, the solvent was removed under vacuum and the residual brown syrup was dissolved in pyridine (40 mL). Acetic anhydride (14 mL, 150 mmol) was added, and the mixture was stirred for 18 h. The solvent was removed under vacuum, the residue was dissolved in DCM and washed with aqueous KHSO4 (3 x), sodium bicarbonate (2 x), and brine (1 x). The organic layer was dried over MgSO4 and concentrated resulting in a dark brown solid which was purified by FC on silica (petroleum ether/ethyl acetate) yielding the corresponding GalNAc derivative.

Ac_4GalNBeoc: The title compound was synthesized with but-3-en-1-yl succinimidyl carbonate (**1a**) according to the general procedure and obtained as a colorless solid (63 %) as a mixture of anomers (α/β = 3.2/1). TLC: R_f = 0.33 (petroleum ether/ethyl acetate 1:1); α-anomer: ^{1}H NMR (400 MHz, $CDCl_3$): δ = 6.23 (d, *J* = 3.5 Hz, 1H, C^1H), 5.70–5.80 (m, 1H, C^9H), 5.42 (d, *J* = 2.3 Hz, 1H, C^4H), 5.19–5.03 (m, 3H, C^3H, $C^{10}H_2$), 4.64 (d, *J* = 9.7 Hz, 1H, NH), 4.41 (dt, *J* = 3.4, 11,4 Hz, 1H, C^2H), 4.22 (m, 1H, C^5H), 4.04-4.15 (m, 4H, C^7H_2, C^6H_2), 2.35–5.33 (m, 2H, C^8H_2), 2.16 (s, 2x3H, CH_3), 2.02 (s, 2x3H, CH_3) ppm; ^{13}C NMR (100 MHz, $CDCl_3$): δ = 170.8, 170.3, 168.8, 155.9 (C=O), 133.9 (C^9), 117.2 (C^{10}), 91.5 (C^1), 68.5 (C^5), 68.0 (C^3), 66.7 (C^4), 61.2, 64.5 (C^6, C^7), 48.6 (C^2), 33.3 (C^8), 20.9, 20.6 (CH_3) ppm; β-anomer: ^{1}H NMR (400 MHz, $CDCl_3$): δ = 6.17 (d, *J* = 4.7 Hz, 1H, C^1H), 5.69–5.80 (m, 1H, C^9H), 5.32–5.28 (m, 1H, C^3H), 5.18–5.03 (m, 4H, NH, C^5H, $C^{10}H_2$), 4.52–5.47 (m, 1H, C^2H), 4.18–4.12 (m, 5H, C^4H, C^7H_2, C^6H_2), 2.35 (m, 2H, C^8H_2), 2.12 (s, 3H, CH_3), 2.07 (s. 2x3H, CH_3), 2.02 (s, 3H, CH_3) ppm; ^{13}C NMR (100 MHz, $CDCl_3$): δ = 170.5, 169.9, 169.3, 168.9, 155.9 (C=O), 133.9 (C^9), 117.2 (C^{10}), 93.9

(C^1) 78.9 (C^5), 73.9 (C^3), 68.6 (C^4), 64.5 (C^7), 62.0 (C^6), 57.8 (C^2), 33.2 (C^8), 20.6, 20.7, 20.8, 21.1 (CH_3) ppm; HRMS (ESI-MS): *m*/*z* calcd. for $C_{19}H_{27}NO_{11}$: 446.1657 [*M*+H]$^+$; found: 468.1471 [*M*+Na]$^+$.

Ac$_4$GalNPeoc: The title compound was synthesized with pent-4-en-1-yl succinimidyl carbonate (**1b**) according to the general procedure and obtained as a colorless solid (49 %) as a mixture of anomers (α/β = 2.2/1). TLC: R_f = 0.5 (petroleum ether/ethyl acetate 1:1); α-anomer: ^{1}H NMR (400 MHz, $CDCl_3$): δ= 6.21 (d, *J* = 3.5 Hz, 1H, C^1H), 5.71–5.81 (m, 2H, $C^{10}H_2$), 5.40 (d, *J* = 2.9 Hz 1H, C^4H), 5.21–5.17 (m, 1H, C^3H), 5.05–4.96 (m, 2H, $C^{11}H_2$), 4.70 (d, *J* = 9.5 Hz, 1H, NH), 4.44–4.40 (m, 1H, C^2H), 4.24–4.19 (m, 1H, C^5H), 4.10–4.01 (m, 4H, C^6H_2, C^7H_2), 2.14 (s, 6H, CH_3), 2.06–2.07 (m, 2H, C^9H_2), 1.99 (s, 3H, CH_3) 2.00 (s, 3H, CH_3), 1.64–1.71 (m, 2H, C^8H_2) ppm; ^{13}C NMR (100 MHz, $CDCl_3$): δ= 170.8, 170.3, 170.1, 168.8, 155.9 (C=O), 137.3 (C^{10}), 114.9 (C^{11}), 91.3 (C^1), 68.4 (C^5), 68.1 (C^3), 66.8 (C^4), 64.9, 61.2 (C^6, C^7), 48.6 (C^2), 29.9 (C^9), 28.1 (C^8), 20.8, 20.7, 20.6 (CH_3) ppm; β-anomer: ^{1}H NMR (400 MHz, $CDCl_3$): δ= 6.19 (d, *J* = 4.7 Hz, 1H, C^1H), 5.84–5.74 (m, 1H, $C^{10}H$), 5.34–5.30 (m, 1H, C^3H), 5.12–4.97 (m, 3H, NH, C^5H, $C^{11}H_2$), 4.54–4.49 (m, C^2H), 4.25–4.04 (m, 5H, C^4H, C^6H_2, C^7H_2), 2.17 (s, 3H, CH_3), 2.11–2.08 (m, 8H, CH_3, CH_3, C^9H_2), 2.04 (s, 3H, CH_3), 1.74–1.67 (m, 2H, C^8H_2) ppm; ^{13}C NMR (100 MHz, $CDCl_3$): δ = 170.7, 170.3, 170.1, 168.9, 156.2 (C=O), 137.8 (C^{10}), 115.2 (C^{11}), 93.3 (C^1), 78.8 (C^5), 73.9 (C^3), 68.6 (C^4), 65.3 (C^7), 61.5 (C^6), 57.6 (C^2), 29.6 (C^9), 27.8 (C^8), 21.1, 21.2, 21.0, 20.8, 20.7 (CH_3) ppm; HRMS (ESI-MS): *m*/*z* calcd. for $C_{20}H_{29}NO_{11}$: 460.1813 [*M*+H]$^+$; found: 482.1628 [*M*+Na]$^+$.

Ac$_4$GalNHeoc: The title compound was synthesized with hex-5-en-1-yl succinimidyl carbonate (**1c**) according to the general procedure and obtained as a colorless solid (76 %) as a mixture of anomers (α/β = 2.6/1). TLC: R_f = 0.45 (petroleum ether/ethyl acetate 1:1); α-anomer: ^{1}H NMR (400 MHz, $CDCl_3$): δ= 6.21 (d, *J* = 3.5 Hz, 1H, C^1H), 5.81–5.70 (m, 1H, $C^{11}H$), 5.40 (d, *J* = 2.3 Hz, 1H, C^4H), 5.21–5.11 (m, 1H, C^3H), 5.00–4.92 (m, 2H, $C^{12}H_2$), 4.68 (d, *J* = 9.6 Hz, 1H, NH), 4.42–4.36 (m, 1H, C^2H), 4.23–4.18 (m, 1H, C^5H), 4.12–4.01 (m, 4H, C^6H_2, C^7H_2), 2.14 (s, 2x3H, CH_3), 2.06–2.03 (m, 2H, $C^{10}H_2$), 2.00 (s, 2x3H, CH_3), 1.59 (m, 2H, C^8H_2), 1.45–1.37 (m, 2H, C^9H_2) ppm; ^{13}C NMR (100 MHz, $CDCl_3$): δ= 170.9, 170.4, 169.9, 168.9 (C=O), 156.1 (C^{13}), 138.3 (C^{11}), 114.9 (C^{12}), 91.6 (C^1), 68.6 (C^5), 68.1 (C^3), 66.9 (C^4), 65.5 (C^7), 61.4 (C^6), 48.7 (C^2), 33.3 (C^{10}), 28.4 (C^8), 25.1 (C^9), 20.8, 20.7 (CH_3) ppm; β-anomer: ^{1}H NMR (400 MHz, $CDCl_3$): δ = 6.16 (d, *J* = 4.7 Hz, 1H, C^1H), 5.81–5.70 (m, 1H, $C^{11}H$), 5.32–5.28 (m, 1H, C^3H), 5.21–5.11 (m, 2H, C^5H, NH), 4.95 (m, 2H, $C^{12}H_2$), 4.52–4.47 (m, 1H, C^2H), 4.20–4.01 (m, 5H, C^4H, C^6H_2, C^7H_2), 2.06–2.03 (m, 2H, $C^{10}H_2$), 2.11 (s, 3H, CH_3), 2.07 (s, 2x3H, CH_3), 2.02 (s, 3H, CH_3), 1.59 (m, 2H, C^8H_2), 1.45–1.37 (m, 2H, C^9H_2) ppm; ^{13}C NMR (100 MHz, $CDCl_3$): δ= 170.9 170.4, 169.9, 168.9 (C=O), 156.1 (C^{13}), 138.3 (C^{11}), 114.9 (C^{12}), 94.1 (C^1), 79.0 (C^5), 74.1

(C^3), 70.4 (C^4), 68.0 (C^4), 66.8 (C^7), 62.2, 61.3 (C^6), 57.9 (C^2), 33.3 (C^{10}), 28.4 (C^8), 25.1 (C^9), 21.2, 21.1, 21.0, 20.8, 20.7 (CH_3) ppm; HRMS (ESI-MS): *m*/*z* calcd. for $C_{21}H_{31}NO_{11}$: 474.1970 $[M+H]^+$; found: 496.1786 $[M+Na]^+$.

Ac_4GalNPtl: The title compound was synthesized with succinimidyl pent-4-enoate (**1d**) according to the general procedure and obtained as a colorless solid (70 %) as a mixture of anomers (α/β = 2.4/1). TLC: R_f = 0.2 (petroleum ether/ethyl acetate 1:1); α-anomer: ^{1}H NMR (400 MHz, $CDCl_3$): δ = 6.21 (d, *J* = 3.6 Hz, 1H, C^1H), 5.79–5.69 (m, 2H, $C^{10}H_2$), 5.55 (m, 1H, NH), 5.39 (m, 1H, C^4H), 5.19–5.16 (m, 1H, C^3H), 5.04–4.95 (m, 2H, C^9H_2), 4.73–4.68 (m, 1H, C^2H), 4.23–4.20 (m, 1H, C^5H), 4.10–4.01 (m, 2H, C^6H_2), 2.33–2.28 (m, 2H, C^8H_2), 2.23–2.19 (m, 2H, C^7H_2), 2.14 (s, 2x3H, CH_3), 1.99 (s, 3H, CH_3) 2.00 (s, 3H, CH_3) ppm; ^{13}C NMR (100 MHz, $CDCl_3$): δ = 172.3, 171.0, 170.3, 170.2, 158.8 (C=O), 136.6 (C^{10}), 115.7 (C^9), 91.3 (C^1), 68.6 (C^5), 68.5 (C^5), 67.8 (C^3), 66.7 (C^4), 61.3 (C^6), 46.8 (C^2), 35.5 (C^7), 29.2 (C^8), 20.9 (CH_3), 20.6 (CH_3) ppm; β-anomer: ^{1}H NMR (400 MHz, $CDCl_3$): δ = 5.70 (d, *J* = 8.7 Hz, 1H, C^1H), 5.81–5.73 (m, 1H, $C^{10}H$), 5.38 (m, 2H, NH, C^4H), 5.10–4.98 (m, 3H, C^3H, C^9H_2), 4.50–4.43 (m, 1H, C^2H), 4.20–4.09 (m, 1H, C^6H_2), 4.02–4.00 (m, 1H, C^5H), 2.36–2.31 (m, 2H, C^8H_2), 2.24–2.21 (m, 2H, C^7H_2), 2.17 (s, 3H, CH_3), 2.12 (s, 3H, CH_3), 2.05 (s, 3H, CH_3), 2.01 (s, 3H, CH_3) ppm; ^{13}C NMR (100 MHz, $CDCl_3$): δ = 172.4, 170.7, 170.1, 164.6 (C=O), 136.5 (C^{10}), 115.7 (C^9), 93.0 (C^1), 71.9 (C^5), 70.3 (C^3), 70.3 (C^3), 66.3 (C^4), 61.3 (C^6), 49.6 (C^2), 35.8 (C^7), 29.2 (C^8), 21.0, 20.8, 20.6, 20.5 (CH_3) ppm; HRMS (ESI-MS): *m*/*z* calcd. for $C_{19}H_{27}NO_{10}$: 430.1708 $[M+H]^+$; found: 452.1524 $[M+Na]^+$.

Adipose-derived stem cell isolation. All used media contained 1% penicillin/streptomycin. ASCs were isolated from human tissue samples obtained from patients undergoing plastic surgery (Dr. Ziegler; Klinik Charlottenhaus, Stuttgart, Germany) as described before.[30] Briefly, tissue was cut into small pieces and digested in Dulbecco`s modified eagle medium (DMEM, BioChrom, Germany) containing 0.1 % collagenase NB4 (Serva Electrophoresis, Germany) and 1 % bovine serum albumin (BSA; Sigma, Germany) for 5 h at 37 °C under constant shaking. The suspension was filtered through a 500 µm sieve and centrifuged for 5 min at 200×g. To remove erythrocytes, the pellet was suspended in erythrocyte lysis buffer and incubated for 10 min at room temperature. The suspension was centrifuged for 5 min at 200xg, the remaining pellet was suspended in phosphate-buffered saline (PBS; Biochrom, Germany) and filtered through a 100 µm meshed sieve. ASCs were initially seeded at a density of 5x103 cells/cm2 in a serum-free MSC growth medium (MSCGM; PELOBiotech, Germany) containing 5 % human platelet lysate (hPL). The phenotype of the ASCs was previously characterized, and it was shown that the cells exhibit the typical surface proteins.[31] All research was carried out following the rules for the investigation of human subjects as defined in the Declaration of Helsinki. Patients provided

written agreement in compliance with the Landesärztekammer Baden-Württemberg (F-2012-078, for normal skin from elective surgeries). ASCs were used up to passage three.

Cytotoxicity of the modified monosaccharides. The biocompatibility of functionalized monosaccharides was evaluated by a lactate dehydrogenase (LDH) assay (TaKaRa Bio Inc.) and a resazurin assay (Sigma Aldrich, Germany). ASCs were seeded in growth medium (DMEM + 10 % FCS) at a density of 50.000 cells/ cm2. After 24 h cells were treated with 100 µM monosaccharide or sterile water and incubated for another 24 h. LDH assay was performed according to the manufacturer's protocol with cell culture supernatant. For the resazurin assay, the culture medium was changed to a medium with resazurin salt (11 µg/mL) and incubated for 3 h at 37 °C and 5 % CO2. The untreated negative control was set as 100 % and values were normalized to control.

Metabolic glycoengineering and isolation of functionalized extracellular matrix. For the generation of functionalized ECM, ASCs were seeded into Petri dishes (d = 14.5 cm) at a density of 25.000 cells/cm2 in DMEM containing 10 % FCS. The next day, 50 µg/mL sodium ascorbate was added to the medium. The medium was changed every second day and removed sodium ascorbate was replaced. On day 4 100µM modified monosaccharides were added to the cell culture medium for MGE. After 72 h incubation cells were lysed using hypotonic 0.7 % ammonium hydroxide solution and isolated ECM was washed with ultrapure water. After isolation, ECM was concentrated using ultracentrifugation tubes (Amicon, Merck, Germany) with a molecular cut-off of 10 kDa. Concentrated ECM was recovered and homogenized using lysis tubes and homogenizer FastPrep-24™ 5G (MP Biomedicals™, Germany).[12] The dry weight of ECM samples was determined by freeze-drying.

Detection of incorporated functional groups. For detection of functional groups, homogenized ECM was dried on TCPS. ECM was incubated with 50 µM biotinylated tetrazine for detection of dienophile groups for 1 h at RT. Samples were washed with PBS and incubated with 6.6 µg/mL streptavidin linked with horseradish peroxidase. Subsequently, TMB was added to the samples and after color change reaction was stopped with 1 M HCl. The supernatant was measured at 450 nm using the plate reader Tecan Saphire II (Tecan, Switzerland). The reference wavelength was set as 620 nm. Unmodified ECM was used as negative control and results were normalized to it.

Preparation of gellan gum-ECM hybrid hydrogels with encapsulated ASC and evaluation of cellular behavior. Hybrid hydrogels were prepared of 1 wt% gellan gum and 0.25 wt% ECM. As a negative control, 1 % gellan gum hydrogels without ECM supplementation were prepared. Liquid hydrogel solution (100 µL) was filled in a plastic ring with 0.6 cm in diameter and covered with PBS with magnesium and calcium (PBS+) to induce cross-linking. Before rheological analysis, hydrogels were swollen for 72 h in PBS+ at RT. For evaluation of stiffness, storage modulus and loss modulus were measured. Oscillatory rheology was performed on a Physica MCR 301 rheometer (Anton Paar) using a parallel plate geometry with a diameter of 8 mm at a temperature of 20 °C. Amplitude sweeps (frequency = 1 Hz, amplitudes between 0.01 % and 10 %) were performed to estimate the linear viscoelastic range, resulting in a comparison of hydrogel stiffness via storage modulus G' and loss modulus G'' at a deformation of 0.1 % and a frequency of 1 Hz. To determine the effect of functionalized ECM on cellular behavior, ASCs were encapsulated into ECM gellan gum-hybrid hydrogels. Therefore, hydrogels with 1 wt% gellan gum, 0.25 wt% ECM, and 300.000 ASCs per 100 µL were prepared. Liquid hydrogel solution (100 µL) was filled in a plastic ring with 0.6 cm in diameter and covered with PBS with magnesium and calcium (PBS+) to induce cross-linking. After 30 min incubation at 37 °C PBS+ was changed to DMEM containing 10 % FCS and 1 % P/S. On day 0 and day 3 after hydrogel preparation, live/dead staining and resazurin assay were performed. For live/dead staining gels were rinsed two times with PBS+ followed by incubation with staining solution, consisting of 200 ng/ml fluorescein diacetate (FDA, Sigma Aldrich, Germany) and 20 µg/mL propidium iodide (PI, Sigma Aldrich, Germany) in DMEM, for 15 min at 37 °C. Nuclei were counterstained with Hoechst33342 (5 µg/mL). Subsequently, gels were rinsed with PBS+ and placed onto a slide for microscopic analysis. Images were taken with an Axio Observer microscope and Axiocam color using the software ZENblue (Carl Zeiss, Germany). Nuclei, viable cells, and dead cells were counted using the software ImageJ. To investigate the metabolic activity of the encapsulated ASCs, a resazurin assay was performed on day 3 after hydrogel preparation. Hydrogels were incubated with resazurin solution (11µg/mL) at 37°C. The absorbance of the supernatant was measured at 570 nm with a correction wavelength set to 595 nm (Tecan Safire 2, multimode microplate reader, Tecan Trading AG, Switzerland). Results were calculated based on the number of viable cells per hydrogel and values were normalized to the control hydrogel without ECM.

Statistics. All experiments were performed using samples from three different biological donors. Data were analyzed by one-way analysis of variance (ANOVA) with a Bonferroni posthoc test using

Origin 2018b. Statistical significances were stated as $p < 0.05$ (*), very significant as $p < 0.01$ (**), and highly significant as $p < 0.001$ (***).

Acknowledgments

This work was supported by the Ministerium für Wissenschaft, Forschung und Kunst Baden-Württemberg (33-7533-7-11.9/7/2) and the Deutsche Forschungsgemeinschaft (SFB 969, project B05). We thank Dr. Silke Keller and Dr. Monika Bach for helpful scientific discussion.

References

[1] C. Frantz, K. M. Stewart, V. M. Weaver, J. Cell Sci. 2010, 123, 4195-4200.
[2] a) A. J. Engler, S. Sen, H. L. Sweeney, D. E. Discher, Cell 2006, 126, 677-689; b) G. C. Reilly, A. J. Engler, J. Biomech. 2010, 43, 55-62.
[3] L. E. Fitzpatrick, T. C. McDevitt, Biomater. Sci. 2015, 3, 12-24.
[4] V. Guneta, Z. Zhou, N. S. Tan, S. Sugii, M. T. C. Wong, C. Choong, Biomater. Sci. 2017, 6, 168-178.
[5] a) N. L'Heureux, N. Dusserre, G. Konig, B. Victor, P. Keire, T. N. Wight, N. A. F. Chronos, A. E. Kyles, C. R. Gregory, G. Hoyt, R. C. Robbins, T. N. McAllister, Nat. Med. 2006, 12, 361-365; b) G. M. Cunniffe, T. Vinardell, J. M. Murphy, E. M. Thompson, A. Matsiko, F. J. O'Brien, D. J. Kelly, Acta Biomater. 2015, 23, 82-90.
[6] A. C. Braun, M. Gutmann, T. Lühmann, L. Meinel, J. Controlled Release 2018, 273, 68-85.
[7] a) O. T. Keppler, R. Horstkorte, M. Pawlita, C. Schmidt, W. Reutter, Glycobiology 2001, 11, 11R-18R; b) D. H. Dube, C. R. Bertozzi, Curr. Opin. Chem. Biol. 2003, 7, 616-625; c) C. Agatemor, M. J. Buettner, R. Ariss, K. Muthiah, C. T. Saeui, K. J. Yarema, Nat. Rev. Chem. 2019, 3, 605-620.
[8] E. M. Sletten, C. R. Bertozzi, Angew. Chem., Int. Ed. 2009, 48, 6974-6998.
[9] a) S. M. Ruff, S. Keller, D. E. Wieland, V. Wittmann, G. E. M. Tovar, M. Bach, P. J. Kluger, Acta Biomater. 2017, 52, 159-170; b) S. Nellinger, S. Keller, A. Southan, V. Wittmann, A.-C. Volz, P. J. Kluger, Curr. Dir. Biomed. Eng. 2019, 5, 393-395.
[10] M. Gutmann, A. Braun, J. Seibel, T. Lühmann, ACS Biomater. Sci. Eng. 2018, 4, 1300-1306.
[11] a) C. W. Tornøe, C. Christensen, M. Meldal, J. Org. Chem. 2002, 67, 3057-3064; b) V. V. Rostovtsev, L. G. Green, V. V. Fokin, K. B. Sharpless, Angew. Chem., Int. Ed. 2002, 41, 2596-2599.
[12] S. Keller, K. Wörgötter, A. Liedek, P. J. Kluger, M. Bach, G. E. M. Tovar, A. Southan, ACS Appl. Mater. Interfaces 2020, 12, 26868-26879.
[13] M. van Dijk, D. T. S. Rijkers, R. M. J. Liskamp, C. F. van Nostrum, W. E. Hennink, Bioconjugate Chem. 2009, 20, 2001-2016.
[14] a) N. J. Agard, J. A. Prescher, C. R. Bertozzi, J. Am. Chem. Soc. 2004, 126, 15046-15047; b) X. Ning, J. Guo, Margreet A. Wolfert, G.-J. Boons, Angew. Chem., Int. Ed. 2008, 47, 2253-2255.
[15] a) M. L. Blackman, M. Royzen, J. M. Fox, J. Am. Chem. Soc. 2008, 130, 13518-13519; b) K. Braun, M. Wiessler, V. Ehemann, R. Pipkorn, H. Spring, J. Debus, B. Didinger, M. Koch, G. Muller, W. Waldeck, Drug Des. Dev. Ther. 2008, 2, 289-301; c) N. K. Devaraj, R. Weissleder, S. A. Hilderbrand, Bioconjugate Chem. 2008, 19, 2297-2299.
[16] L. M. Haiber, M. Kufleitner, V. Wittmann, Front. Chem. 2021, 9, 654932.
[17] a) A. Niederwieser, A.-K. Späte, L. D. Nguyen, C. Jüngst, W. Reutter, V. Wittmann, Angew. Chem., Int. Ed. 2013, 52, 4265-4268; b) A.-K. Späte, V. F. Schart, S. Schöllkopf, A. Niederwieser, V. Wittmann, Chem. Eur. J. 2014, 20, 16502-16508; c) J. E. G. A. Dold, J. Pfotzer, A.-K. Späte, V. Wittmann, ChemBioChem 2017, 18, 1242-1250; d) A. Kitowski, G. J. L. Bernardes, ChemBioChem 2020, 21, 2696-2700; e) J. E. G. A. Dold, V. Wittmann, ChemBioChem 2021, 22, 1243-1251.
[18] a) D. M. Patterson, L. A. Nazarova, B. Xie, D. N. Kamber, J. A. Prescher, J. Am. Chem. Soc. 2012, 134, 18638-18643; b) A.-K. Späte, H. Bußkamp, A. Niederwieser, V. F. Schart, A. Marx, V. Wittmann, Bioconjugate Chem. 2014, 25, 147-154; c) D. M. Patterson, K. A. Jones, J. A. Prescher, Mol. BioSyst. 2014, 10, 1693-1697; d) A.-K. Späte, V. F. Schart, J. Häfner, A. Niederwieser, T. U. Mayer, V. Wittmann, Beilstein J. Org. Chem. 2014, 10, 2235-2242; e) D.-C. Xiong, J. Zhu, M.-J. Han, H.-X. Luo, C. Wang, Y. Yu, Y. Ye, G. Tai, X.-S. Ye, Org. Biomol. Chem. 2015, 13, 3911-3917; f) F. Doll, A. Buntz, A.-K. Späte, V. F. Schart, A. Timper, W. Schrimpf, C. R. Hauck, A. Zumbusch, V. Wittmann, Angew. Chem., Int. Ed. 2016, 55, 2262–2266; g) J. Hassenrück, V. Wittmann, Beilstein J. Org. Chem. 2019, 15, 584-601.
[19] P. Agarwal, B. J. Beahm, P. Shieh, C. R. Bertozzi, Angew. Chem., Int. Ed. 2015, 54, 11504-11510.

[20] A.-K. Späte, J. E. G. A. Dold, E. Batroff, V. F. Schart, D. E. Wieland, O. R. Baudendistel, V. Wittmann, ChemBioChem 2016, 17, 1374-1383.
[21] M. Wiessler, W. Waldeck, R. Pipkorn, C. Kliem, P. Lorenz, H. Fleischhacker, M. Hafner, K. Braun,
Int. J. Med. Sci. 2010, 7, 213-223.
[22] V. F. Schart, J. Hassenrück, A.-K. Späte, J. E. G. A. Dold, R. Fahrner, V. Wittmann, ChemBioChem 2019, 20, 166-171.
[23] Y.-J. Lee, Y. Kurra, W. R. Liu, ChemBioChem 2016, 17, 456-461.
[24] I. Jeon, D. Lee, I. J. Krauss, S. J. Danishefsky, J. Am. Chem. Soc. 2009, 131, 14337-14344.
[25] D. E. Place, T. D. Kanneganti, J. Exp. Med. 2019, 216, 1474-1486.
[26] a) M. E. L. Lago, L. P. da Silva, C. Henriques, A. F. Carvalho, R. L. Reis, A. P. Marques, Bioengineering 2018, 5; b) L. R. Stevens, K. J. Gilmore, G. G. Wallace, M. I. H. Panhuis, Biomater. Sci. 2016, 4, 1276-1290; c) C. J. Ferris, K. J. Gilmore, G. G. Wallace, M. I. H. Panhuis, Soft Matter 2013, 9, 3705-3711; d) M. B. Oliveira, C. A. Custodio, L. Gasperini, R. L. Reis, J. F. Mano, Acta Biomater. 2016, 41, 119-132.
[27] a) Kshitiz, J. Park, P. Kim, W. Helen, A. J. Engler, A. Levchenko, D. H. Kim, Integr. Biol. 2012, 4, 1008-1018; b) Y. N. Wu, Z. Yang, J. B. K. Law, A. Y. He, A. A. Abbas, V. Denslin, T. Kamarul, J. H. P. Hui, E. H. Lee, Tissue Eng., Part A 2017, 23, 43-54.
[28] a) G. D. Kusuma, M. C. Yang, S. P. Brennecke, A. J. O'Connor, B. Kalionis, D. E. Heath, ACS Biomater. Sci. Eng. 2018, 4, 1760-1769; b) R. Rakian, T. J. Block, S. M. Johnson, M. Marinkovic, J. Wu, Q. Dai, D. D. Dean, X.-D. Chen, Stem Cell Res. Ther. 2015, 6, 235; c) A. I. Hoch, V. Mittal, D. Mitra, N. Vollmer, C. A. Zikry, J. K. Leach, Biomaterials 2016, 74, 178-187; d) H. Lin, G. Yang, J. Tan, R. S. Tuan, Biomaterials 2012, 33, 4480-4489.
[29] S. Nellinger, I. Schmidt, S. Heine, A. C. Volz, P. J. Kluger, Biotechnol. Bioeng. 2020, 117, 3160-3172.
[30] A.-C. Volz, B. Huber, A. M. Schwandt, P. J. Kluger, Differentiation 2017, 95, 21-30.
[31] A.-C. Volz, P. J. Kluger, Cytotherapy 2018, 20, 576-588.

6 GENERAL DISCUSSION

The ECM as the natural environment of the cells provides chemical and physical cues that can be sensed by the residing cells and affect their behavior (e.g. migration, proliferation, differentiation) [1,2]. With this ability, ECM is an important actor of organisms' physiology and pathophysiology. It is known to influence a variety of processes including wound healing and scar formation and play a crucial role in tumor development [183–185]. This makes ECM an ideal biomaterial for scaffolds in tissue engineering and regenerative medicine. Due to its highly complex composition and structure, to date, it is not possible to recreate the native ECM *in vitro* by the combination of individual ECM proteins. Thus, this material needs to be isolated from humans (autologous or allogeneic) or animals (xenogeneic) tissues or cells. A promising alternative to dECM from native tissue is the generation of cdECM *in vitro.* This cdECM is produced by cells in culture and can be isolated using relatively gentle methods [85]. In this thesis, it was demonstrated that cdECM exhibits relevant differences towards dECM (see Paper I – Characterization and Comparison p. 19) [186], and with its bioactivity regarding neo-angiogenesis it provides a promising biomaterial for vascularized tissue engineering and regenerative medicine approaches (see Paper II – Support of Prevascular-like Structure Formation p. 50) [187]. In addition, the successful equipment of cdECM with specific addressable functional groups that enables a cell-friendly catalyst-free modification of cdECM via inverse electron demand Diels Alder reaction was shown (see Paper III – Functionalization of cdECM p. 74) [166].

Due to the advantages of native dECM as a biomaterial several ECM-based products are in clinical application. For example, AlloDerm® (BioHorizons) [188] and Oasis® (Smith & Nephew) [189] are applied for skin regeneration and GraftJacket® (Wright Medical; approved for clinical application by the FDA in 2014) [190] and Allopatch HD™ (MTF Sports Medicine) [191] are products for tendon and ligament repair. These developments further promoted the refinement of decellularization techniques. However, inadequate decellularization and processing of the dECM can have a serve impact on experimental outcomes in tissue engineering or implant survival in regenerative medicine [192]. Zhang *et al*. proposed a list of challenges that need to be addressed for the clinical transformation of ECM-based products (**Figure 11**) [73]. Hereafter, the potential of cdECM for application in tissue engineering and regenerative medicine is discussed against the background of the proposed challenges.

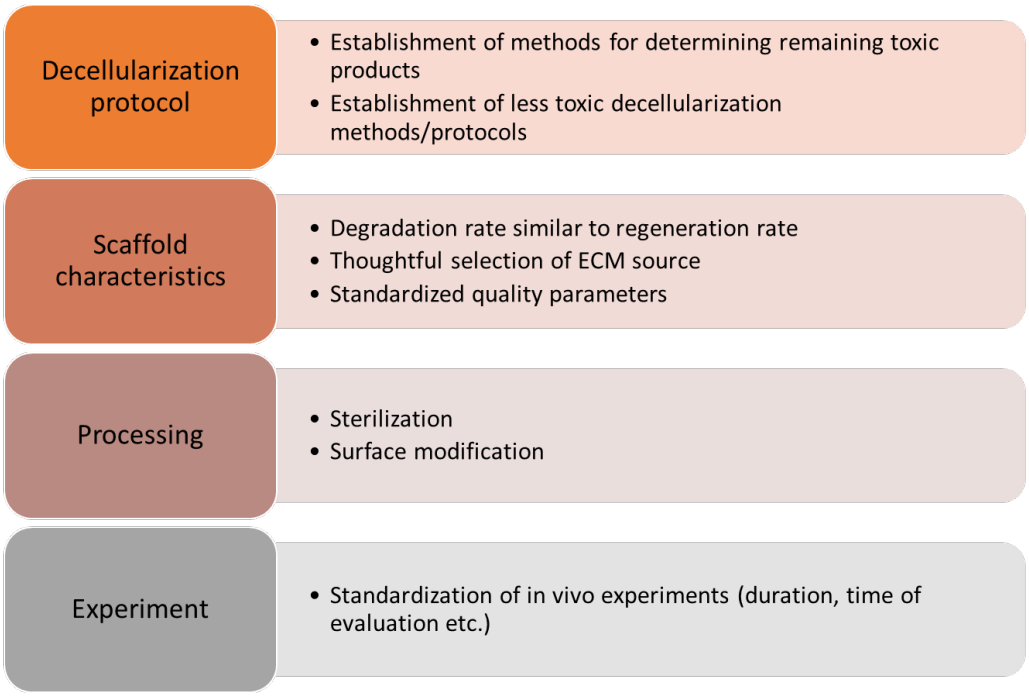

Figure 11: Challenges of ECM applied in tissue engineering and regenerative medicine. For successful application of ECM materials in tissue engineering and regenerative medicine various challenges have to be addressed. Modified after [73].

Decellularization protocol

Over the last years, decellularization protocols and techniques undergo great development. However, decellularization of native tissues or organs – especially dense tissue like muscle or tendon – in general needs the use of harsh and most **toxic chemicals** (e.g. enzymes and detergents) and/ or **destructive methods** (e.g. freeze-thaw-cycles and sonication). If the washing of the resulting dECM is not sufficient or the substances bind to ECM proteins, residues of these toxic substances can remain in the dECM and may harm the host tissue or reseeded cells [73,103]. In contrast, the *in vitro* generated cdECM exhibits a less dense structure. Due to the loosely packed structure of cdECM, it can be isolated using fewer or without toxic substances which minimizes the risk of remaining toxic product in the isolated cdECM. Bourgine *et al*. successfully used programmed cell death – apoptosis – for the removal of cells from cdECM [193–195]. They further suggested the use of cell lines that undergo apoptosis upon exposure to a specific stimulus for facilitated decellularization of cdECM [196]. Throughout induced apoptosis is an interesting approach, it brings some limitations in tissue engineering and regenerative medicine approaches. For example, remaining apoptosis inducer and apoptosis-associated cytokines might affect reseeded cells *in vitro* and infiltration and ingrowth *in vivo* [73]. All currently available decellularization methods entail the hurdle of possible remaining substances that affect the experimental outcome *in vitro* as well as *in vivo*. For adequate quality control, Zhang *et al*.

proposed the establishment and standardization of **methods for the detection** of remaining toxic substances in the ECM material (**Figure 8**) [73]. Possible methods include spectroscopic measurements like Raman spectroscopy. The looser packed structure of cdECM might facilitate the detection of remaining decellularization chemicals by such methods, which might be a great advantage of cdECM products.

Scaffold characteristics

As the interaction of ECM and the residing cells is finely balanced, the used ECM material should be carefully characterized and **standardized quality parameters** should be defined [73]. It is known that the characteristics of ECM material are highly dependent on donor characteristics like age, health, and sex [105,107–109,197,198]. These differences should also come into account when interpreting the experimental results. In this thesis, macromolecular and structural differences between dECM from adipose tissue and cdECM from stem cells and adipogenic differentiated ASCs were highlighted. These include chemical composition (e.g. collagen content and sGAG content), structural features (e.g. fiber diameter), and physical characteristics (e.g. swelling degree) [186]. All of them have the potential to relevantly influence cellular behavior and therefore the results of performed experiments. Thus, for comprehensive interpretation of generated results using different ECM materials, researchers should know these differences and involve them in the interpretation of the obtained results and their conclusions. These results confirm the **first and second hypothesis** of this work (see Paper I – Characterization and comparison; p. 19). The methods for standardized characterization of ECM should be carefully selected. As ECM is a highly complex structure, basic characterization methods reach their limits. For example, Keller *et al.* demonstrated that simple colorimetric assays for the determination of total protein content are not suitable for ECM [199]. Thus, every method should be validated for the application in ECM characterization. For **standardization** and reproducibility of cdECM generation, production under serum-free conditions has to be established and performed. Serum proteins have the potential to bind to ECM structures, can remain in the isolated cdECM, and might be released when reseeded or implanted and alter cellular response to the cdECM material [53,54]. In addition, a well-known issue in the use of serum for cell culture is batch-to-batch variation. Serum is a natural product that underlies donor variations. As these variations in composition might lead to variable impacts on cellular cdECM production and variability in bound proteins to ECM material, they need to be excluded.

In general, as all cellular structures are removed and ECM proteins are highly conserved between species, ECM is seen as a non-immunogenic biomaterial. However, next to the ethical concerns

and the risk of pathogen transfer, an issue of xenogeneic ECM, especially for clinical applications, is the xenoantigen alpha-Gal (Galalpha1-3Galbeta1-(3)4GlcNAc-R) that is synthesized in ECM molecules of nonprimate mammals and New World monkeys [200,201]. Primates, including humans, lost the gene during evolution and produce anti-Gal antibodies due to constant exposure of the Gal epitope by intestinal bacteria. This leads to **immunogenic responses** like a hyperacute rejection of xenografts in humans. The alpha-Gal xenoantigen can be removed by the treatment of the ECM with galactosidase. However, this treatment further affects the ECM after the decellularization process. Another possibility is the knock-out of the gene in transgenic animals intended for the generation of xenografts [202]. Studies demonstrated that Gal knock-out ECMs were rejected over periods of several months due to the formation of antibodies specific to porcine antigens [203,204]. To minimize the risk of serve immune responses the use of autologous ECM material would be preferable. However, the availability of autologous grafts or ECM sources is restricted in most cases and the additional burden of surgical harvesting of autologous material makes it a hardly feasible method. For the production of autologous cdECM, only little amounts of the patient's cells would be needed. These isolated cells can be expanded and used for autologous cdECM generation. At this point the major drawback of cdECM comes into effect: to date, only low amounts of cdECM can be generated. Efforts are made to develop scale-up technologies for cdECM generation. The key steps for scale-up cdECM production are cell expansion, maximizing the amount of secreted cdECM, and optimization of cdECM isolation [121]. Yielding a relevant amount of cdECM in a short time would open up the possibility of using cdECM as a biomaterial in tissue engineering and regenerative medicine as stand-alone scaffold material.
Next to immunogenicity, investigating the **immunomodulatory effect** of ECM scaffolds on cells/ tissue is an important point. Studies demonstrated that a certain degree of inflammation is beneficial for tissue regeneration. However, serve and long-lasting inflammation damages the implantation site and the scaffold leading to rejection in the worst case [205–207]. Within the framework of inflammation, the polarization of macrophages plays a crucial role. Macrophages can be polarized into the proinflammatory M1 macrophages and the anti-inflammatory M2 macrophages, which are essential for regenerative processes [208,209]. For an improved assessment of the immune response after reseeding or implantation, detailed investigations of the underlying mechanisms should be performed.
Due to the varying donors, a strict **selection of tissue sources** and **standardization of processing** of dECM, as it is suggested by Zhang *et al*., is difficult. As cdECM is produced by cultured cells monitoring of these cells as the source of the cdECM and standardization of processing is relatively easy implementable. Cell culture parameters like cell density, temperature, oxygen supply,

nutrient supply, and culture medium can be defined and monitored over the production time. In particular for primary cells, the spontaneous change of cellular characteristics is well known. There are methods in development (e.g. spectroscopic methods) for non-invasive monitoring of cellular processes/changes allowing even more precise monitoring.

ECM consists of naturally degradable proteins (e.g. collagen, PGs, and glycoproteins) that can be degraded with non-toxic degradation products by naturally occurring enzymes like matrix metalloproteases [210,211]. The **degradation rate** is an important parameter for implanted ECM scaffolds but also for scaffolds in engineered tissue constructs. If the degradation is faster than the production of new host ECM, tissue defects might occur or the tissue construct becomes unstable and cannot be used for further experiments. Following the degradation rate of the scaffold should be at the same speed as the regenerative capacity of the host tissue or reseeded cells [73]. As ECM exhibits natural binding sites for degradation enzymes like metalloproteases, it can be easily degraded by infiltrating or encapsulated cells. Crosslinking of the ECM scaffold, for example using genipin [212,213], may reduce the degradation rate. However, the chemical crosslinking of ECM protein alters the chemical and structural features of the ECM. One major advantage of cdECM is the possibility of specific functionalization using MGE enabling site-directed modification of the cdECM. This method opens up almost endless possibilities in cdECM modification beginning with the linking of enzymatic proteins over bioactive protein (e.g. growth factors or antibiotic molecules) to cross-linking of the cdECM itself and combinations of them. A widely used strategy for this method is the incorporation of azide functionalized monosaccharides and the modification of the resulting cdECM via CuAAC. The concern with this reaction is the need for copper as a catalyst, which can have cytotoxic effects when remaining in the cdECM. In this thesis, an alternative reaction that does not need any catalyst was demonstrated: the Diels Alder with inverse electron demand. Therefore, dienophile functionalized monosaccharides were used for the metabolic glycoengineering and the resulting cdECM was modified with tetrazine functionalized molecules **(confirming fourth hypothesis**) (see Paper III – Functionalization of cdECM; p.74). Functionalization of cdECM using azide-alkyne-cycloaddition or Diels Alder reaction offers the possibility to specifically crosslink the cdECM in finely tuned stages. Specific linkers enable the crosslinking of the cdECM structures themselves without altering the chemical and structural features of the cdECM.

Processing

To improve biocompatibility and remove pathogens that may elicit an immune response, decellularized scaffolds should be sterilized/ disinfected. Current **sterilization** methods can be

divided into chemical and physical methods. Chemical methods include treatment with ethylene oxide, antibiotics, and pancreatic acid. Ethylene oxide is a relatively mature method however it might affect ECM structure and produces toxic substances that might remain in the ECM material [214,215]. Antibiotics do not affect ECM structure but are ineffective on viruses and spores and the antimicrobial spectrum of each antibiotic is different. Pancreatic acid acts also antimicrobial, however, it destroys the chemical and physical characteristics of the ECM material [214]. A physical method is (gamma-)irradiation which is known to alter the physical, chemical, and biological compatibility of the ECM material [73,214,215]. Thus, sterilization of ECM products poses the problem that the common sterilization methods that meet the requirements of comprehensive disinfection damage the structure of the ECM to some degree which in turn have an impact on the cells and subsequently the experimental results or clinical outcome. Thus, generation of cdECM under sterile cell culture conditions is a huge advantage. It can be assumed that the cdECM is sterile by nature which would solve the problem of sterilization.

Regarding specific **(surface) modification** of the ECM material cdECM exhibits the advantage of specific functionalization/modification via MGE as described above. Modification of dECM is accompanied by alterations in chemical and/ or structural features of the ECM. Using specific addressable functional groups enables the modification of cdECM without affecting the chemical appearance or structure.

Experiments

ECM is a highly bioactive material that influences the cellular behavior of cells including differentiation of stem cells, activation of immune cells, and development of tissue organization and vascular structures. This bioactivity is based on different aspects of ECM. First, the impact of macromolecules and their organization within the ECM material. Second, ECM-bound protein-like growth factors and chemokines, and third the bioactivity of degradation products of the ECM and matrix-bound vesicles [51,52,216]. Next to dECM, this ability was also shown for cdECM. In this thesis, the enhancing effect of cdECM - especially cdECM from adipogenic differentiated ASCs – on the spontaneous formation of prevascular-like structures by mvECs was demonstrated (**confirming third hypothesis**) (see Paper II – Support of prevascular-like structure formation; p.50). These structures cannot be found on coating with the ECM protein collagen I, underlining the fact that individual ECM proteins cannot replace the natural ECM. The generation of functional vascular structures, in particular small vessels like capillaries, remains a challenge in tissue engineering. An autologous/ allogeneic (bio)material that enhances the formation of capillary structures may support efforts in this research area.

Due to the high number of different types of ECM, sources of ECM, decellularization protocols, and experimental designs comparability of the different studies is not given in most cases. In addition, donor variations and culture parameters can affect the experimental outcome. For an adequate comparison of different ECM materials (dECMs from different tissues as well as dECM and cdECM), a **standardization** of the experimental setup should be established [73]. This would facilitate the direct comparison of experiments using different ECM materials. These standards should include timepoints for reseeding of *in vitro* products and implantation of *in vivo* products, timepoints for evaluation of specific parameters like cellular survival and functionality, and in particular for implanted constructs the timepoint for endpoint analysis which represents the basis for the evaluation of the implant [73].

7 CONCLUSION AND OUTLOOK

The ECM represents the natural environment of cells in tissues and therefore is an interesting biomaterial for various tissue engineering and regenerative medicine approaches/ applications. In the present thesis, the macromolecular and structural differences of the native dECM and the cdECM were highlighted. The dECM was shown to contain a higher amount of mature collagens whereas cdECM exhibits a higher amount of sGAGs which were shown to have a beneficial impact on regenerative processes. In addition, the fiber diameter of cdECM was found to be lower compared to dECM which results in distinct topographical features. These differences have the potential to strongly affect cellular behavior and thus on the experimental outcome of *in vitro* and in *in vivo* studies. Thus, the demonstrated differences should be considered when interpreting obtained results and when choosing a biomaterial for a specific application. Future studies should focus on a more detailed characterization of native dECM and cdECM from various tissues and generations, decellularization, and processing methods. Next to macromolecular, structural, and physical characterization, this includes the determination of ECM-bound bioactive molecules, degradation products, and MBVs. A comprehensive characterized material would enable more in-depth studies of ECM-cell interactions and the effect of possible alterations in ECM on cellular behavior. This would ensure the reproducible outcome of *in vitro* and *in vivo* experiments.

The regenerative effect of cdECM was shown by investigating the impact on vascular structure formation. It was successfully demonstrated that cdECM has a supporting effect on the spontaneous formation of prevascular-like structures by mvECs. This effect was stronger on cdECM from adipogenic differentiated ASCs compared to cdECM from stem cells which might be traced back to pro-angiogenic factors found in cdECM substrates. As vascularization remains a challenge in tissue engineering and regenerative medicine, this regenerative effect by supporting vascular structure formation might be of advantage for various applications and a promising starting point for further investigations. The inductive potential of cdECM on vascular-like structure formation should be investigated in 3D approaches. These could be cdECM-hybrid hydrogels with varying cdECM concentrations or pure cdECM hydrogels. Also, the effect of co-cultured cells (e.g. pericytes) should be studied. These cells have the potential to enhance the effect of the cdECM material by supporting new built structures and lumenization.

A promising method for specific modification of cdECM is the functionalization of ECM structures with specific addressable functional groups by MGE and subsequent linking of molecules via site-directed chemical reactions. In this thesis, the functionalization of cdECM with dienophile groups

was demonstrated. These dienophile groups allow the catalyst-free, cell-friendly modification of cdECM via IEDDA reaction. These results highlight cdECM as a promising alternative to native dECM as it can be modified without affecting the structure of the ECM. This opens up a wide range of possible modification and specific adjustment depending on purpose. One interesting direction would be the further development of cdECM modified with antibiotic molecules for wound dressing. This would combine the regenerative capacity of cdECM, essential for wound healing with antibiotic properties to avoid infections and serve inflammation.

The major drawback of cdECM is the relatively low amount that can be generated to date. For relevant clinical applications, scale-up technologies for cdECM production should be established. Various approaches are made in this field however to date the amount of yielded cdECM is too low for successful transformation to the clinic.

REFERENCES

[1] C. Frantz, K.M. Stewart, V.M. Weaver, The extracellular matrix at a glance, J. Cell Sci. 123 (2010) 4195 LP – 4200. https://doi.org/10.1242/jcs.023820.

[2] A.D. Theocharis, S.S. Skandalis, C. Gialeli, N.K. Karamanos, Extracellular matrix structure, Adv. Drug Deliv. Rev. 97 (2016) 4–27. https://doi.org/10.1016/j.addr.2015.11.001.

[3] F.T. Bosman, I. Stamenkovic, Functional structure and composition of the extracellular matrix, J. Pathol. 200 (2003) 423–428. https://doi.org/10.1002/PATH.1437.

[4] M.A. Wozniak, K. Modzelewska, L. Kwong, P.J. Keely, Focal adhesion regulation of cell behavior, Biochim. Biophys. Acta - Mol. Cell Res. 1692 (2004) 103–119. https://doi.org/10.1016/J.BBAMCR.2004.04.007.

[5] B. Geiger, A. Bershadsky, Assembly and mechanosensory function of focal contacts, Curr. Opin. Cell Biol. 13 (2001) 584–592. https://doi.org/10.1016/S0955-0674(00)00255-6.

[6] N.K. Karamanos, Extracellular matrix: key structural and functional meshwork in health and disease, FEBS J. 286 (2019) 2826–2829. https://doi.org/10.1111/febs.14992.

[7] P. Laurila, I. Leivo, Basement membrane and interstitial matrix components form separate matrices in heterokaryons of PYS-2 cells and fibroblasts, J. Cell Sci. 104 (Pt 1) (1993) 59–68. https://doi.org/10.1242/JCS.104.1.59.

[8] S. Spada, A. Tocci, F. Di Modugno, P. Nisticò, Fibronectin as a multiregulatory molecule crucial in tumor matrisome: from structural and functional features to clinical practice in oncology, J. Exp. Clin. Cancer Res. 2021 401. 40 (2021) 1–14. https://doi.org/10.1186/S13046-021-01908-8.

[9] N.K. Karamanos, A.D. Theocharis, Z. Piperigkou, D. Manou, A. Passi, S.S. Skandalis, D.H. Vynios, V. Eronique Orian-Rousseau, S. Ricard-Blum, C.E.H. Schmelzer, L. Duca, M. Durbee, N.A. Afratis, L. Troeberg, M. Franchi, V. Masola, M. Onisto, N.K. Karamanos, A.D. Theocharis, A guide to the composition and functions of the extracellular matrix, (n.d.). https://doi.org/10.1111/febs.15776.

[10] A. Teti1, A. Teti, Regulation of cellular functions by extracellular matrix., J. Am. Soc. Nephrol. 2 (1992) S83. https://doi.org/10.1681/ASN.V210S83.

[11] I. GERSH, H.R. CATCHPOLE, The Nature of Ground Substance of Connective Tissue, Perspect. Biol. Med. 3 (1960) 282–319. https://doi.org/10.1353/PBM.1960.0019.

[12] M. Marieswaran, I. Jain, B. Garg, V. Sharma, D. Kalyanasundaram, A review on biomechanics of anterior cruciate ligament and materials for reconstruction, Appl. Bionics

Biomech. 2018 (2018). https://doi.org/10.1155/2018/4657824.

[13] N. Afratis, C. Gialeli, D. Nikitovic, T. Tsegenidis, E. Karousou, A.D. Theocharis, M.S. Pavão, G.N. Tzanakakis, N.K. Karamanos, Glycosaminoglycans: Key players in cancer cell biology and treatment, FEBS J. 279 (2012) 1177–1197. https://doi.org/10.1111/j.1742-4658.2012.08529.x.

[14] A. Köwitsch, G. Zhou, T. Groth, Medical application of glycosaminoglycans: a review, J. Tissue Eng. Regen. Med. 12 (2018) e23–e41. https://doi.org/10.1002/term.2398.

[15] M. Wang, X. Liu, Z. Lyu, H. Gu, D. Li, H. Chen, Glycosaminoglycans (GAGs) and GAG mimetics regulate the behavior of stem cell differentiation, Colloids Surfaces B Biointerfaces. 150 (2017) 175–182. https://doi.org/10.1016/J.COLSURFB.2016.11.022.

[16] H. Sodhi, A. Panitch, Glycosaminoglycans in Tissue Engineering: A Review, Biomol. 2021, Vol. 11, Page 29. 11 (2020) 29. https://doi.org/10.3390/BIOM11010029.

[17] R. V. Iozzo, A.D. Murdoch, Proteoglycans of the extracellular environment: clues from the gene and protein side offer novel perspectives in molecular diversity and function, FASEB J. 10 (1996) 598–614. https://doi.org/10.1096/fasebj.10.5.8621059.

[18] J.E. Scott, Supramolecular organization of extracellular matrix glycosaminoglycans, in vitro and in the tissues, FASEB J. 6 (1992) 2639–2645. https://doi.org/10.1096/FASEBJ.6.9.1612287.

[19] L.E. Bertassoni, M. V. Swain, The contribution of proteoglycans to the mechanical behavior of mineralized tissues, J. Mech. Behav. Biomed. Mater. 38 (2014) 91–104. https://doi.org/10.1016/J.JMBBM.2014.06.008.

[20] J.R. Couchman, Transmembrane signaling proteoglycans, Annu. Rev. Cell Dev. Biol. 26 (2010) 89–114. https://doi.org/10.1146/annurev-cellbio-100109-104126.

[21] J.R. Couchman, C.A. Pataki, An Introduction to Proteoglycans and Their Localization, J. Histochem. Cytochem. 60 (2012) 885–897. https://doi.org/10.1369/0022155412464638.

[22] S. Ricard-Blum, The Collagen Family, Cold Spring Harb. Perspect. Biol. 3 (2011) 1–19. https://doi.org/10.1101/cshperspect.a004978.

[23] A.B. Balaji, H. Pakalapati, M. Khalid, R. Walvekar, H. Siddiqui, Natural and synthetic biocompatible and biodegradable polymers, 2017. https://doi.org/10.1016/B978-0-08-100970-3.00001-8.

[24] A. Sorushanova, L.M. Delgado, Z. Wu, N. Shologu, A. Kshirsagar, R. Raghunath, A.M. Mullen, Y. Bayon, A. Pandit, M. Raghunath, D.I. Zeugolis, A. Sorushanova, L.M. Delgado, Z. Wu, N. Shologu, D.I. Zeugolis, A. Kshirsagar, A. Pandit, R. Raghunath, M. Raghunath, A.M. Mullen, Y. Bayon, The Collagen Suprafamily: From Biosynthesis to Advanced Biomaterial

Development, Adv. Mater. 31 (2019) 1801651. https://doi.org/10.1002/ADMA.201801651.

[25] M. Yamauchi, M. Sricholpech, Lysine post-translational modifications of collagen, Essays Biochem. 52 (2012) 113–133. https://doi.org/10.1042/BSE0520113.

[26] R.A.F. Gjaltema, R.A. Bank, Molecular insights into prolyl and lysyl hydroxylation of fibrillar collagens in health and disease, Crit. Rev. Biochem. Mol. Biol. 52 (2017) 74–95. https://doi.org/10.1080/10409238.2016.1269716.

[27] K.E. Kadler, C. Baldock, J. Bella, R.P. Boot-Handford, Collagens at a glance, J. Cell Sci. 120 (2007) 1955–1958. https://doi.org/10.1242/jcs.03453.

[28] S.D. Vallet, S. Ricard-Blum, Lysyl oxidases: From enzyme activity to extracellular matrix cross-links, Essays Biochem. 63 (2019) 349–364. https://doi.org/10.1042/EBC20180050.

[29] Y. Luo, D. Sinkeviciute, Y. He, M. Karsdal, Y. Henrotin, A. Mobasheri, P. Önnerfjord, A. Bay-Jensen, The minor collagens in articular cartilage, Protein Cell. 8 (2017) 560–572. https://doi.org/10.1007/s13238-017-0377-7.

[30] M. Sun, E.Y. Luo, S.M. Adams, T. Adams, Y. Ye, S.S. Shetye, L.J. Soslowsky, D.E. Birk, Collagen XI regulates the acquisition of collagen fibril structure, organization and functional properties in tendon, Matrix Biol. 94 (2020) 77–94. https://doi.org/10.1016/j.matbio.2020.09.001.

[31] P.S. Amenta, N.A. Scivoletti, M.D. Newman, J.P. Sciancalepore, D. Li, J.C. Myers, Proteoglycan-collagen XV in human tissues is seen linking banded collagen fibers subjacent to the basement membrane, J. Histochem. Cytochem. 53 (2005) 165–176. https://doi.org/10.1369/jhc.4A6376.2005.

[32] B.R. Olsen, Collagen IX, Int. J. Biochem. Cell Biol. 29 (1997) 555–558. https://doi.org/10.1016/S1357-2725(96)00100-8.

[33] M. Cescon, F. Gattazzo, P. Chen, P. Bonaldo, Collagen VI at a glance, J. Cell Sci. 128 (2015) 3525–3531. https://doi.org/10.1242/jcs.169748.

[34] A. Nyström, D. Velati, V.R. Mittapalli, A. Fritsch, J.S. Kern, L. Bruckner-Tuderman, Collagen VII plays a dual role in wound healing, J. Clin. Invest. 123 (2013) 3498–3509. https://doi.org/10.1172/JCI68127.

[35] A.O. Eghrari, S.A. Riazuddin, J.D. Gottsch, Overview of the Cornea: Structure, Function, and Development, in: Prog. Mol. Biol. Transl. Sci., Elsevier B.V., 2015: pp. 7–23. https://doi.org/10.1016/bs.pmbts.2015.04.001.

[36] G. Shen, The role of type X collagen in facilitating and regulating endochondral ossification of articular cartilage, Orthod. Craniofacial Res. 8 (2005) 11–17.

https://doi.org/10.1111/j.1601-6343.2004.00308.x.

[37] K. Natsuga, M. Watanabe, W. Nishie, H. Shimizu, Life before and beyond blistering: The role of collagen XVII in epidermal physiology, Exp. Dermatol. 28 (2019) 1135–1141. https://doi.org/10.1111/exd.13550.

[38] M. Hurskainen, F. Ruggiero, P. Hägg, T. Pihlajaniemi, P. Huhtala, Recombinant human collagen XV regulates cell adhesion and migration, J. Biol. Chem. 285 (2010) 5258–5265. https://doi.org/10.1074/jbc.M109.033787.

[39] K.S. Midwood, J.E. Schwarzbauer, Elastic Fibers: Building Bridges Between Cells and Their Matrix, Curr. Biol. 12 (2002) R279–R281. https://doi.org/10.1016/S0960-9822(02)00800-X.

[40] C.M. Kielty, M.J. Sherratt, C.A. Shuttleworth, Elastic fibres, J. Cell Sci. 115 (2002) 2817–2828. https://doi.org/10.1242/JCS.115.14.2817.

[41] B.B. Aaron, J.M. Gosline, Elastin as a random-network elastomer: A mechanical and optical analysis of single elastin fibers, Biopolymers. 20 (1981) 1247–1260. https://doi.org/10.1002/BIP.1981.360200611.

[42] M. RP, Methods in elastic tissue biology: elastin isolation and purification, Methods. 45 (2008) 32–41. https://doi.org/10.1016/J.YMETH.2008.01.007.

[43] K. FW, The synthesis of soluble and insoluble elastin in chicken aorta as a function of development and age. Effect of a high cholesterol diet, Can. J. Biochem. 57 (1979) 1273–1280. https://doi.org/10.1139/O79-169.

[44] C.E.H. Schmelzer, L. Duca, Elastic fibers: formation, function, and fate during aging and disease, FEBS J. (2021). https://doi.org/10.1111/FEBS.15899.

[45] D. EC, Stability of elastin in the developing mouse aorta: a quantitative radioautographic study, Histochemistry. 100 (1993) 17–26. https://doi.org/10.1007/BF00268874.

[46] H. M, L. CA, R. L, Tropoelastin gene expression in the developing vascular system of the chicken: an in situ hybridization study, Anat. Embryol. (Berl). 188 (1993) 481–492. https://doi.org/10.1007/BF00190142.

[47] T. USHIKI, Collagen Fibers, Reticular Fibers and Elastic Fibers. A Comprehensive Understanding from a Morphological Viewpoint, Arch. Histol. Cytol. 65 (2002) 109–126. https://doi.org/10.1679/AOHC.65.109.

[48] H. MIYATA, M. ABE, K. TAKEHANA, K. IWASA, T. HIRAGA, Electron Microscopic Studies on Reticular Fibers in the Pig Sheathed Artery and Splenic Cords, J. Vet. Med. Sci. 55 (1993) 821–827. https://doi.org/10.1292/JVMS.55.821.

[49] S. Ricard-Blum, S.D. Vallet, Fragments generated upon extracellular matrix remodeling: Biological regulators and potential drugs, Matrix Biol. 75–76 (2019) 170–189.

https://doi.org/10.1016/j.matbio.2017.11.005.

[50] S. Ricard-Blum, R. Salza, Matricryptins and matrikines: Biologically active fragments of the extracellular matrix, Exp. Dermatol. 23 (2014) 457–463. https://doi.org/10.1111/exd.12435.

[51] L. Huleihel, G.S. Hussey, J.D. Naranjo, L. Zhang, J.L. Dziki, N.J. Turner, D.B. Stolz, S.F. Badylak, Matrix-bound nanovesicles within ECM bioscaffolds, Sci. Adv. 2 (2016). https://doi.org/10.1126/SCIADV.1600502.

[52] G.S. Hussey, C.P. Molina, M.C. Cramer, Y.Y. Tyurina, V.A. Tyurin, Y.C. Lee, S.O. El-Mossier, M.H. Murdock, P.S. Timashev, V.E. Kagan, S.F. Badylak, Lipidomics and RNA sequencing reveal a novel subpopulation of nanovesicle within extracellular matrix biomaterials, Sci. Adv. 6 (2020) 4361. https://doi.org/10.1126/SCIADV.AAY4361.

[53] O. Saksela, M. Laiho, Growth factors in the extracellular matrix, FASEB J. 11 (1997) 51–59. https://doi.org/10.1096/FASEBJ.11.1.9034166.

[54] J. Zhu, R.A.F. Clark, Fibronectin at Select Sites Binds Multiple Growth Factors and Enhances their Activity: Expansion of the Collaborative ECM-GF Paradigm, J. Invest. Dermatol. 134 (2014) 895–901. https://doi.org/10.1038/JID.2013.484.

[55] N. Khalilgharibi, Y. Mao, To form and function: on the role of basement membrane mechanics in tissue development, homeostasis and disease, Open Biol. 11 (2021). https://doi.org/10.1098/RSOB.200360.

[56] Y. Kubo, S. Kaidzu, I. Nakajima, … K.T.-I.V.C.&, undefined 2000, Organization of extracellular matrix components during differentiation of adipocytes in long-term culture, Springer. (n.d.). https://doi.org/10.1290/1071.

[57] C. Leclech, C.F. Natale, A.I. Barakat, The basement membrane as a structured surface – role in vascular health and disease, J. Cell Sci. 133 (2021). https://doi.org/10.1242/jcs.239889.

[58] M.J. Randles, M.J. Humphries, R. Lennon, Proteomic definitions of basement membrane composition in health and disease, Matrix Biol. 57–58 (2017) 12–28. https://doi.org/10.1016/j.matbio.2016.08.006.

[59] D.P. Keeley, E. Hastie, R. Jayadev, L.C. Kelley, Q. Chi, S.G. Payne, J.L. Jeger, B.D. Hoffman, D.R. Sherwood, Comprehensive Endogenous Tagging of Basement Membrane Components Reveals Dynamic Movement within the Matrix Scaffolding, Dev. Cell. 54 (2020) 60-74.e7. https://doi.org/10.1016/J.DEVCEL.2020.05.022.

[60] H. Colognato, P.D. Yurchenco, REVIEWS A PEER REVIEWED FORUM Form and Function: The Laminin Family of Heterotrimers, (2000). https://doi.org/10.1002/(SICI)1097-0177(200006)218:2.

[61] M. Aumailley, The laminin family, Http://Dx.Doi.Org/10.4161/Cam.22826. 7 (2012) 48–55. https://doi.org/10.4161/CAM.22826.

[62] S. Li, D. Edgar, R. Fässler, W. Wadsworth, P.D. Yurchenco, The Role of Laminin in Embryonic Cell Polarization and Tissue Organization, Dev. Cell. 4 (2003) 613–624. https://doi.org/10.1016/S1534-5807(03)00128-X.

[63] K.M. Malinda, A.B. Wysocki, J.E. Koblinski, H.K. Kleinman, M.L. Ponce, Angiogenic laminin-derived peptides stimulate wound healing, Int. J. Biochem. Cell Biol. 40 (2008) 2771–2780. https://doi.org/10.1016/J.BIOCEL.2008.05.025.

[64] National Institutes of Health, Clinical Applications of Biomaterials, Consens. Dev. Conf. Statement. November 1 (1982) 1–19.

[65] C.P. Bergmann, A. Stumpf, Biomaterials, Top. Mining, Metall. Mater. Eng. (2013) 9–13. https://doi.org/10.1007/978-3-642-38224-6_2.

[66] K.D. Jandt, Evolutions, revolutions and trends in biomaterials science -A perspective, Adv. Eng. Mater. 9 (2007) 1035–1050. https://doi.org/10.1002/ADEM.200700284.

[67] B.D. Ratner, G. Zhang, A History of Biomaterials, Biomater. Sci. (2020) 21–34. https://doi.org/10.1016/B978-0-12-816137-1.00002-7.

[68] X. Yu, X. Tang, S. V. Gohil, C.T. Laurencin, Biomaterials for Bone Regenerative Engineering, Adv. Healthc. Mater. 4 (2015) 1268–1285. https://doi.org/10.1002/ADHM.201400760.

[69] M.J. Cooke, S.R. Phillips, D.S.H. Shah, D. Athey, J.H. Lakey, S.A. Przyborski, Enhanced cell attachment using a novel cell culture surface presenting functional domains from extracellular matrix proteins, Cytotechnology. 56 (2008) 71–79. https://doi.org/10.1007/S10616-007-9119-7.

[70] D. Lam, H.A. Enright, J. Cadena, S.K.G. Peters, A.P. Sales, J.J. Osburn, D.A. Soscia, K.S. Kulp, E.K. Wheeler, N.O. Fischer, Tissue-specific extracellular matrix accelerates the formation of neural networks and communities in a neuron-glia co-culture on a multi-electrode array, Sci. Reports 2019 91. 9 (2019) 1–15. https://doi.org/10.1038/s41598-019-40128-1.

[71] F. Tan, M. Al-Rubeai, Customizable Implant-specific and Tissue-Specific Extracellular Matrix Protein Coatings Fabricated Using Atmospheric Plasma, Front. Bioeng. Biotechnol. 0 (2019) 247. https://doi.org/10.3389/FBIOE.2019.00247.

[72] T. Hoshiba, T. Yamaoka, CHAPTER 1 Extracellular Matrix Scaffolds for Tissue Engineering and Biological Research, (2019) 1–14. https://doi.org/10.1039/9781788015998-00001.

[73] X. Zhang, X. Chen, H. Hong, R. Hu, J. Liu, C. Liu, Decellularized extracellular matrix scaffolds: Recent trends and emerging strategies in tissue engineering, Bioact. Mater. 10 (2022) 15–31. https://doi.org/10.1016/J.BIOACTMAT.2021.09.014.

[74] W.E. Poel, Preparation of acellular homogenates from muscle samples, Science (80-.). 108 (1948) 390–391. https://doi.org/10.1126/science.108.2806.390-a.

[75] J.T. Hjelle, E.C. Carlson, K. Brendel, E. Meezan, Biosynthesis of basement membrane matrix by isolated rat renal glomeruli, Kidney Int. 15 (1979) 20–32. https://doi.org/10.1038/KI.1979.3.

[76] S.F. Badylak, R. Tullius, K. Kokini, K.D. Shelbourne, T. Klootwyk, S.L. Voytik, M.R. Kraine, C. Simmons, The use of xenogeneic small intestinal submucosa as a biomaterial for Achille's tendon repair in a dog model, J. Biomed. Mater. Res. 29 (1995) 977–985. https://doi.org/10.1002/JBM.820290809.

[77] H.C. Ott, T.S. Matthiesen, S.K. Goh, L.D. Black, S.M. Kren, T.I. Netoff, D.A. Taylor, Perfusion-decellularized matrix: using nature's platform to engineer a bioartificial heart, Nat. Med. 2008 142. 14 (2008) 213–221. https://doi.org/10.1038/nm1684.

[78] H.C. Ott, B. Clippinger, C. Conrad, C. Schuetz, I. Pomerantseva, L. Ikonomou, D. Kotton, J.P. Vacanti, Regeneration and orthotopic transplantation of a bioartificial lung, Nat. Med. 2010 168. 16 (2010) 927–933. https://doi.org/10.1038/nm.2193.

[79] T.H. Petersen, E.A. Calle, L. Zhao, E.J. Lee, L. Gui, M.S.B. Raredon, K. Gavrilov, T. Yi, Z.W. Zhuang, C. Breuer, E. Herzog, L.E. Niklason, Tissue-engineered lungs for in vivo implantation, Science (80-.). 329 (2010) 538–541. https://doi.org/10.1126/SCIENCE.1189345/SUPPL_FILE/PETERSEN-SOM.REVISION.1.PDF.

[80] B.E. Uygun, A. Soto-Gutierrez, H. Yagi, M.L. Izamis, M.A. Guzzardi, C. Shulman, J. Milwid, N. Kobayashi, A. Tilles, F. Berthiaume, M. Hertl, Y. Nahmias, M.L. Yarmush, K. Uygun, Organ reengineering through development of a transplantable recellularized liver graft using decellularized liver matrix, Nat. Med. 2010 167. 16 (2010) 814–820. https://doi.org/10.1038/nm.2170.

[81] J.J. Song, J.P. Guyette, S.E. Gilpin, G. Gonzalez, J.P. Vacanti, H.C. Ott, Regeneration and experimental orthotopic transplantation of a bioengineered kidney, Nat. Med. 2013 195. 19 (2013) 646–651. https://doi.org/10.1038/nm.3154.

[82] E. Garreta, R. Oria, C. Tarantino, M. Pla-Roca, P. Prado, F. Fernández-Avilés, J.M. Campistol, J. Samitier, N. Montserrat, Tissue engineering by decellularization and 3D bioprinting, Mater. Today. 20 (2017) 166–178. https://doi.org/10.1016/J.MATTOD.2016.12.005.

[83] C. Mandrycky, Z. Wang, K. Kim, D.H. Kim, 3D bioprinting for engineering complex tissues, Biotechnol. Adv. 34 (2016) 422–434. https://doi.org/10.1016/J.BIOTECHADV.2015.12.011.

[84] F. Pati, J. Jang, D.H. Ha, S. Won Kim, J.W. Rhie, J.H. Shim, D.H. Kim, D.W. Cho, Printing three-dimensional tissue analogues with decellularized extracellular matrix bioink, Nat.

Commun. 5 (2014) 1–11. https://doi.org/10.1038/ncomms4935.

[85] L.E. Fitzpatrick, T.C. McDevitt, Cell-derived matrices for tissue engineering and regenerative medicine applications, Biomater. Sci. 3 (2015) 12–24. https://doi.org/10.1039/c4bm00246f.

[86] P.M. Crapo, T.W. Gilbert, S.F. Badylak, An overview of tissue and whole organ decellularization processes, Biomaterials. 32 (2011) 3233–3243. https://doi.org/10.1016/j.biomaterials.2011.01.057.

[87] K. Schenke-Layland, F. Opitz, M. Gross, C. Döring, K.J. Halbhuber, F. Schirrmeister, T. Wahlers, U.A. Stock, Complete dynamic repopulation of decellularized heart valves by application of defined physical signals—an in vitro study, Cardiovasc. Res. 60 (2003) 497–509. https://doi.org/10.1016/J.CARDIORES.2003.09.002.

[88] M.C. VeDepo, M.S. Detamore, R.A. Hopkins, G.L. Converse, Recellularization of decellularized heart valves: Progress toward the tissue-engineered heart valve, J. Tissue Eng. 8 (2017). https://doi.org/10.1177/2041731417726327.

[89] F. Juthier, A. Vincentelli, J. Gaudric, D. Corseaux, O. Fouquet, C. Calet, T. Le Tourneau, V. Soenen, C. Zawadzki, O. Fabre, S. Susen, A. Prat, B. Jude, Decellularized heart valve as a scaffold for in vivo recellularization: Deleterious effects of granulocyte colony-stimulating factor, J. Thorac. Cardiovasc. Surg. 131 (2006) 843–852. https://doi.org/10.1016/J.JTCVS.2005.11.037.

[90] M. OA, C. B, P. JN, T.-P. C, H. DA, B. BA, G. JM, Decellularized Adipose Tissue: Biochemical Composition, in vivo Analysis and Potential Clinical Applications, Adv. Exp. Med. Biol. 1212 (2020) 57–70. https://doi.org/10.1007/5584_2019_371.

[91] M. Song, Y. Liu, L. Hui, Preparation and characterization of acellular adipose tissue matrix using a combination of physical and chemical treatments, Mol. Med. Rep. 17 (2018) 138–146. https://doi.org/10.3892/mmr.2017.7857.

[92] I. Belviso, V. Romano, A.M. Sacco, G. Ricci, D. Massai, M. Cammarota, A. Catizone, C. Schiraldi, D. Nurzynska, M. Terzini, A. Aldieri, G. Serino, F. Schonauer, F. Sirico, F. D'Andrea, S. Montagnani, F. Di Meglio, C. Castaldo, Decellularized Human Dermal Matrix as a Biological Scaffold for Cardiac Repair and Regeneration, Front. Bioeng. Biotechnol. 0 (2020) 229. https://doi.org/10.3389/FBIOE.2020.00229.

[93] J. AM, C. Z, G. G, L. SJ, Y. JJ, S. S, A. A, Decellularized Skin Extracellular Matrix (dsECM) Improves the Physical and Biological Properties of Fibrinogen Hydrogel for Skin Bioprinting Applications, Nanomater. (Basel, Switzerland). 10 (2020) 1–10. https://doi.org/10.3390/NANO10081484.

[94] Y. Ji, J. Zhou, T. Sun, K. Tang, Z. Xiong, Z. Ren, S. Yao, K. Chen, F. Yang, F. Zhu, X. Guo, Diverse preparation methods for small intestinal submucosa (SIS): Decellularization, components, and structure, J. Biomed. Mater. Res. - Part A. 107 (2019) 689–697. https://doi.org/10.1002/JBM.A.36582.

[95] M. Parmaksiz, A. Dogan, S. Odabas, A.E. Elçin, Y.M. Elçin, Clinical applications of decellularized extracellular matrices for tissue engineering and regenerative medicine, Biomed. Mater. 11 (2016) 022003. https://doi.org/10.1088/1748-6041/11/2/022003.

[96] M. Parmaksiz, A.E. Elçin, Y.M. Elçin, Decellularization of bovine small intestinal submucosa, Methods Mol. Biol. 1577 (2018) 129–138. https://doi.org/10.1007/7651_2017_33.

[97] R. DJ, R. GC, A.S. E, G. M, B. AJ, M. S, Decellularization and sterilization of porcine urinary bladder matrix for tissue engineering in the lower urinary tract, Regen. Med. 3 (2008) 145–156. https://doi.org/10.2217/17460751.3.2.145.

[98] K. CY, N. HQ, W. YC, Characterization of Porcine Urinary Bladder Matrix Hydrogels from Sodium Dodecyl Sulfate Decellularization Method, Polymers (Basel). 12 (2020) 1–16. https://doi.org/10.3390/POLYM12123007.

[99] A.B. Lovati, M. Bottagisio, M. Moretti, Decellularized and Engineered Tendons as Biological Substitutes: A Critical Review, Stem Cells Int. 2016 (2016). https://doi.org/10.1155/2016/7276150.

[100] A. de Lima Santos, C.G. da Silva, L.S. de Sá Barreto, K.R.M. Leite, M.J.S. Tamaoki, L.M. Ferreira, F.G. de Almeida, F. Faloppa, A new decellularized tendon scaffold for rotator cuff tears – evaluation in rabbits, BMC Musculoskelet. Disord. 2020 211. 21 (2020) 1–12. https://doi.org/10.1186/S12891-020-03680-W.

[101] P.J. Schaner, N.D. Martin, T.N. Tulenko, I.M. Shapiro, N.A. Tarola, R.F. Leichter, R.A. Carabasi, P.J. DiMuzio, Decellularized vein as a potential scaffold for vascular tissue engineering, J. Vasc. Surg. 40 (2004) 146–153. https://doi.org/10.1016/J.JVS.2004.03.033.

[102] S. Xu, F. Lu, L. Cheng, C. Li, X. Zhou, Y. Wu, H. Chen, K. Zhang, L. Wang, J. Xia, G. Yan, Z. Qi, Preparation and characterization of small-diameter decellularized scaffolds for vascular tissue engineering in an animal model, Biomed. Eng. OnLine 2017 161. 16 (2017) 1–15. https://doi.org/10.1186/S12938-017-0344-9.

[103] T.W. Gilbert, T.L. Sellaro, S.F. Badylak, Decellularization of tissues and organs, Biomaterials. 27 (2006) 3675–3683. https://doi.org/10.1016/J.BIOMATERIALS.2006.02.014.

[104] K. Dzobo, K.S.C.M. Motaung, A. Adesida, Recent Trends in Decellularized Extracellular Matrix Bioinks for 3D Printing: An Updated Review, Int. J. Mol. Sci. 2019, Vol. 20, Page 4628. 20 (2019) 4628. https://doi.org/10.3390/IJMS20184628.

[105] R.M. Spiers, J. Marzi, E.M. Brauchle, S.E. Cross, R.H. Vaughan, P.A. Bateman, S.J. Hughes, K. Schenke-Layland, P.R.V. Johnson, Donor age significantly influences the Raman spectroscopic biomolecular fingerprint of human pancreatic extracellular matrix proteins following collagenase-based digestion, Acta Biomater. 99 (2019) 269–283. https://doi.org/10.1016/J.ACTBIO.2019.09.013.

[106] T.D. Johnson, R.C. Hill, M. Dzieciatkowska, V. Nigam, A. Behfar, K.L. Christman, K.C. Hansen, Quantification of decellularized human myocardial matrix: A comparison of six patients, PROTEOMICS – Clin. Appl. 10 (2016) 75–83. https://doi.org/10.1002/PRCA.201500048.

[107] S.B. Seif-Naraghi, D. Horn, P.A. Schup-Magoffin, M.M. Madani, K.L. Christman, Patient-to-patient variability in autologous pericardial matrix scaffolds for cardiac repair, J. Cardiovasc. Transl. Res. 4 (2011) 545–556. https://doi.org/10.1007/S12265-011-9293-Z.

[108] T.D. Johnson, J.A. Dequach, R. Gaetani, J. Ungerleider, D. Elhag, V. Nigam, A. Behfar, K.L. Christman, Human versus porcine tissue sourcing for an injectable myocardial matrix hydrogel, Biomater. Sci. 2 (2014) 735–744. https://doi.org/10.1039/c3bm60283d.

[109] S. Gilpin, J. Guyette, G. Gonzalez, … X.R.-T.J. of H. and, undefined 2014, Perfusion decellularization of human and porcine lungs: bringing the matrix to clinical scale, Elsevier. (n.d.). https://www.sciencedirect.com/science/article/pii/S1053249813015118 (accessed March 12, 2022).

[110] D.A. Beacham, M.D. Amatangelo, E. Cukierman, Preparation of Extracellular Matrices Produced by Cultured and Primary Fibroblasts, Curr. Protoc. Cell Biol. 33 (2006) 10.9.1-10.9.21. https://doi.org/10.1002/0471143030.CB1009S33.

[111] C. Quint, M. Arief, A. Muto, A. Dardik, L.E. Niklason, Allogeneic human tissue-engineered blood vessel, J. Vasc. Surg. 55 (2012) 790–798. https://doi.org/10.1016/J.JVS.2011.07.098.

[112] B.Q. Le, C. van Blitterswijk, J. de Boer, An Approach to In Vitro Manufacturing of Hypertrophic Cartilage Matrix for Bone Repair, Bioeng. 2017, Vol. 4, Page 35. 4 (2017) 35. https://doi.org/10.3390/BIOENGINEERING4020035.

[113] Y. Yang, H. Lin, H. Shen, B. Wang, G. Lei, R.S. Tuan, Mesenchymal stem cell-derived extracellular matrix enhances chondrogenic phenotype of and cartilage formation by encapsulated chondrocytes in vitro and in vivo, Acta Biomater. 69 (2018) 71–82. https://doi.org/10.1016/J.ACTBIO.2017.12.043.

[114] V. Guneta, Q.L. Loh, C. Choong, Cell-secreted extracellular matrix formation and differentiation of adipose-derived stem cells in 3D alginate scaffolds with tunable properties, J. Biomed. Mater. Res. Part A. 104 (2016) 1090–1101. https://doi.org/10.1002/jbm.a.35644.

[115] M.S. Carvalho, J.C. Silva, J.M.S. Cabral, C.L. da Silva, D. Vashishth, Cultured cell-derived extracellular matrices to enhance the osteogenic differentiation and angiogenic properties of human mesenchymal stem/stromal cells, J. Tissue Eng. Regen. Med. 13 (2019) 1544–1558. https://doi.org/10.1002/TERM.2907.

[116] X. Mingyuan, P. Qianqian, X. Shengquan, Y. Chenyi, L. Rui, S. Yichen, X. Jinghong, Hypoxia-inducible factor-1α activates transforming growth factor-β1/Smad signaling and increases collagen deposition in dermal fibroblasts, Oncotarget. 9 (2018) 3188. https://doi.org/10.18632/ONCOTARGET.23225.

[117] Y. Horino, S. Takahashi, T. Miura, Y. Takahashi, Prolonged hypoxia accelerates the posttranscriptional process of collagen synthesis in cultured fibroblasts, Life Sci. 71 (2002) 3031–3045. https://doi.org/10.1016/S0024-3205(02)02142-2.

[118] Q. Xing, Z. Qian, M. Tahtinen, A. Hui Yap, K. Yates, F. Zhao, Q. Xing, Z. Qian, M. Tahtinen, A.H. Yap, K. Yates, F. Zhao, Aligned Nanofibrous Cell-Derived Extracellular Matrix for Anisotropic Vascular Graft Construction, Adv. Healthc. Mater. 6 (2017) 1601333. https://doi.org/10.1002/ADHM.201601333.

[119] M. Li, A. Zhang, J. Li, J. Zhou, Y. Zheng, C. Zhang, D. Xia, H. Mao, J. Zhao, Osteoblast/fibroblast coculture derived bioactive ECM with unique matrisome profile facilitates bone regeneration, Bioact. Mater. 5 (2020) 938–948. https://doi.org/10.1016/J.BIOACTMAT.2020.06.017.

[120] J. Li, K.C. Hansen, Y. Zhang, C. Dong, C.Z. Dinu, M. Dzieciatkowska, M. Pei, Rejuvenation of chondrogenic potential in a young stem cell microenvironment, Biomaterials. 35 (2014) 642–653. https://doi.org/10.1016/J.BIOMATERIALS.2013.09.099.

[121] W.W. Chan, F. Yu, Q.B. Le, S. Chen, M. Yee, D. Choudhury, Towards Biomanufacturing of Cell-Derived Matrices, Int. J. Mol. Sci. 2021, Vol. 22, Page 11929. 22 (2021) 11929. https://doi.org/10.3390/IJMS222111929.

[122] S.R. Pinnell, Regulation of collagen biosynthesis by ascorbic acid: a review., Yale J. Biol. Med. 58 (1985) 553. /pmc/articles/PMC2589959/?report=abstract (accessed March 12, 2022).

[123] S. Han, Y. Li, B.P. Chan, Extracellular Protease Inhibition Alters the Phenotype of Chondrogenically Differentiating Human Mesenchymal Stem Cells (MSCs) in 3D Collagen Microspheres, PLoS One. 11 (2016) e0146928. https://doi.org/10.1371/JOURNAL.PONE.0146928.

[124] C. Chen, F. Loe, A. Blocki, Y. Peng, M. Raghunath, Applying macromolecular crowding to enhance extracellular matrix deposition and its remodeling in vitro for tissue engineering

and cell-based therapies, Adv. Drug Deliv. Rev. 63 (2011) 277–290. https://doi.org/10.1016/J.ADDR.2011.03.003.

[125] H. H, Secretory factors from human adipose tissue and their functional role, Proc. Nutr. Soc. 64 (2005) 163–169. https://doi.org/10.1079/PNS2005428.

[126] C.M. Pond, The Evolution of Mammalian Adipose Tissues, Adipose Tissue Biol. Second Ed. (2017) 1–59. https://doi.org/10.1007/978-3-319-52031-5_1.

[127] C. M, O. T, F. R, Biochemistry of adipose tissue: an endocrine organ, Arch. Med. Sci. 9 (2013) 191–200. https://doi.org/10.5114/AOMS.2013.33181.

[128] X. Y, L. S, B. E, C. Y, Adipose angiogenesis: quantitative methods to study microvessel growth, regression and remodeling in vivo, Nat. Protoc. 5 (2010) 912–920. https://doi.org/10.1038/NPROT.2010.46.

[129] J. M, P. J, S. K, J. E, S. PA, G. BG, L. M, S. A, R. M, L. TC, C. B, C. LM, L. M, Separation of human adipocytes by size: hypertrophic fat cells display distinct gene expression, FASEB J. 20 (2006) 1540–1542. https://doi.org/10.1096/FJ.05-5678FJE.

[130] C. WP, S. EL, M. OA, Adipose tissue stem cells meet preadipocyte commitment: going back to the future, J. Lipid Res. 53 (2012) 227–246. https://doi.org/10.1194/JLR.R021089.

[131] D. M, L.B. K, M. I, S.-C. I, M. F, K. D, D. R, K. A, P. Dj, H. E, Minimal criteria for defining multipotent mesenchymal stromal cells. The International Society for Cellular Therapy position statement, Cytotherapy. 8 (2006) 315–317. https://doi.org/10.1080/14653240600855905.

[132] N. PJ, The biology of PECAM-1, J. Clin. Invest. 99 (1997) 3–8. https://doi.org/10.1172/JCI119129.

[133] M. P, P. P, P. P, L. I, D. JP, Visceral obesity: the link among inflammation, hypertension, and cardiovascular disease, Hypertens. (Dallas, Tex. 1979). 53 (2009) 577–584. https://doi.org/10.1161/HYPERTENSIONAHA.108.110320.

[134] T. LE, M. RA, C. EJ, Extracellular Matrix and Dermal Fibroblast Function in the Healing Wound, Adv. Wound Care. 5 (2016) 119–136. https://doi.org/10.1089/WOUND.2014.0561.

[135] L.E. Flynn, The use of decellularized adipose tissue to provide an inductive microenvironment for the adipogenic differentiation of human adipose-derived stem cells, Biomaterials. 31 (2010) 4715–4724. https://doi.org/10.1016/j.biomaterials.2010.02.046.

[136] P.M. Martin, A. Shridhar, C. Yu, C. Brown, L.E. Flynn, Decellularized adipose tissue scaffolds for soft tissue regeneration and adipose-derived stem/stromal cell delivery, Methods Mol. Biol. 1773 (2018) 53–71. https://doi.org/10.1007/978-1-4939-7799-4_6.

[137] D.A. Young, D.O. Ibrahim, D. Hu, K.L. Christman, Injectable hydrogel scaffold from decellularized human lipoaspirate, Acta Biomater. 7 (2011) 1040–1049. https://doi.org/10.1016/j.actbio.2010.09.035.

[138] F. Pati, D.H. Ha, J. Jang, H.H. Han, J.W. Rhie, D.W. Cho, Biomimetic 3D tissue printing for soft tissue regeneration, Biomaterials. 62 (2015) 164–175. https://doi.org/10.1016/j.biomaterials.2015.05.043.

[139] Y. Zhao, J. Fan, S. Bai, Biocompatibility of injectable hydrogel from decellularized human adipose tissue *in vitro* and *in vivo*, J. Biomed. Mater. Res. Part B Appl. Biomater. 107 (2019) 1684–1694. https://doi.org/10.1002/jbm.b.34261.

[140] A.E.B. Turner, C. Yu, J. Bianco, J.F. Watkins, L.E. Flynn, The performance of decellularized adipose tissue microcarriers as an inductive substrate for human adipose-derived stem cells, Biomaterials. 33 (2012) 4490–4499. https://doi.org/10.1016/j.biomaterials.2012.03.026.

[141] S.H. Kim, D. Kim, M. Cha, S.H. Kim, Y. Jung, The Regeneration of Large-Sized and Vascularized Adipose Tissue Using a Tailored Elastic Scaffold and dECM Hydrogels, Int. J. Mol. Sci. 2021, Vol. 22, Page 12560. 22 (2021) 12560. https://doi.org/10.3390/IJMS222212560.

[142] W. Zhang, A. Du, S. Liu, M. Lv, S. Chen, Research progress in decellularized extracellular matrix-derived hydrogels, Regen. Ther. 18 (2021) 88–96. https://doi.org/10.1016/J.RETH.2021.04.002.

[143] B.A. Bunnell, M. Flaat, C. Gagliardi, B. Patel, C. Ripoll, Adipose-derived stem cells: Isolation, expansion and differentiation, Methods. 45 (2008) 115–120. https://doi.org/10.1016/J.YMETH.2008.03.006.

[144] A. Paganelli, L. Benassi, E. Rossi, C. Magnoni, Extracellular matrix deposition by adipose-derived stem cells and fibroblasts: a comparative study, Arch. Dermatol. Res. 312 (2020) 295–299. https://doi.org/10.1007/S00403-019-01997-8/FIGURES/2.

[145] V. Guneta, Z. Zhou, N.S. Tan, S. Sugii, M.T.C. Wong, C. Choong, Recellularization of decellularized adipose tissue-derived stem cells: Role of the cell-secreted extracellular matrix in cellular differentiation, Biomater. Sci. 6 (2018) 168–178. https://doi.org/10.1039/c7bm00695k.

[146] J.C. Blum, T.L. Schenck, A. Birt, R.E. Giunta, P.S. Wiggenhauser, Artificial decellularized extracellular matrix improves the regenerative capacity of adipose tissue derived stem cells on 3D printed polycaprolactone scaffolds:, Https://Doi.Org/10.1177/20417314211022242. 12 (2021). https://doi.org/10.1177/20417314211022242.

[147] E. Rossi, J. Guerrero, P. Aprile, A. Tocchio, E.A. Kappos, I. Gerges, C. Lenardi, I. Martin, A. Scherberich, Decoration of RGD-mimetic porous scaffolds with engineered and devitalized extracellular matrix for adipose tissue regeneration, Acta Biomater. 73 (2018) 154–166. https://doi.org/10.1016/j.actbio.2018.04.039.

[148] K. Horisawa, Specific and quantitative labeling of biomolecules using click chemistry, Front. Physiol. 5 (2014). https://doi.org/10.3389/FPHYS.2014.00457.

[149] J.M. Baskin, C.R. Bertozzi, Bioorthogonal Click Chemistry: Covalent Labeling in Living Systems, QSAR Comb. Sci. 26 (2007) 1211–1219. https://doi.org/10.1002/QSAR.200740086.

[150] E.M. Sletten, C.R. Bertozzi, Bioorthogonal Chemistry: Fishing for Selectivity in a Sea of Functionality, Angew. Chemie Int. Ed. 48 (2009) 6974–6998. https://doi.org/10.1002/ANIE.200900942.

[151] K. Nwe, M.W. Brechbiel, Growing Applications of "Click Chemistry" for Bioconjugation in Contemporary Biomedical Research, Cancer Biother. Radiopharm. 24 (2009) 289. https://doi.org/10.1089/CBR.2008.0626.

[152] C.A. DeForest, B.D. Polizzotti, K.S. Anseth, Sequential click reactions for synthesizing and patterning three-dimensional cell microenvironments, Nat. Mater. 2009 88. 8 (2009) 659–664. https://doi.org/10.1038/nmat2473.

[153] L. Wang, M. Zhao, S. Li, U.J. Erasquin, H. Wang, L. Ren, C. Chen, Y. Wang, C. Cai, "Click"Immobilization of a VEGF-MimeticPeptide on Decellularized Endothelial Extracellular Matrix to EnhanceAngiogenesis, ACS Appl. Mater. Interfaces. 6 (2014) 8401. https://doi.org/10.1021/AM501309D.

[154] S.M. Ruff, S. Keller, D.E. Wieland, V. Wittmann, G.E.M. Tovar, M. Bach, P.J. Kluger, clickECM: Development of a cell-derived extracellular matrix with azide functionalities, Acta Biomater. 52 (2017) 159–170. https://doi.org/10.1016/j.actbio.2016.12.022.

[155] D.H. Dube, C.R. Bertozzi, Metabolic oligosaccharide engineering as a tool for glycobiology, Curr. Opin. Chem. Biol. 7 (2003) 616–625. https://doi.org/10.1016/j.cbpa.2003.08.006.

[156] V. Hong, N.F. Steinmetz, M. Manchester, M.G. Finn, Labeling Live Cells by Copper-Catalyzed Alkyne−Azide Click Chemistry, Bioconjug. Chem. 21 (2010) 1912–1916. https://doi.org/10.1021/BC100272Z.

[157] Nicholas J. Agard, and Jennifer A. Prescher, C.R. Bertozzi*, A Strain-Promoted [3 + 2] Azide−Alkyne Cycloaddition for Covalent Modification of Biomolecules in Living Systems, J. Am. Chem. Soc. 126 (2004) 15046–15047. https://doi.org/10.1021/JA044996F.

[158] A.-K. Späte, V.F. Schart, S. Schöllkopf, A. Niederwieser, V. Wittmann, Terminal Alkenes as

Versatile Chemical Reporter Groups for Metabolic Oligosaccharide Engineering, Chem. – A Eur. J. 20 (2014) 16502–16508. https://doi.org/10.1002/CHEM.201404716.

[159] D.J.E.G.A. Dold, P.D.V. Wittmann, Metabolic Glycoengineering with Azide- and Alkene-Modified Hexosamines: Quantification of Sialic Acid Levels, Chembiochem. 22 (2021) 1243. https://doi.org/10.1002/CBIC.202000715.

[160] D. JEGA, P. J, S. AK, W. V, Dienophile-Modified Mannosamine Derivatives for Metabolic Labeling of Sialic Acids: A Comparative Study, Chembiochem. 18 (2017) 1242–1250. https://doi.org/10.1002/CBIC.201700002.

[161] D. F, B. A, S. AK, S. VF, T. A, S. W, H. CR, Z. A, W. V, Visualization of Protein-Specific Glycosylation inside Living Cells, Angew. Chem. Int. Ed. Engl. 55 (2016) 2262–2266. https://doi.org/10.1002/ANIE.201503183.

[162] J. Hassenrück, V. Wittmann, Cyclopropene derivatives of aminosugars for metabolic glycoengineering, Beilstein J. Org. Chem. 15 (2019) 584–601. https://doi.org/10.3762/bjoc.15.54.

[163] A. P, B. BJ, S. P, B. CR, Systemic Fluorescence Imaging of Zebrafish Glycans with Bioorthogonal Chemistry, Angew. Chem. Int. Ed. Engl. 54 (2015) 11504–11510. https://doi.org/10.1002/ANIE.201504249.

[164] S. AK, D. JE, B. E, S. VF, W. DE, B. OR, W. V, Exploring the Potential of Norbornene-Modified Mannosamine Derivatives for Metabolic Glycoengineering, Chembiochem. 17 (2016) 1374–1383. https://doi.org/10.1002/CBIC.201600197.

[165] V.F. Schart, J. Hassenrück, A.-K. Späte, J.E.G.A. Dold, R. Fahrner, V. Wittmann, V.F. Schart, J. Hassenrück, A.-K. Späte, J.E.G.A. Dold, R. Fahrner, V. Wittmann, Triple Orthogonal Labeling of Glycans by Applying Photoclick Chemistry, ChemBioChem. 20 (2019). https://doi.org/10.1002/cbic.201800740.

[166] N. S, R. MA, S. A, W. V, K. PJ, An Advanced “clickECM” That Can be Modified by the Inverse-Electron-Demand Diels-Alder Reaction, Chembiochem. (2021). https://doi.org/10.1002/CBIC.202100266.

[167] Z.K. Otrock, R.A.R. Mahfouz, J.A. Makarem, A.I. Shamseddine, Understanding the biology of angiogenesis: Review of the most important molecular mechanisms, Blood Cells, Mol. Dis. 39 (2007) 212–220. https://doi.org/10.1016/J.BCMD.2007.04.001.

[168] K. Gaengel, G. Genové, A. Armulik, C. Betsholtz, Endothelial-mural cell signaling in vascular development and angiogenesis, Arterioscler. Thromb. Vasc. Biol. 29 (2009) 630–638. https://doi.org/10.1161/ATVBAHA.107.161521.

[169] P.L. Olive, C. Vikse, M.J. Trotter, Measurement of oxygen diffusion distance in tumor cubes

using a fluorescent hypoxia probe, Int. J. Radiat. Oncol. Biol. Phys. 22 (1992) 397–402. https://doi.org/10.1016/0360-3016(92)90840-E.

[170] R.H. Thomlinson, L.H. Gray, The Histological Structure of Some Human Lung Cancers and the Possible Implications for Radiotherapy, Br. J. Cancer 1955 94. 9 (1955) 539–549. https://doi.org/10.1038/bjc.1955.55.

[171] X. Meng, Y. Xing, J. Li, C. Deng, Y. Li, X. Ren, D. Zhang, Rebuilding the Vascular Network: In vivo and in vitro Approaches, Front. Cell Dev. Biol. 9 (2021) 937. https://doi.org/10.3389/FCELL.2021.639299/BIBTEX.

[172] J. Rouwkema, N.C. Rivron, C.A. van Blitterswijk, Vascularization in tissue engineering, Trends Biotechnol. 26 (2008) 434–441. https://doi.org/10.1016/J.TIBTECH.2008.04.009.

[173] J.W. Nichol, S.T. Koshy, H. Bae, C.M. Hwang, S. Yamanlar, A. Khademhosseini, Cell-laden microengineered gelatin methacrylate hydrogels, Biomaterials. 31 (2010) 5536–5544. https://doi.org/10.1016/J.BIOMATERIALS.2010.03.064.

[174] D.B. Kolesky, K.A. Homan, M.A. Skylar-Scott, J.A. Lewis, Three-dimensional bioprinting of thick vascularized tissues, Proc. Natl. Acad. Sci. 113 (2016) 3179–3184. https://doi.org/10.1073/PNAS.1521342113.

[175] L.E. Bertassoni, M. Cecconi, V. Manoharan, M. Nikkhah, J. Hjortnaes, A.L. Cristino, G. Barabaschi, D. Demarchi, M.R. Dokmeci, Y. Yang, A. Khademhosseini, Hydrogel bioprinted microchannel networks for vascularization of tissue engineering constructs, Lab Chip. 14 (2014) 2202–2211. https://doi.org/10.1039/C4LC00030G.

[176] G. Yang, B. Mahadik, J.Y. Choi, J.P. Fisher, Vascularization in tissue engineering: fundamentals and state-of-art, Prog. Biomed. Eng. 2 (2020) 012002. https://doi.org/10.1088/2516-1091/AB5637.

[177] D. Ingber, J.F.-L. investigation; a journal of technical, undefined 1988, Inhibition of angiogenesis through modulation of collagen metabolism., Europepmc.Org. (n.d.). https://europepmc.org/article/med/2455830 (accessed November 1, 2021).

[178] S.M. Sweeney, G. DiLullo, S.J. Slater, J. Martinez, R. V. Iozzo, J.L. Lauer-Fields, G.B. Fields, J.D. San Antonio, Angiogenesis in Collagen I Requires α2β1 Ligation of a GFP*GER Sequence and Possibly p38 MAPK Activation and Focal Adhesion Disassembly, J. Biol. Chem. 278 (2003) 30516–30524. https://doi.org/10.1074/JBC.M304237200.

[179] K.T. Morin, R.T. Tranquillo, In vitro models of angiogenesis and vasculogenesis in fibrin gel, Exp. Cell Res. 319 (2013) 2409–2417. https://doi.org/10.1016/J.YEXCR.2013.06.006.

[180] M.N. Nakatsu, R.C.A. Sainson, J.N. Aoto, K.L. Taylor, M. Aitkenhead, S. Pérez-del-Pulgar, P.M. Carpenter, C.C.W. Hughes, Angiogenic sprouting and capillary lumen formation

modeled by human umbilical vein endothelial cells (HUVEC) in fibrin gels: the role of fibroblasts and Angiopoietin-1☆, Microvasc. Res. 66 (2003) 102–112. https://doi.org/10.1016/S0026-2862(03)00045-1.

[181] B. Jiang, R. Suen, J.A. Wertheim, G.A. Ameer, Targeting Heparin to Collagen within Extracellular Matrix Significantly Reduces Thrombogenicity and Improves Endothelialization of Decellularized Tissues, Biomacromolecules. 17 (2016) 3940–3948. https://doi.org/10.1021/ACS.BIOMAC.6B01330.

[182] G.R. Fercana, S. Yerneni, M. Billaud, J.C. Hill, P. VanRyzin, T.D. Richards, B.M. Sicari, S.A. Johnson, S.F. Badylak, P.G. Campbell, T.G. Gleason, J.A. Phillippi, Perivascular extracellular matrix hydrogels mimic native matrix microarchitecture and promote angiogenesis via basic fibroblast growth factor, Biomaterials. 123 (2017) 142–154. https://doi.org/10.1016/J.BIOMATERIALS.2017.01.037.

[183] P. Rousselle, M. Montmasson, C. Garnier, Extracellular matrix contribution to skin wound re-epithelialization, Matrix Biol. 75–76 (2019) 12–26.

[184] N.N. Potekaev, O.B. Borzykh, G. V. Medvedev, D. V. Pushkin, M.M. Petrova, A. V. Petrov, D. V. Dmitrenko, E.I. Karpova, O.M. Demina, N.A. Shnayder, The Role of Extracellular Matrix in Skin Wound Healing, J. Clin. Med. 2021, Vol. 10, Page 5947. 10 (2021) 5947. https://doi.org/10.3390/JCM10245947.

[185] F. Graf, P. Horn, A.D. Ho, M. Boutros, C. Maercker, The extracellular matrix proteins type I collagen, type III collagen, fibronectin, and laminin 421 stimulate migration of cancer cells, FASEB J. 35 (2021). https://doi.org/10.1096/FJ.202002558RR.

[186] S. Nellinger, I. Mrsic, | Silke Keller, | Simon Heine, | Alexander Southan, M. Bach, A.-C. Volz, T. Chassé, P.J. Kluger, Cell-derived and enzyme-based decellularized extracellular matrix exhibit compositional and structural differences that are relevant for its use as a biomaterial, Biotechnol. Bioeng. (2022). https://doi.org/10.1002/BIT.28047.

[187] S. Nellinger, I. Schmidt, S. Heine, A.C. Volz, P.J. Kluger, Adipose stem cell-derived extracellular matrix represents a promising biomaterial by inducing spontaneous formation of prevascular-like structures by mvECs, Biotechnol. Bioeng. 117 (2020) 3160–3172. https://doi.org/10.1002/bit.27481.

[188] I. Juhasz, B. Kiss, L. Lukacs, I. Erdei, Z. Peter, E. Remenyik, Long-term followup of dermal substitution with acellular dermal implant in burns and postburn scar corrections, Dermatol. Res. Pract. 2010 (2010). https://doi.org/10.1155/2010/210150.

[189] E.N. Mostow, G.D. Haraway, M. Dalsing, J.P. Hodde, D. King, Effectiveness of an extracellular matrix graft (OASIS Wound Matrix) in the treatment of chronic leg ulcers: A

randomized clinical trial, J. Vasc. Surg. 41 (2005) 837–843. https://doi.org/10.1016/J.JVS.2005.01.042.

[190] I. Wong, J. Burns, S. Snyder, Arthroscopic GraftJacket repair of rotator cuff tears, J. Shoulder Elb. Surg. 19 (2010) 104–109. https://doi.org/10.1016/J.JSE.2009.12.017.

[191] V. Agrawal, Healing rates for challenging rotator cuff tears utilizing an acellular human dermal reinforcement graft, Int. J. Shoulder Surg. 6 (2012) 36. https://doi.org/10.4103/0973-6042.96992.

[192] P. Simon, M.T. Kasimir, G. Seebacher, G. Weigel, R. Ullrich, U. Salzer-Muhar, E. Rieder, E. Wolner, Early failure of the tissue engineered porcine heart valve SYNERGRAFT® in pediatric patients, Eur. J. Cardio-Thoracic Surg. 23 (2003) 1002–1006. https://doi.org/10.1016/S1010-7940(03)00094-0.

[193] P.E. Bourgine, B.E. Pippenger, A. Todorov, L. Tchang, I. Martin, Tissue decellularization by activation of programmed cell death, Biomaterials. 34 (2013) 6099–6108. https://doi.org/10.1016/J.BIOMATERIALS.2013.04.058.

[194] P.E. Bourgine, E. Gaudiello, B. Pippenger, C. Jaquiery, T. Klein, S. Pigeot, A. Todorov, S. Feliciano, A. Banfi, I. Martin, Engineered Extracellular Matrices as Biomaterials of Tunable Composition and Function, Adv. Funct. Mater. 27 (2017) 1605486. https://doi.org/10.1002/ADFM.201605486.

[195] P.E. Bourgine, C. Scotti, S. Pigeot, L.A. Tchang, A. Todorov, I. Martin, Osteoinductivity of engineered cartilaginous templates devitalized by inducible apoptosis, Proc. Natl. Acad. Sci. U. S. A. 111 (2014) 17426–17431. https://doi.org/10.1073/PNAS.1411975111.

[196] P. Bourgine, C. Le Magnen, S. Pigeot, J. Geurts, A. Scherberich, I. Martin, Combination of immortalization and inducible death strategies to generate a human mesenchymal stromal cell line with controlled survival, Stem Cell Res. 12 (2014) 584–598. https://doi.org/10.1016/J.SCR.2013.12.006.

[197] M.F. Tenreiro, H. V. Almeida, T. Calmeiro, E. Fortunato, L. Ferreira, P.M. Alves, M. Serra, Interindividual heterogeneity affects the outcome of human cardiac tissue decellularization, Sci. Reports 2021 111. 11 (2021) 1–11. https://doi.org/10.1038/s41598-021-00226-5.

[198] T.D. Johnson, R.C. Hill, M. Dzieciatkowska, V. Nigam, A. Behfar, K.L. Christman, K.C. Hansen, Quantification of Decellularized Human Myocardial Matrix: A Comparison of Six Patients, Proteomics. Clin. Appl. 10 (2016) 75. https://doi.org/10.1002/PRCA.201500048.

[199] S. Keller, A. Liedek, D. Shendi, M. Bach, G.E.M. Tovar, P.J. Kluger, A. Southan, Eclectic characterisation of chemically modified cell-derived matrices obtained by metabolic

glycoengineering and re-assessment of commonly used methods, RSC Adv. 10 (2020) 35273–35286. https://doi.org/10.1039/d0ra06819e.

[200] U. Galili, The α-Gal epitope (Galα1-3Galβ1-4GlcNAc-R) in xenotransplantation, Biochimie. 83 (2001) 557–563. https://doi.org/10.1016/S0300-9084(01)01294-9.

[201] S.F. Badylak, T.W. Gilbert, Immune response to biologic scaffold materials, Semin. Immunol. 20 (2008) 109–116. https://doi.org/10.1016/J.SMIM.2007.11.003.

[202] L. Lai, D. Kolber-Simonds, K.W. Park, H.T. Cheong, J.L. Greenstein, G.S. Im, M. Samuel, A. Bonk, A. Rieke, B.N. Day, C.N. Murphy, D.B. Carter, R.J. Hawley, R.S. Prather, Production of alpha-1,3-galactosyltransferase knockout pigs by nuclear transfer cloning, Science. 295 (2002) 1089–1092. https://doi.org/10.1126/SCIENCE.1068228.

[203] K. Kuwaki, Y.L. Tseng, F.J.M.F. Dor, A. Shimizu, S.L. Houser, T.M. Sanderson, C.J. Lancos, D.D. Prabharasuth, J. Cheng, K. Moran, Y. Hisashi, N. Mueller, K. Yamada, J.L. Greenstein, R.J. Hawley, C. Patience, M. Awwad, J.A. Fishman, S.C. Robson, H.J. Schuurman, D.H. Sachs, D.K.C. Cooper, Heart transplantation in baboons using alpha1,3-galactosyltransferase gene-knockout pigs as donors: initial experience, Nat. Med. 11 (2005) 29–31. https://doi.org/10.1038/NM1171.

[204] G. Chen, H. Qian, T. Starzl, H. Sun, B. Garcia, X. Wang, Y. Wise, Y. Liu, Y. Xiang, L. Copeman, W. Liu, A. Jevnikar, W. Wall, D.K.C. Cooper, N. Murase, Y. Dai, W. Wang, Y. Xiong, D.J. White, R. Zhong, Acute rejection is associated with antibodies to non-Gal antigens in baboons using Gal-knockout pig kidneys, Nat. Med. 11 (2005) 1295–1298. https://doi.org/10.1038/NM1330.

[205] K.S. Jones, Effects of biomaterial-induced inflammation on fibrosis and rejection, Semin. Immunol. 20 (2008) 130–136. https://doi.org/10.1016/J.SMIM.2007.11.005.

[206] G.S. Selders, A.E. Fetz, M.Z. Radic, G.L. Bowlin, An overview of the role of neutrophils in innate immunity, inflammation and host-biomaterial integration, Regen. Biomater. 4 (2017) 55–68. https://doi.org/10.1093/RB/RBW041.

[207] R. Klopfleisch, F. Jung, The pathology of the foreign body reaction against biomaterials, J. Biomed. Mater. Res. Part A. 105 (2017) 927–940. https://doi.org/10.1002/JBM.A.35958.

[208] B.N. Brown, J.E. Valentin, A.M. Stewart-Akers, G.P. McCabe, S.F. Badylak, Macrophage phenotype and remodeling outcomes in response to biologic scaffolds with and without a cellular component, Biomaterials. 30 (2009) 1482–1491. https://doi.org/10.1016/j.biomaterials.2008.11.040.

[209] T.U. Luu, W.F. Liu, Regulation of Macrophages by Extracellular Matrix Composition and Adhesion Geometry, Regen. Eng. Transl. Med. 4 (2018) 238–246.

https://doi.org/10.1007/s40883-018-0065-z.

[210] P. Lu, K. Takai, V.M. Weaver, Z. Werb, ExtracellularMatrix Degradation andRemodeling in Development and Disease, Cold Spring Harb Perspect Biol. (2011). https://doi.org/10.1101/cshperspect.a005058.

[211] R.D. Record, D. Hillegonds, C. Simmons, R. Tullius, F.A. Rickey, D. Elmore, S.F. Badylak, In vivo degradation of 14C-labeled small intestinal submucosa (SIS) when used for urinary bladder repair, Biomaterials. 22 (2001) 2653–2659. https://doi.org/10.1016/S0142-9612(01)00007-2.

[212] S. Sart, Y. Yan, E. Lochner, C. Zeng, T. Ma, Y. Li, Crosslinking of extracellular matrix scaffolds derived from pluripotent stem cell aggregates modulates neural differentiation, Acta Biomater. 30 (2016) 222–232. https://doi.org/10.1016/j.actbio.2015.11.016.

[213] K. Výborný, J. Vallová, Z. Kočí, K. Kekulová, K. Jiráková, P. Jendelová, J. Hodan, Š. Kubinová, Genipin and EDC crosslinking of extracellular matrix hydrogel derived from human umbilical cord for neural tissue repair, Sci. Reports 2019 91. 9 (2019) 1–15. https://doi.org/10.1038/s41598-019-47059-x.

[214] A.M. Matuska, P.S. Mcfetridge, J. Crayton, P. Family, The effect of terminal sterilization on structural and biophysical properties of a decellularized collagen-based scaffold; implications for stem cell adhesion, J. Biomed. Mater. Res. Part B Appl. Biomater. 103 (2015) 397–406. https://doi.org/10.1002/JBM.B.33213.

[215] C.L. Dearth, T.J. Keane, C.A. Carruthers, J.E. Reing, L. Huleihel, C.A. Ranallo, E.W. Kollar, S.F. Badylak, The effect of terminal sterilization on the material properties and in vivo remodeling of a porcine dermal biologic scaffold, Acta Biomater. 33 (2016) 78–87. https://doi.org/10.1016/J.ACTBIO.2016.01.038.

[216] V. Agrawal, S. Tottey, S.A. Johnson, J.M. Freund, B.F. Siu, S.F. Badylak, Recruitment of progenitor cells by an extracellular matrix cryptic peptide in a mouse model of digit amputation, Tissue Eng. Part A. 17 (2011) 2435–2443. https://doi.org/10.1089/TEN.TEA.2011.0036.

DECLARATION OF INDEPENDENCE

Ich erkläre hiermit, dass ich die zur Promotion eingereichte Arbeit mit dem Titel " Adipose stem cell-derived extracellular matrix – comparative characterization and evaluation as a biomaterial" selbstständig verfasst, nur die angegebenen Quellen und Hilfsmittel benutzt und wörtlich oder inhaltlich übernommene Zitate also solche gekennzeichnet habe. Ich erkläre, dass die Richtlinien zur Sicherung guter wissenschaftlicher Praxis der Universität Tübingen beachtet wurden. Ich versichere an Eides statt, dass diese Angaben wahr sind und dass ich nichts verschwiegen habe. Mir ist bekannt, dass die falsche Angabe einer Versicherung an Eides statt mit Freiheitsstrafe bis zu drei Jahren oder mit Geldstrafe bestraft wird.

Tübingen, 14.03.2022

Svenja Nellinger

APPENDICES

Appendix I: Generation of an azide-modified extracellular matrix by adipose-derived stem cells using metabolic engineering

Current Directions in Biomedical Engineering 2019;5(1):1-3

Svenja Nellinger*, Silke Keller, Alexander Southan, Valentin Wittmann, Ann-Cathrin Volz and Petra J. Kluger

Generation of an azide-modified extracellular matrix by adipose-derived stem cells using metabolic glycoengineering

Abstract: Natural extracellular matrix (ECM) represents an ideal biomaterial for tissue engineering and regenerative medicine approaches. For further functionalization, there is a need for specific addressable functional groups within this biomaterial. Metabolic glycoengineering (MGE) provides a technique to incorporate modified monosaccharide derivatives into the ECM during their assembly, which was shown by us earlier for the production of a modified fibroblast-derived dermal ECM. In this study, adipose-derived stem cells (ASCs) were treated with the azide-modified monosaccharide derivate 1,3,4,6-tetra-O-acetyl-N-azidoacetylgalactosamine ($Ac_4GalNAz$). Toxicity and viability assays after 24 h and 72 h incubation revealed high biocompatibility of $Ac_4GalNAz$ in contact with ASCs. The successful incorporation of the functional azide groups into the glycocalyx and the ECM of the ASCs was proven by conjugation with a fluorescent dye via a copper-catalyzed click reaction. Thus, $Ac_4GalNAz$ in combination with ASCs was confirmed to achieve an azide-modified ECM as a multifunctional biomaterial for further applications.

Keywords: Adipose-derived stem cells, clickECM, extracellular matrix, metabolic glycoengineering, azide-modified

https://doi.org/10.1515/cdbme-2019-XXXX

*Corresponding author: **Svenja Nellinger:** Reutlingen University, Alteburgstr 150, Reutlingen, Germany, e-mail: svenja.nellinger@reutlingen-university.de
Silke Keller, Alexander Southan: University of Stuttgart, Stuttgart, Germany
Valentin Wittmann: University of Konstanz, Konstanz, Germany
Ann-Cathrin Volz, Petra J. Kluger: Reutlingen University, Reutlingen, Germany

1 Introduction

The extracellular matrix (ECM) represents the natural environment of cells in an organism, wherein it is synthesized and assembled by tissue-specific cells. Next to native ECM, derived from decellularized mature tissues, cell-specific matrices can also be obtained from the in vitro culture of these cells. Varying with the specific tissue or cell source, the ECM contains variable amounts of collagens, other fibrous and non-fibrous proteins, proteoglycans and glycoproteins and exhibits different physical properties. Native and cell-derived ECMs are used and studied in a variety of applications as potential biomaterials such as cell-influencing coatings [1, 2], hybrid scaffolding materials for tissue engineering [3, 4], and bioinks [5, 6]. A wide range of potential applications requires the modification of the ECM with specific addressable functional groups. Chemical modification of ECM compounds is challenging as it might affect matrix integrity. To address these issues, metabolic glycoengineering (MGE) represents a promising tool. This method is based on the incorporation of chemically modified monosaccharide derivatives into the natural intra- and extracellular oligosaccharide structures of the cell by its natural metabolic pathways [7, 8]. These functionalities can subsequently be addressed by bioorthogonal chemical ligation reactions [9, 10] for tuning chemical and physical properties and for visualization of glycoconjugates. Previously, we employed MGE with the azide-modified monosaccharide derivate 1,3,4,6-tetra-O-acetyl-N-azidoacetylgalactosamine ($Ac_4GalNAz$) to generate a human fibroblast-derived dermal ECM containing azide groups [11] that can be addressed by copper-catalyzed azide-alkyne cycloaddition [12, 13]. For this functionalized ECM (clickECM) we could show that the composition and functionality of the ECM was not affected by the MGE procedure and the modification with azide groups [11]. Later, also Gutmann et al. reported a similar approach using the corresponding azide-modified glucosamine derivative [14].

In this study, we aimed to prove whether the glycocalyx and ECM of adipose-derived stem cells (ASCs) can be modified with azide groups using $Ac_4GalNAz$ in MGE (Figure 1). Generation of an azide-modified stem cell ECM would be very promising for a wide range of applications especially in tissue engineering and regenerative medicine by representing a stem cell niche material with tunable chemical and physical properties. Such a unique biomaterial cannot be achieved by decellularization of tissues, as the stem cell niches are very small in vivo and integrated in matured neighboring tissues. Therefore, azide-modified ECM of ASCs provides multiple opportunities of further functionalization and application.

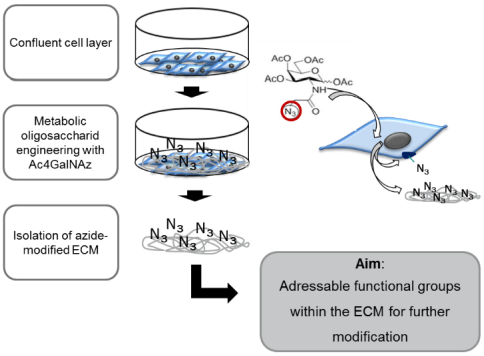

Figure 1: Schematic overview of the metabolic glycoengineering process with ASCs and $Ac_4GalNAz$. Cells were grown to confluency followed by the addition of $Ac_4GalNAz$. The incorporation of azide-groups into the glycocalyx and ECM occurs by MGE. Subsequently the azide-modified ECM was isolated by lysis of the cells. Generated azide-modified ECM could prospectively be used for further applications such as specific modifications of the ECM with molecules and for the use in tissue engineering and bioprinting approaches. (Modified after Ruff et al. [11])

2 Materials and Methods

2.1 Isolation and expansion of ASCs

ASCs were isolated from human tissue samples obtained from patients undergoing plastic surgery (Dr. Ziegler; Klinik Charlottenhaus, Stuttgart, Germany) as described before [15]. All research was carried out in accordance with the rules for investigation of human subjects as defined in the Declaration of Helsinki. Patients provided written agreement in compliance with the Landesärztekammer Baden-Württemberg (F-2012- 078, for normal skin from elective surgeries). ASCs were initially seeded at a density of $5x10^3$ cells cm^{-2} in serum-free MSC growth medium (PELOBiotech, #PB-C-MH-675-0511-XF) containing 5 % human platelet lysate.

2.2 Biocompatibility assay

The biocompatibility of $Ac_4GalNAz$ was evaluated by a lactate dehydrogenase (LDH) assay (TaKaRa Bio Inc. #630117) and a resazurin assay (Sigma Aldrich, #R7017). ASCs were treated with 100 µM $Ac_4GalNAz$ or phosphate buffered saline (PBS) for 24 h and 72 h. LDH assay was performed according to manufacturer's protocol with cell culture supernatant. For the resazurin assay, culture medium was changed to medium with resazurin salt (11 µg/mL) and incubated for 3 h at 37 °C and 5 % CO2.

2.3 Detection of incorporated azide groups

Incorporated azide-groups were detected via copper-catalyzed azide-alkyne cycloaddition using an alkyne-linked fluorophore as described by Ruff et al. [11]. Isolated paraformaldehyde-fixed ECM was stained according to the manufacturer's instructions. Cell nuclei were counterstained with 1 µg/mL 4',6-diamidino-2-phenylindole (DAPI, Serva Electrophoresis) in PBS for 10 min at RT. Fluorescence images (z-stacks) were taken using a Zeiss Axio Observer.

2.4 Statistics

All experiments were performed with cells from three different biological donors. Data was compared by a one-way analysis of variance and a Tukey post-hoc test using OriginPro 2018b.

3 Results and Discussion

Biocompatibility of $Ac_4GalNAz$ was proven by LDH and resazurin assay (Figure 2). Control groups (Ctr) were incubated with PBS and absorption values were normalized to the control groups. LDH assay revealed no cytotoxic effects of $Ac_4GalNAz$ after 24 h and 72 h.

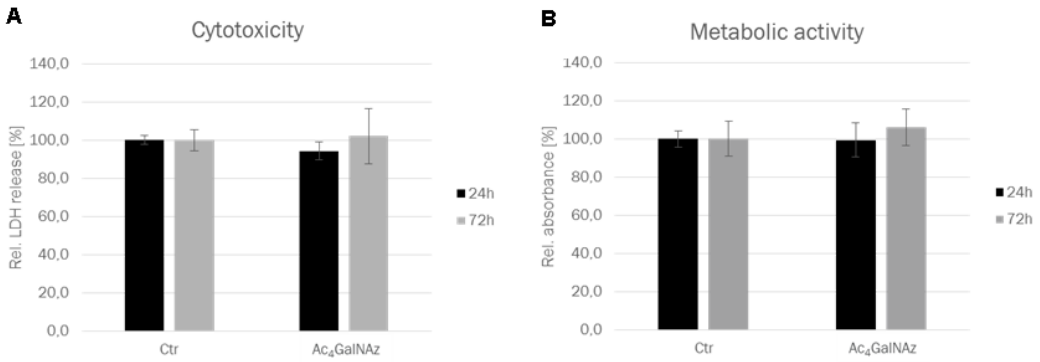

Figure 2: Biocompatibility of Ac4GalNAz in ACSs. ASCs were incubated with 100 µM Ac4GalNAz for 24 h and 72 h. Controls were treated with PBS. A: LDH Assay revealed no significant influence of azide-modified monosaccharide on cell death after 24 h and 72 h. B: Resazurin assay showed no significant influence of azide-modified monosaccharide on metabolic activity after 24 h and 72 h.

Metabolization of resazurin salt was comparable for cells treated with Ac_4GalNAz to the control group. Thus, resazurin assay revealed no significant influence of Ac_4GalNAz on metabolic activity of ASCs. These results are in line with previous studies using fibroblasts [11].

ECM of ASCs can be successfully isolated and harvested as thin sheet of protein network (Fig. 3 A;i) or left as thin gel-like film on the bottom of the petri dish (Figure. 3 A;ii). Incorporation of azide-groups into the glycocalyx and ECM of ASCs was proven by reaction with fluorophore-linked alkyne. In the untreated control group, no specific fluorescence staining was observed (Figure 3B). The cells treated with Ac_4GalNAz exhibited a high specific fluorescence staining of the incorporated azide-groups. It was shown that azide groups were successfully incorporated into the glycocalyx of the cells. Moreover, for ECM isolated from ASCs and thereafter treated with Ac_4GalNAz, showed a specific fluorescence of stained azide groups. This confirmed the incorporation of Ac_4GalNAz in the stem cell ECM. The azide groups were ubiquitously distributed in the glycocalyx and the ECM, comparable to the findings of Ruff et al. [11]

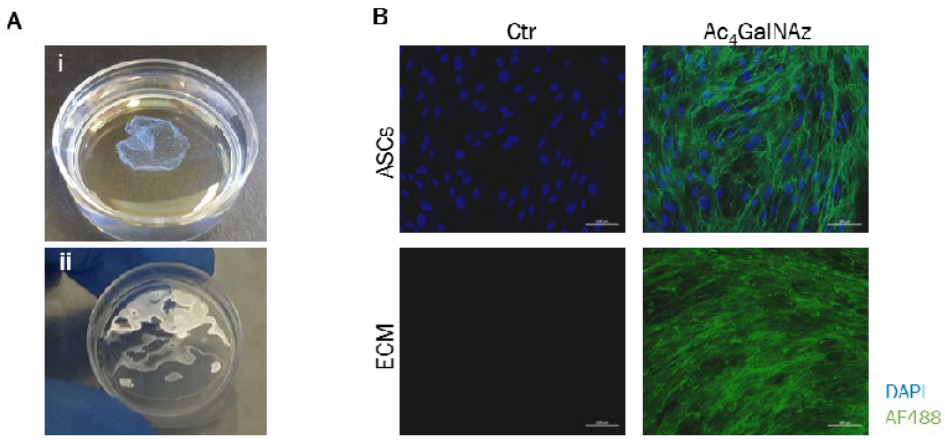

Figure 3: Characterization of ECM as biomaterial. A: Macroscopic pictures of isolated ECM. i: Isolated ECM floating in PBS. ECM can be isolated and collected as a gel-like sheet of a collagen network. ii: Isolated ECM on the bottom of a petri dish. After cell lysis and washing steps, the collagen network appears as a gel-like coating on the bottom of a petri dish (d=35 mm) **B: Fluorescence staining of the incorporated Ac_4GalNAz in ASCs and cell-derived ECM**. Staining of the azide-groups shows the successful incorporation of azide groups into the glycocalyx and ECM of the ASCs. Negative controls (Ctr.) exhibit no fluorescence staining. Cell nuclei are counterstained with DAPI. (Scale bar: 100 µm)

4 Conclusion

No negative impact on cell survival and metabolic activity of ASCs was detectable. Further, it was shown that stem cell ECM of ASCs can be successfully modified with azide groups, which can be further addressed by alkyne-groups via copper-catalyzed azide-alkyne cycloaddition. Based on these results, Ac_4GalNAz may be considered a suitable azide-modified monosaccharide derivative to be used in MGE with ASCs. Thereby, this approach opens up a wide field of medical and material applications of ASC-derived ECM by yielding a multifunctional biomaterial with tuneable chemical and physical properties.

Author Statement

Research funding: We acknowledge the financial support of the Ministry of Science, Research and the Arts of Baden-Württemberg, Germany (#33-7533-7-11.9/7/2).

Conflict of interest: Authors state no conflict of interest. Informed consent: Informed consent has been obtained from all individuals included in this study. Ethical approval: The research related to human use complies with all the relevant national regulations, institutional policies and was performed in accordance with the tenets of the Helsinki Declaration, and has been approved by the authors' institutional review board or equivalent committee.

References

[1] Guneta V, Loh QL, Choong C. Cell-secreted extracellular matrix formation and differentiation of adipose-derived stem cells in 3D alginate scaffolds with tunable properties. Journal of biomedical materials research Part A 2016;104:1090-101.

[2] Vafaei S, Tabaei SR, Guneta V, Choong C, Cho NJ. Hybrid Biomimetic Interfaces Integrating Supported Lipid Bilayers with Decellularized Extracellular Matrix Components. Langmuir 2018;34:3507-16.

[3] Flynn LE. The use of decellularized adipose tissue to provide an inductive microenvironment for the adipogenic differentiation of human adipose-derived stem cells. Biomaterials 2010;31:4715-24.

[4] Adam Young D, Bajaj V, Christman KL. Award winner for outstanding research in the PhD category, 2014 Society for Biomaterials annual meeting and exposition, Denver, Colorado, April 16-19, 2014: Decellularized adipose matrix hydrogels stimulate in vivo neovascularization and adipose formation. Journal of biomedical materials research Part A 2014;102:1641-51.

[5] Pati F, Jang J, Ha DH, Kim SW, Rhie JW, Shim JH, et al. Printing three-dimensional tissue analogues with decellularized extracellular matrix bioink. Nat Commun 2014;5.

[6] Pati F, Ha DH, Jang J, Han HH, Rhie JW, Cho DW. Biomimetic 3D tissue printing for soft tissue regeneration. Biomaterials 2015;62:164-75.

[7] Wratil PR, Horstkorte R, Reutter W. Metabolic Glycoengineering with N-Acyl Side Chain Modified Mannosamines. Angew Chem, Int Ed 2016;55:9482-512.

[8] Palaniappan KK, Bertozzi CR. Chemical Glycoproteomics. Chem Rev 2016;116:14277-306.

[9] Prescher JA, Bertozzi CR. Chemistry in living systems. Nat Chem Biol 2005;1:13-21.

[10] Sletten EM, Bertozzi CR. Bioorthogonal Chemistry: Fishing for Selectivity in a Sea of Functionality. Angew Chem, Int Ed 2009;48:6974-98.

[11] Ruff SM, Keller S, Wieland DE, Wittmann V, Tovar GEM, Bach M, et al. clickECM: Development of a cell-derived extracellular matrix with azide functionalities. Acta biomaterialia 2017;52:159-70.

[12] Rostovtsev VV, Green LG, Fokin VV, Sharpless KB. A Stepwise Huisgen Cycloaddition Process: Copper(I)-Catalyzed Regioselective "Ligation" of Azides and Terminal Alkynes. Angew Chem, Int Ed 2002;41:2596-9.

[13] Tornøe CW, Christensen C, Meldal M. Peptidotriazoles on Solid Phase: [1,2,3]-Triazoles by Regiospecific Copper(I)-Catalyzed 1,3-Dipolar Cycloadditions of Terminal Alkynes to Azides. J Org Chem 2002;67:3057-64.

[14] Gutmann M, Braun A, Seibel J, Lühmann T. Bioorthogonal Modification of Cell Derived Matrices by Metabolic Glycoengineering. ACS Biomater Sci Eng 2018;4:1300-6.

[15] Huber B, Borchers K, Tovar GE, Kluger PJ. Methacrylated gelatin and mature adipocytes are promising components for adipose tissue engineering. Journal of biomaterials applications 2016;30:699-710.

Appendix II: Cell-derived extracellular matrix as maintaining biomaterial for adipogenic differentiation

DE GRUYTER Current Directions in Biomedical Engineering 2020;6(3): 20203106

Svenja Nellinger, Simon Heine, Ann-Cathrin Volz and Petra J. Kluger*

Cell-derived Extracellular Matrix as maintaining Biomaterial for adipogenic differentiation

Abstract: The extracellular matrix (ECM) naturally surrounds cells in humans, and therefore represents the ideal biomaterial for tissue engineering. ECM from different tissues exhibit different composition and physical characteristics. Thus, ECM provides not only physical support but also contains crucial biochemical signals that influence cell adhesion, morphology, proliferation and differentiation. Next to native ECM from mature tissue, ECM can also be obtained from the *in vitro* culture of cells. In this study, we aimed to highlight the supporting effect of cell-derived- ECM (cdECM) on adipogenic differentiation. ASCs were seeded on top of cdECM from ASCs (scdECM) or pre-adipocytes (acdECM). The impact of ECM on cellular activity was determined by LDH assay, WST I assay and BrdU assay. A supporting effect of cdECM substrates on adipogenic differentiation was determined by oil red O staining and subsequent quantification. Results revealed no effect of cdECM substrates on cellular activity. Regarding adipogenic differentiation a supporting effect of cdECM substrates was obtained compared to control. With these results, we confirm cdECM as a promising biomaterial for adipose tissue engineering.

Keywords: extracellular matrix, adipose-derived stem cells, differentiation, biomaterial.

https://doi.org/10.1515/cdbme-2020-3106

1 Introduction

Biomaterials should provide an adequate environment for cultures cells and thereby play a crucial role in tissue engineering process. To date there are a variety of available materials for adipose tissue engineering such as gelatine [1], collagen [2], alginate [3] or combinations thereof. However, these materials cannot represent the complexity of the natural ECM and the typical organization of native tissue. ECM represents the natural environment of cells in an organism, wherein it is synthesized and assembled by tissue-specific cells. The ECM of a tissue provides not only physical support but also delivers crucial biochemical signals that influence cell adhesion, morphology, proliferation and differentiation [4]. The composition and physical characteristics of the ECM vary between different tissues and different stages of cell differentiation. Next to native ECM, derived from mature decellularized tissues, cell-specific matrices can also be obtained from the *in vitro* culture of these cells. Native and cell-derived ECMs (cdECM) are used and studied in numerous applications as potential biomaterials such as cell-influencing coatings [5], hybrid scaffolding materials for tissue engineering [6], and bioinks [7].

In this work, we investigated the potentially supporting effect of cdECM on ASCs regarding cytotoxicity, metabolic activity, proliferation and adipogenic differentiation.

2 Materials and Methods

All research was carried out in accordance with the rules for investigation of human subjects as defined in the Declaration of Helsinki. Patients provided written agreement in compliance with the Landesärztekammer Baden-Württemberg (F-2012- 078, for normal skin from elective surgeries).

2.1 Cell isolation and expansion

ASCs were isolated from human adipose tissue samples obtained from patients undergoing plastic surgery (Dr. Ziegler, Klinik Charlottenhaus, Stuttgart, Germany) as described before. ASCs were initially seeded at a density of $5x10^3$ cells/ cm^2 in serum-free MSC growth medium (PELOBiotech, #PB-C-MH-675-0511-XF) containing 5 % human platelet lysate.

***Corresponding author: Petra J. Kluger,** Reutlingen University, Alteburgstr. 150, Reutlingen, Germany, e-mail: petra.kluger@reutlingen-university.de
Svenja Nellinger, Simon Heine, Ann-Cathrin Volz, Reutlingen Research Institute, Alteburgstr. 150, Reutlingen, Germany

2.2 Generation of cdECM and reseeding

ASCs were seeded into 24-well plates at a density of $2.5x10^4$ cells/cm^2 in serum-free MSCGM containing 5 % human platelet lysate. At confluency, medium was changed to either serum-containing growth medium (GM) (Dulbecco's modified Eagle Medium (DMEM) with 10 % fetal calf serum (FCS) = scdECM) or adipogenic differentiation medium (DMEM with 10 % FCS, 1 µg/mL insulin, 1 µM dexamethasone, 100 µM indomethacin, 500 µM 3-isobutyl-1-methylxanthine = acdECM) both supplemented with 50 µg/mL Na-L-ascorbate. The medium was changed every other day. At day 7, cells were lysed using hypotonic ammonium hydroxide solution and cdECM was washed with ultrapure water. Direct after cdECM isolation ASCs were seeded on top of the cdECM at a density of $2.5x10^4$ cells/cm^2 in GM. As a control, ASCs were seeded on TCPS.

At confluency medium was changed to differentiation medium. For this study, two different adipogenic differentiation media were used. A full supplemented adipogenic differentiation medium (DMEM with 10 % FCS, 1 µg/mL insulin, 1 µM dexamethasone, 100 µM indomethacin, 500 µM 3-isobutyl-1- methylxanthine = Diff. medium) and an adipogenic differentiation medium supplemented with 1 µg/mL insulin (GM + insulin). As control, ASCs were cultured in GM.

2.3 Assays for cellular activity

At day three after reseeding, assays were performed to determine the influence of cdECM substrates on ASCs activity. For evaluation of cytotoxicity of the substrates a lactate dehydrogenase (LDH) assay was performed. LDH is released into the cell culture medium after cell death. Metabolic activity of ASCs cultured on the different substrates was evaluated by WST I assay. WST I is a tetrazolium salt which is cleaved to formazan by cellular mitochondrial dehydrogenase and therefore can be used to measure metabolic activity. ASCs proliferation was determined by colorimetric BrdU assay (Sigma Aldrich, Germany). Within this assay, bromolated nucleotides are incorporated into the DNA during replication and can therefore be used to determine the proliferation rate of ASCs. Incorporated BrdU was detected by horse radish peroxidase conjugated antibody and TMB turnover was measured using a plate reader at 650nm.

2.4 Oil red O staining and quantification

To determine the amount of accumulated lipids and thereby the degree of adipogenic differentiation, ASCs were stained with Oil red O. Cells were fixed with Roti-Histofix for 15 min. Subsequently, cells were incubated with 60 % isopropanol for 5 min followed by 10 min incubation with Oil red O solution (60% Oil red O stock solution (5 mg/mL) in Millipore water). For quantification, the staining solution was extracted with 100 % isopropanol for 15 min under shaking conditions. Absorbance was measured at 520 nm with a plate reader (Tecan safire²). Light microscopic pictures were taken before extracting Oil red O off the cells with an Axio Observer (Carl Zeiss).

2.5 Statistics

All experiments were performed with cells from three different biological donors. Data was compared by a one-way analysis of variance and a Tukey post-hoc test using OriginPro 2018b.

3 Results

3.1 ASC activity

To determine potential cytotoxic effects of cdECM, LDH release was measured at day three after reseeding (Figure 1). Results revealed no cytotoxic effect of cdECM on ASCs (TCPS: 100.0 (± 8.8) %; acdECM: 123.8 (± 48.4) %; scdECM: 89 (± 23.3) %). Influence of cdECM on metabolic activity and proliferation was determined by WST I assay (TCPS: 100.0 (±1.0) %; acdECM: 99.2 (± 14.2) %: scdECM: 130.2 (± 6.9) %) and BrdU assay (TCPS: 100.0 (± 4.6) %; acdECM: 148.0 (± 61.8) %; scdECM: 98.2 (± 22.2) %), respectively.

3.2 Adipogenic differentiation

For determining a potential effect of cdECM on adipogenic differentiation, ASCs were seeded on top of acdECM and scdECM and were cultured in GM, GM with insulin (insulin) or fully supplemented adipogenic differentiation medium (full suppl.). As a control, ASCs were cultured on TCPS. To analyse lipid accumulation as an indicator for adipogenic differentiation Oil red O staining was performed at day 14 (Figure 3). Light microscopic analysis revealed no adipogenic differentiation in GM on all substrates. For insulin, some lipid

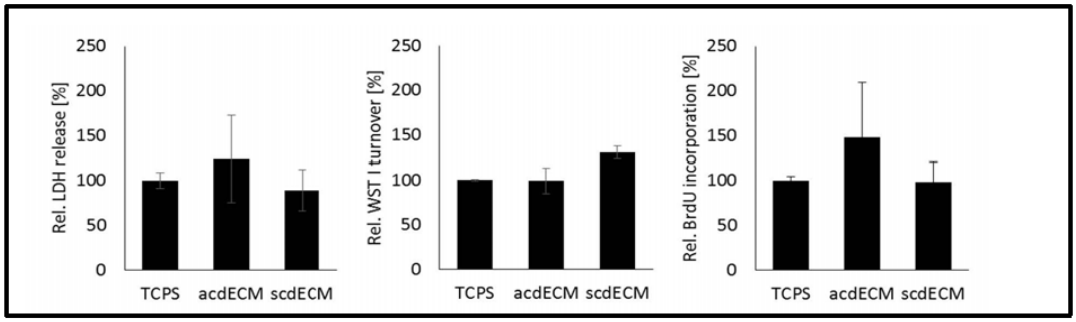

Figure 1: Cellular activity of ASCs cultured on cdECM substrates. ASCs were seeded on top of TCPS, acdECM and scdECM at a density of 2.5 x 10^4 cells/cm^2 in GM. At day three LDH, WST I and BrdU assays were performed. None of the assays revealed any influence of cdECM substrates on cell death, metabolic activity or proliferation rate of ASCs.

accumulation can be observed on acdECM and scdECM but not on TCPS. Full supplemented medium led to extensive lipid accumulation on all substrates. Quantification of Oil red O staining was performed at day 14 (Figure 3). No adipogenic differentiation can be observed in GM on all substrates (TCPS: 100.0(±23.0) %; acdECM: 107.6 (± 23.7) %; scdECM: 103.2 (±22.2) %). For insulin supplemented medium a significantly higher lipid accumulation can be found in ASCs cultured on cdECM substrates compared to TCPS (TCPS: 100.0 (± 20.3) %; acdECM: 163.0 (± 18.1) %: scdECM: 150.4 (± 19.5) %). In fully supplemented adipogenic differentiation medium a higher degree of lipid accumulation can be observed on acdECM compared to scdECM and TCPS (TCPS: 100.0 (± 9.2) %; acdECM: 146.7 (± 9.1) %; scdECM: 91.9 (± 37.3) %).

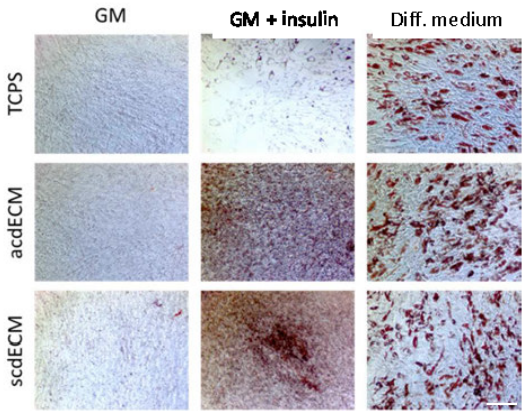

Figure 2: Oil red O staining of ASCs cultured on different substrates. ASCs were seeded on top of cdECM substrates and TCPS at a density of 2.5 x 10^4 cells/cm^2 and were cultured in GM, insulin supplemented medium and fully supplemented adipogenic differentiation medium for 14 days. ASCs cultured in GM exhibit no lipid accumulation. ASCs cultured in insulin supplemented medium exhibit higher degree of lipid accumulation on cdECM substrates compared to TCPS. In fully supplemented medium lipid accumulation can be found on all substrates. Scale bar: 200µm

4 Discussion

The present study confirms cdECM as promising biomaterial for adipose tissue engineering. ASCs cultured in insulin supplemented medium led to a significantly higher lipid accumulation on cdECM substrates compared to TCPS. These results indicate a supporting effect of cdECM on adipogenic differentiation in combination with soluble differentiation factors. The incorporation of lipids, analysed in this study, is a process occurring at a late stage of adipogenic differentiation. Insulin is well known to induce adipogenic differentiation and thus accelerate the supporting effect of cdECM, but does not induce differentiation as strong as fully supplemented adipogenic differentiation medium [8, 9]. These results are in line with Guneta et al. who found the expression of genes associated with adipogenic differentiation in ASCs cultured on cdECM [5]. Interestingly in fully supplemented adipogenic differentiation medium a supporting effect of acdECM on adipogenic differentiation can be found indicating the promising effect of acdECM. The complex composition of the ECM is not fully characterized. Individual components of the ECM like collagen and laminin are widely used in tissue engineering approaches [10]. Next to structural proteins native ECM is also decorated with growth factors and degradation products of the ECM are known to induce cellular response [4]. A major advantage of cdECM over ECM from mature tissue is the independence of yielded ECM amount from the size of donated tissue samples. In conclusion, these results highlight the promising effect of cdECM as biomaterial for adipose tissue engineering by supporting adipogenic differentiation.

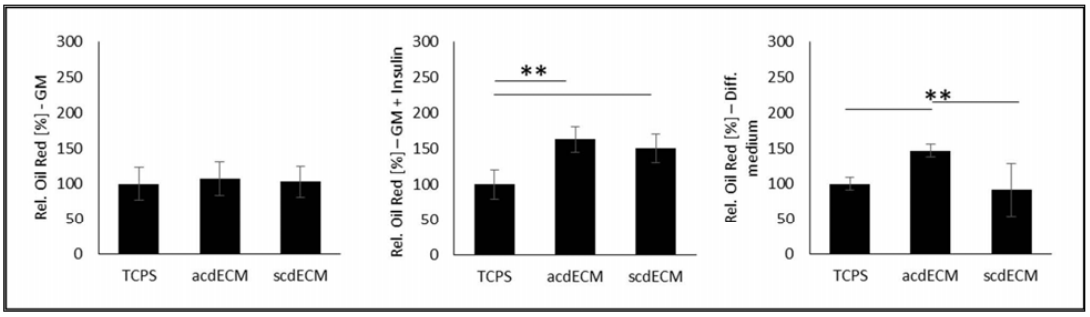

Figure 3: Adipogenic differentiation on different substrates. ASCs were seeded on top of cdECM substrates and TCPS at a density of 2.5 x10^4 cells/cm^2 and were cultured in GM, GM supplemented with insulin and fully supplemented adipogenic differentiation medium for 14 days. In GM no lipid accumulation can be observed on all substrates. In insulin supplemented medium significantly increased lipid accumulation can be found on cdECM substrates compared to controls for both time points. In fully supplemented adipogenic differentiation medium, enhanced lipid accumulation can be observed at day 14 on acdECM. (** $p \leq 0.01$)

Author Statement

Research funding: We acknowledge the financial support of the Ministry of Science, Research and the Arts of Baden-Württemberg, Germany; Landesgraduiertenförderung.
Conflict of interest: Authors state no conflict of interest. Informed consent: Informed consent has been obtained from all individuals included in this study. Ethical approval: The research related to human use complies with all the relevant national regulations, institutional policies and was performed in accordance with the tenets of the Helsinki Declaration, and has been approved by the authors' institutional review board or equivalent committee.

References

[1] Phull MK, Eydmann T, Roxburgh J, Sharpe JR, Lawrence-Watt DJ, Phillips G, et al. Novel macro-microporous gelatin scaffold fabricated by particulate leaching for soft tissue reconstruction with adipose-derived stem cells. Journal of materials science Materials in medicine 2013;24:461-7.

[2] Zoller N, Schreiner S, Petry L, Hoffmann S, Steinhorst K, Kleemann J, et al. Collagen I Promotes Adipocytogenesis in Adipose-Derived Stem Cells In Vitro. Cells 2019;8.

[3] Hirsch T, Laemmle C, Behr B, Lehnhardt M, Jacobsen F, Hoefer D, et al. Implant for autologous soft tissue reconstruction using an adipose-derived stem cell-colonized alginate scaffold. Journal of plastic, reconstructive & aesthetic surgery : JPRAS 2018;71:101-11.

[4] Frantz C, Stewart KM, Weaver VM. The extracellular matrix at a glance. Journal of cell science 2010;123:4195-200.

[5] Guneta V, Zhou Z, Tan NS, Sugii S, Wong MTC, Choong C. Recellularization of decellularized adipose tissue-derived stem cells: role of the cell-secreted extracellular matrix in cellular ' differentiation. Biomater Sci-Uk 2017;6:168-78.

[6] Guneta V, Loh QL, Choong C. Cell-secreted extracellular matrix formation and differentiation of adipose-derived stem cells in 3D alginate scaffolds with tunable properties. Journal of biomedical materials research Part A 2016;104:1090-101.

[7] Pati F, Ha DH, Jang J, Han HH, Rhie JW, Cho DW. Biomimetic 3D tissue printing for soft tissue regeneration. Biomaterials 2015;62:164-75.

[8] Ding J, Nagai K, Woo JT. Insulin-dependent adipogenesis in stromal ST2 cells derived from murine bone marrow. Bioscience, biotechnology, and biochemistry 2003;67:314-21.

[9] Zhang HH, Huang JX, Duvel K, Boback B, Wu SL, Squillace RM, et al. Insulin Stimulates Adipogenesis through the Akt-TSC2-mTORC1 Pathway. PloS one 2009;4.

[10] Fernandes H, Moroni L, van Blitterswijk C, de Boer J. Extracellular matrix and tissue engineering applications. J Mater Chem 2009;19:5474-84.